The Role of Mitochondrial ATP-Binding Cassette Transporter ABCB6 in Metabolism and Energy Balance

By

Robert T Tessman

Submitted to the graduate degree program in Toxicology and the Graduate Faculty of the University of Kansas in partial fulfillment of the requirements for the degree of Doctor of Philosophy.

_____

Committee Chair: Partha Kasturi, PhD

_____

Bruno Hagenbuch, PhD

_____

Hao Zhu, PhD

_____

Tiangang Li, PhD

_____

Luciano DiTacchio, PhD

Date Defended: April 19th, 2019

The dissertation committee for Robert T Tessman certifies that this is the approved version of the following dissertation:

The role of Mitochondrial ATP-Binding Cassette Transporter ABCB6 in Metabolism and Energy Balance

Committee Chair: Partha Kasturi, PhD

Date Approved: April 19th, 2019

Abstract

Obesity and the associated health risks represent a world-wide health and financial crisis. Lack of physical activity combined with excessive caloric intake are the root cause of the problem. Despite the increased advocation for healthy lifestyle choices, the trend has yet to reverse and indeed, seems to be on the rise especially among pre-teens and adolescents, a constituent that had not been previously part of the obesity epidemic.

Mitochondria are the “fuel-burners” of the body and like other combustion devices, become inefficient in the context of fuel surplus. Moreover, with chronic over-feeding, the physiological mechanisms that regulate energy balance become permanently dysfunctional leading to the progression of pathologies such as Type II diabetes and cardiovascular disease.

Medical and scientific evidence confirms that mitochondria are integral to the responses necessary to adapt to over-nutrition. However, success in mitochondria-based therapies has been extremely limited in the context of metabolic diseases. Our knowledge of the regulation of mitochondrial function, dynamics, signaling, and transport processes in different tissues and organ systems is extremely limited and this knowledge gap is a serious impediment to progress toward targeting mitochondria for treatment of metabolic diseases.

In this study, we successfully genetically manipulated the expression of mitochondrial transporter ABCB6. The physiological function of this transporter is unknown but non-functional mutations of this protein have been linked to several heritable human diseases.

This study establishes that ABCB6 plays a role in the maintenance of energy homeostasis. Whole-body *Abcb6* knockout adult male and female mice have increased body mass with no increases in food consumption. Increased body mass is due to increased adiposity. ABCB6 deficiency results in steatosis, glucose intolerance, insulin resistance, and lower energy expenditure. Exposure to high-fat diet exacerbates these metabolic derangements.

Genetically targeting ABCB6 expression specifically in liver results in disruption of whole-body energy metabolism as well with a loss of metabolic flexibility. Loss of hepatic ABCB6 results in fragmented mitochondria while overexpression leads to mitochondrial elongation, dysregulating dynamic mitochondrial functional responses to energy status. In this liver-specific model, hepatic metabolites are significantly altered with either ABCB6 knockdown or overexpression. Metabolites that have a profound impact on energy metabolism such as bile acids, amino acids, and phospholipids were significantly altered in this model.

Interestingly, we discovered that ABCB6 expression is responsive to nutrient status and circadian patterns. ABCB6 expression is upregulated in the fasted state and rapidly downregulated in response to feeding. Also, ABCB6 expression is reduced in cases of chronic over-nutrition such as, diet and genetic mouse models of obesity as well as in clinically obese humans. These findings suggest that ABCB6 acts as a nutrient sensor and mediates a homeostatic response through dynamic mitochondrial changes in form and function.

Acknowledgments

I would like to express my sincere appreciation for my mentor Dr. Partha Kasturi. Dr. Kasturi is a man of impeccable standards in his career and in his personal life and sets an outstanding example in these areas. When I was battling the trials of the research process, he was a kind confidant, allowing me to vent when I needed to but then always putting me back on a positive track with words of encouragement and wisdom. I am grateful for the training I have gotten from him, most of all, the ability to think in a “logical progression” (one of our often-used phrases) as a scientist should. Thank you Partha!

I would also like to thank the members of my committee, Drs. Bruno Hagenbuch, Tiangang Li, Luciano DiTacchio, and Hao Zhu. I valued their comments and support throughout this process and appreciate all their assistance day in and day out. I am also grateful to many fellow students who made this fun and accepted an old-timer like me as one of their own.

To my children Steven, Brittany, Jarred, TJ, Faith, and Abigail, I want to thank you for your gift of understanding as I “went back to school” as your father. Because your mother and I needed to move to allow me to gain this training, you willingly gave up your right to be close (physically) to us and I promise to honor that sacrifice by making full use this accomplishment.

This dissertation is dedicated to my devoted and loving wife Michelle. Everything I have achieved, you have made possible. I could not possibly have attempted all of this without you. I am eternally grateful for all that you do, your unconditional love, and your kind and generous heart.

Table of Contents

List of Figures.

List of Abbreviations

Abbreviation	Full Name
ABC	ATP binding cassette
ADP	Adenosine diphosphate
ATP	Adenosine triphosphate
Ca^{2+}	Calcium ion
DNA	Deoxynucleic acid
ETC	Electron transport chain
FAD	Flavin adenine dinucleotide
FFA	Free fatty acid
GTP	Guanosine-5'-triphosphate
H&E	Hematoxylin and eosin staining
HDL	High-density lipoprotein
HFD	High fat diet
IMM	Inner mitochondrial membrane
mRNA	messenger ribonucleic acid
Na^{+}	Sodium ion
OMM	outer mitochondrial membrane
OXPHOS	oxidative phosphorylation
RNAi	RNA interference
ROS	Reactive oxygen species
RTPCR	Real-time polymerase chain reaction
TCA	Tricarboxylic acid
TG	Triglyceride
VCO^{2}	Volume carbon dioxide
VLDL	Very low-density lipoprotein
VO^{2}	Volume oxygen

Chapter 1. Background and Introduction

1.1 Mitochondria: Energetic Symbionts

It would be difficult to overstate the importance of mitochondria regarding eukaryotic physiology. Thought to have been first discovered in the 1840's, mitochondria were later described to be ubiquitous in all eukaryotic life and to be "elemental organisms" living inside cells carrying out vital functions by Richard Altmann and others (Ernster *et al.*, 1981). Following a series of discoveries that mitochondria could produce energy and had an independent genome (circular DNA), Lynn Margulis published her theory of endosymbiosis in 1967 which stated that mitochondria as we know them, probably came to be when an independent prokaryotic life form was endocytosed by a distant relative of current eukaryotes. The prokaryotic entity was permanently hosted by the eukaryote and the ensuing symbiotic relationship is thought to have made possible the existence of multi-celled organisms because of the increased ability to provide the bioenergetics necessary for differentiation, growth and development (Gray, 2017). Although energy production is the best-known attribute of mitochondria, there are a plurality of known alternate functions of these organelles and current investigation uncovers novel roles for mitochondria at a rapid pace. They are integral to nearly every physiological process and pathology. Hence, the fervent research of mitochondria and their impact on health and disease is not surprising.

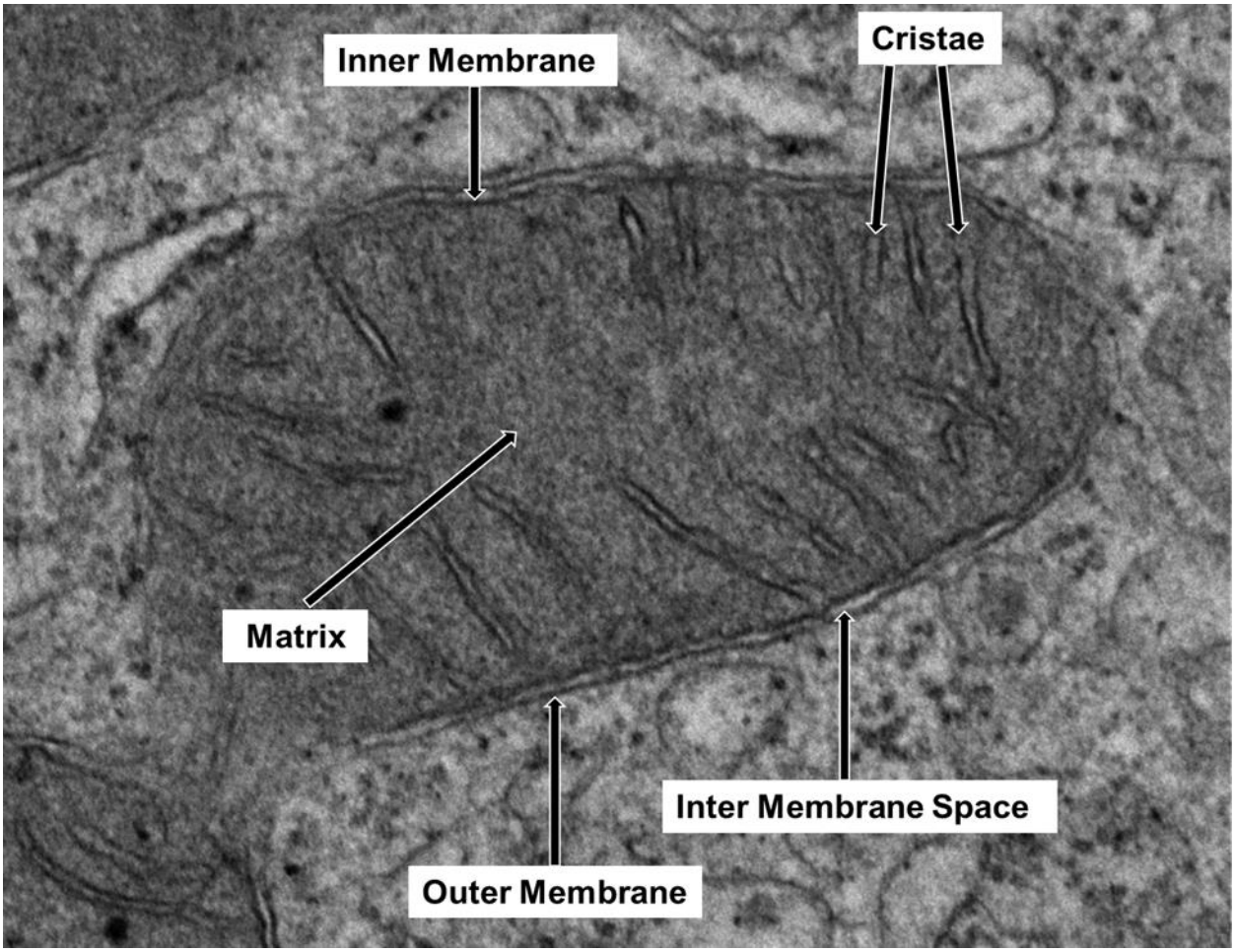

Figure 1.1 Basic mitochondrial structure

Physical Properties of Mitochondria

Figure 1.1 is an image from an electron microscope that relates the basic structure of mitochondria. Individual mitochondria measure from 0.5 to 10 microns and are enveloped by a double membrane. The outer mitochondrial membrane is relatively porous allowing for diffusion of small molecules. Protein channels called porins also allow for proteins less than 5000 Daltons to pass through the outer membrane. Proteins larger than this must be transported via active transport processes.

The area between the two membranes is called the intermembrane space. Within the intermembrane space, there are discrete contact points between the two membranes thought to be important in several aspects such as metabolite exchange, protein transport, and dynamic morphological changes (Reichert *et al.*, 2002) .

The inner mitochondrial membrane has many folds (cristae) that greatly increase surface area. The provided increased area is necessary for an abundance of proteins that perform key mitochondrial functions. Along with a high protein to lipid ratio, the inner membrane has a unique lipid composition with low triglyceride levels, a higher degree of fatty acid unsaturation, and cardiolipin, a phospholipid specific to mitochondria. The interdependent functions of lipid composition and IMM proteins are thought be crucial to mitochondrial function (Gohil *et al.*, 2009).

The area interior to the inner membrane and its folds is known as the mitochondrial matrix which contains the enzymes that contribute to the mitochondrion's bioenergetic production as well as nucleoids which contain double-stranded, circular mitochondrial DNA and mitochondrial protein translational machinery.

Although mitochondria were possibly once independent organisms, the evolution of increased interdependence between this organelle and the host cell is clear. Mitochondrial DNA and protein translational components provide just 1% of the known mitochondrial proteins with nuclear DNA and cytosolic transcription and translation providing the rest (Boengler *et al.*, 2011).

Mitochondrial Energy Production

Just as mitochondria rely upon the cell for their protein synthesis, cells rely upon mitochondria for energy production. Indeed, 90-95 % of adenosine triphosphate (ATP), the main source of cellular biochemical energy, is produced by mitochondria with the balance coming from glycolysis (Skulachev, 1999). These "powerhouses of the cell" can utilize different substrates (Figure 1.2) such as carbohydrates, lipids, and proteins to produce ATP.

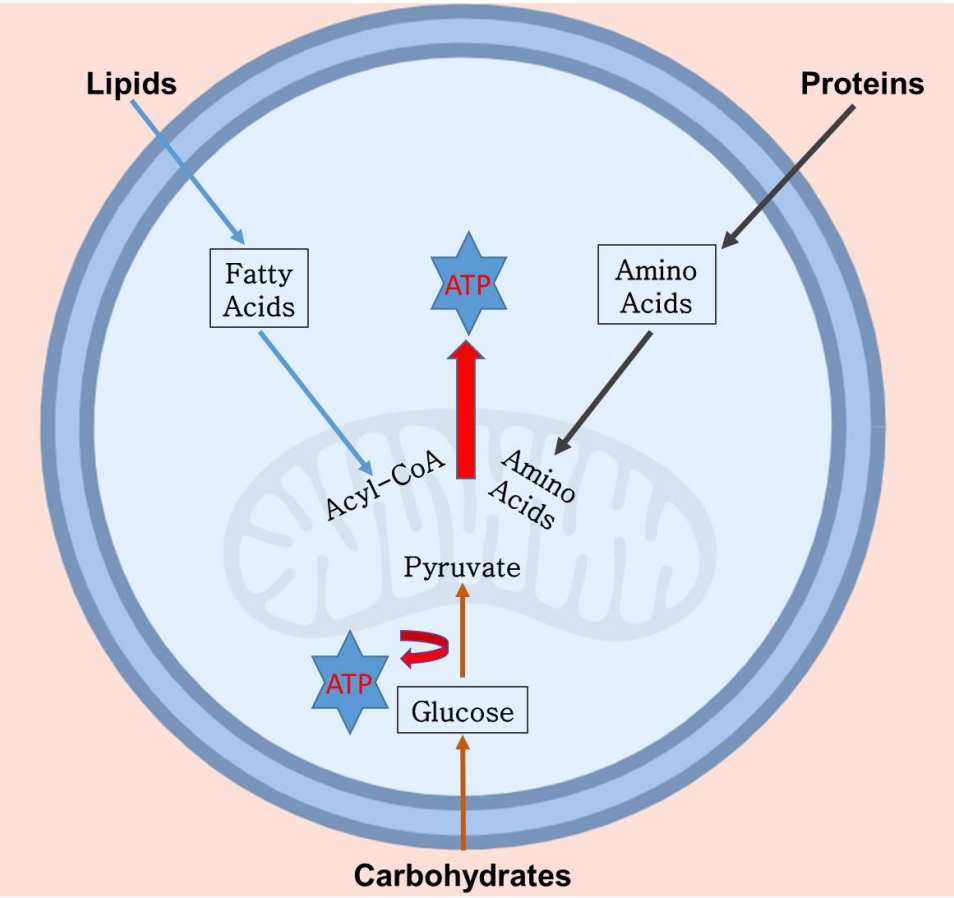

Figure 1.2 Mitochondria utilize multiple macromolecules to produce ATP.

Because there are relatively long periods between food intake for most mammals, the ability to utilize stored fat or protein reserves is a crucial physiological aspect. The coordination of the trafficking and utilization of nutrients between highly metabolic tissues and storage depots is highly dependent upon this “metabolic flexibility” provided by mitochondria.

The tricarboxylic acid (TCA) or “Krebs Cycle” and oxidative phosphorylation are the main components of non-glycolytic energy production. Oxidation of carbon sources by the TCA cycle occurs in the mitochondrial matrix and a myriad of transport, anaplerotic, and cataplerotic processes allow for metabolic flexibility, or the ability of an organism to use multiple substrates for energy production. Oxidation of these substrates by the TCA cycle results in the reduction of nicotinamide adenine dinucleotide (NAD) and flavin adenine dinucleotide (FAD) which act as “electron carriers” in the form of NADH and $FADH_2$. Acceptance of electrons from these carriers allows complexes in the electron transport chain to “pump” protons into the intermembrane space which results in the creation of an electrochemical gradient and membrane potential. This “proton motive” force is returned to the mitochondrial matrix through ATP synthase, a protein complex embedded in the inner membrane. The flow of protons produces mechanical energy through ATP synthase which allows the formation of ATP by combining ADP with inorganic phosphate. The ATP produced by this “oxidative phosphorylation” can then be shuttled out of the mitochondria for use in the rest of the cell in exchange for ADP via the ADP/ATP translocase protein. Acetyl CoA, a two-carbon molecule, is the common metabolite in carbohydrate, fatty acid, and amino acid metabolism. It is used in the TCA cycle to generate carbon dioxide, ATP or GTP, NADH, and $FADH_2$. During carbohydrate

oxidation, acetyl CoA can be derived from glycolysis in the cytosol. Glucose molecules are catabolized into two molecules of pyruvate which are then transported into the mitochondria and oxidized by pyruvate dehydrogenase to form acetyl-CoA. Acetyl-CoA is combined with oxaloacetate to form citrate. This six-carbon molecule undergoes various TCA cycle chemical reactions that result in the production of carbon dioxide, NADH, $FADH_2$, and ATP/GTP. Mitochondrial oxidation of fatty acids provides both acetyl CoA as an input to the TCA cycle and NADH used in the electron transport chain. Amino acids, derived from the catalysis of endogenous proteins or from the diet, after deamination, can also act as substrates for use in the TCA cycle.

There are many human pathologies related to defects in mitochondrial energy production including: Leigh Syndrome, mitochondrial encephalopathy lactic acidosis and stroke-like episodes (MELAS), deafness–dystonia syndrome (DDP), and Friedreich ataxia (Shoffner, 2001; Smeitink *et al.*, 2001).

Mitochondrial energetic functions are also required to maintain health. Metabolic flexibility represents the ability to utilize various energy substrates to match energetic demand which results in achieving energy balance. In the modern world, this adaptability has become particularly important. Due to easy access to calorie-rich foods and a concurrent decrease in typical daily physical exertion, metabolic diseases have become a pandemic. The disruption of energy balance (over-nutrition plus reduced energy expenditure) results in mitochondrial dysfunction which is central to the development of Metabolic Syndrome, a collection of conditions including increased visceral adiposity, hyperglycemia, high cholesterol, hypertriglyceridemia, hypertension, and insulin resistance (Mitchell *et al.*, 2012). Mitochondrial dysfunction is often

etiological in these pathologies. For example, disruption of mitochondrial ability to utilize fats as an energy source (incomplete fatty acid oxidation) results in the buildup of lipotoxic metabolites which are known to interfere with insulin signaling and increased inflammation (Sunny *et al.*, 2015). Disruption of insulin signaling is often an initial step in the progression toward non-alcoholic fatty liver disease (NAFLD) and increased fat storage.

Obesity and the ensuing metabolic disease pathologies are currently the greatest health concerns in most developed countries and represent a staggering financial burden. Targeting mitochondrial dysfunction that has resulted from over-nutrition is an obvious approach to abrogate metabolic syndrome-related disease. However, there are several roadblocks to this approach. Mitochondria function and regulation varies greatly in a tissue-specific manner and our knowledge of these differences is incomplete. Also, congenital mitochondrial mutations are not often homogeneous due to selective segregation during development and because of mitochondrial replication processes. Partial loss of function due to heteroplasmy confounds efforts to assign dysfunction to specific genetic alterations. Because of these factors, mitochondrial diseases are currently addressed through palliative efforts and cannot currently be cured (Nunnari *et al.*, 2012).

1.2 Alternative Functions of Mitochondria

Other than energy production, mitochondria also perform a multitude of crucial “alternative functions”. For example, in some tissues, proton motive force can be “uncoupled” from ATP synthesis by increasing the permeability of the inner

mitochondrial membrane through the action of uncoupling proteins. Protons can then bypass ATP synthase to enter the mitochondrial matrix which instead of providing chemical energy in the form of ATP, results in heat production. This process of thermogenesis allows maintenance of body temperature. Recent research indicates there may be potential therapeutic value in the pharmacological regulation of thermogenesis. Interventions that increase thermogenesis may allow for the treatment of obesity while treatment to pharmacologically reduce thermogenesis may treat fever or ischemic insult from stroke (Tupone *et al.*, 2014).

There are also numerous critical biosynthetic pathways that rely upon mitochondria. For instance, the majority of iron in the body is stored in heme-containing proteins (Ajioka *et al.*, 2006) and heme biosynthesis is a coordinated process between mitochondrial and cytosolic enzymes and transporters (Xu *et al.*, 2013). Additionally, the first and rate-limiting step in steroidogenesis is performed by the cholesterol side-chain cleavage enzyme (p450scc) which resides in the inner mitochondrial membrane (Miller, 2017). Another crucial function reliant upon mitochondria is amino acid metabolism. The TCA cycle produces oxaloacetate and 2-oxoglutarate which contribute to the production of the amino acids, aspartate/asparagine, glutamine/glutamate, arginine, and proline (Johnson *et al.*, 2014). Essential branched-chain amino acids such as leucine, isoleucine, and valine, are crucial for maintenance of muscle mass, neurotransmitter synthesis, maternal health and embryonic growth (Zhang *et al.*, 2017). The catabolic enzymes required for use of BCAAs are located within mitochondria (Hutson *et al.*, 2005).

Citrate, a metabolite of the TCA cycle, can be exported from mitochondria as a building block for the synthesis of fatty acids, a component of cellular membrane phospholipids. Indeed, phospholipid synthesis is a coordinated effort of both cytosolic and mitochondrial pathways as evidenced by the existence of mitochondrial and extramitochondrial redundant pathways for the production of phosphatidylcholine (PC), phosphatidylethanolamine (PE), and phosphatidylserine (PS) (Scharwey *et al.*, 2013). Because these glycerophospholipids are required for membrane formation, functional mitochondria are a fundamental requirement for cell growth and proliferation. Mitochondria also produce cardiolipin, a mitochondrial-specific phospholipid that is required for mitochondrial function.

Transient changes in cellular calcium levels trigger signals that result in a wide array of events from cell death to proliferation (Contreras *et al.*, 2010). During cytosolic calcium overload, mitochondria provide a protective uptake through the mitochondrial calcium uniporter. Mitochondrial calcium efflux can also be utilized to maintain homeostasis when cytosolic calcium concentrations normalize through mitochondrial Na^{+}/Ca^{2+} antiporters (Contreras, et al., 2010).

The urea cycle represents another protective function of mitochondria. Amino acid catabolism produces the toxic waste product ammonia which must be converted to urea for excretion. The first two steps of the five-step process take place in mitochondria. Several mitochondrial transporters are required for urea production (Morris, 2002).

1.3 Mitochondrial Dynamics and Cell Signaling

Mitochondria are crucial mediators of cellular signaling. They act as a communication and signaling hub because their structure and function are physiologically responsive to intracellular signals and by extension, extracellular signals. The molecular mechanisms for the transmission of extracellular signals to mitochondria are a current area of investigation. Signaling molecules are also sent from the mitochondria to the nucleus (retrograde signaling) to affect cellular responses. Mitochondria directly participate in signaling through interaction or trafficking of proteins, lipids, and ions on the outer mitochondrial membrane, by the production of metabolites, and through alterations in morphology and motility (Tait *et al.*, 2012).

It is important to consider that mitochondria are not static entities and that contributions of mitochondria to cellular function and signaling are dependent upon the dynamic control of intrinsic mitochondrial properties such as membrane potential, TCA flux and ETC activity which are themselves interrelated. In addition, mitochondria are motile and undergo morphological changes. Indeed, two neighboring individual mitochondria can either fuse (Figure 1.3) into one, or a single mitochondrion can “split” into two daughter mitochondria. These fusion/fission processes allow for the sharing and segregation of mitochondrial components as well as the fine-tuning of mitochondrial function. Mitochondrial also interact with other cellular organelles such as the endoplasmic reticulum and lysosomes to facilitate signaling and intra-cellular communication. Mitochondrial dynamics is a term used to comprehensively describe mitochondrial motility, intracellular localization and morphology. Mitochondrial dynamics

are inseparably linked to the major cellular signaling categories of cell death, reactive oxygen species (ROS), and ATP production in response to demand.

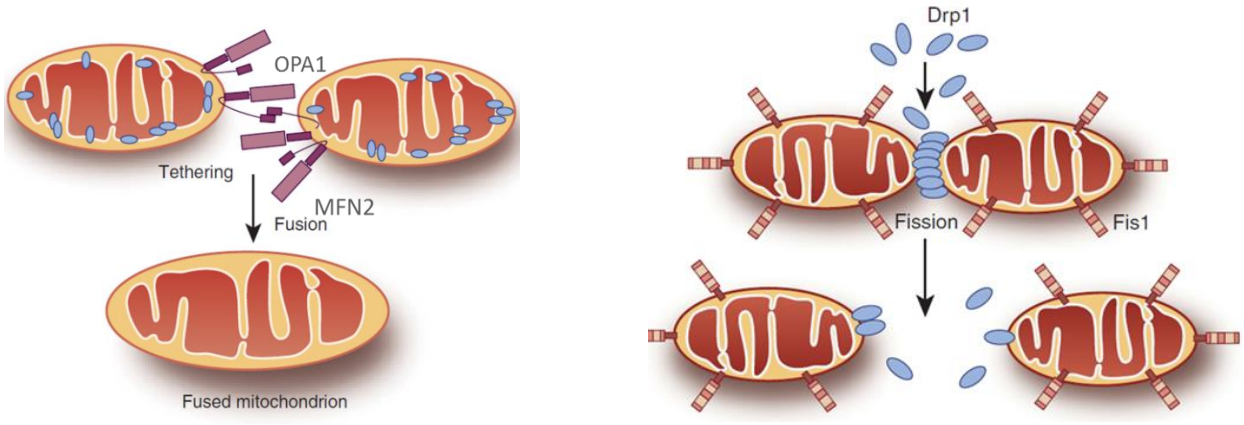

Figure 1.3 Mitochondrial fusion and fission. Reprinted with permission from Zhan M, et al. Mitochondrial dynamics and emerging role in renal pathophysiology. 2013. Kidney International. 83(4):586-581. https://doi.org/10.1038/ki.2012.441 (Zhan *et al.*, 2013)

Mitochondrial Motility

Mitochondria are tethered to the cytoskeleton which allows translocation in an energy consuming process. Intracellular localization of mitochondria is known to play important roles in cellular responses. For example, hypoxia has been shown to induce perinuclear clustering of mitochondria. This translocation allows proximity-driven ROS signaling that produces a nuclear transcriptional response to abate detrimental ROS-mediated effects (Al-Mehdi *et al.*, 2012). Spatial distribution of mitochondria in parotid acinar cells is thought to be integral to calcium mediated function within these highly polarized cells. Firstly, the intercellular distribution of mitochondria acts as a buffer to protect the basolateral portion of the cell from calcium waves produced due to

specialized cellular functions via mitochondrial calcium buffering. Secondly, mitochondria are positioned so that the calcium-driven ATP production is selectively utilized for exocytosis (Bruce *et al.*, 2004). Perhaps the most profound example of the need for mitochondrial motility is found in neurons. These cells, which can be up to a meter in length, require most mitochondria at the synapse to support neuronal firing. However, mitochondrial biogenesis takes place in the soma, at a great distance from the synapse. Mitochondria must translocate in order to provide ATP at the proximal location of neurons (Course *et al.*, 2016). Also, mitochondria are requisite for the production of neurotransmitters at synaptic gaps (Course, et al., 2016). Neurons themselves have a long lifespan and have high energetic demand. Consequently, older mitochondria within neurons must fuse with newer ones to maintain genome integrity and function as they traverse the distance of axons illustrating the necessity of both major facets of mitochondrial dynamics; translocation and fusion/fission. Additionally, there are large neurotransmitter-stimulated calcium influxes at neuronal synapses. The aforementioned calcium buffering function of mitochondria is protective against excitotoxity at these synaptic gaps further illustrating the vital role of mitochondrial mobility (Nunnari, et al., 2012).

Mitochondrial Fusion and Fission

Mitochondrial morphology is controlled by a balance between the processes of mitochondrial fusion, or the physical joining of separate mitochondria, and fission, the division of a single mitochondria to multiple mitochondria. A loss of fusion activity itself results in fragmented mitochondria and an increase of fusion results in elongated,

tubular morphology whereas a gain of fission results in more fragmentation and its loss results in a return to the elongated form. Mitochondrial motility and fusion/fission activities and the regulation thereof vary greatly depending upon cellular status or environment. The variability of these processes within different anatomical structures contributes to the pleiotropic phenotypes seen during the loss of mitochondrial dynamic functions (Nunnari, et al., 2012).

The process of mitochondrial fusion and fission are carried out by a group of dynamin-like GTPases. In mammals, the proteins involved in fusion are Mitofusin1 (MFN1), Mitofusin 2 (MFN2), and Optic atrophy type 1 (OPA1). Fusion is a two-step process (Meeusen *et al.*, 2004) in which outer membrane proteins MFN1 and MFN2 accomplish the fusion of the outer membrane. Inner membrane fusion is dependent upon OPA1.

Increased mitochondrial fusion is often seen in metabolically active cells and the process results in an extensive electrically connected network allowing for the distribution of membrane potential across cellular oxygen gradients thereby spatially distributing energy production. Fusion is often described as a protective response against cellular stressors such as energy deprivation and ROS. Mitochondrial fusion acts as a defense against ROS-mediated mitochondrial DNA damage by facilitating the “mixing” of gene products responsible for oxidative phosphorylation. In a process termed complementation, the combining of mitochondrial contents allows for well-functioning components in one mitochondrion to compensate for damaged components of another. It is also thought that defective components are segregated during fusion to

prepare for eventual removal which can be mediated via fission (Westermann, 2008) (Youle *et al.*, 2012).

The first step of mitochondrial membrane fusion is a remarkable process in which, protein complexes in distinct mitochondria are coordinately formed *in trans* allowing the fusion of four membranes (two outer and two inner) despite the repellant negative charges of individual mitochondria. Studies in yeast systems indicate that outer membrane fusion can be initiated by reversible ubiquitylation (Wiedemann *et al.*, 2013). However, knowledge of molecular mechanisms of initiation events in mammals is incomplete. Numerous cellular events are known to coincide with fusion such as energy deficiency, calcium efflux, and cellular division. For example, in some plants and kidney cells, all mitochondria fuse as a single interconnected entity to allow proper distribution of mitochondrial DNA prior to cytokinesis. This is in stark contrast to less drastic and transient fusion events in response to changes in energy demand. Considering the plurality of cellular events associated with mitochondrial fusion, it is likely that initiation arises from distinct mechanisms. The mechanistic details of the process of mitochondrial outer membrane fusion itself are also unclear but ablation of GTP binding/hydrolysis in fusion proteins completely abolishes membrane fusion (Wiedemann, et al., 2013). There are two mechanistic models of mitochondrial fusion considered to be likely. First, the nucleotide binding state of mitofusins may promote recruitment of other proteins required to complete the process or secondly, mitofusin GTP hydrolysis may provide the mechanochemical energy required to allow fusion through membrane conformational changes or close apposition (Wiedemann, et al., 2013). It is known that mitofusins can form both homo and heterodimers (MFN1/MFN1

MFN2/MFN2, MFN1/MFN2) and that coordination of trans mitofusins interaction is mediated by heptad repeats (HR1 and HR2) (Eura *et al.*, 2003). Interaction of trans HR domains between mitofusins are thought to tether mitochondrial pairs but not at a distance to allow spontaneous fusion. This tethered complex forms an intermediate complex after which, the GTPase activity of both mitofusins bring to completion outer membrane fusion (Koshiba *et al.*, 2004), (Meeusen, et al., 2004).

As mentioned above, inner membrane fusion is a distinct process, but it is unknown what causes the transition from outer to inner membrane fusion. However, it has been demonstrated that following trans mitofusin complex formation, the lipid bilayer contents from each prospective mitochondrion are mixed (Frohman, 2015). Mixing of membrane components may be a factor in the accomplishment of complete mitochondrial fusion.

The inner membrane dynamin-like GTPase OPA1 facilitates inner mitochondrial membrane fusion and is required for mitochondrial fusion in mammals (Song *et al.*, 2007). OPA1 knockout mice die in mid-gestation and mutations in OPA1 are known to be causative of the heritable human ocular disease, optic atrophy type 1. OPA1 has 8 isoforms due to alternate mRNA splicing and these various isoforms are subject to post-translational proteolytic processing resulting in long and short forms. Unprocessed OPA1 contains a mitochondrial targeting sequence and cleavage may be regulated based upon its import into the inner membrane (Wiedemann, et al., 2013). Drosophila models deficient in short-form OPA1 display drastically fragmented mitochondria demonstrating the long form alone is insufficient for fusion (McQuibban *et al.*, 2003). Also, disruptions in the ratio of long and short forms results in mitochondrial morphology alterations (Herlan *et al.*, 2004) indicating the need for both isoforms to maintain normal

fusion. Paradoxically, both OPA1 knockout and overexpression models display fragmented mitochondria. OPA1 has also been shown to be involved in the maintenance of cristae morphology as yeast systems deficient for OPA1 have disorganized, poorly invaginated cristae. It has been postulated therefore, that the disruption of fusion in both models may be secondary to OPA1 mediated cristae structure (Wiedemann, et al., 2013). Mechanistic details of inner membrane fusion are scarce but GTP availability and mitochondrial membrane potential are crucial aspects. Dissipation of mitochondrial membrane potential using ionophores or limiting GTP concentrations allows outer membrane fusion but blocks inner membrane fusion demonstrating both that outer membrane and inner membrane fusion are distinct steps and that GTP hydrolysis and maintenance of membrane potential are necessary for complete mitochondrial fusion (Mattenberger *et al.*, 2003), (Meeusen, et al., 2004).

Mitochondrial fission is mediated by dynamin-related protein 1 (DRP1). Disruption of DRP1 function results in elongated, tubular mitochondrial morphology (Youle, et al., 2012). DRP1 is localized mainly in the cytosol but a portion of the population is situated on the outer mitochondrial membrane and possibly acts as a marker of future fission events (Chan, 2006). The process occurs in four stages which are translocation of cytosolic DRP1 to the outer mitochondrial membrane, assembly of DRP1 oligomers, GTP hydrolysis, and disassembly (Hu *et al.*, 2017). Mitochondrial fission can be initiated by calcium efflux from the endoplasmic reticulum (ER) to the mitochondria or from CDK1 during mitosis. Also, increased ROS can initiate fission via PKC1 delta (Hu, et al., 2017). Several accessory proteins have been shown to play a role in the recruitment of DRP1 from the cytosol to the mitochondrial outer membrane including mitochondrial

fission factor (MFF), mitochondrial fission 1 protein (FIS1), and mitochondrial elongation factors 1 and 2 (MiD51 and MiD49).

Endoplasmic reticulum mitochondrial-associated membranes seem to act as markers as a guide for fission sites and DRP1 recruitment (Willems *et al.*, 2015). Exact mechanistic details of DRP1 recruitment are still under investigation and are model/species dependent. Once the recruitment stage is complete, DRP1 undergoes oligomerization. Conserved regions of individual DRP1 units fold back on each other to form a stalk. This complex induces a spiral effect that brings GTPase regions of DRP1 units into a position that favors hydrolysis and the mechanochemical force required for constriction is produced enabling the scission of outer and inner membranes (van der Bliek *et al.*, 2013).

Mitochondrial fission machinery is regulated by multiple post-translational modifications including SUMOlation, s-nitrosylation, ubiquitination, O-GlcNAcylation, and phosphorylation of DRP1. There are several phosphorylation sites that positively and negatively regulate DRP1 activity (Hu, et al., 2017). Accessory proteins such as MFF are also regulated via phosphorylation.

Because mitochondria cannot be formed de novo, mitochondrial fission is required for cell division. Fission allows for the increased population of mitochondria that newly formed cells require. Like fusion, fission is often the consequence of cellular stress but rather, occurs in late stages when the protective response of fusion has reached capacity. Fission allows for the clearance of defective mitochondria and recycling of materials through autophagy (Youle, et al., 2012).

Mitochondrial Dynamics and Cell Death

Mitochondria carry out well-characterized functions involved in regulating programed cell death in response to both extracellular (extrinsic) and intracellular (intrinsic) stimuli. Apoptosis is a critical factor for the formation of anatomical structures during development and for maintenance of cellular populations in tissues and organs throughout adulthood and during the aging process (Elmore, 2007). During programmed cell death, cellular components are degraded in a controlled manner with no adverse effects to surrounding cells. The extrinsic apoptotic pathway (receptor-mediated) is initiated via “death receptors” such as first apoptosis signal (FAS) and tumor necrosis factor (TNF) receptors that are activated by immune responses or trauma from without the cell. The intrinsic pathway also called “mitochondrial-mediated apoptosis”, is initiated via mitochondrial outer membrane permeabilization (MOMP) and release of pro-apoptotic factors such as cytochrome c, apoptosis inducing factor (AIF), and endonuclease G from the mitochondria. There is extensive crosstalk between extrinsic and intrinsic pathways with mitochondria playing crucial roles in both. Mitochondrial morphology is tightly linked to apoptosis (Figure 1.4). In general, fission is pro-apoptotic. During the early stage of apoptosis, cytosolic DRP1 is recruited to the OMM resulting in fragmentation and cytochrome C release. RNAi induced knockdown of DRP1 prevents cytochrome c release mitigating apoptosis (Youle, et al., 2012). Bcl-2-associated X protein (BAX), a well characterized mediator of apoptosis resides in the cytosol in non-apoptotic cells and like DRP1, is recruited to the OMM co-localizing with DRP1 and MFN2 which induces cytochrome c release. Again, knockdown of DRP1 prevents cytochrome c release despite BAX translocation (Youle, et al., 2012). However, fission

is not universally pro-apoptotic but rather is dependent upon the source of stimuli. In the case of an apoptotic calcium wave through a mitochondrial network, fragmentation can block the transmission of the calcium signal thereby blocking apoptosis (Perfettini *et al.*, 2005). Mitochondrial fusion is generally anti-apoptotic. Bcl-2 homologous antagonist/killer (BAK) and BAX have been shown to promote fusion in healthy cells via maintenance of MFN2 distribution on the OMM (Youle, et al., 2012). Knockdown of MFN1 and MFN2 promotes fragmentation and sensitivity to apoptotic stimuli while overexpression delayed BAX translocation and cytochrome c release (Suen *et al.*, 2008). Further, the bulk of cytochrome c resides in cristae junctions and its release is dependent upon OPA1 cristae remodeling activity. Like the mitofusins, efficient knockdown of OPA1 can induce apoptosis (Suen, et al., 2008) illustrating the anti-apoptotic roles of mitochondrial fusion mediators.

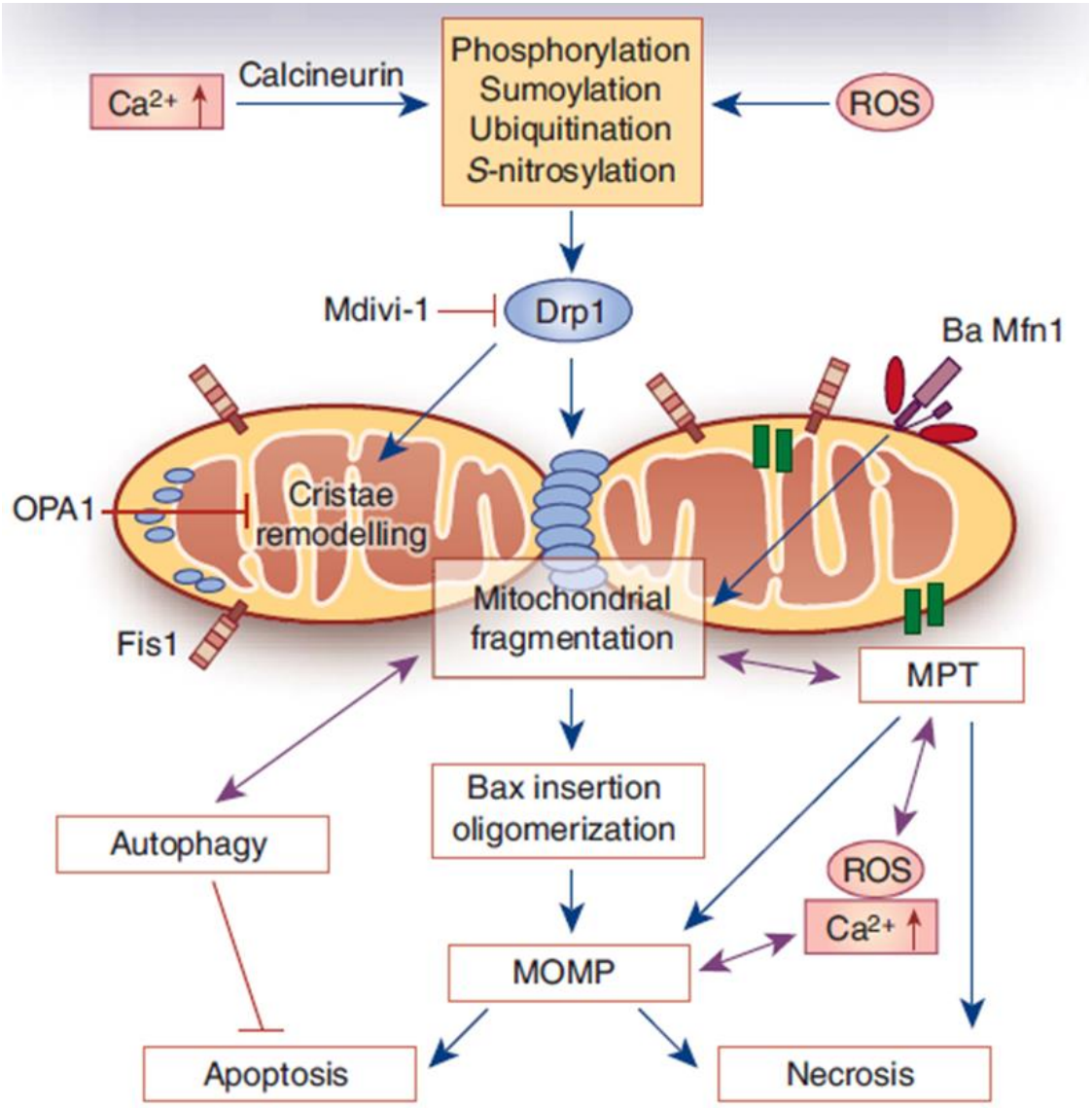

Figure 1.4 Mitochondrial dynamics and cell death are inter-related processes. Reprinted with permission from Zhan M, et al. Mitochondrial dynamics and emerging role in renal pathophysiology. 2013. Kidney International. 83(4):586-581. https://doi.org/10.1038/ki.2012.441 (Zhan, et al., 2013)

Mitochondrial Dynamics and Reactive Oxygen Species

As a consequence of respiration, mitochondria are the main cellular source of reactive oxygen species (ROS). The main sites of mitochondrial ROS production are Complexes I & III in the electron transport chain (ETC). During the process of electron transfer, some electrons “leak” rather than being transferred from complex I and complex II to complex III resulting in a single electron reduction of molecular oxygen thus forming the superoxide anion. Superoxide cannot readily pass through membranes and is quickly converted to hydrogen peroxide by mitochondrial dismutase. Hydrogen peroxide is freely diffusible and is converted to water by peroxidases and peroxidoxins within mitochondria and by catalase in the cytosol and peroxisomes. In the presence of metals, superoxide and hydrogen peroxide can be converted to the highly reactive hydroxyl radical. Free radical species such as these can cause cellular damage including membrane disruption by lipid peroxidation, DNA damage via hydrogen abstraction, and oxidation-mediated disruption of protein function.

Eukaryotes have developed endogenous anti-oxidant defenses such as the “non-critical” nucleophile glutathione. In addition to the enzymatic conversion (via peroxidases) of free radicals to water, glutathione acts as an antioxidant by donating its electrons to free radicals. The oxidized form (GSSG) is then recycled to the reduced form (GSH) by glutathione reductase. Despite the potential damage caused by these reactive species, healthy cells maintain a constant low level of ROS. Indeed, some reactive oxygen species are valuable signaling molecules that are necessary for proper development and cellular function (Di Meo *et al.*, 2016). A physiological level of ROS promotes cellular production of antioxidant molecules necessary for defense against

environmental sources of ROS such as ionizing radiation and xenobiotics (Yamashita *et al.*, 1997). Further, ROS levels dictate cellular proliferation/death balance and innate immune responses (Zuo *et al.*, 2015).

There is sufficient evidence to demonstrate that mitochondrial form and function mediate ROS dependent cellular responses. Indeed, ROS levels regulate mitochondrial fusion and fission and reciprocally, mitochondrial morphology can modulate ROS levels. Mitochondria within cells exposed to exogenous hydrogen peroxide have increased fragmentation while subsequent exogenous antioxidant treatment results in increased fusion (Willems, et al., 2015) demonstrating that fission fusion balance is affected by ROS levels. The interrelation of mitochondrial dynamics, function, and ROS is illustrated by studies that show greatly reduced complex I activity results in mitochondrial fragmentation and increased ROS (Willems, et al., 2015). Other studies demonstrate DRP1-dependent fragmentation due to increased nitric oxide levels which is attenuated by nitric oxide scavengers (Willems, et al., 2015). In yeast, peroxidation of the mitochondrial-specific phospholipid cardiolipin, results in the functional disruption of the fusion protein OPA1. In this case and in the cases of hydrogen peroxide exposure and reduced complex I activity, loss of membrane potential is a common theme. Mitochondria with low membrane potential are often targeted for degradation through mitophagy. Decreased membrane potential increases E3 ubiquitin ligase Parkin activity which in turn regulates the degradation of DRP1 and MFN2 illustrating the connection between ROS levels, mitochondrial function, and mitophagy. Fragmentation facilitates the removal of defective mitochondria through mitophagy. Conversely, mitochondria that have undergone fusion may avoid degradation because their increased size

prevents entry into the autophagosome (Nunnari, et al., 2012). ROS-induced s-nitrosylation influences Parkin, a E3 ubiquitin ligase that regulates DRP1 and MFN2 degradation which ultimately controls mitochondrial morphology. Additionally, several fusion/fission proteins undergo ROS-mediated posttranslational modifications (PTMs) that regulate their function illustrating an interdependent relationship between cellular redox status, mitochondrial dynamics and mitochondrial quality control.

Mitochondrial Dynamics and Energy Balance

Mitochondria are highly responsive to cellular energetic demands. Reciprocally, mitochondrial ATP production dictates overall cellular function. Bioenergetic balance is coordinated by regulation of cellular activity and energy production in response to nutrient availability (Benard *et al.*, 2010). Nutrient availability is sensed by mammalian target of rapamycin kinases that broadly influence metabolic state (anabolism/catabolism). Energy status is determined by the adenosine monophosphate (AMP) to adenosine triphosphate ratio (ATP) and NAD^+/NADH levels which are sensed by amp-activated protein kinase (AMPK) and sirtuins respectively. These energy sensors regulate energy production via mitochondrial biogenesis regulation, influencing catabolic/anabolic state, and through the regulation of energy substrate usage (metabolic flexibility).

Metabolic control analysis (MCA) is the study of cellular energy flux. It involves investigating the expression and activity of enzymes involved in transport and oxidation of energy substrates and the subsequent production of ATP. Performance of MCA is highly complex due to the diversity of the energetic needs of various organs and

tissues. For example, the regulation of mitochondrial bioenergetics in cardiac and skeletal muscle are dictated mainly by ETC activity while in the brain, liver and kidney, the main determinant is ATP production (Benard, et al., 2010). Indeed, not only are there vast differences in total mitochondrial content and protein expression levels between tissues but proteomics reveals that subsets of mitochondrial proteins are unique to various organ systems illustrating the complexity of mitochondrial biology.

In addition to the regulation of metabolic control via the cytosolic nutrient and energy sensors, mitochondrial fusion and fission rapidly fine tunes energy balance in response to energetic status and demand. Increasing evidence suggests that there is an interdependent relationship between cellular energetic status and mitochondrial dynamics that maintains overall energy homeostasis.

Mechanisms that link nutritional state, mitochondrial dynamics, and mitochondrial energy production are active areas of investigation but clearly, mitochondrial morphology is influenced by nutritional state. Diet induced obesity rat models result in decreased mitochondrial fusion in skeletal muscle parallel to decreased MFN2 (Bach *et al.*, 2005). Additionally, genetic and diet induced obesity models result in increased fission protein expression and increased fragmentation (Putti *et al.*, 2015). However, fusion and fission responses to increased energy substrates are dependent upon the type of energy substrate concerned. Mice fed lard-based diet exhibit increased mitochondrial fragmentation in parallel with decreased MFN2 expression. Conversely, diets supplemented with polyunsaturated fats had increases in mitochondrial fusion which was negated with siRNA knockdown of MFN2 indicating that fusion/fission machinery is responsive and highly selective to nutritional inputs (Zhang *et al.*, 2011).

Nutrient deprivation also results in selective mitochondrial morphology responses. In one cell-based model, glucose or serum starvation results in increased fragmentation while nitrogen-based nutrient deprivation results in increased fusion. Mixed nutrient deprivation results in increased fusion. Caloric restriction however, results in increases in DRP1 and FIS1 with no change in fusion proteins (Khraiwesh *et al.*, 2013). One could infer from these data that dynamic responses are dependent upon the type of nutrient deficiency and the length of starvation period (Putti, et al., 2015).

In the above listed studies, the general finding is that mitochondrial fragmentation is accompanied by reduced mitochondrial function and increased ROS production whereas increased fusion results in increased oxidative phosphorylation efficiency. It is postulated that mitochondrial fragmentation could occur as a protective mechanism in the context of high nutrient status by increasing total surface area to facilitate oxidation of the surplus substrate supply. An exception is seen in the case of prolonged caloric restriction. Increased fragmentation in this case was thought to support mitochondrial biogenesis to increase ATP production in this context. This view is supported by an increased mitochondrial number per cell with decreased ROS production and no decrease in ATP production. This agrees with studies that show caloric restriction increases longevity because of reduced ROS production. There are limited studies supporting the idea that increased mitochondrial fusion directly causes increased mitochondrial function and efficiency (Mitra *et al.*, 2009), (Tondera *et al.*, 2009) and mechanistic details are scarce in this regard. However, some studies suggest that mitochondrial remodeling proteins enable the formation of “super complexes” of individual ETC members that are in complex to afford a synergistic efficiency (Genova

et al., 2014). Other studies demonstrate that fusion allows a complementation of mitochondrial DNA, a situation in which two separate mitochondria, each with a different set of genetic mutations compensate for gene defects by the “sharing” of their respective genomes. This principle was illustrated when two cell lines, one with a normal genome, and one with mitochondrial DNA mutations that caused respiratory defects were hybridized. After a few days, respiratory capacity was restored in the loss of function mutation group, ostensibly due to the transmission of functional genes from the healthy group to the other (Ono *et al.*, 2001). Mouse fibroblasts deficient for MFN1 and MFN2 can maintain mitochondrial DNA content but rapidly lose membrane potential. However, cells with fragmented mitochondria that still possess some fusion activity maintain their respiratory capacity (Westermann, 2012) indicating that mitochondrial DNA complementation rather than morphology supports the increase in function.

Mitochondrial fission positively influences mitochondrial function through selective degradation of dysfunctional mitochondria. After a fission event, daughter mitochondria with low membrane potential have lower fusion protein expression making it unlikely that they will undergo fusion in the future and will be targeted for mitophagy thereby maintaining a healthy mitochondrial population. This contrasts with pathogenic fragmentation seen in response to chronic overfeeding or genetic disruptions in which diminished ATP production and increased ROS is seen (Jheng *et al.*, 2012).

The above examples illustrate the interdependent relationships that exist between mitochondrial dynamics, nutritional state, energy demand, and energy production. However, there is a considerable gap of knowledge with respect to control mechanisms.

Individual mitochondria acquire genome diversity (heteroplasmy) in different cell populations and indeed, even within the same cell, evidence suggests there are subpopulations of mitochondria making these groups functionally unique (Benador *et al.*, 2018). Also, due to the disparate, yet connected functionality of different organs in the maintenance of whole-body energy balance, the regulation of mitochondrial dynamics is necessarily context dependent. Methods previously and currently used to study mitochondrial function include the utilization of immortal or primary cells and mitochondrial isolation ex vivo. These methodologies are artefactual and extremely limited in giving a clear picture of how mitochondrial dynamics influences energy homeostasis under normal physiology in vivo and much less, under pathogenic conditions. New technologies such as nuclear magnetic resonance (NMR) analysis of mitochondrial transport chain activity in situ, will advance the field of study of this crucial aspect of cellular biology.

1.4 Mitochondrial Transporters

Just as mitochondria themselves are not static entities, dynamic control of the transport of substrates, waste products, lipids, and proteins to and from mitochondria are a requisite for life. As mentioned previously, mitochondria are enveloped in a double membrane. The outer membrane is comprised mainly of lipids and permeable to molecules of 10 kilodaltons or less but the inner membrane is highly organized, proteinaceous and impermeable to diffusion except for very small molecules such as oxygen and water. ATP produced within mitochondria is needed throughout the cell and is derived from ADP. Thus, ATP/ADP exchange is a crucial transport function within the

cell. Further, most enzymes required for mitochondrial function are synthesized in the cytosol. Therefore, the most obvious needs for mitochondrial transport are an exchange of ADP/ATP, bidirectional trafficking of TCA cycle substrates, and import of nuclear encoded mitochondrial proteins, all of which require active transport processes.

ATP-Binding Cassette Transporters (ABC transporters) belong to one of the largest super families of proteins and are highly conserved throughout evolution (Davidson *et al.*, 2008). As active transporters, they couple the binding and hydrolysis of ATP to the active transport of various substrates across lipid membranes or from one double-membrane leaflet to another (Quazi *et al.*, 2012). ABC transporters consist of two hydrophilic nucleotide binding domains (NBDs) and at least two hydrophobic transmembrane domains (TMDs). The nucleotide binding region is highly conserved and serves as a common transport mechanism among the superfamily of proteins (Locher, 2009). The NBD consists of Walker A and B sequence motifs that allow the binding and hydrolysis of ATP and a signature, “C” region located upstream of the Walker B site that contains the consensus sequence (LSGGQ) which distinguishes ABC transporters from other ATP binding proteins (Kay *et al.*, 2012). The NBDs are located on the cytosolic face and typically pump compounds out of the cell or into organelles such as the endoplasmic reticulum, mitochondria, peroxisomes, and lysosomes (Procko *et al.*, 2009). The transmembrane domains typically consist of six membrane spanning segments and serve as substrate binding sites and are less conserved allowing for transport of a diverse array of substrates within the ABC family members (Kaminski *et al.*, 2006). Eukaryotic ABC transporters are divided into seven subfamilies (A through G) according to sequence similarity and phylogenic analysis (Vasiliou *et al.*, 2009). ABC transporters

are further divided into full or half transporter categories. Full transporters contain two NBDs and two TMDs within a single polypeptide chain and are a complete, fully functional unit. Half-transporters contain only one NBD and one TMD and must homo or heterodimerize to form a fully functional transporter. Figure 1.5 is a graphic depiction of the basic organization and structure of ABC transporters.

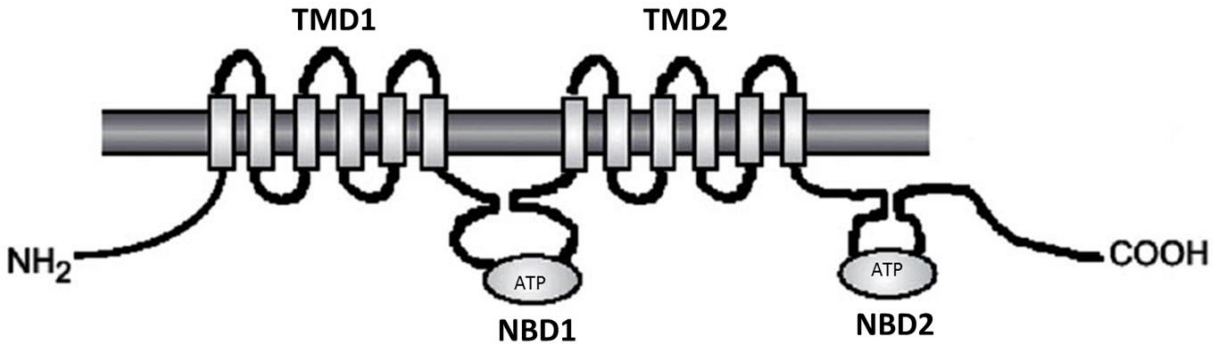

Figure 1.5 Basic structure of an ABC transporter. (TMD)-transmembrane domain. (NBD)-Nucleotide binding domain.

There are four known mitochondrial ABC transporters all belonging to the “B” subfamily. ABCB7, ABCB8, and ABCB10 are localized to the inner membrane and have proposed functions including iron-sulfur cluster and heme biosynthesis. ABCB6 is the only ABC transporter known to be localized to the outer mitochondrial membrane. Due to the highly hydrophobic nature of ABC transporter TMDs, they would be predicted to be directed co-translationally to the ER membrane. However, it has been demonstrated that a long, positively charged N-terminal leader sequence re-routes the mitochondrial

ABC transporters to the mitochondria (Zhang, et al., 2011). The exception to this proposed mechanism is ABCB6 which has no defined mitochondrial targeting sequence and has been found in the secretory locations of the ER, Golgi, and plasma membrane (Tsuchida *et al.*, 2008). How ABCB6 is targeted to mitochondria is an active area of investigation.

ABCB6 is a member of the “B” subfamily which is further divided by homology into the multidrug resistance (MDR) and the transporter associated with antigen processing (TAP) classes. The ABC B subfamily is unique in that the entire set of transporters within the class are present in all mammals (Locher, 2009). Another distinguishing characteristic of this subfamily is that it includes both full and half transporters. The conservation of ABC B subfamily members in humans and mice demonstrate that murine model is useful for understanding ABCB6 functionality in humans. ABCB6 was initially cloned while screening for novel drug resistance-related genes in the liver using a partial ABCB1 or P-glycoprotein sequence as a probe. Subsequently, the full-length protein was independently cloned and named UMAT (ubiquitously expressed mammalian ABC half-transporter) or MTABC3 (mammalian mitochondrial ABC protein 3 (Hirsch-Ernst *et al.*, 1998; Mitsuhashi *et al.*, 2000). These terms are synonymous with ABCB6 as it is referred to in the currently accepted nomenclature. ABCB6 is a transmembrane protein with the full transporter having two TMDs and two NBDs. The NBD shows similar homology to other ABC transporters and faces the cytosol (Kurashima-Ito *et al.*, 2006). ABCB6 is nearly universally expressed with high protein expression seen in liver, gallbladder, stomach, duodenum, kidney, bladder, testis, epididymis, thyroid, and bronchus (Uhlen *et al.*, 2015).

Non-functional or null mutations in *Abcb6* have been shown to be involved in several human diseases and pathologies. ABCB6 is known to be localized in the plasma membrane (PM) of red blood cells and thought to be involved in the export of porphyrins. Studies have identified ABCB6 as the genetic basis of the Langereis blood type. Patients with *Abcb6* null alleles are at for risk hemorrhagic complications during transfusions (Helias *et al.*, 2012). In another blood-related pathology, *Abcb6* mutations are responsible for Familial Pseudo Hyperkalemia, a condition that results in increased potassium in whole blood or serum (Andolfo *et al.*, 2013). Dyschromatosis universalis hereditaria presents as areas of hyper or hypo skin pigmentation. Ocular coloboma is an inherited developmental disease that results in incomplete closure of the optic fissure. Loss of function of ABCB6 is causative for both conditions (Wang *et al.*, 2012), (Zhang *et al.*, 2013). Studies in mice indicate that ABCB6 plays a role in the development in atherosclerosis (Murphy *et al.*, 2014). The variation in the severity of these disease phenotypes associated with ABCB6 suggest incomplete penetrance. Moreover, the pleiotropic nature of these conditions supports multiple and/or tissue-dependent physiological roles.

ABCB6 is highly conserved and unique in its mitochondrial outer membrane localization. Because of this, considerable efforts have been taken to ascertain its physiological function. Initially, because of its sequence similarity (46%) to the yeast mitochondrial iron transporter ATM1p, it was thought that ABCB6 may be an ATM1p ortholog and would play a role in iron homeostasis. However, it was discovered that ABCB7 was actually the functional ortholog of ATM 1p (Pondarre *et al.*, 2007). Abc6 is highly expressed in the gut of Caenorhabditis elegans and is required for iron uptake

from diet again suggesting a role in iron/heme-related processes (Krishnamurthy *et al.*, 2011). Additional in vitro and ex vivo studies demonstrated that ABCB6 binds heme-related molecules (porphyrins) suggesting a role in heme biosynthesis (Krishnamurthy *et al.*, 2006). However, cohort studies using Lan - samples identified no impairment of erythropoiesis (a heme-dependent process) and only slight increase in porphyrin in subject red blood cells with no incidents of anemia (Helias, et al., 2012). This study refutes the presumed role of the plasma membrane form of ABCB6 in porphyrin export and suggests another plasma membrane transporter may compensate for the loss of ABCB6. Whole-body and liver specific *Abcb6* mouse knockout models show no significant decrease in heme or upregulation of other heme biosynthesis pathway genes (Chavan *et al.*, 2015) suggesting the absence of need for outer membrane heme active transport or an additional, yet unidentified transport process.

A significant challenge in determining the physiological roles of ABC transporters is their promiscuity. Although they are perhaps best known for promotion of drug resistance in humans through cellular efflux of hydrophilic pharmaceuticals, the discovery that ABCB4 was responsible for the secretion of PC into bile (Borst *et al.*, 2000), lead to the idea that ABC transporters can and do transport hydrophobic substrates including lipids. This concept has been confirmed in several instances. Streptococcus produce the toxin doxorubicin, a hydrophobic entity that can enter cells through simple diffusion. Intuitively, bacteria that produce these toxins would require efflux transporters to protect themselves from the poisons they produce. Indeed, that is the case as the streptococcus that produces doxorubicin also encodes an ABC transporter that transports it out of the cell (Borst, et al., 2000). Nearly half of the 48

human ABC transporters transport lipids or lipid-related compounds like cholesterol and bile acids in addition to hydrophilic substrates (Schou *et al.*, 2012). Examples include ABCD4 which transports long-chain fatty acids into peroxisomes, and ABCB4 which transports phosphatidylcholine via floppase activity. (Neumann *et al.*, 2017).

Interestingly, ABC transporter conformation and activity are affected by their cellular environment which they help to maintain (Neumann, et al., 2017). It has been demonstrated that this interrelationship has physiological consequences regarding energy metabolism. ABCB11, a bile acid transporter influences glucose and lipid homeostasis through the signaling actions of bile acids (Ma *et al.*, 2014). Genetic alterations in ABCA1 result in high-density lipoprotein (HDL) deficiency (Tangier disease) which disrupts reverse cholesterol transport. Abcg1 is expressed in macrophages, adipose tissue, and pancreatic beta cells and is responsible for the regulation of insulin secretion, cholesterol homeostasis, and adiposity in a context-dependent manner (Schou, et al., 2012), (Frisdal *et al.*, 2015).

Our current studies focus on the role of the ABC transporter ABCB6 in the maintenance of energy homeostasis. We discovered that genetic manipulation of *Abcb6* expression in mice resulted in observable phenotypes including, lower than predicted Mendelian KO progeny and altered growth pattern. Liver microarray data from these studies supported these phenotypes as they showed disturbances in organismal survival, lipid metabolism, metabolic disease, and carbohydrate metabolism (Table 1) (Chavan, et al., 2015). These initial observations prompted the current study which explores the influence of ABCB6 protein expression on energy metabolism.

Table 1.1 Microarray IPA analysis of *Abcb6* knock out mouse liver

Category	Functions Annotation	p-Value	z-Score	# Genes
Activated Functions				
Organismal Survival	organismal death	1.57E $^{-02}$	3.924	92
	perinatal death	9.99E $^{-04}$	3.831	35
	neonatal death	5.23E $^{-03}$	3.113	25
Lipid Metabolism	concentration of lipid	7.47E $^{-03}$	2.11	32
	concentration of cholesterol	1.45E $^{-02}$	2.774	13
	concentration of phospholipid	4.80E $^{-02}$	2.213	7
Metabolic Disease	adiposity	1.45E $^{-02}$	2.213	8
Inhibited Functions				
Carbohydrate Metabolism	synthesis of carbohydrate	6.58E $^{-04}$	-2.18	13

Chapter 2. Statement of Purpose

2.1 Study Objective

The world's current population is the most obese in history according to the National Health and Nutrition Examination Survey. Except for a relatively small percentage of congenital etiologies, the increase in obesity is due to lifestyle choices. Nonetheless, interventions of diet and exercise mostly fail due to lack of sustained compliance which necessitates alternative treatment options. Obesity in and of itself is not necessarily pathological. However, there is voluminous clinical evidence that incidents of various pathologies are closely associated with increased body fat including diabetes mellitus, insulin resistance, and the metabolic syndrome.(Bray, 2004).

Progression toward obesity begins with positive energy balance. Imbalances in the type of dietary calories are also implicated in increased adiposity. Mitochondria are the first defense against obesity as they are key to metabolic flexibility. Chronic positive energy balance dysregulates mitochondrial adaptive responses and eventually causes mitochondrial dysfunction. Parallel to this process, capacity to store a surfeit of energy is overwhelmed leading to dyslipidemia and increased postprandial blood glucose. This leads to systemic stress and further mitochondrial dysfunction in a feed-forward manner. Non-alcoholic fatty liver, type II diabetes, hypercholesterolemia, and hypertension are manifestations of this maladaptive process and could ultimately be described as a failure of metabolic flexibility.

It is known that dynamic regulation of mitochondrial form and function in response to changes in nutritional status is required for metabolic flexibility but there are no pharmacological therapies that target this axis. Additionally, current

understanding of how mitochondrial transport systems affect mitochondrial dynamics is extremely limited. In this study, we show that the alteration of expression of a single mitochondrial transporter, ABCB6 disrupts mitochondrial dynamics leading to metabolic syndrome.

Previous studies demonstrated that loss of ABCB6 resulted in alterations of hepatic function and metabolism. Overall observable phenotypes were pleiotropic but among them was a disturbance in growth and body weight. Further, it was discovered that ABCB6 expression was regulated by nutrient status. Despite past and ongoing efforts, ABCB6 transport and other possible physiological functions remain unknown. The current study explores ABCB6 regulation and the impact of ABCB6 expression on energy metabolism.

Specific Aim 1 tests the hypothesis that the loss of ABCB6 *in vivo* results in disrupted metabolic homeostasis. We utilized a whole-body *Abcb6* knock out mouse to study the metabolic effects of ABCB6 loss. Specifically, we tracked body weight and food consumption from post-weaning to adulthood, analyzed lipid and glucose metabolic pathways, and determined the impact of these pathway disturbances on substrate utilization and energy expenditure.

Specific Aim 2 tests the hypothesis that ABCB6 expression is driven by nutrient availability and ensuing changes of ABCB6 expression controls mitochondrial form and function in response to energetic state. To determine that alterations in mitochondrial dynamics were directly attributable to ABCB6 expressional changes,

we utilized a genetic model that allowed for temporal, tissue-specific control of ABCB6 expression. Under these conditions, we monitored mitochondrial form and function as well as hepatic metabolic functions and the impact of these changes on whole-body homeostasis.

Specific Aim 3 tests the hypothesis that alteration of ABCB6 expression modifies the hepatic metabolome. We used hepatocyte-specific *Abcb6* deficient and over expressing mice to study the resulting changes in liver metabolites in both high-nutrient and low-nutrient states to discover novel ABCB6 transport substrates.

2.2 Study Significance

We have established a model that consistently and predictably alters mitochondrial form and function. Therefore, it is possible to ascertain the impact of the disruption of mitochondrial dynamics throughout the entire lifespan, including development, in a whole-body or tissue-dependent manner. Additionally, these studies allowed progress toward understanding the possible *in vivo* role of ABCB6. More importantly, the outcome of this and future studies could direct therapies for a myriad of congenital metabolic pathologies as well as interventions for metabolic syndrome due to chronic over-nutrition. This model promises to further elucidate the interconnected feedback signals between energy supply and the physiological responses required for homeostasis.

2.3 Innovation

Our current study is the only one, to our knowledge that studies the impact of mitochondrial ABC transporter, ABCB6 on energy metabolism. Also, ours is the only model that allows for inducible, tissue-specific, alteration of ABCB6 *in vivo.*

We demonstrate that altered expression of a mitochondrial ABC transporter affects mitochondrial form and function. More specifically, *Abcb6* deficiency or overexpression impairs nutrient-mediated fusion and fission responses in mice. This study highlights the connection between mitochondrial transporters, energy sensing processes, and mitochondrial dynamic bioenergetics which introduces a novel approach to understanding the regulation of metabolic flexibility.

The liver-specific studies described in this dissertation illustrate how disruption of hepatic mitochondrial form and function has a dramatic effect on overall energy utilization and balance. There are limited models describing how impaired mitochondrial dynamics within a single tissue affect whole-body homeostasis. Analysis of non-hepatic tissues in our liver-specific model will further elucidate organ-organ crosstalk in various energy states thereby expanding our knowledge of whole-body energy physiology.

Currently, our knowledge of the regulation of ABCB6 expression is extremely limited. We introduce a novel mechanism in the regulation of ABCB6.

Chapter 3. Characterization of *Abcb6* Null Mice

3.1 Abstract

ABCB6 is a member of the ATP binding cassette superfamily of transport proteins that has been shown to play a role in heme biosynthesis. Here, we assess the effect of disrupting mouse ABCB6 *in vivo* and report on its unanticipated role in metabolic regulation and body-weight homeostasis. *Abcb6* deficient mice show early signs of mature onset obesity, which is more severe in males than in females. *Abcb6*-deficient mice show accumulation of abdominal fat, hepatic steatosis, and high fasting plasma levels of insulin leading to glucose intolerance and insulin resistance. Gene expression analyses of liver and visceral white fat from *Abcb6*-deficient mice show deregulation of metabolic programs, including fatty acid, glucose metabolism and lipid signaling. Indirect calorimetry analysis of *Abcb6* deficient mice before the onset of obesity show disturbances in energy expenditure and physical activity. We identify disturbances in mitochondrial form and function as key factors affected by *Abcb6* deletion in the liver. These findings reveal a role for a mitochondrial ATP binding cassette protein in the regulation of metabolism.

3.2 Introduction

The ATP binding cassette (ABC) superfamily of active transporters is composed of many functionally diverse proteins (Dean *et al.*, 2001a; Dean *et al.*, 2001b). These proteins are fundamental to membrane transport of a broad variety of substrates including amino acids, lipids, lipopolysaccharides, inorganic ions, peptides, sugars, metals, drugs and proteins (Dean, 2009; Dean, et al., 2001a; Schmitz *et al.*, 2000). These proteins utilize energy derived from the hydrolysis of ATP to `pump' substrate across the membrane against a concentration gradient. The ABC transporters not only move a variety of substrates into and out of the cell but are also involved in intracellular compartmental transport (Dean, et al., 2001a; Dean, et al., 2001b) and are often vital to the health and survival of the organism.

The ATP binding cassette transporter subfamily member B6 (*ABCB6*) gene encodes a membrane protein of 842 amino acids with a transmembrane domain (TMD) followed by a nucleotide binding domain (NBD) (Chavan *et al.*, 2013; Krishnamurthy, et al., 2006). Hydrophobicity and sequence homology analysis suggests that the TMD contains six transmembrane helices with the N and C termini located in the cytoplasm. The minimal functional unit has been suggested to be a homodimer residing in the outer mitochondrial membrane (Chavan, et al., 2013; Krishnamurthy, et al., 2006). ABCB6 has been characterized as a mitochondrial transporter involved in the translocation of coproporphyrinogen III (CPIII) from the cytoplasm into the mitochondria (Chavan, et al., 2013; Krishnamurthy, et al., 2006). CPIII a byproduct of heme synthesis in the cytoplasm requires active transport into the mitochondria to complete heme synthesis

(Krishnamurthy *et al.*, 2007). Thus, ABCB6 has been characterized with a physiological role in heme synthesis.

Recent localization and genome association studies have suggested that mammalian Abcb6 has several other functions and localization. ABCB6 has been localized to the plasma membrane and specifies the new blood group system Langereis (Lan) (Helias, et al., 2012). Loss of ABCB6 function has been associated with developmental defects including ocular coloboma (Wang, et al., 2012). Further, exogenous expression of ABCB6 has been correlated with increased cell growth and proliferation while loss of ABCB6 expression results in delayed progression through the mitotic phase of the cell cycle (Polireddy *et al.*, 2011). These studies together suggest that ABCB6 might have non-heme functions in mammals.

To test the role of ABCB6 *in vivo*, we have analyzed the phenotypes associated with ABCB6 loss. Here, we report on an unanticipated function of ABCB6 in controlling body weight and regulating metabolism. *Abcb6* knockout mice display a phenotype characterized by obesity, glucose intolerance, insulin resistance, liver steatosis and adipose tissue expansion. Dysregulated hepatic function and adipose tissue expansion coincide with significant alterations in gene expression and are preceded by significant alteration in daily energy expenditure and physical activity. Lastly, we identify that in liver, the key factor affected by *Abcb6* deletion, is altered mitochondrial form and function.

3.3 Results

Mature-onset obesity in mice lacking ABCB6

To study the physiological function of ABCB6 *in vivo* we generated a whole-body constitutive *Abcb6* knockout mouse by homologous recombination. As we previously reported, mice lacking ABCB6 show a pleiotropic phenotype including embryonic lethality and short stature (Chavan, et al., 2015). However, a subset of *Abcb6* knockout mice were alive and fertile (Chavan, et al., 2015). Surprisingly, *Abcb6-KO* mice that survived embryonic lethality and overcame short stature, displayed a gradual increase in body weight. To establish a chronology of overweight occurrence in the absence of ABCB6, we performed regular weight and food consumption recordings of individual mice under a standard diet over a 20-week period. By 20 weeks of age *Abcb6* deficient male mice showed a significant increase in body weight (Figure 1A-1C, right panel; 16% increase over WT males). In contrast to male mice, the difference in body weight among females was less pronounced (Figure 1A-1C, left panels; 6% increase over WT females). The increase in body weight in either male or female mice could not be attributed to increase in food intake (Figures 1D and 1E). Together, these findings indicate that ABCB6 deletion leads to early signs of mature-onset obesity, which is more pronounced in males than in females.

Figure 3.1

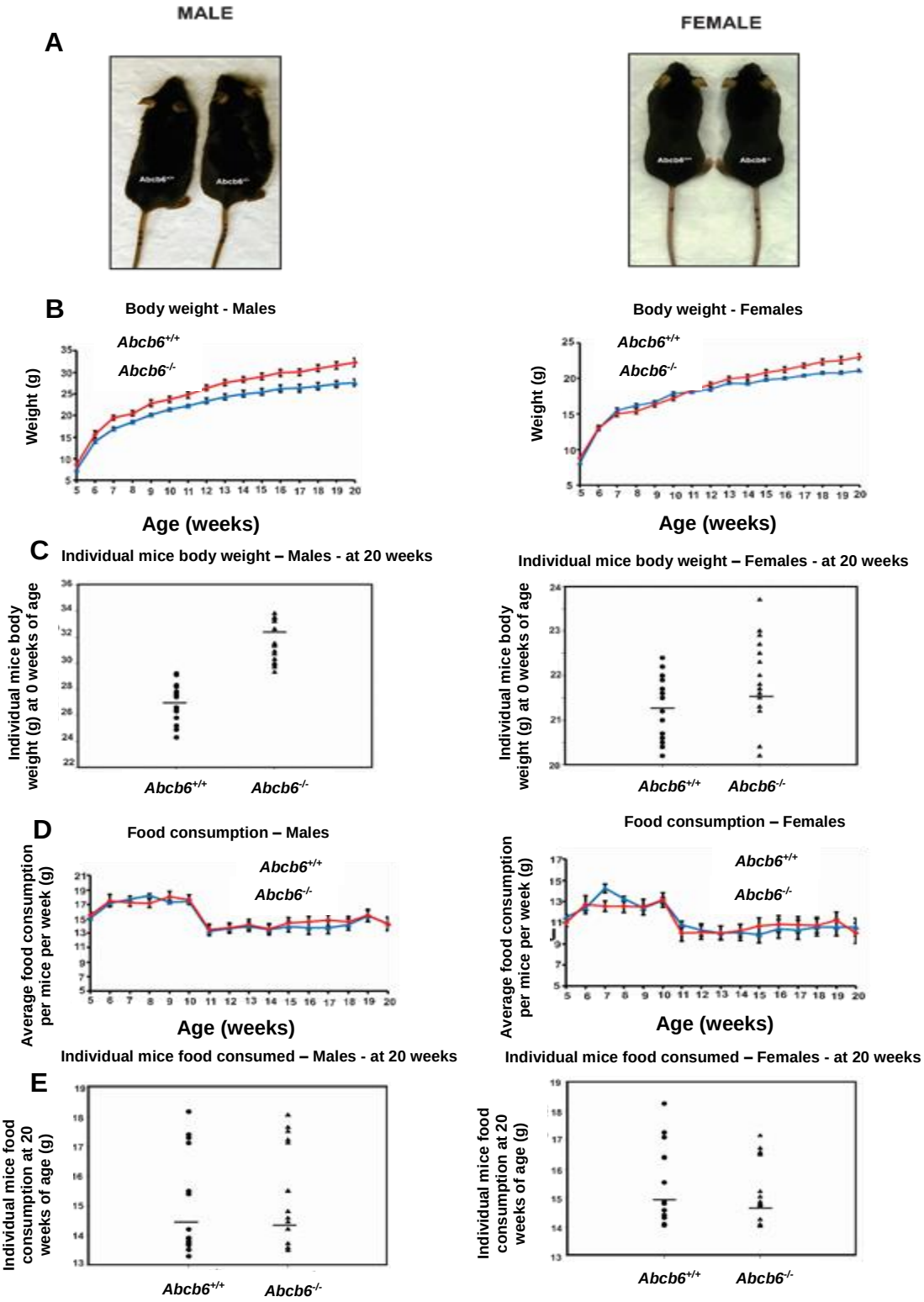
MALE
FEMALE
A
B
Body weight - Males
Body weight - Females
Abcb6+/+
Abcb6-/-
Weight (g)
Age (weeks)
C
Individual mice body weight – Males - at 20 weeks
Individual mice body weight – Females - at 20 weeks
Individual mice body weight (g) at 0 weeks of age
D
Food consumption – Males
Food consumption – Females
Average food consumption per mice per week (g)
Individual mice food consumed – Males - at 20 weeks
Individual mice food consumed – Females - at 20 weeks
E
Individual mice food consumption at 20 weeks of age (g)

Figure 3.1 Abc6 deficiency leads to early signs of mature onset obesity

(A) *Abcb6*-KO male mice display morphological signs of obesity when compared to *Abcb6-WT* controls. Shown are representative photographs of 20-week old male (left) and female (right) mice. (B) Body weight curves of *Abcb6-WT* and *Abcb6-KO* mice over a period of 20 weeks. (C) Animals were fed a normal chow diet and weighed once every week. Data represent mean value ± SD Statistical significance was determined by two-tailed Student's t test. $^{a}p < 0.05$ Individual value plot showing the actual weight of each mice at 20 weeks of age. 15 mice per genotype. (D) Relative food intake curves per mice per week. Data represent mean value ± SD. (E) Individual value plot showing the relative food intake per mice at 20 weeks. Data represent mean value ± SD.

Abcb6-deficient mice accumulate more fat in visceral tissues and show signs of liver steatosis

We next determined whether increased body weight in *Abcb6*-deficient mice could be attributed to a difference in body composition. To this end we performed ECHOMRI which allows quantification of whole-body fat mass and the fat-to-lean ratio. We found that *Abcb6* deficient mice had a significant relative increase in fat mass and a statistically non-significant decrease in lean mass (Figure 3.2A) at 20 weeks of age. We next examined if the larger fat mass of *Abcb6* deficient mice reflects a proportionate increase in organ size. Direct measurements of organ weights from mice maintained on standard diet showed a significant increase in liver, intraabdominal fat, and brown fat mass relative to total body weight in *Abcb6*-deficient male mice compared to wild-type controls (Figures 3.2B). The gross morphology of liver, intrabdominal fat and brown fat was consistent with the increased mass of these tissues in *Abcb6*-deficient male mice (Figures 3.2C). Further, no significant differences in the weight of spleen, and kidney

was observed in either the male or the female *Abcb6* deficient mice compared to their respective controls (data not shown). Hematoxylin and eosin staining (H&E) of liver and white fat sections revealed increased hepatic lipid deposits and a larger size of adipocytes (Figure 3.2D) in *Abcb6* deficient mice. Oil red O staining of liver sections confirmed accumulation of large lipid droplets suggestive of liver steatosis (Figure 3.2D). The oil red O-stained area per section was significantly higher in *Abcb6*-deficient mouse livers compared to wild-type controls (Figure 3.2E). Finally, we found increased amounts of liver triglycerides in *Abcb6*-deficient mice compared to wild-type controls, further indicative of liver steatosis (Figure 3.2F). The increased adiposity in *Abcb6* deficient mice was consistent with decreased adipocyte number (Figure 3.2G). Interestingly, the increased adiposity in *Abcb6* deficient mice was not associated with inflammation, because we did not find any difference in F4/80 staining of white fat sections in *Abcb6*-deficient samples compared to the wild-type controls (Figure 3.2H). Of note, we observed accumulation of white fat also around brown fat in *Abcb6*-deficient mice, which was coincidental with larger intracellular lipid droplets in brown fat tissues (Figures 3.2C).

Abcb6-deficient mice are glucose resistant and show some signs of metabolic syndrome

In humans, increased body mass and fatty liver are indicative of metabolic defects, a condition associated with glucose intolerance and insulin resistance (Castro *et al.*, 2014; Moller *et al.*, 2005). To address whether *Abcb6*-deficiency lead to features of glucose intolerance and insulin insensitivity, we tested the ability of *Abcb6*-deficient mice to

respond to glucose and insulin. To this end, we performed glucose and insulin tolerance tests (GTTs and ITTs, respectively) on 20-week-old mice. Although blood glucose, taken after an overnight fast, was not significantly different between the genotypes, a small but significant increase in higher values of glucose were observed in *Abcb6*-deficient mice after an intraperitoneal glucose tolerance test (Figure 3.2I). In contrast to blood glucose levels *Abcb6* deficient mice showed a small but significant increase in serum insulin levels (Figure 3.2J). The presence of greater insulin resistance in the *Abcb6* deficient mice was confirmed by the insulin tolerance test; at a dose of 0.75 U/kg, the Abcb6 deficient mice showed a small but significantly lower decrease in blood glucose (Figure3.2J). The area under the curve (AUC) values for the GTT and ITT assays were significantly higher in *Abcb6*-deficient mice compared to wild-type controls (Figure 3.2K).

Figure 3.2

A

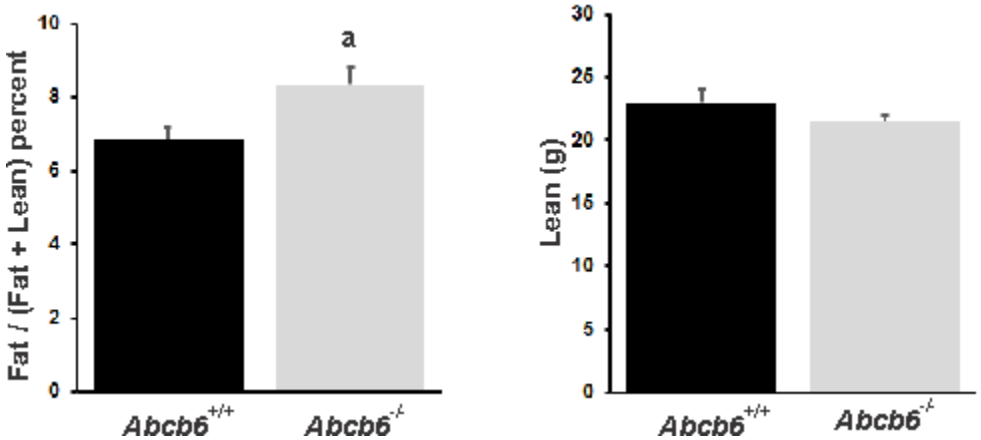

Figure 3.2 cont

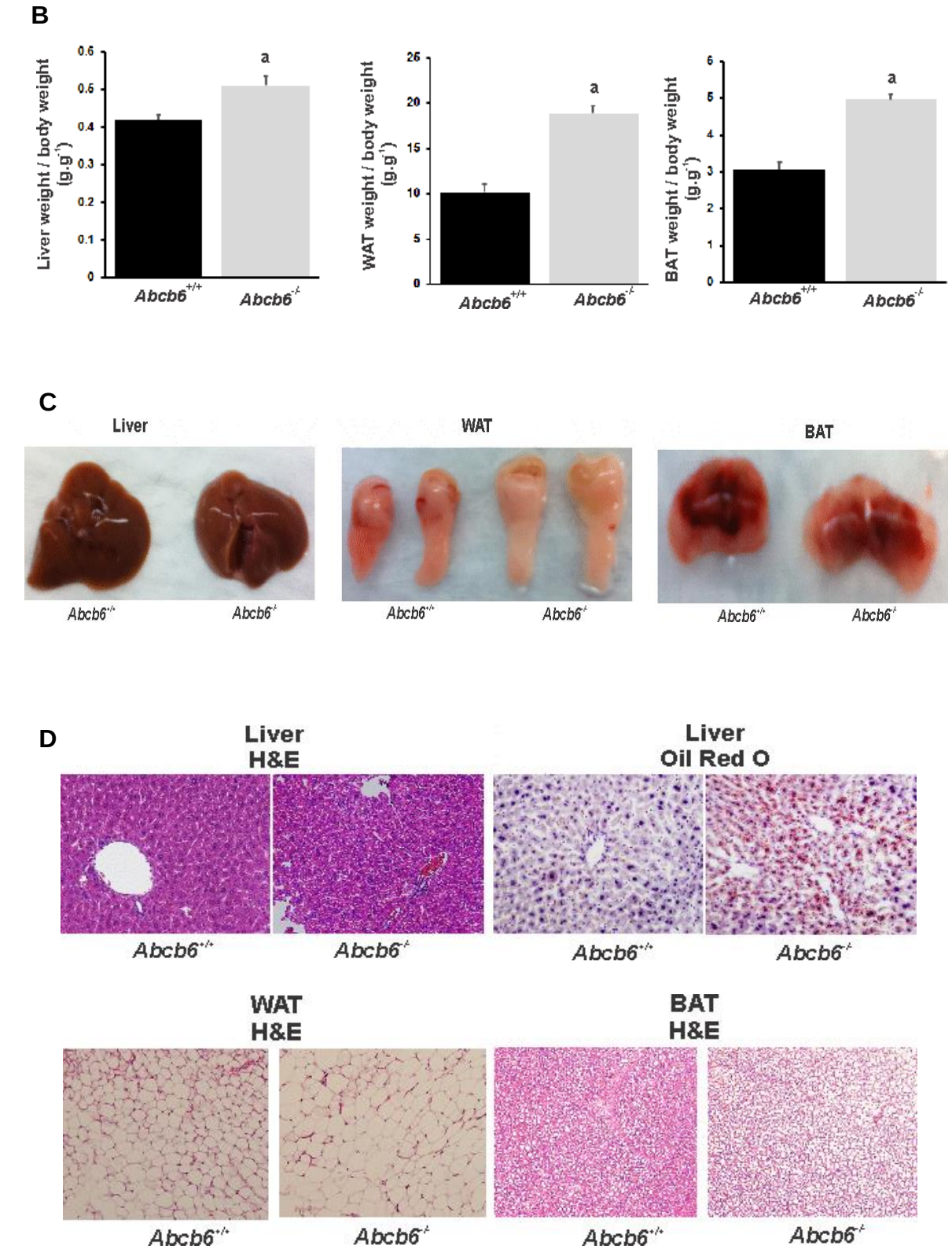

Figure 3.2 continued

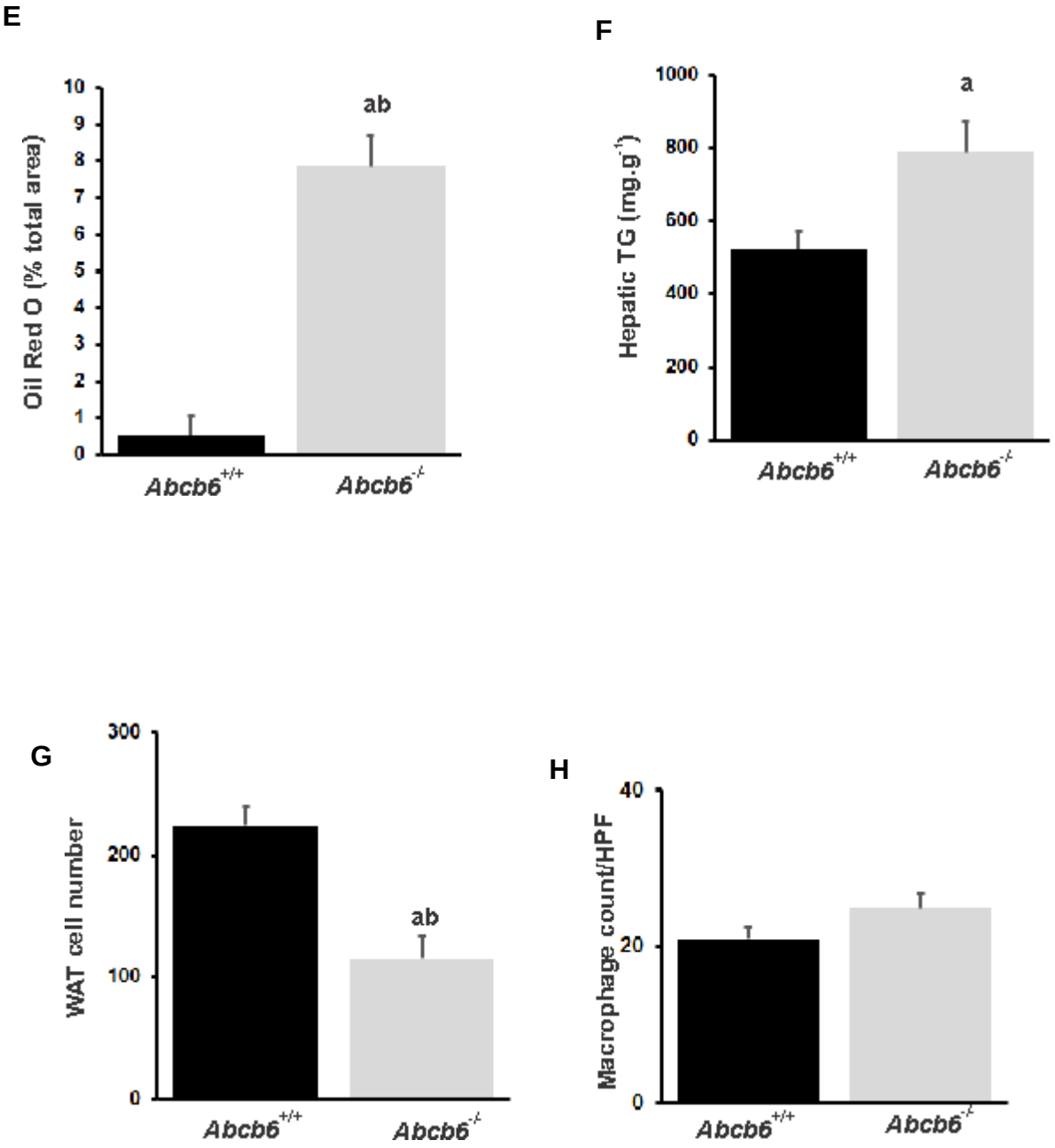

Figure 3.2 continued

I

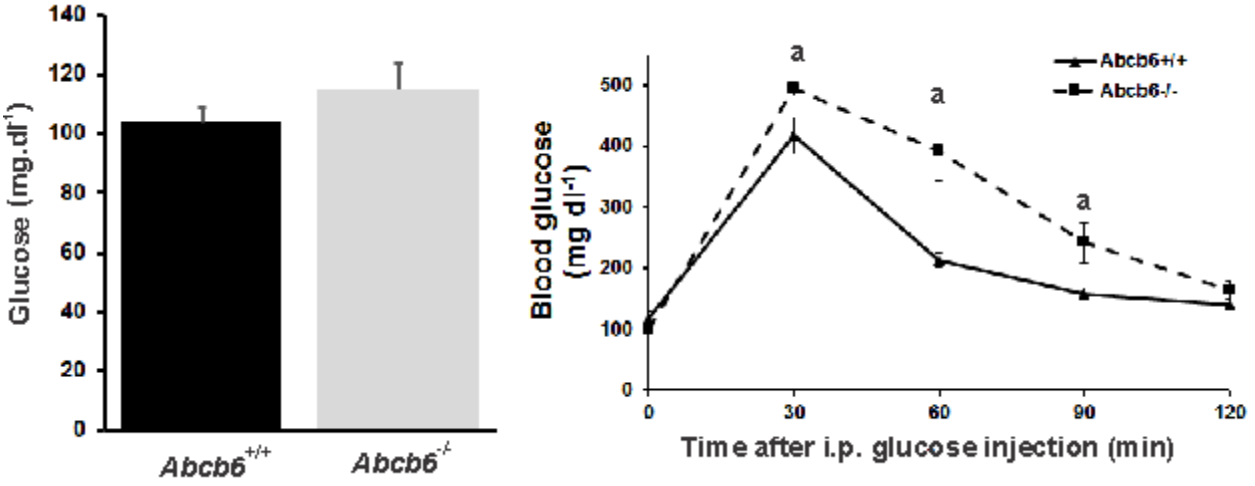

J

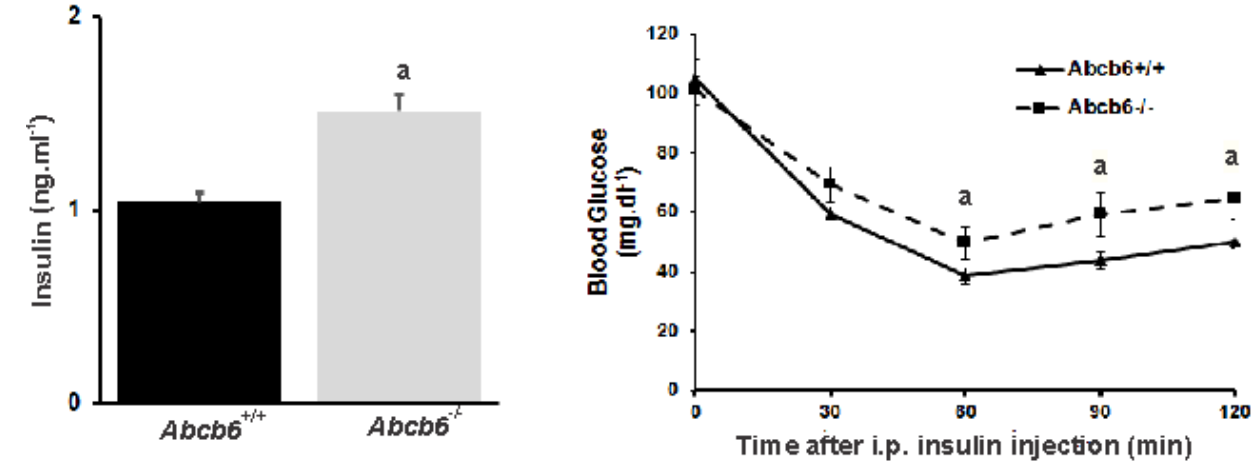

Figure 3.2 continued

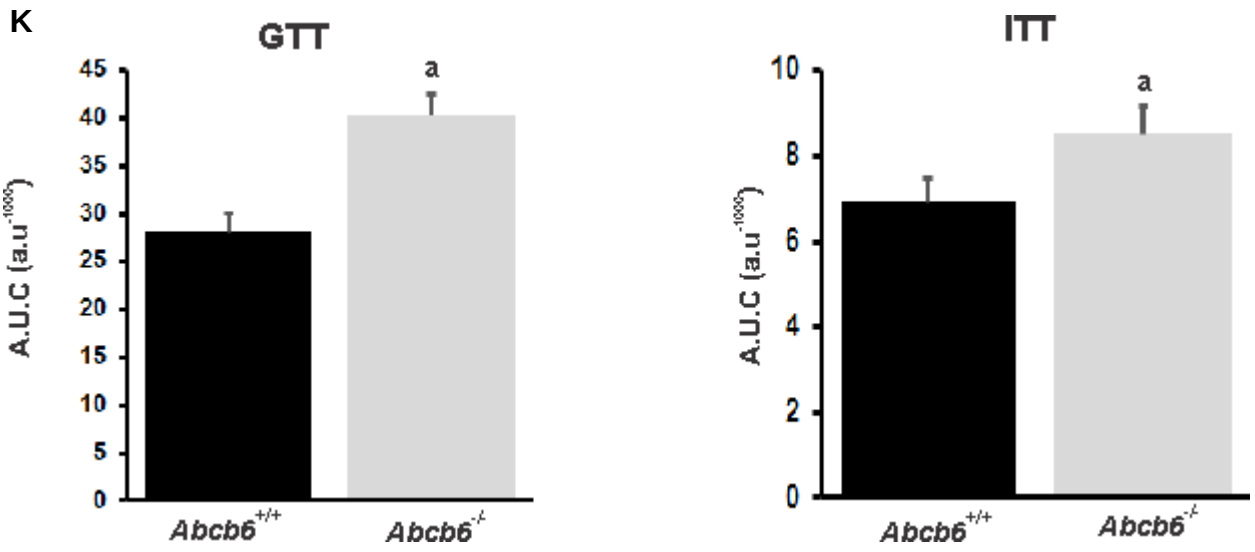

Figure 3.2 *Abcb6*-Deficient male mice accumulate more fat and are insulin resistant

(A) Relative fat mass and lean mass of 20-week-old male mice n=15 mice per genotype (B) Organ weight-to-total body weight ratios, WAT, White adipose tissue; BAT, brown adipose tissue, n = 15 mice per genotype (C) Representative macroscopic images of the indicated tissues and organs (D) Representative light microscopy images of H&E sections, and oil red O staining of the indicated tissues, WAT, white adipose tissue; BAT, brown adipose tissue (E) Quantification of oil red O-positive areas in liver sections of the indicated genotypes (F) Quantification of triglyceride content in liver samples, n=15 mice per genotype (G) Quantification of the adipocyte number in abdominal fat depots (H) Average macrophage count per high power field [HPF (200x optical field)]. Ten adjacent HPF were used and the average number of positive cells per HPF was calculated. (I) Fasting glucose levels and GTT data of fifteen 20-week-old wild-type and *Abcb6* knockout mice (J) Fasting inulin and ITT data of fifteen 20-week-old wild-type and *Abcb6* knockout mice (K) Quantification of the area under the GTT and ITT curve

(AUC), a.u., arbitrary units Values represent means ± SD. Statistical significance was determined by two-tailed Student's t test. ap < 0.05, abp< 0.01

Abcb6-deficient mice show altered hepatic and adipose gene expression that favor the altered hepatic and adipose phenotype

To investigate the biological processes underlying the altered hepatic and adipose phenotype, we assessed the effects of *Abcb6* deficiency on gene transcription and protein translation in liver and adipose of 20-week-old mice. We focused our attention on liver first, due to its role in regulating metabolic homeostasis. We used an Affymetrix GeneChip microarray to assess gene expression changes. Of the total 45,105 transcripts analyzed 501 genes were differentially expressed between *Abcb6-WT* and *Abcb6*-deficient mice ($p< 0.05$ with a fold change > 1.5; 336 downregulated and 165 upregulated genes). Ingenuity Pathway analysis of all differentially expressed genes indicated a significant dysregulation in genes which impact different metabolic pathways including lipid, fatty acid, cholesterol and carbohydrate metabolism as well as in genes involved in developmental process, organismal survival, reproduction and transport (Figure 3.3A pie diagram to the left). To confirm and extend the GeneChip results further we examined liver mRNA and protein response focusing on protein products related to fatty acid and lipid metabolism. Consistent with the microarray data we found a modest but significant difference in the expression of mRNA and protein that regulate hepatic fat and lipid homeostasis in the livers of *Abcb6* deficient mice compared to wild type control mice (Figure 3.3B & 3.3C). Quantification of the protein bands in the immunoblots allowed confirmation of the presence of significant differences in the expression of proteins involved in hepatic fat and lipid homeostasis (Figure 3.3B & 3.3C right panels).

We next turned our attention to the intra-abdominal fat. Differential gene expression analysis, using the PRIMEPCR pathway analysis plate (BioRad), revealed 62 genes that were significantly deregulated in *Abcb6* deficient male mice as compared to age-matched controls. Ingenuity Pathway analysis of all differentially expressed genes indicated a significant deregulation in genes involved in regulating metabolic process, including fat and lipid metabolism (Figure 3.3A pie diagram to the right). To confirm and extend the microarray expression analysis we examined the intrabdominal mRNA and protein response focusing on protein products related to fatty acid and lipid metabolism. As observed in the liver protein response, we found a modest but significant difference in the expression proteins that regulate adipose fat and lipid homeostasis in *Abcb6* deficient mice compared to wild type control mice (Figure 3.3D & 3.3E). Quantification of the protein bands in the immunoblots allowed confirmation of the presence of significant differences in the expression of proteins involved in adipose fat and lipid homeostasis (3.3D & 3.3E right panels).

Figure 3.3

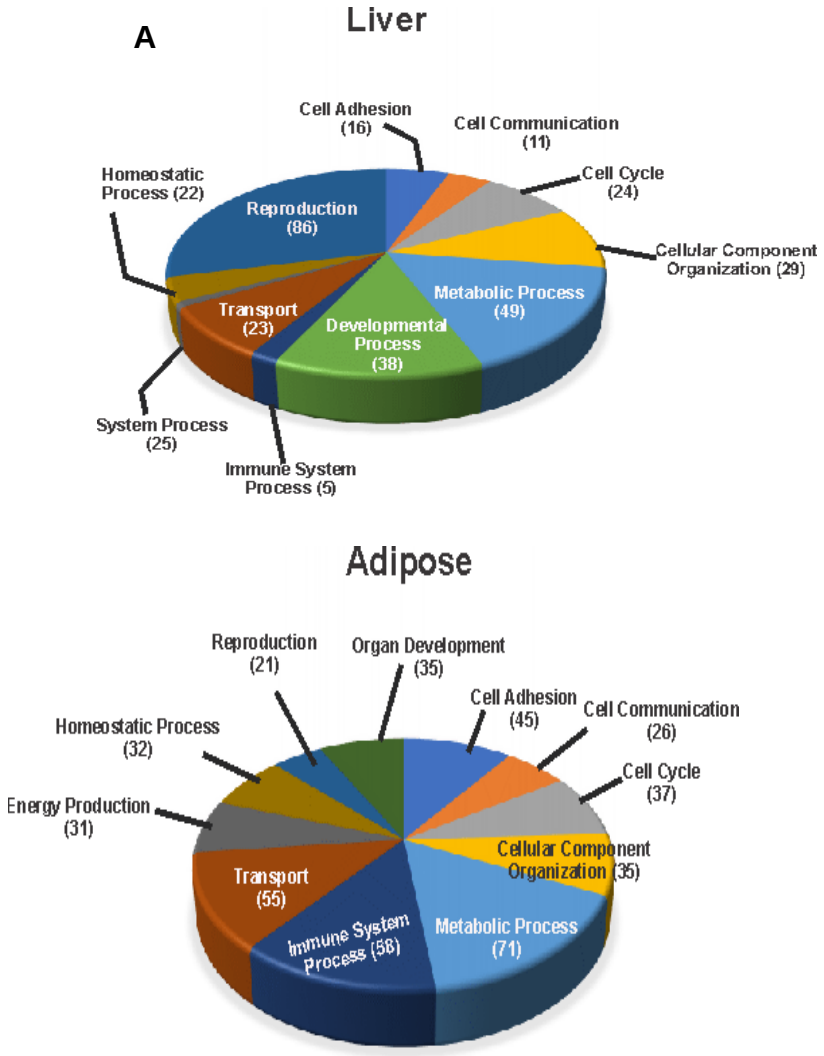
A
Liver
Cell Adhesion (16)
Cell Communication (11)
Cell Cycle (24)
Cellular Component Organization (29)
Metabolic Process (49)
Developmental Process (38)
Immune System Process (5)
System Process (25)
Transport (23)
Homeostatic Process (22)
Reproduction (86)
Adipose
Reproduction (21)
Organ Development (35)
Cell Adhesion (45)
Cell Communication (26)
Cell Cycle (37)
Cellular Component Organization (35)
Metabolic Process (71)
Immune System Process (58)
Transport (55)
Energy Production (31)
Homeostatic Process (32)

Figure 3.3 continued

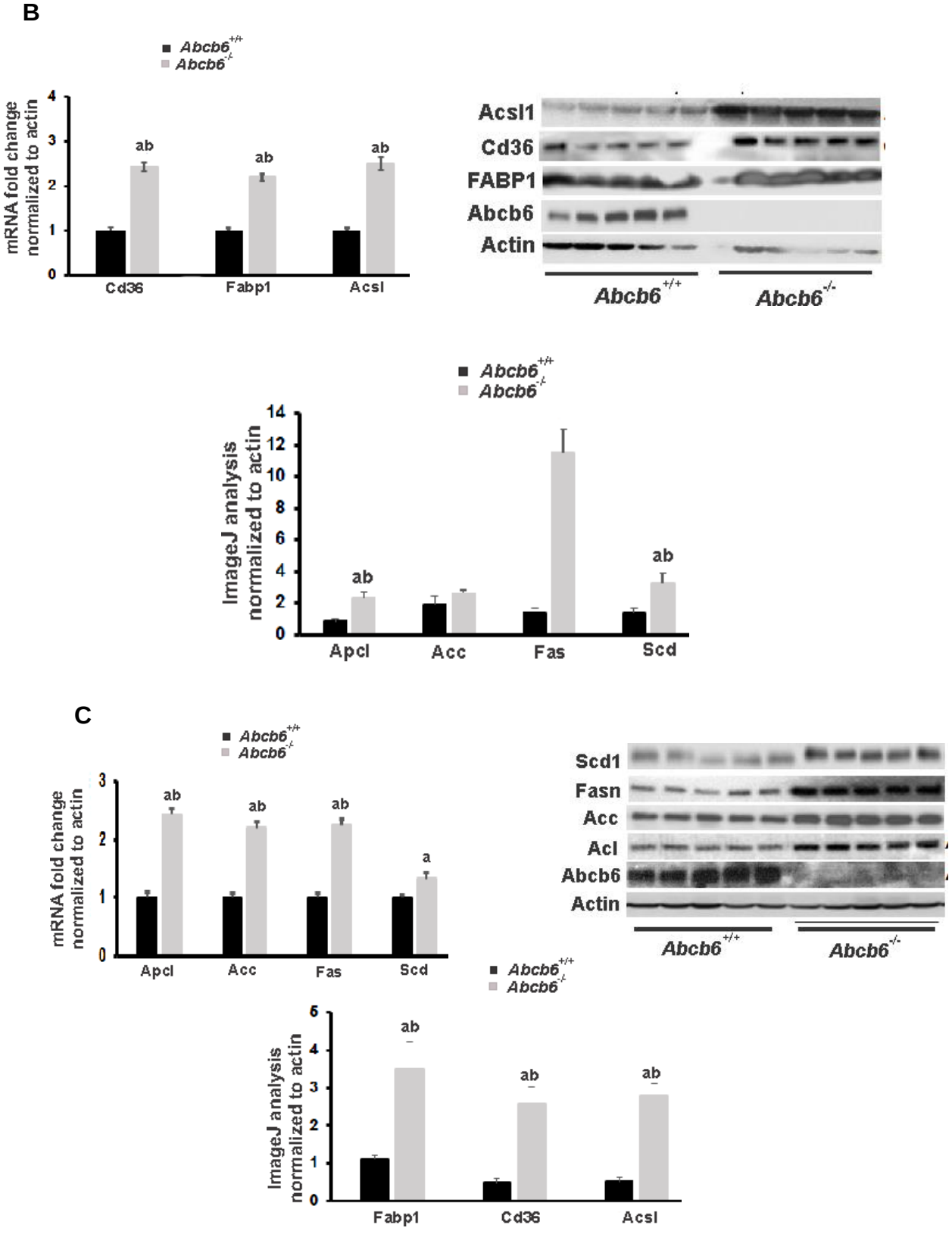

Figure 3.3 continued

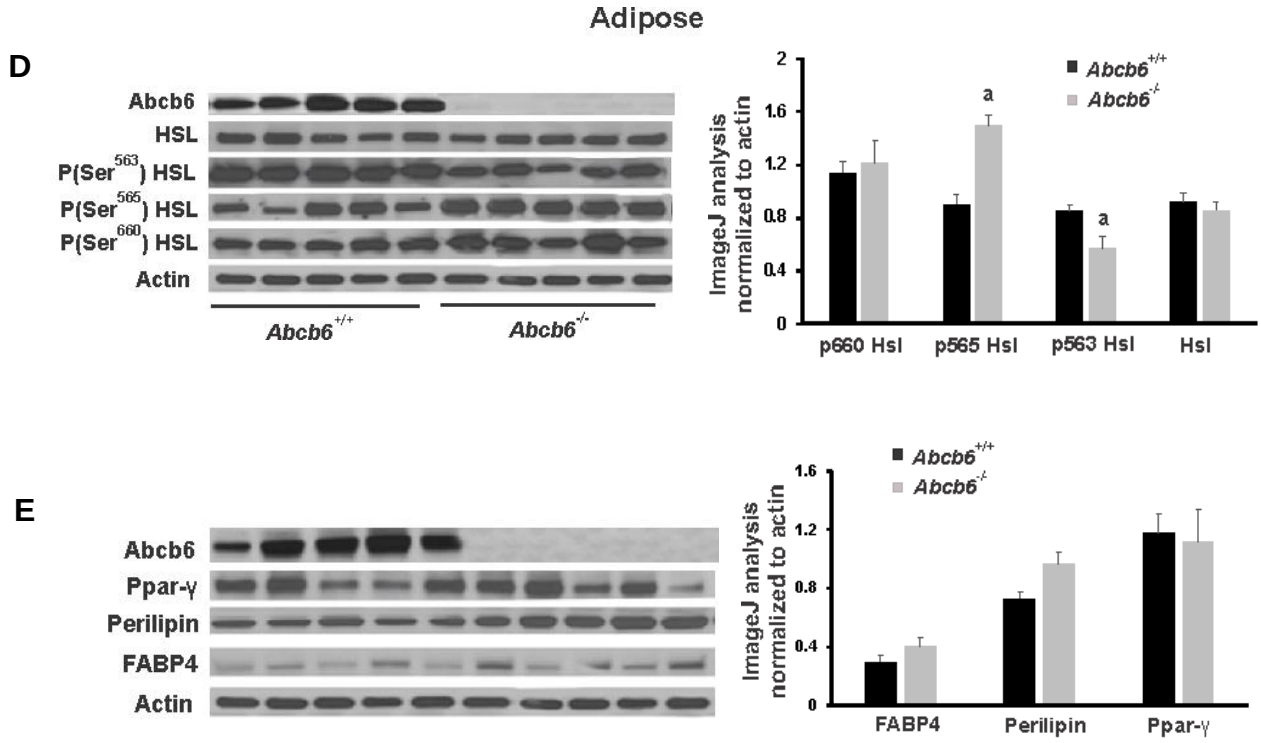

Figure 3.3 *Abcb6* Deficiency alters liver and adipose metabolism leading to steatosis and adipose expansion respectively

(A) Gene ontology analysis and classification of differentially expressed genes into biological processes. (B) qPCR and western blot validation of selected mRNA and proteins involved in fat mobilization. Gene expression changes were normalized to actin and fold changes were normalized to *Abcb6-WT* mice. (C) qPCR and western blot validation of selected mRNA and proteins involved in de-novo lipogenesis. (D) Western blot validation of selected proteins involved in adipose tissue lipolysis. (E) Western blot validation of selected proteins involved in adipose tissue lipid homeostasis. Values represent mean ± SD. Statistical significance was determined by two-tailed Student's t test. ap < 0.05, abp< 0.01 ImageJ was used to normalize protein bands in western blots against the respective loading controls (Actin).

Abcb6 deficient mice have decreased energy expenditure and physical activity.

We next sought to define the basis for the altered body composition in the *Abcb6* deficient mice. To this end, we performed indirect calorimetry analysis to determine whether increased body weight in *Abcb6* deficient mice could be due to differences in energy expenditure (EE). Cohorts of male mice at 6 weeks of age, prior to when the effect of *Abcb6* deletion on body weight is evident, were placed on a standard diet and subjected to indirect calorimetry analysis. We found significant differences in both day and night time EE in *Abcb6* deficient male mice (Figures 3.4A & 3.4I). We also found significant differences in VO_2 and VCO_2 between the genotypes (Figures 3.4B & 3.4C and 3.4J & 3.4K). More importantly we observed lower respiratory exchange rate (RQ) in *Abcb6*-deficient males compared to wild-type males in both light and dark cycles (Figures 3.4D & 3.4L). Finally, measurements of physical activity taken during the calorimetry studies revealed a modest but significantly decreased nighttime but not daytime locomotor activity in *Abcb6* deficient male mice compared to wild-type mice (Figure 3.4E & 3.4F and 3.4M & 3.4N). Together, these results suggest that the substantially increased deposition of fat in *Abcb6* deficient mice could be partly attributable to a modest decrease in EE and physical activity.

Figure 3.4

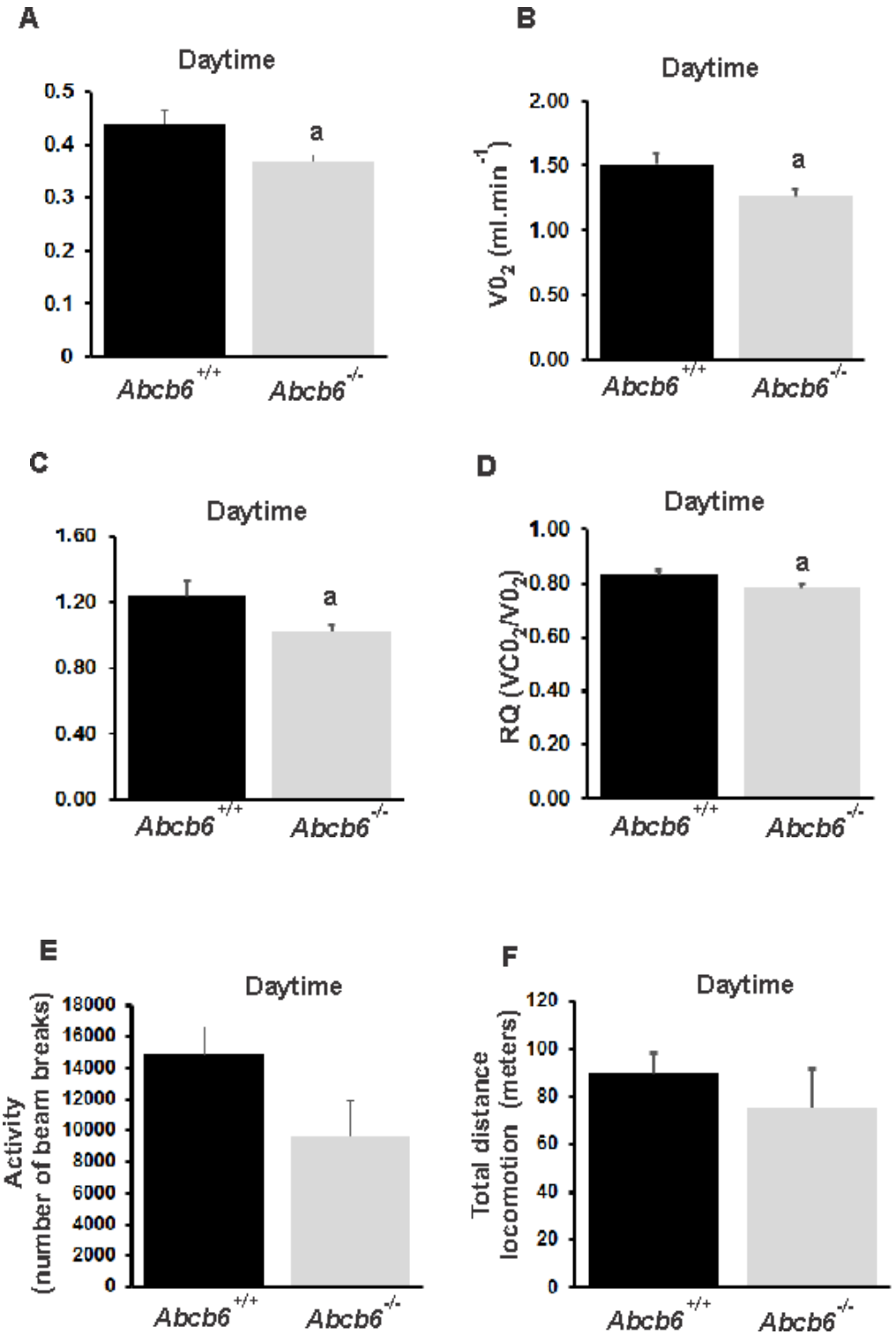
A
Daytime
0.5
0.4
0.3
0.2
0.1
0
a
Abcb6+/+
Abcb6-/-
B
Daytime
VO2 (ml.min-1)
2.00
1.50
1.00
0.50
0.00
a
Abcb6+/+
Abcb6-/-
C
Daytime
1.60
1.20
0.80
0.40
0.00
a
Abcb6+/+
Abcb6-/-
D
Daytime
RQ (VCO2/VO2)
1.00
0.80
0.60
0.40
0.20
0.00
a
Abcb6+/+
Abcb6-/-
E
Daytime
Activity (number of beam breaks)
18000
16000
14000
12000
10000
8000
6000
4000
2000
0
Abcb6+/+
Abcb6-/-
F
Daytime
Total distance locomotion (meters)
120
100
80
60
40
20
0
Abcb6+/+
Abcb6-/-

Figure 3.4 continued

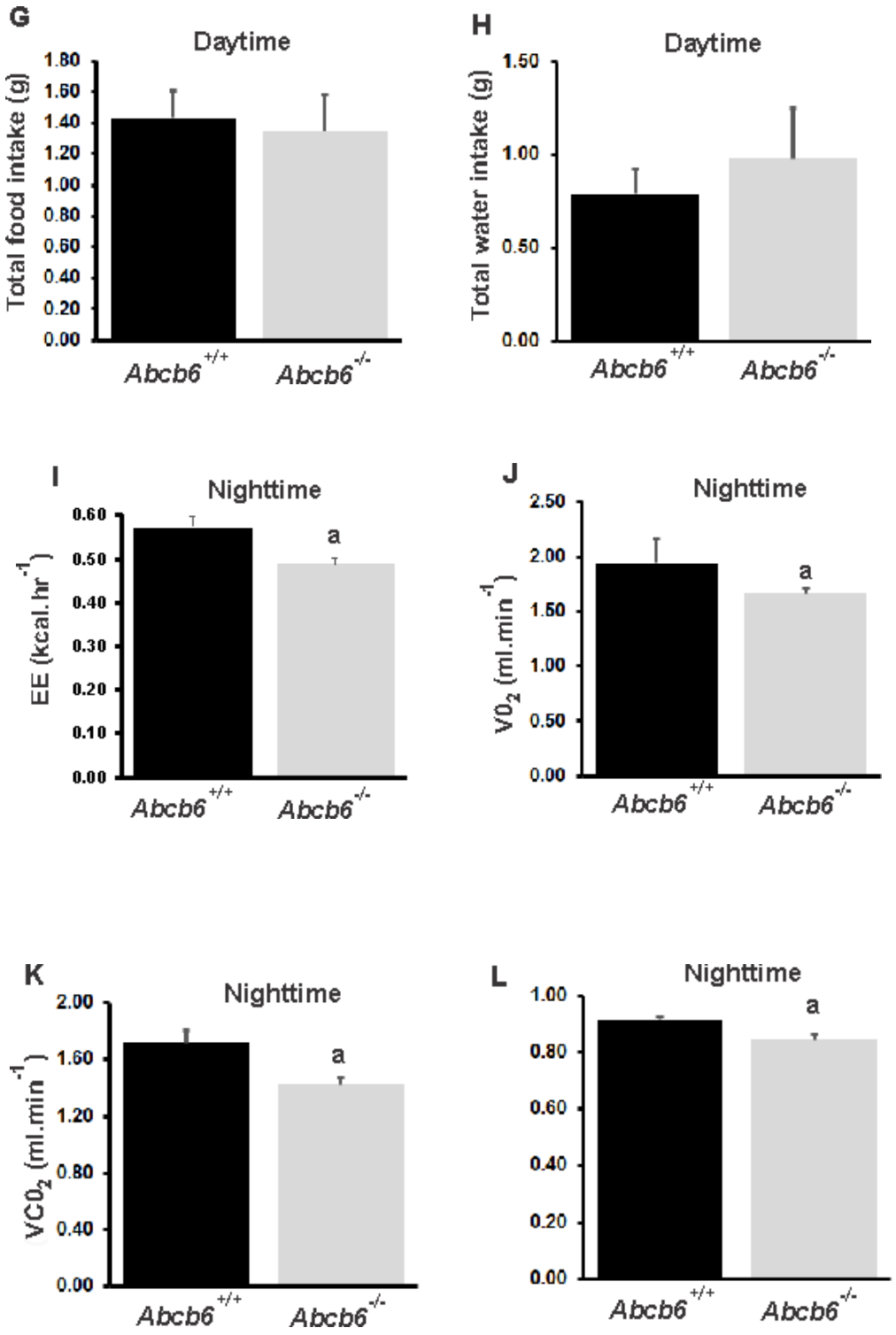

Figure 3.4 continued

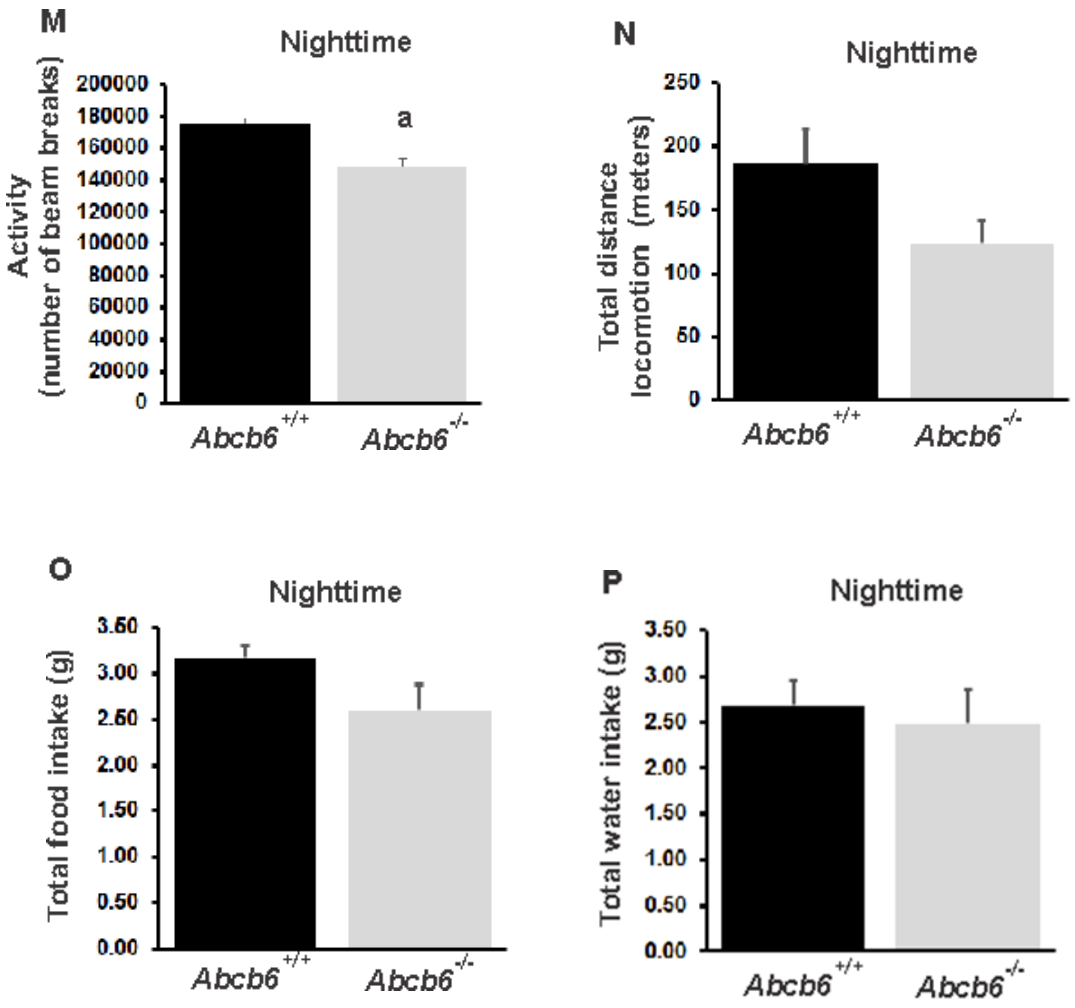

Figure 3.4 *Abcb6* Deficiency affects diurnal energy expenditure

(A-D) Average daytime (A) energy expenditure, (B) volume of O2, (C) volume of CO2, and (D) RER (E-F) Average daytime (E) activity, (F) distance travelled, (G) average food intake and (H) average water intake. (I-L) Average nighttime (I) energy expenditure, (J) volume of O2, (K) volume of CO2, and (L) RER. (M-P) Average nighttime (M) activity, (N) distance travelled, (O) average food intake and (P) average water intake. Indirect calorimetric analysis of 6 – week-old *Abcb6-WT* and *Abcb6-KO* mice monitored during a week period in metabolic cages. Values represent mean ± SD. Statistical significance was determined by two-tailed Student's t test. ap < 0.05

High-fat diet further aggravates obesity and diabetes in Abcb6-deficient mice

To further understand the origin of obesity and liver steatosis associated with *Abcb6* deficiency, we subjected 6-week-old *Abcb6*$^{+/+}$ and *Abcb6*$^{-/-}$ mice to high-fat diet (HFD) and followed weight gain in a longitudinal manner (weekly measurements). HFD resulted in a significant increase in body weight compared to wild-type controls, (Figure 3.5A and 3.5B). The increased body weight of *Abcb6* deficient mice fed a HFD could not be attributed to differences in daily food intake (Figure 3.5B inset).

Next, we performed direct measurements of organ weights from mice maintained on HFD. We observed a significant increase in liver, intra-abdominal, and brown fat mass (Figure 3.5D & 3.5E) relative to total body weight in *Abcb6*-deficient mice compared to wild-type controls on HFD. Hematoxylin and eosin staining (H&E) of white fat revealed a larger size of adipocytes in *Abcb6* deficient mice (Figure 3.5F). Oil red O staining of liver sections confirmed accumulation of large lipid droplets (Figure 3.5F). Finally, we found increased amounts of liver triglycerides in *Abcb6*-deficient mice (Figure 3.5I). Of note, we observed accumulation of white fat also around brown fat in *Abcb6*-deficient mice, which was coincidental with larger intracellular lipid droplets in brown fat tissues (Figures 3.5F).

To further understand the metabolic effects of HFD in *Abcb6* deficiency, we analyzed several metabolic parameters in the plasma of mice of both genotypes. Glucose and insulin plasma levels were increased in *Abcb6* deficient mice (Figure 3.5C). The GTTs and ITTs confirmed that *Abcb6*-deficient mice are significantly more glucose resistant and insulin-insensitive than wild-type mice on the same diet (Figure 3.5G and 3.5H). We also found that the levels of cholesterol, serum triglycerides and free fatty acids were

elevated in *Abcb6* deficient mice compared to their wild type counterparts (Figures3. 5I – 3.5M). Taken together, these results suggest that ABCB6 impairment has adverse metabolic consequences that can lead to diet induced obesity in mouse.

Figure 3.5

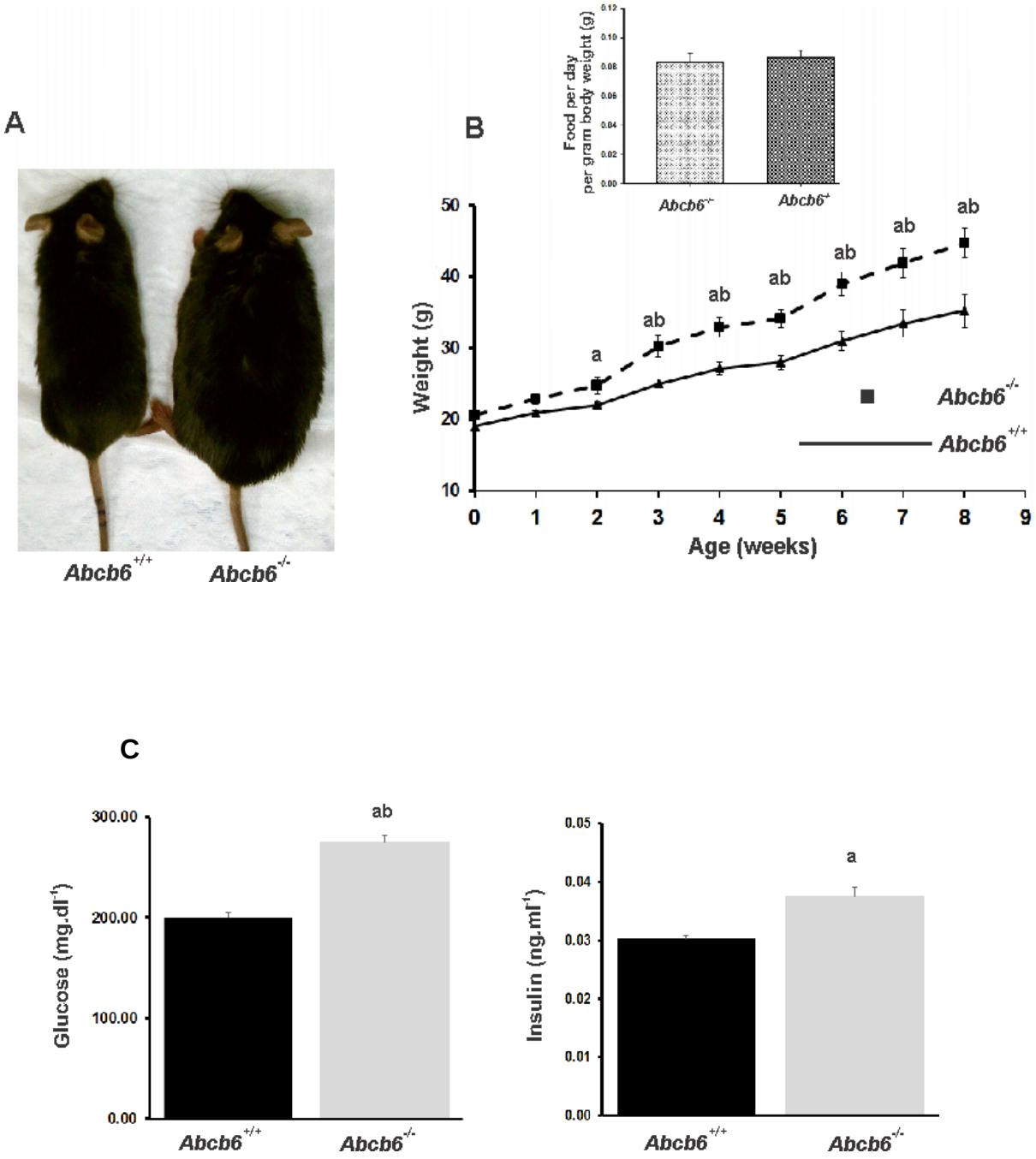

Figure 3.5 continued

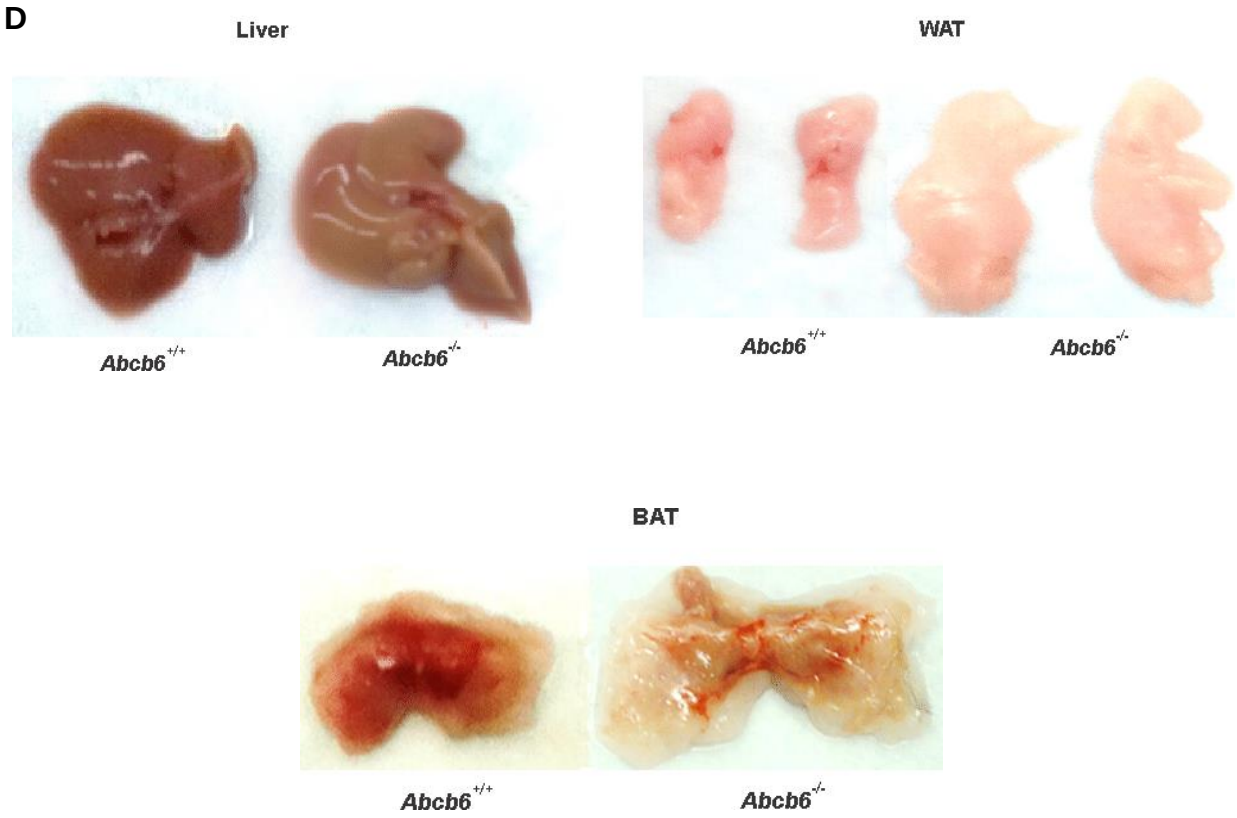

Figure 3.5 continued

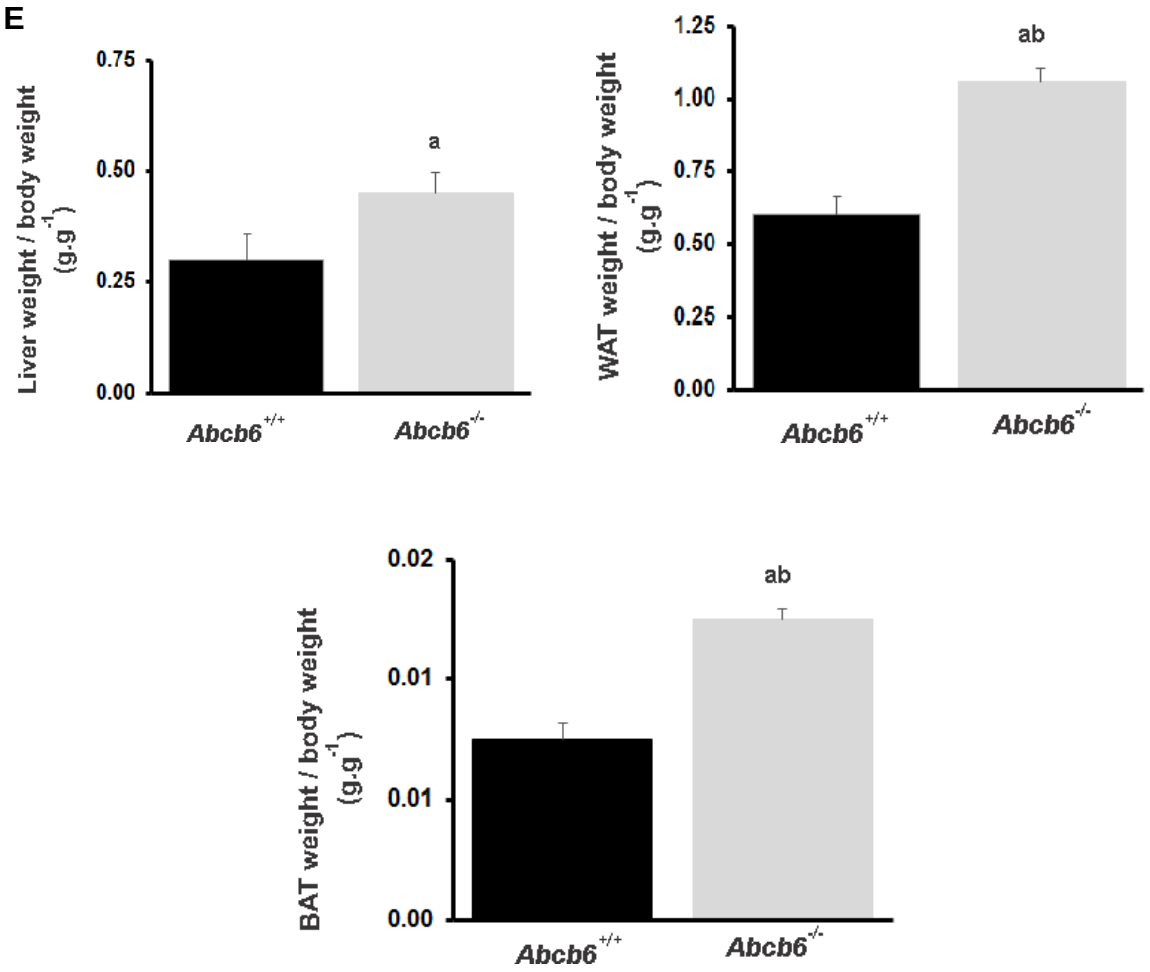

Figure 3.5 continued

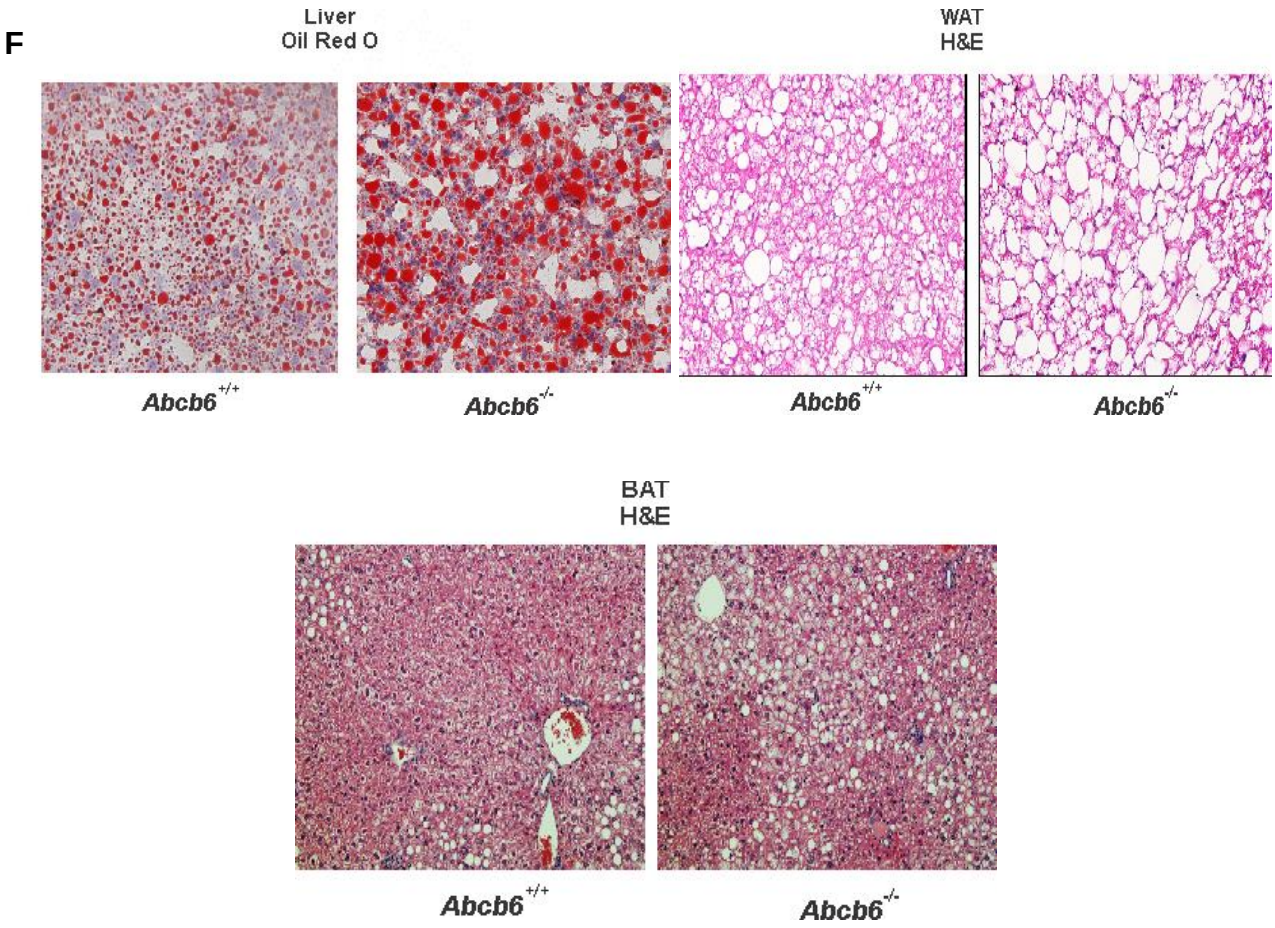

Figure 3.5 continued

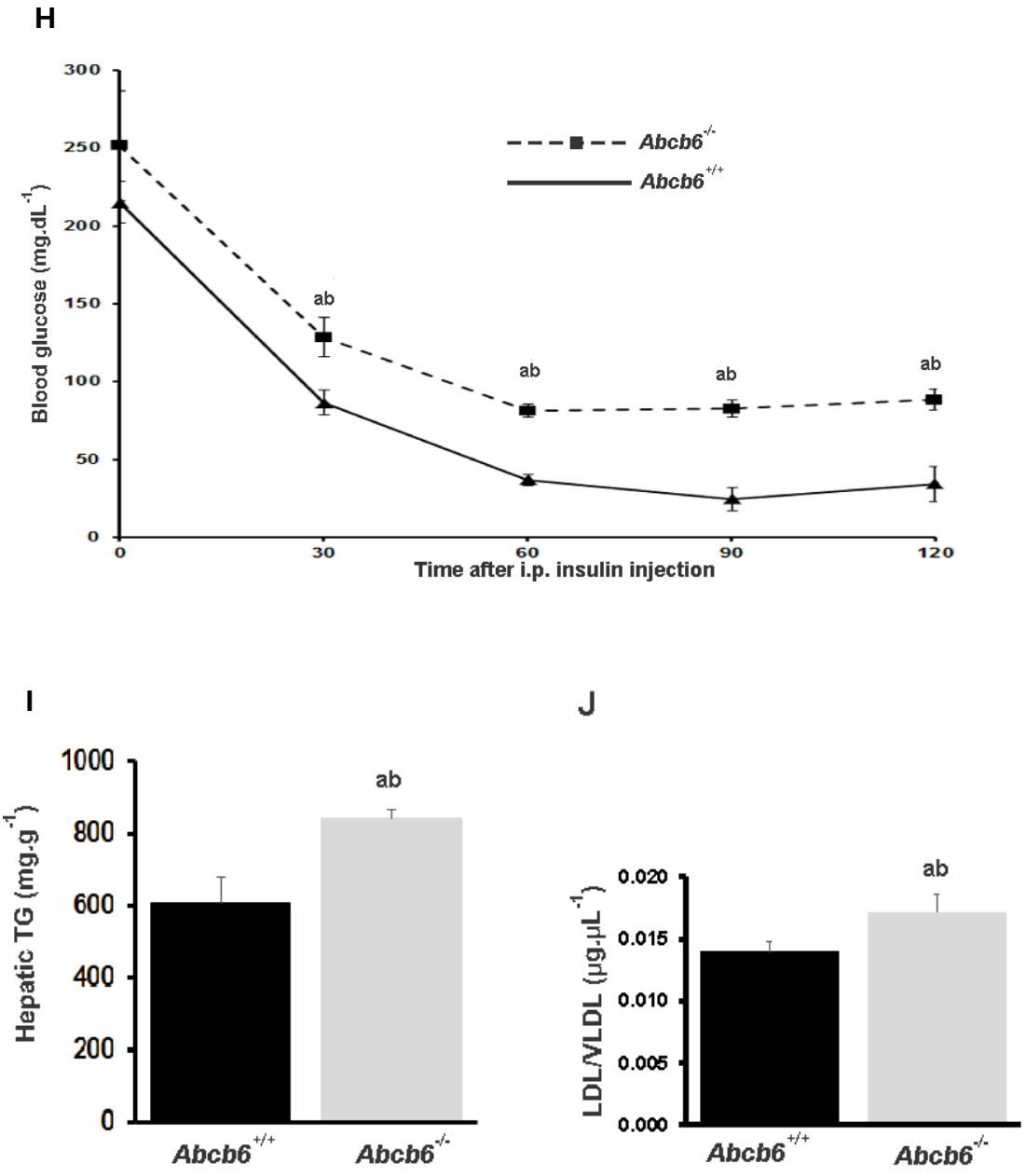

Figure 3.5 continued

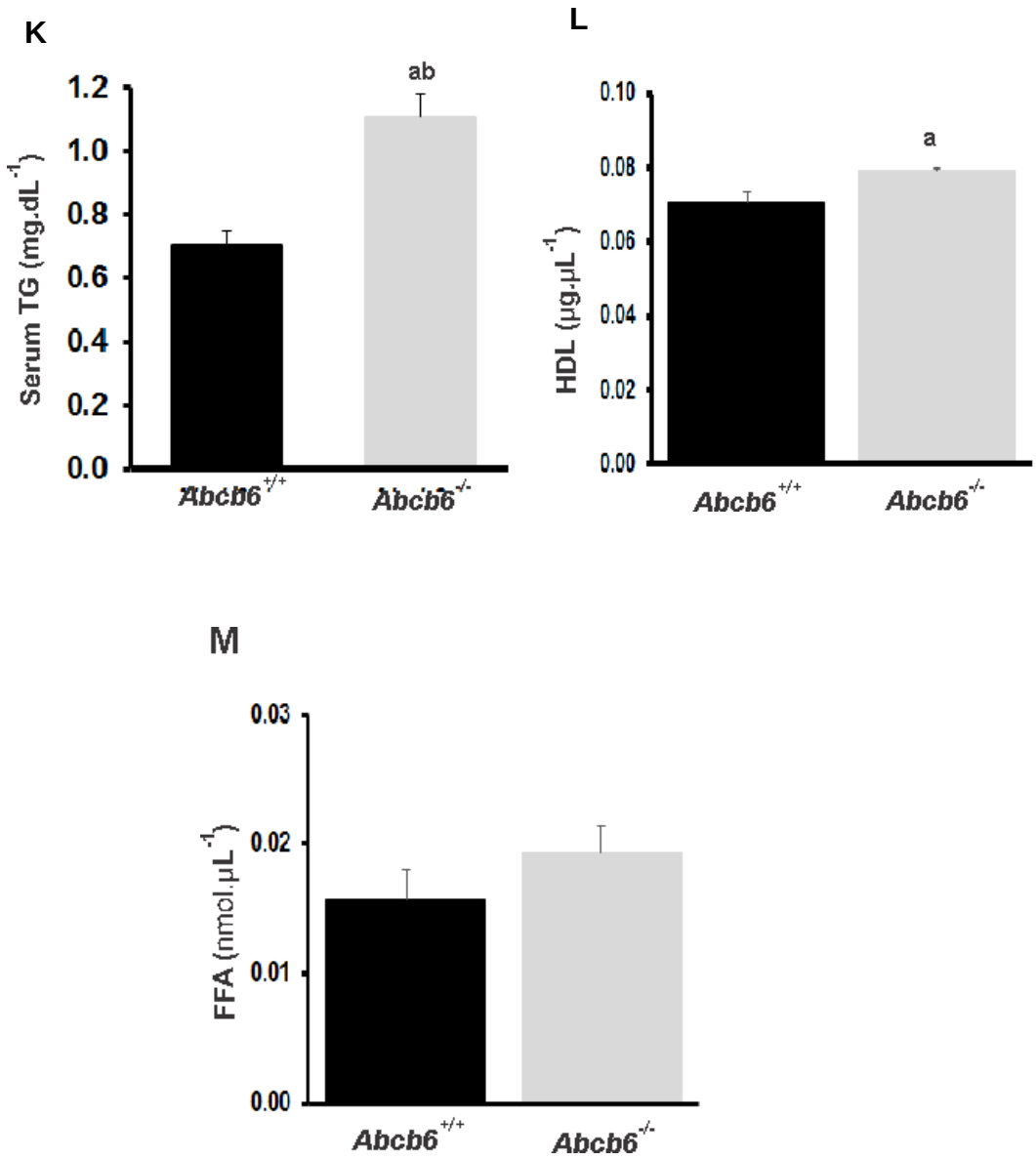

Figure 3.5 Enhanced weight gain and disruption of glucose metabolism in *Abcb6* deficient mice subjected to HFD

(A) Representative image of male mice of the indicated genotype and age subjected to HFD for 8 weeks. (B) Weight curves of male mice of the indicated genotype on HFD (60% calories from fat) commencing at 5 weeks of age. Inset in (B) relative food intake monitored during the HFD feeding. (C) Fasting glucose and insulin levels in male mice of the indicated genotype. (D) Representative macroscopic images of the indicated tissues and organs. (E) Organ weight-to-total body weight ratios, WAT, White adipose tissue; BAT, brown adipose tissue, n = 15 mice per genotype. (F) Representative light microscopy images of H&E sections, and oil red O staining of the indicated tissues, WAT, white adipose tissue; BAT, brown adipose tissue. (G) Glucose tolerance test (GTT) data in *Abcb6-WT* and *Abcb6-KO* mouse fed HFD for 8 weeks. (H) Insulin tolerance test (ITT) data in Abcb6-WT and *Abcb6-KO* mice fed HFD for 8 weeks. (I-M) Analysis of hepatic and plasma parameters in wild-type and Abcb6-deficient mice on HFD. (I) Hepatic TG, (J) Plasma LDL/VLDL ratio, (K) Plasma TG, (L) Plasma HDL (M) Plasma FFA. TG, Triglycerides; LDL, low density lipoproteins; VLDL, very low-density lipoproteins, HDL, high density lipoprotein; FFA, free fatty acids.

Values represent mean ± SD. Statistical significance was determined by two-tailed Student's t test. ap < 0.05, abp < 0.01

ABCB6 expression is suppressed under obese conditions

Given the significant association between Abcb6 deficiency, and obesity we wondered if ABCB6 expression is differentially regulated under obese conditions. To test this hypothesis, we extracted proteins from livers and intra-abdominal adipose tissue of HFD induced obese mice and mice that are obese because of leptin deficiency (ob/ob). We found that ABCB6 expression was suppressed in the livers and white

adipose tissue of both HFD induced obese mice and leptin deficient obese mice (Figures 3.6A and 3.6B). We next sought to extend these observations and test whether ABCB6 expression was differentially regulated in obese humans compared to their 'non-obese' counterparts. Towards this end we analyzed ABCB6 expression in clinically obese (BMI≥ 30, with hepatic steatosis of 20% or more by histology) and non-obese (BMI≤ 25, with no significant steatosis) human livers. As observed in the livers of obese mice we found decreased ABCB6 expression in obese human livers (Figure 3.6C). Together these results suggest a strong association between ABCB6 expression and metabolic homeostasis.

Figure 3.6

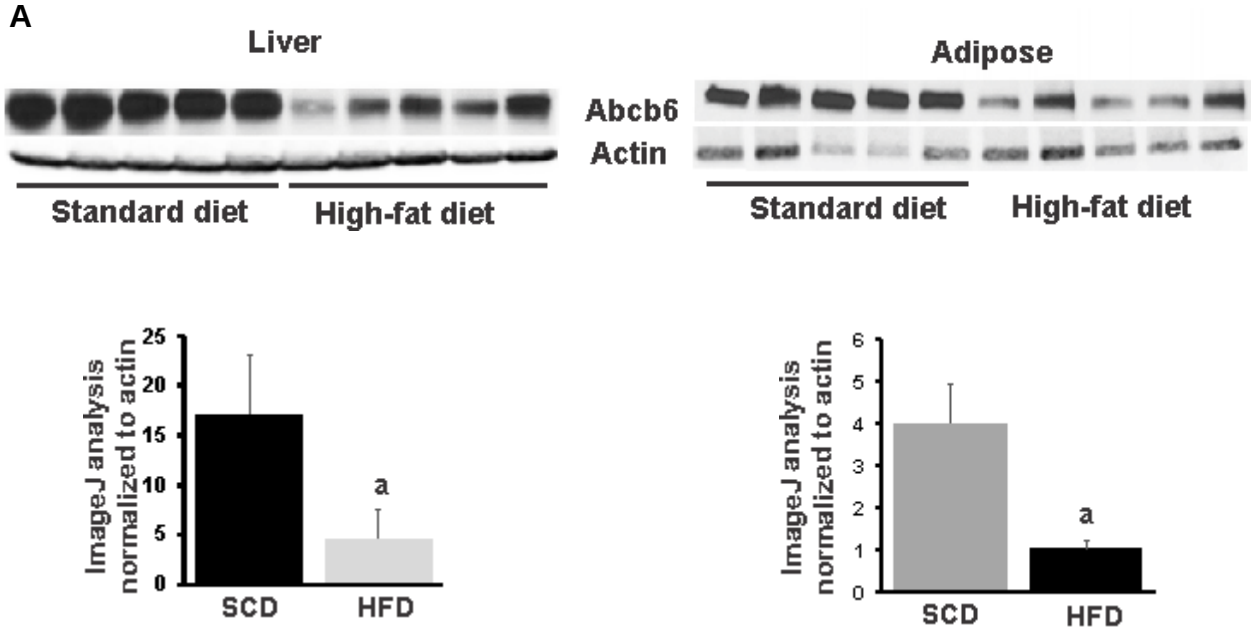

Figure 3.6 continued

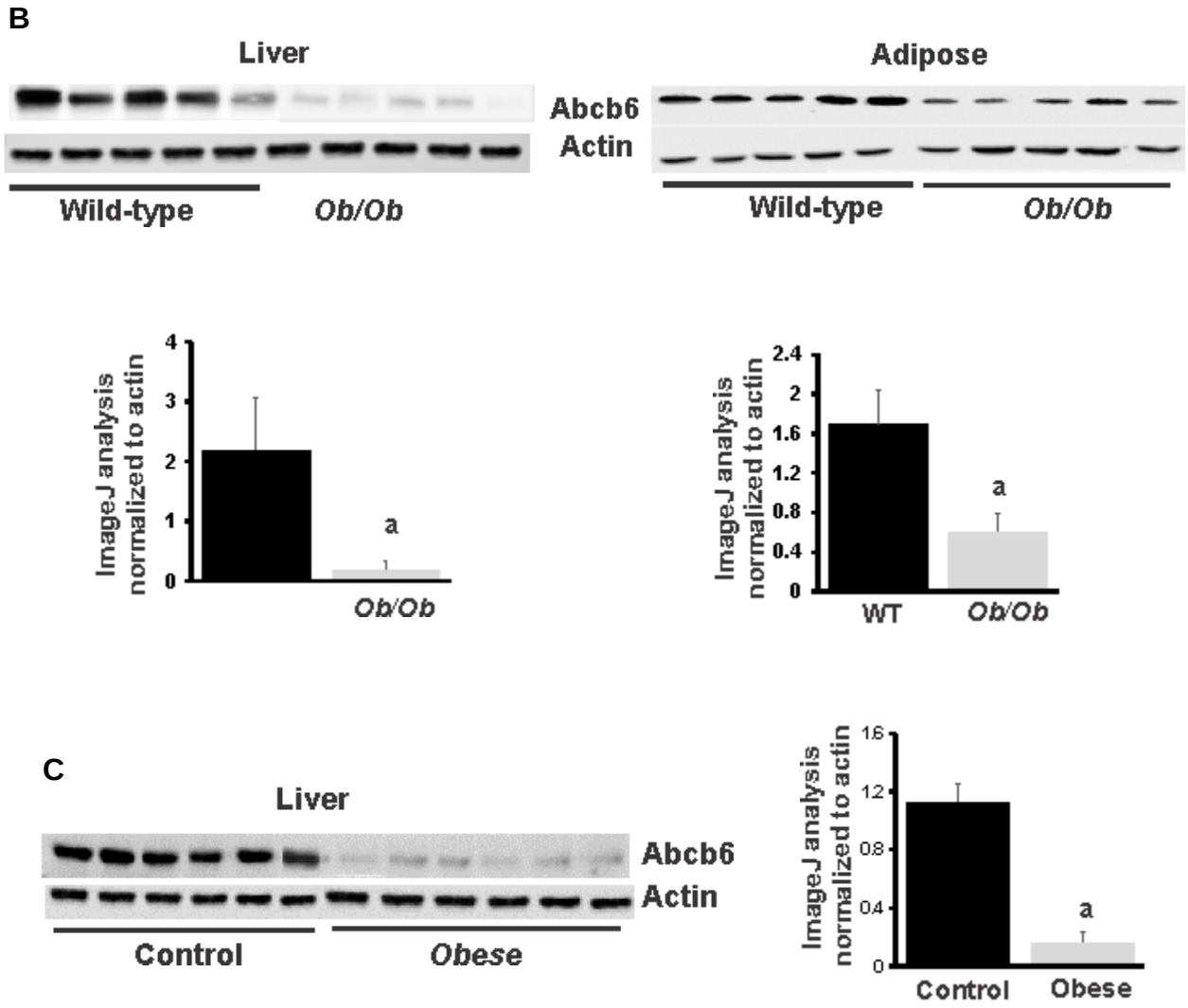

Figure 3.6 Conditions that lead to obesity affects ABCB6 expression in liver and adipose tissue

(A) Representative figure showing the effects of HFD feeding on ABCB6 abundance in liver (upper left) and adipose tissue (upper right). (Lower panels) Quantification of the protein bands in the immunoblots normalized to actin (n=15 mice per genotype). (B) Representative figure showing ABCB6 expression in liver (middle left) and adipose (middle right) in leptin deficient

(ob/ob) mice. (Lower panels) Quantification of the protein bands in the immunoblots normalized to actin (n=15 mice per genotype). (C) Representative figure showing hepatic ABCB6 expression in obese (BMI≥ 30, with hepatic steatosis of 20% or more by histology) and non-obese (BMI≤ 25, with no significant steatosis) human. Values represent mean ± SD. Statistical significance was determined by two-tailed Student's t test. ap < 0.05.

Abcb6 deficient mice display altered mitochondrial form and function

Over the past decade, it has become evident that shifts in energy expenditure are often linked to changes in mitochondrial function and such altered mitochondrial function also underlie systemic metabolic abnormalities that characterize the many clinical features of metabolic disease (Kim *et al.*, 2008; Krishnamurthy, et al., 2011; Pintus *et al.*, 2012). Given that ABCB6 is a mitochondrial protein we wondered if some of the observed phenotype in *Abcb6* deficiency could result from altered mitochondrial function. To test this, we evaluated liver mitochondrial morphology and liver mitochondrial function in 6-week-old *Abcb6*-deficient male and female mice, prior to when the effect of *Abcb6* deletion on body weight is evident. We found loss of ABCB6 resulted in swollen mitochondria with indistinct cristae in liver tissue (Figure 3.7A and 3.7B left panels) and decreased mitochondrial function in primary hepatocytes (Figure 3.7A and 3.7B middle panels) and crude mitochondria isolated from *Abcb6*-deficient livers (Figure 3.7A and 3.7B right panels). Interestingly, we found that the mitochondrial form and function changes observed in *Abcb6*-deficient mice livers on standard chow diet was analogous to those observed in wildtype mice that developed obesity in response to high-fat diet feeding (Figure 3.7D) or developed obesity because of leptin deficiency (ob/ob mice; Figure 3.7C). Together, these results suggest a strong

association between ABCB6 expression and mitochondrial form and function in obesity linked metabolic disease.

The oxidative phosphorylation system, consisting of the four-multimeric enzyme complexes (CI–CIV) of the respiratory chain, and the ATP synthase complex (CV), drive the synthesis of ATP in most cells and defines the bioenergetic efficiency of the mitochondria. We wondered whether altered expression and/or activity of oxidative phosphorylation complexes contributed to the differential bioenergetic capacity of the hepatic mitochondria in *Abcb6* deficient mice. To test this, we measured the activity of each (CI, CII, CIII, and CIV) of the respiratory complexes and found a significant decrease in the activity of CI, CIII and CIV complexes in *Abcb6* deficient mice (Figure 3.7E left panel). We next determined if the changes in enzyme activity resulted from changes in respiratory complex expression. Towards this end we performed a denaturing gel electrophoresis of mitochondrial proteins isolated from *Abcb6*-deficienand *Abcb6 WT* control mice liver. Surprisingly, western blot analysis revealed no significant difference in the protein levels of any of the complexes in *Abcb6*-deficient mice compared to the *Abcb6WT* controls (Figure 3.7E middle panel). Quantification of the protein bands in the immunoblots allowed confirmation of the lack of significant differences in the expression of respiratory complexes between the *Abcb6* genotypes (Figure 3.7E right panel). Together these results suggest that the decreased hepatic mitochondrial bioenergetics in *Abcb6* deficiency could partly arise from a decrease in the activity of respiratory complexes CI and CIII without any significant change in their expression.

Figure 3.7

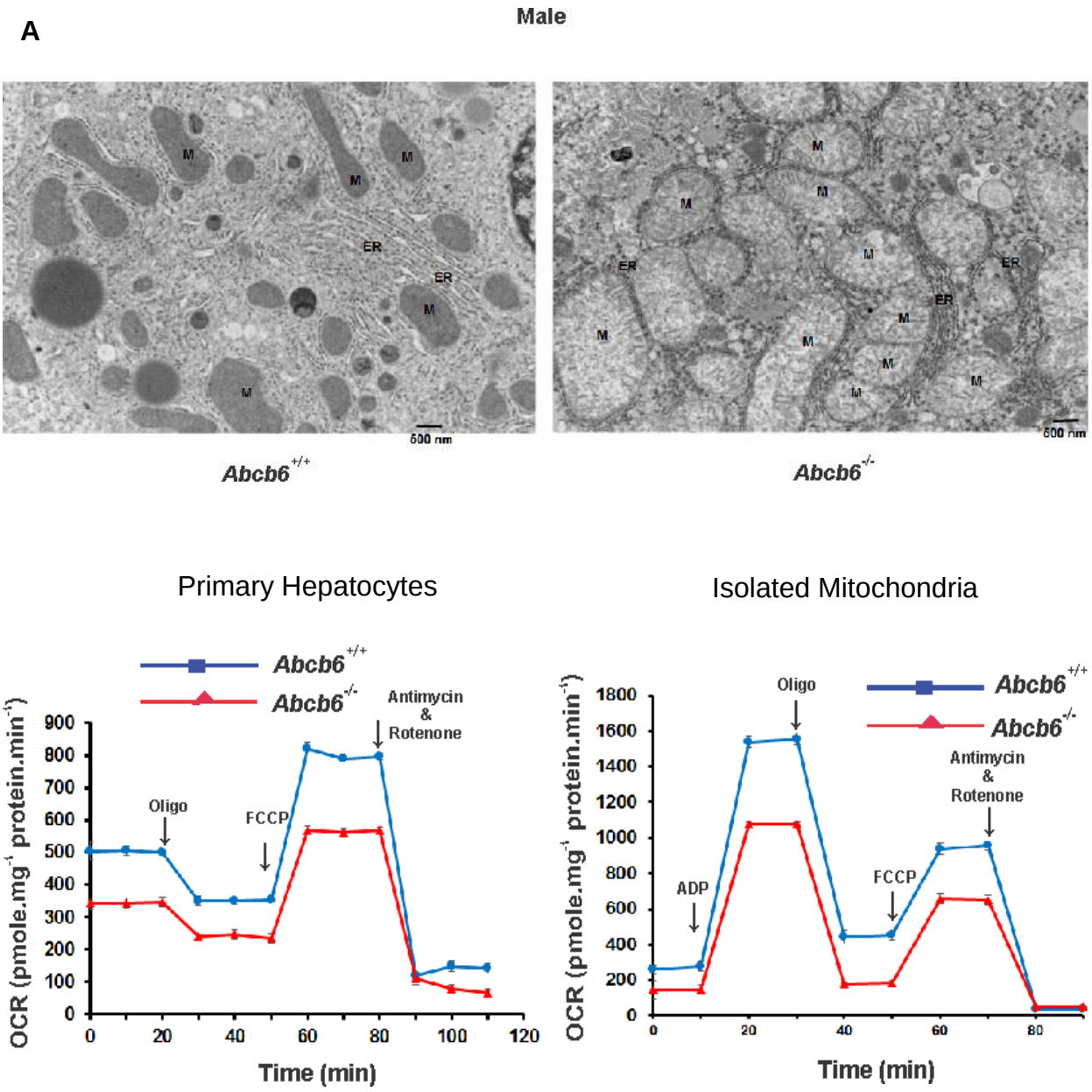
A
Male
M
ER
600 nm
Abcb6+/+
Abcb6-/-
Primary Hepatocytes
Isolated Mitochondria
Abcb6+/+
Abcb6-/-
Oligo
FCCP
Antimycin
&
Rotenone
ADP
OCR (pmole.mg-1 protein.min-1)
Time (min)

Figure 3.7 continued

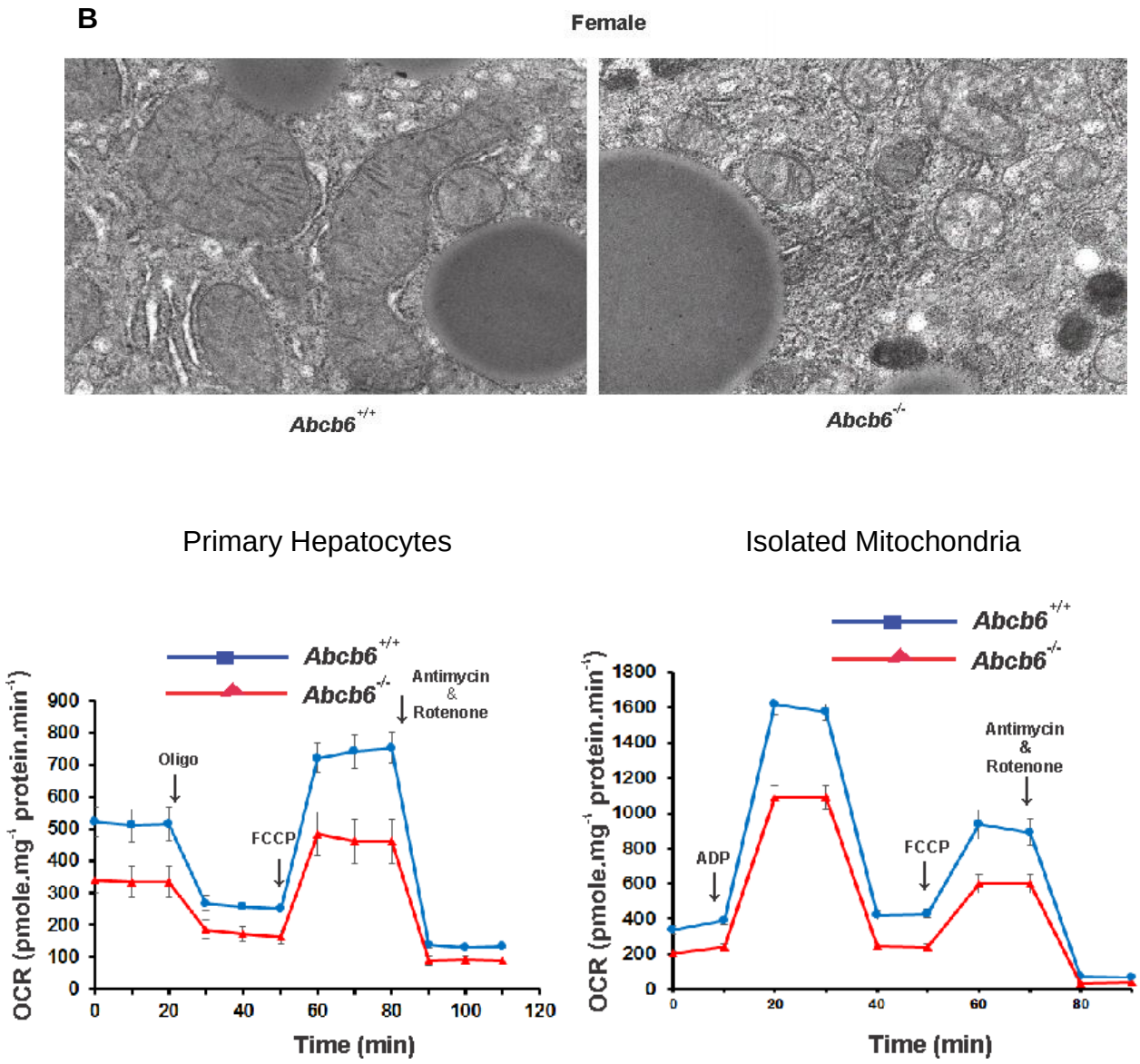

Figure 3.7 continued

C

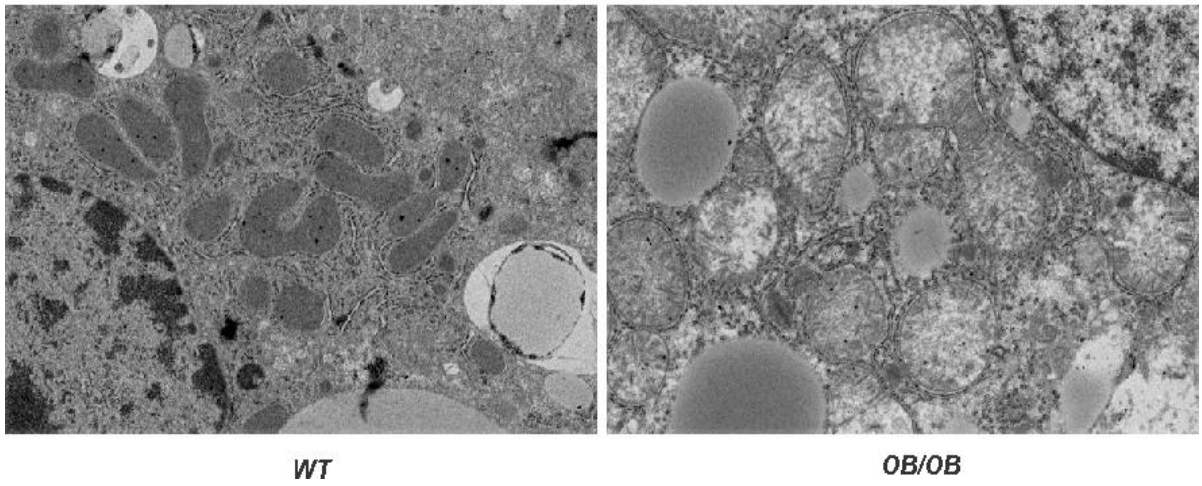

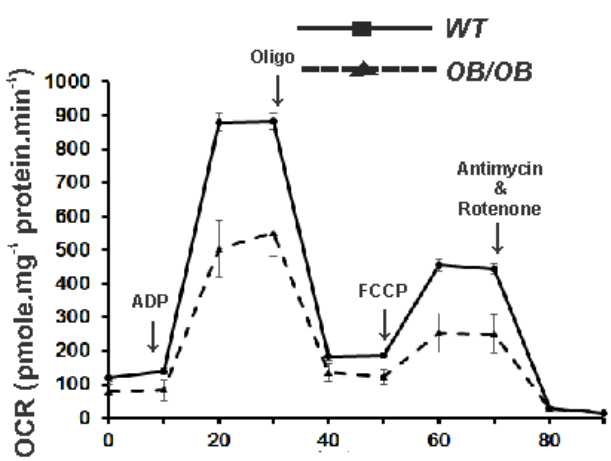

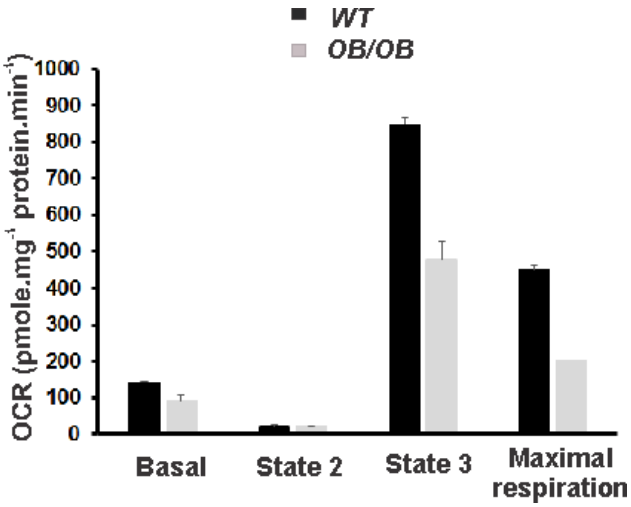

Figure 3.7 continued

D

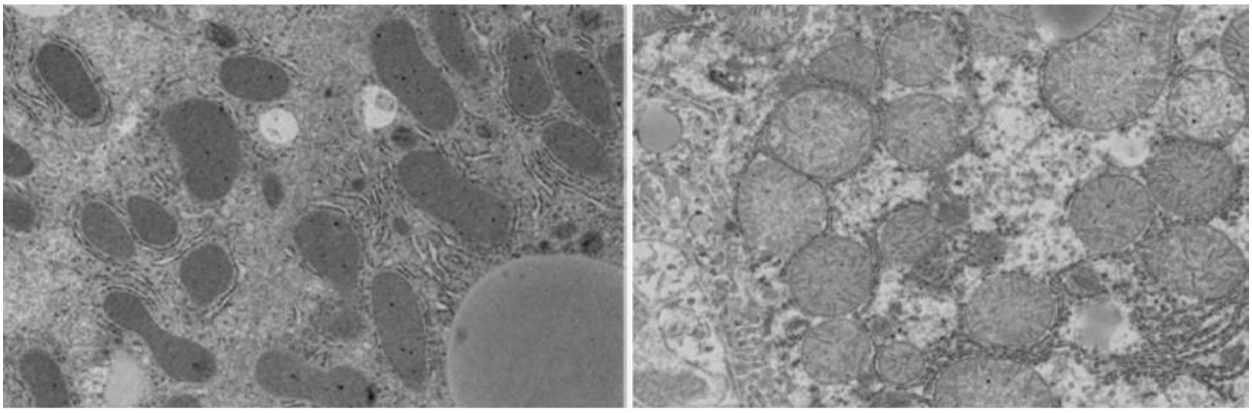

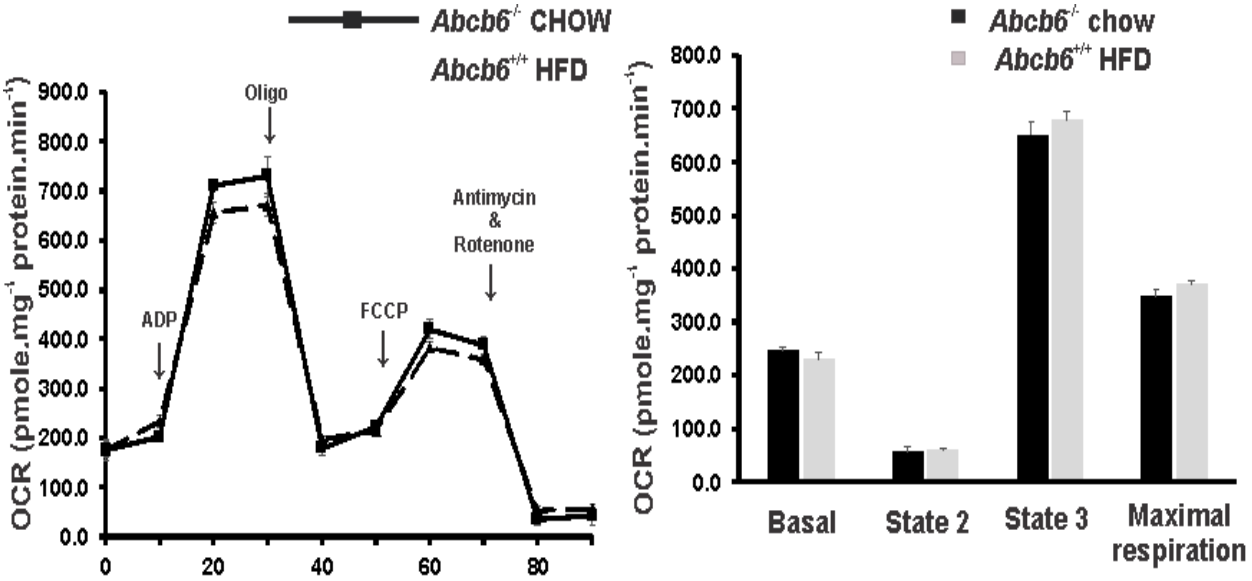

Figure 3.7 continued

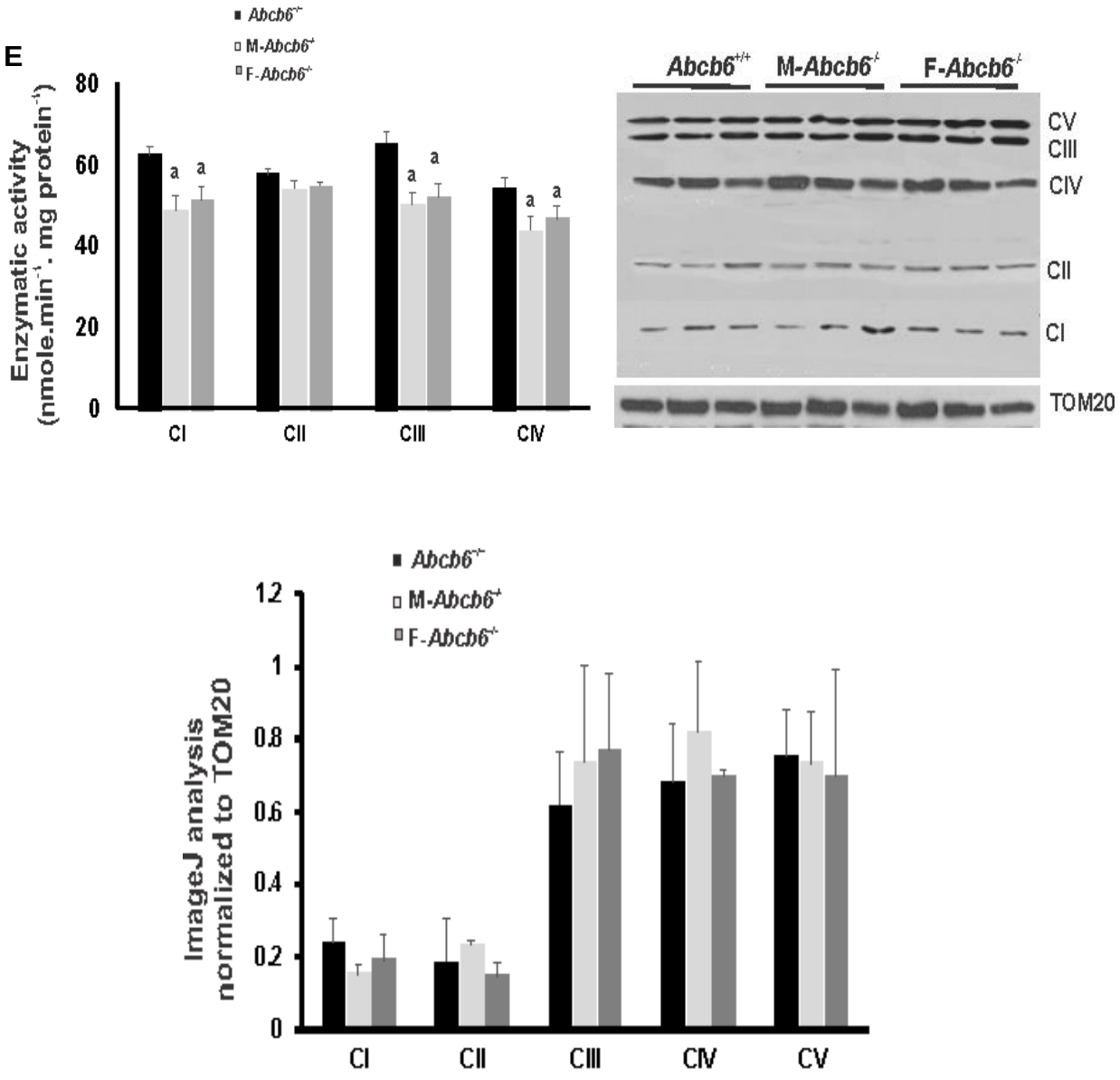

Figure 3.7 ABCB6 expression affects hepatic bioenergetic capacity

(A) Representative electron microscopic image showing the effects of *Abcb6* deficiency on hepatic mitochondrial morphology, primary hepatocyte bioenergetics and isolated mitochondrial bioenergetics in 6-week-old *Abcb6-WT* and *Abcb6-KO* male mice. (B) Representative electron microscopic image showing the effects of *Abcb6* deficiency on hepatic mitochondrial morphology, primary hepatocyte bioenergetics, and isolated mitochondrial bioenergetics in 6-week-old *ABCB6-WT* and Abcb6-KO female mice. (C) Representative electron microscopic image showing the effects of obesity on hepatic mitochondrial morphology and isolated mitochondrial bioenergetics in 8 -week-old leptin deficient ob/ob mice fed a standard chow diet. (D) Representative electron microscopic image showing the effects of diet induced obesity on hepatic mitochondrial morphology and isolated mitochondrial bioenergetics in mice fed HFD for 8 weeks. (E) Quantification of OXPHOS complex activity and expression in *Abcb6* deficient mice at 6 weeks of age.

3.4 Discussion

Overall our study sheds light on a yet unanticipated role for mammalian ABCB6 in normal body weight control. Our data establish that ABCB6 acts as a molecular determinant of metabolic homeostasis. *Abcb6* deficiency leads to a multisystem metabolic derangement reflected by glucose intolerance, insulin resistance, liver steatosis, and excess fat accumulation. Ultimately, this manifests as late onset obesity in the *Abcb6* knockout mice.

Although the mechanism underlying the metabolic phenotype of *Abcb6* deficiency remains to be delineated, our observation draws an interesting link between mitochondrial transport, mitochondrial function, metabolic flexibility and metabolic regulation. The best explanation we could identify for the differential gain in fat mass in

Abcb6-deficient mice is decreased EE as measured by indirect calorimetry. Regarding the source of the decreased EE in *Abcb6* deficient mice, the altered mitochondrial form and function observed in *Abcb6* deficiency provides an important clue, particularly given that these alterations in mitochondrial form and function as well as decreased EE occur simultaneously and prior to when the effect of *Abcb6* deletion on body weight is evident.

A number of studies have described reduced levels of mRNA for mitochondrial genes (Heilbronn *et al.*, 2007; Mootha *et al.*, 2003; Morino *et al.*, 2005; Patti *et al.*, 2003), decreased mitochondria DNA (Boushel *et al.*, 2007; Ritov *et al.*, 2005) and lower protein expression of respiratory chain subunits (Heilbronn, et al., 2007) in mitochondria isolated from insulin-resistant individuals. However, several features point to a more complex role for ABCB6 in mitochondrial bioenergetics and mitochondrial function. These include the decreased activity of the mitochondrial respiratory complexes without any change in the either the transcriptional or translational efficiency of many liver mRNAs encoding mitochondrial electron transport components. We speculate that change in mitochondrial form observed in *Abcb6* deficiency might be a contributing factor for decreased mitochondrial function. Such a functional change would be analogous to the Barth syndrome, a fatal X-linked recessive disease characterized by cardioskeletal myopathy (Barth *et al.*, 2004), where defective mitochondrial form correlates with reduced mitochondrial bioenergetics leading to severe cellular dysfunction (McKenzie *et al.*, 2006). Alterations in mitochondrial form have also been identified during aging (Frenzel *et al.*, 2010; Lombardi *et al.*, 2009; Lopez-Lluch *et al.*, 2015), as well as in metabolic disease (Arruda *et al.*, 2014) including type 2 diabetes (Antoun *et al.*, 2015).

Obesity is a major global public health concern that has now reached epidemic proportions. Obese individuals are faced with a markedly increased risk of cardiovascular disease, type 2 diabetes, osteoarthritis, and several metabolic syndromes. Of the many genes that have been reported to impact obesity in mice, only a handful of heritable genes have been identified in human genetic studies. Results from our studies suggest that ABCB6 expression correlates inversely with body weight gain. Although, gene association studies have established a strong link between loss of ABCB6 function with a variety of human diseases (Chavan, et al., 2015; Cui *et al.*, 2013; Wang, et al., 2012; Zhang, et al., 2013), it remains to be seen whether such loss of function mutations in *ABCB6* are also associated with human metabolic syndromes. Nevertheless, our finding that ABCB6 expression is down regulated in obese conditions, and loss of ABCB6 results in weight gain, and substantial metabolic phenotype supports the case for *Abcb6* as a causal gene in metabolic disease and provides a strong impetus to the investigation of the physiologic roles of the human *Abcb6* SNPs in metabolic disease.

In conclusion, our studies demonstrate that *Abcb6* deficient mice, both male and female, present impaired hepatic mitochondrial function and are susceptible to diet induced obesity, glucose intolerance, hepatic steatosis and adipose tissue expansion. Given that ABCB6 is ubiquitously expressed and that loss of ABCB6 results in a wide variety of human pathologies, it will be important to evaluate if ABCB6 has tissue specific effects that are dependent on mitochondrial function.

Chapter 4: ABCB6 Fine-tunes Metabolic Flexibility in Response to Physiological Signals

4.1 Abstract

Hepatic mitochondria undergo cyclical changes in their shape, size, and distribution to adapt their bioenergetic and biosynthetic output to the ever-changing anabolic/catabolic state of the liver. This adaptability allows organisms to switch freely between alternative fuels, according to physiological and nutritional circumstances, and is essential to maintain metabolic homeostasis. Here we provide evidence that the mitochondrial outer-membrane protein ABCB6 plays a pivotal role, in controlling systemic energy and body weight homeostasis, through temporal regulation of mitochondrial dynamics. In mice ABCB6 expression is in sync-with diurnal bioenergetic demands, and chronic loss or gain of hepatic ABCB6 results in lack of bioenergetic and biosynthetic adaptation of the mitochondria, leading to metabolic inflexibility and the development of metabolic disease. Our data suggest that ABCB6 acts as a conserved pivot for the adaptive metabolic responses to promote the bioenergetic and biosynthetic adaptation of the mitochondria, to the ever-changing anabolic/catabolic state of the liver.

4.2 Introduction

Organisms sense nutrients in the environment and adapt their metabolism based on the available energy. This adaptability, termed ‘metabolic flexibility’, allows organisms the ability to switch from fatty acid oxidation during the fasted state to enhanced glucose metabolism during the fed state (Kohler, 1985) (Gao *et al.*, 2014; Smith *et al.*, 2018b). During the last decade, mitochondria have independently emerged as key regulators of metabolic flexibility (Gao, et al., 2014; Liesa *et al.*, 2013; Stephenson *et al.*, 2014). Mitochondrion’s ability to regulate cellular processes such as ATP synthesis, autophagy/mitophagy, and apoptosis in response to changing energetic levels maintains metabolic homeostasis. Dysregulation in mitochondrial function has been shown to result in metabolic inflexibility leading to the inability of the organism to adapt its metabolism to energetic changes, resulting in the development of metabolic diseases such as obesity and insulin resistance (Corpeleijn *et al.*, 2009; Galgani *et al.*, 2008; Gao, et al., 2014; Smith, et al., 2018b).

Two main mechanisms allow mitochondria to adjust ATP synthesis to changes in energetic demand and to control metabolic flexibility (i) acute change of both mitochondrial dynamics (fusion and fission) and post-translational modifications, and (ii) longer-term modification of mitochondrial quantity.(Gao, et al., 2014). Evidence suggests that mitochondrial response to nutrients is mediated by the acute change; mitochondrial dynamics, which is shaped by fusion and fission (Gao, et al., 2014). In nutrient excess, cells maintain their mitochondria in a fragmented state, while during fasting/starvation mitochondria tend to persist in a fused state (Gomes *et al.*, 2011a; Liesa, et al., 2013; Molina *et al.*, 2009). While the complete lack of fusion or fission

results in embryonic lethality (Chen *et al.*, 2003; Davies *et al.*, 2007; Ishihara *et al.*, 2009), shifts in balance between fusion and fission are an important adaptive process required to retain mitochondrial flexibility and health upon changes to our environment (Kulkarni *et al.*, 2016; Sebastian *et al.*, 2012; Wang *et al.*, 2015). However, our understanding of the potential mechanisms that regulate the dynamic shifts in fusion and fission, to remodel mitochondrial architecture upon whole-body physiology remain largely incomplete.

In this report, we show that ABCB6, a mitochondrial outer membrane ATP binding cassette protein, is an important regulator of mitochondrial form and function in the liver. Loss of ABCB6 in hepatocytes leads to a pronounced shortcoming in mitochondrial morphology that favors fission. In contrast liver-specific overexpression of ABCB6 favors fusion which results in elongated mitochondria. In addition, we find that ABCB6 expression is in sync-with diurnal bioenergetic demands, and that chronic loss or gain of ABCB6 results in lack of biosynthetic adaptation of the mitochondria to the changing anabolic/catabolic state of the liver leading to metabolic inflexibility. Although, the exact mechanism by which ABCB6 regulates mitochondrial dynamics and metabolic homeostasis is not completely clear, the strength of evidence presented in this report favors the hypothesis that ABCB6 is a potential regulator of mitochondrial form and function and suggests a role for ABCB6 in linking environmental stimuli to mitochondrial dynamics and metabolic flexibility.

4.3 Results

Genetically engineered hepatic ABCB6 deficient mice exhibit altered mitochondrial form.

We used adeno associated viral delivery of Cre-recombinase, driven by liver specific Thyroxine- binding globulin (TBG) promoter, to eliminate hepatic ABCB6 expression postnatally (Figure 4.1A). This approach eliminated ABCB6 expression by > 85% ten days post infection (Figure 4.1B). In the rest of this dissertation, liver specific ABCB6 deficient mice are designated by the acronym *Abcb6LKO,* liver-specific overexpressing mice by *Abcb6LOE,* and *Abcb6* wild-type control mice are designated by the acronym *Abcb6WT*.

Although, ABCB6 has been shown to regulate heme synthesis *in vitro* (Krishnamurthy, et al., 2006), loss of ABCB6 in the present mouse model did not affect hepatic heme levels (Figure 4.1C), nor were there any compensatory responses in the expression of heme synthesis pathway genes (Figure 4.1D). However, quite surprisingly, mice with liver-specific deletion of ABCB6 (Figures 4.1E-1G) displayed a shift in mitochondria size distribution, toward rounder, shorter organelles, compared to wild-type littermate controls (*Abcb6WT*) (Figure 4.1H). We performed a systematic evaluation of these mitochondrial alterations and found an overall increase (~26%) in the mitochondrial number in *Abcb6LKO* mice (338 in Abcb6LKO vs 269 in *Abcb6WT* mice per image of 980 μm^2; (Figure 4.1I). However, we found that on an average the area of the individual mitochondrion decreased by ~16% in *Abcb6LKO* mice (0.606 μm^2 in *Abcb6LKO* livers vs 0.724 μm^2 in *Abcb6WT* livers; (Figure 1K) without any significant difference in the total mitochondrial area between the two groups of animals (Figure 4.1J). We found that this

change in decreased mitochondrion area in *Abcb6LKO* mice was due to a shift in mitochondria size distribution toward rounder (Figure 4.1H), shorter organelles (Figure 4.1L-1N).

Figure 4.1

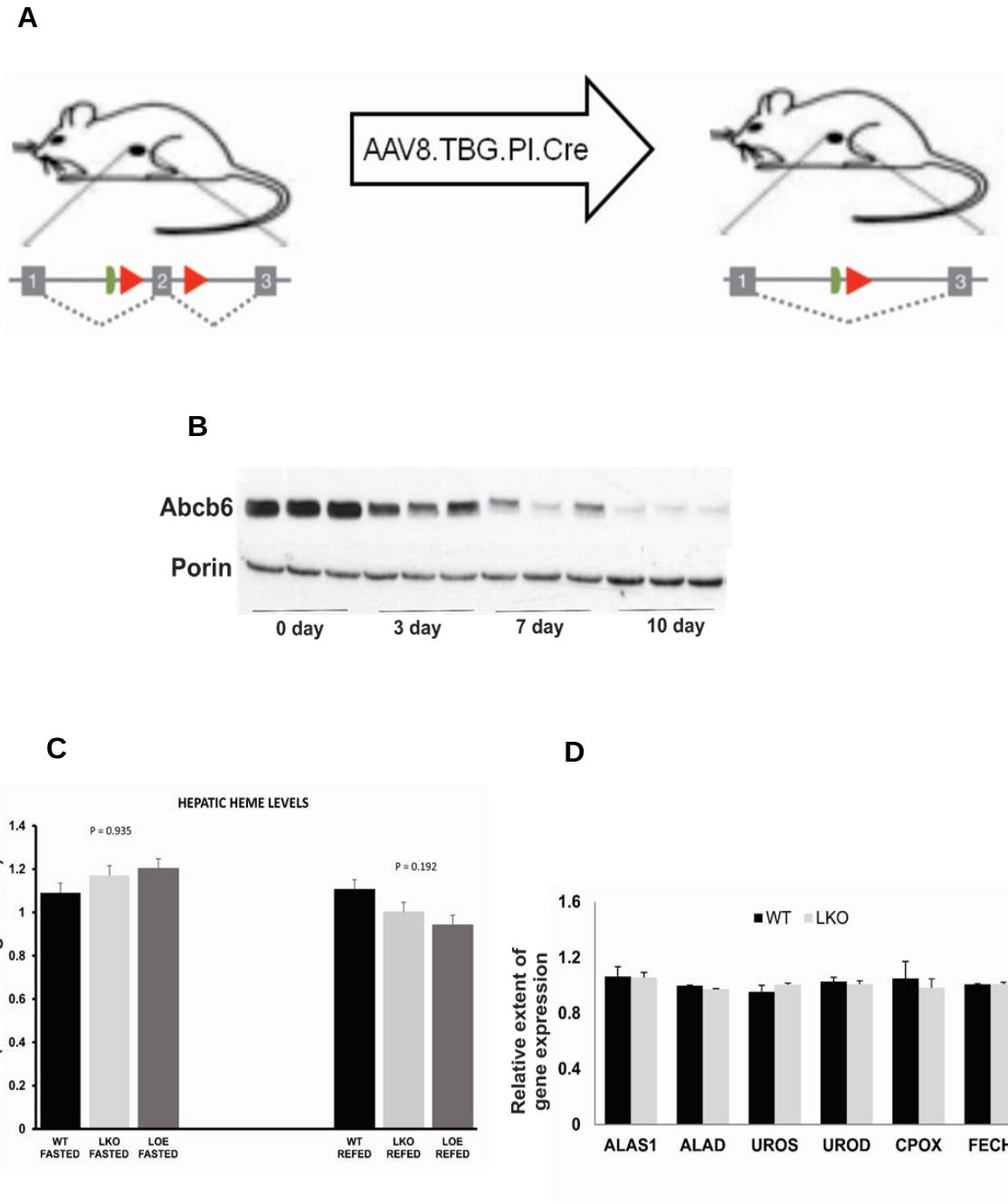

Figure 4.1 cont

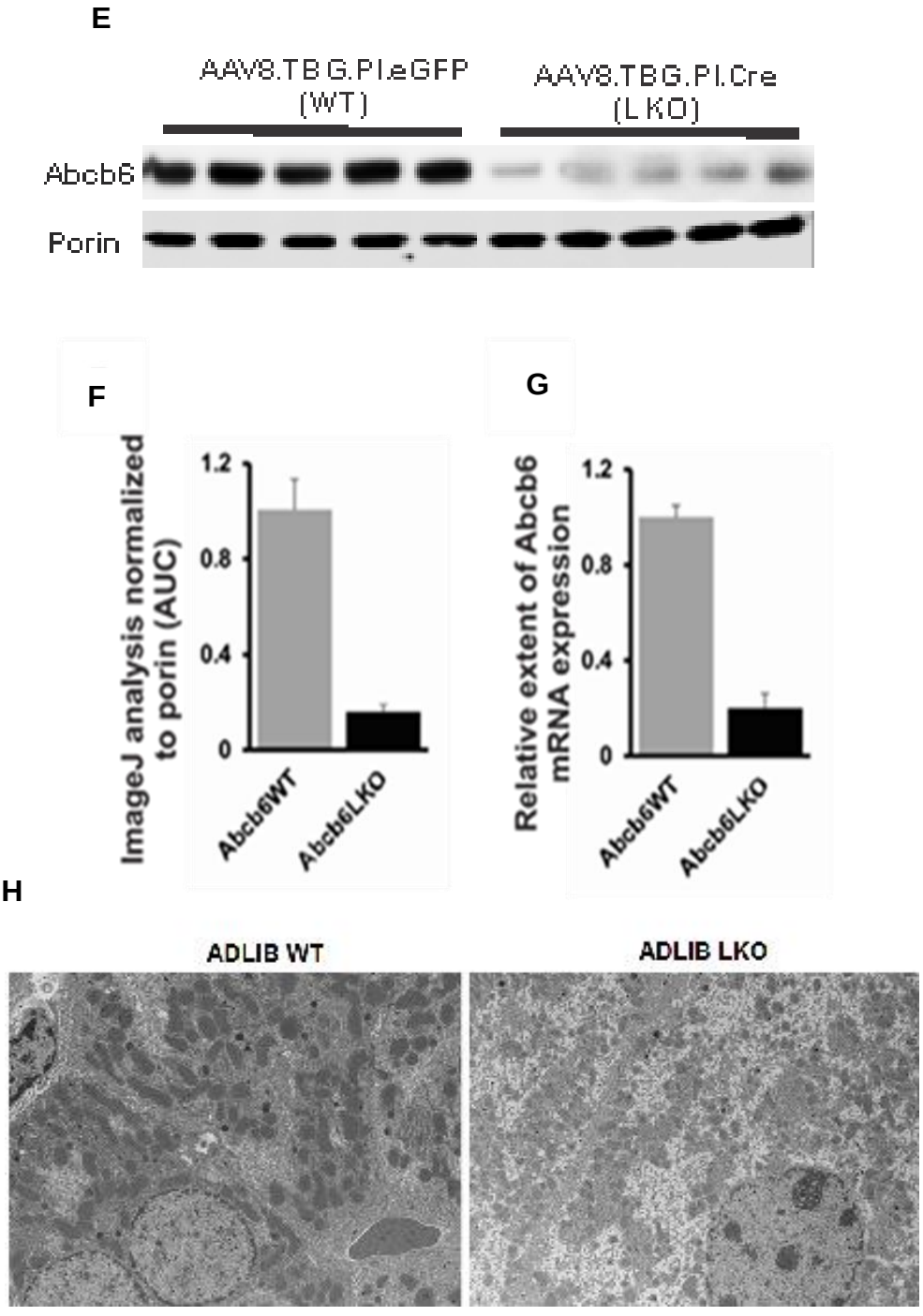

Figure 4.1 continued

I

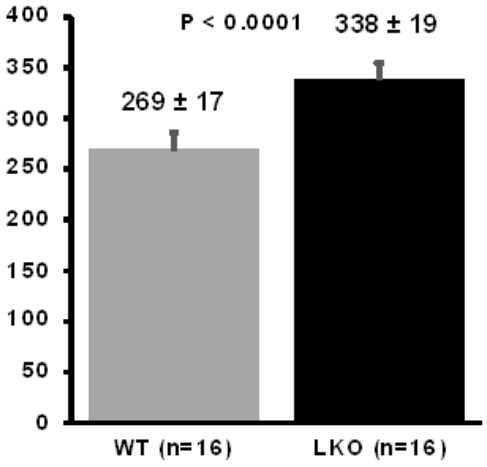

J

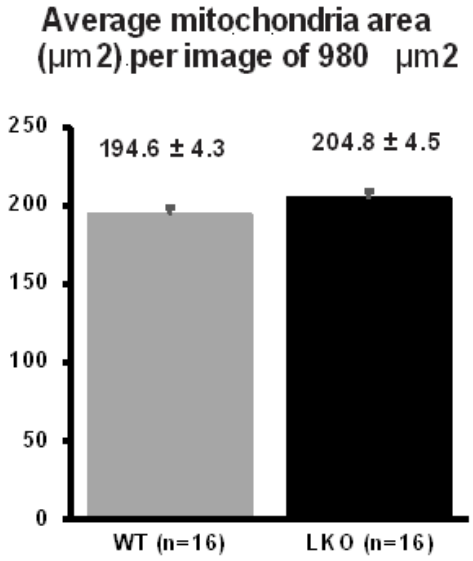

K

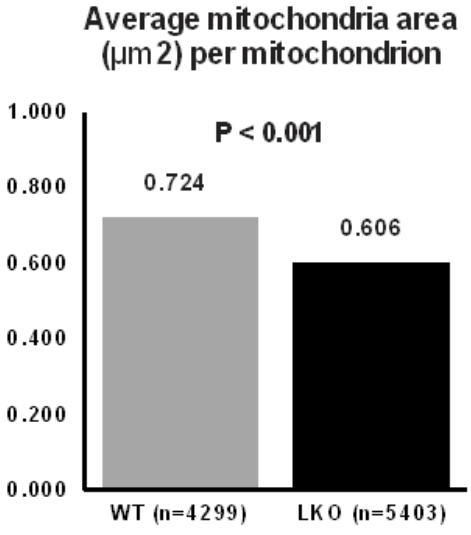

L

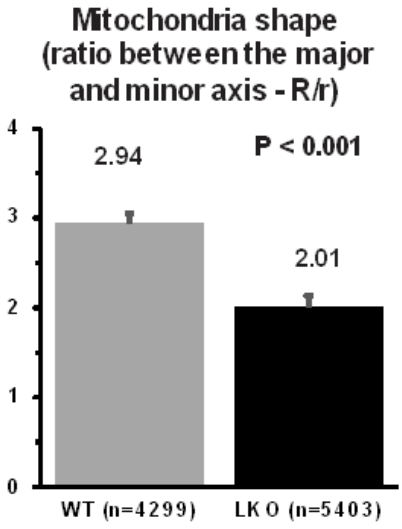

Figure 4.1 continued

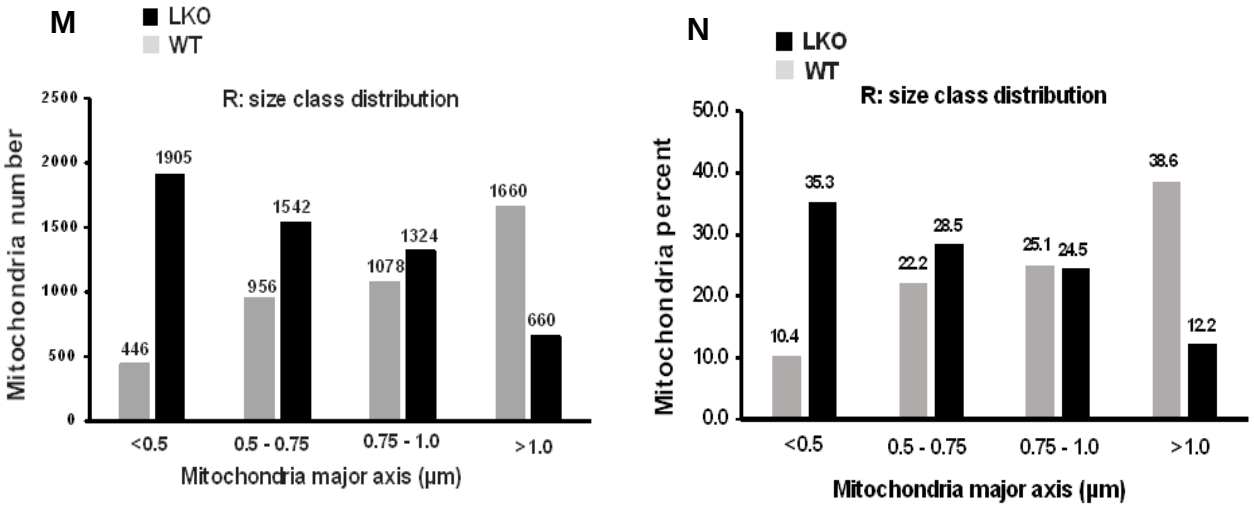

Figure 4.1 Loss of hepatic ABCB6 is linked to fragmentation of the mitochondrial network

(A) Schematic representation of the generation of tissue specific *Abcb6* knockout mice using the Cre-loxP system. The floxed *Abcb6* gene mouse line contains loxP sites flanking exon 2. Injection of AAV8 viral particles carrying the Cre-recombinase under the control of liver specific (TBG) promoter deletes the intervening DNA sequence resulting in loss of exon 2. (B) Immunoblot analysis of ABCB6 expression in *Abcb6*-floxed mice injected with AAV8-TBG-PI. Cre. (C) Hepatic heme levels in *Abcb6WT, Abcb6LKO*, and *Abcb6LOE* mice. (D) RTPCR analysis of hepatic enzymes involved in heme biosynthesis in *Abcb6WT* and *Abcb6LKO* mice. Histograms represent mean ± SD.

(E) Representative western blot analysis of ABCB6 and Porin in *Abcb6LKO* and *Abcb6WT* mice at 10 days post infection. Porin is used as a loading control. (F) ImageJ analysis of protein bands normalized to porin. Average of three independent studies with 5 mice per group per study. Histograms are mean ± SD (G) RTPCR analysis of *Abcb6* transcript levels in *Abcb6LKO* and *Abcb6WT* mice. Average of three independent studies with 5 mice per group per study. Histograms are mean ± SD (H) Representative EM image of liver mitochondria used to study mitochondrial number, area and morphology. (I-N) Effect of hepatic *Abcb6* deficiency on (I)

average mitochondria number per image, (J) average mitochondria area per image, (K) average area per mitochondrion, (L) mitochondria shape, (M) mitochondria number major axis class distribution, (N) mitochondria percent major axis class distribution. Mitochondrial network dynamics were calculated in 16 images (2 images per mice per genotype) each of 980 μm^2 representing 8 *Abcb6LKO* and 8 *Abcb6WT* mice. Values represent mean ± SD.

Genetically engineered hepatic ABCB6 overexpressing mice exhibit altered mitochondrial form

We next tested whether ectopic overexpression of ABCB6 in wildtype mice would affect mitochondrial morphology. We used adenoviral associated viral delivery of *Abcb6* gene, driven by liver specific TBG-promoter to ectopically express ABCB6 in the livers of *Abcb6WT* mice. This delivery method resulted in a ~ 4-fold increase in ABCB6 expression in the livers of *Abcb6WT* mice by 10 days post infection (Figure 4.2A-4.2C). In the rest of the dissertation liver specific ABCB6 overexpressing mice are designated by the acronym *Abcb6LOE*.

We found that ectopic overexpression of ABCB6 resulted in mitochondria that were significantly more elongated than those observed in *Abcb6WT* mice that received control AAV particles (Figure 4.2D). A systematic evaluation of these mitochondrial alterations demonstrated an overall decrease (~ 18%) in the mitochondrial number (174 *Abcb6LOE* mice vs 266 in *Abcb6WT* mice per image of 980 μm^2; Figure 4.2E), and an overall increase in the area of the individual mitochondrion in *Abcb6LOE* mice (1.191 μm^2 in *Abcb6LOE* livers vs 0.782 μm^2 in *Abcb6WT* livers; Figure 4.2G). However, we did not find any significant difference in the total mitochondrial area between the two groups of animals (Figure 4.2F). As with the *Abcb6LKO* mice the change in individual mitochondrion

area and number in *Abcb6LOE* mice appear to result from a shift in mitochondria size distribution toward longer, elongated organelles (Figures 4.2H – 4.2J). Together these results causally link ABCB6 expression to mitochondrial morphology.

Figure 4.2

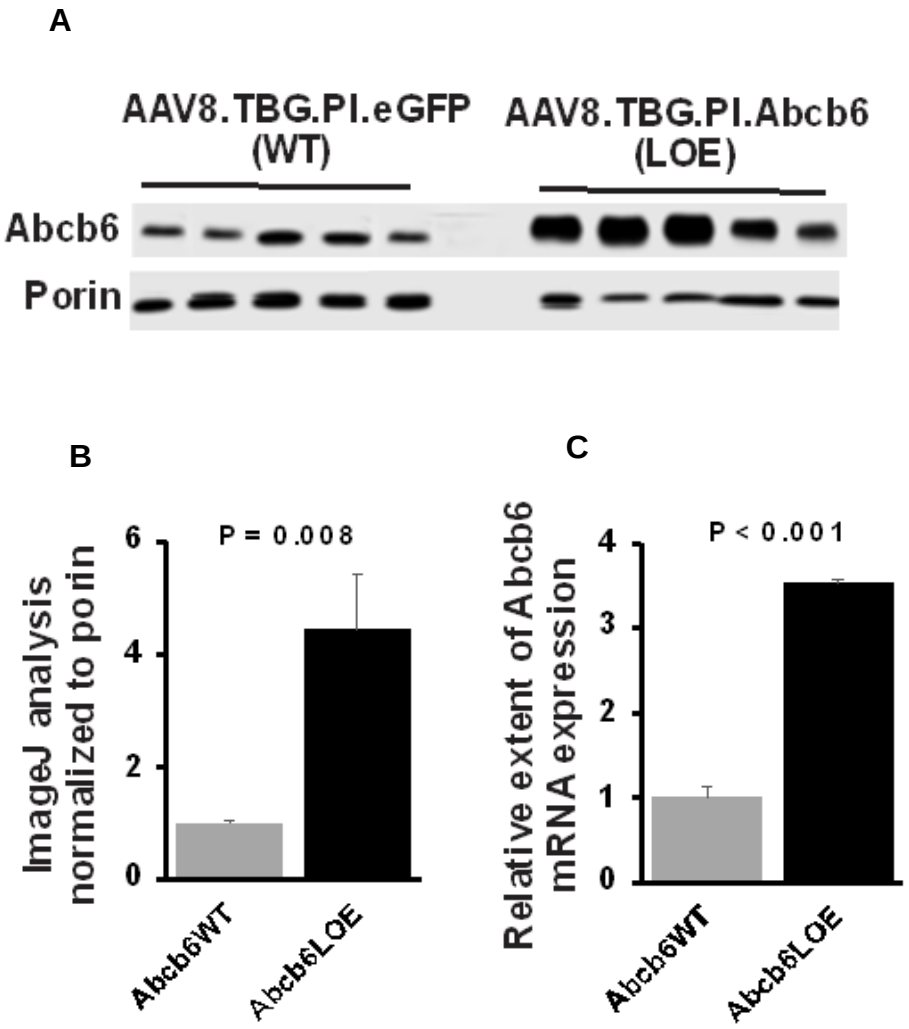

Figure 4.2 continued

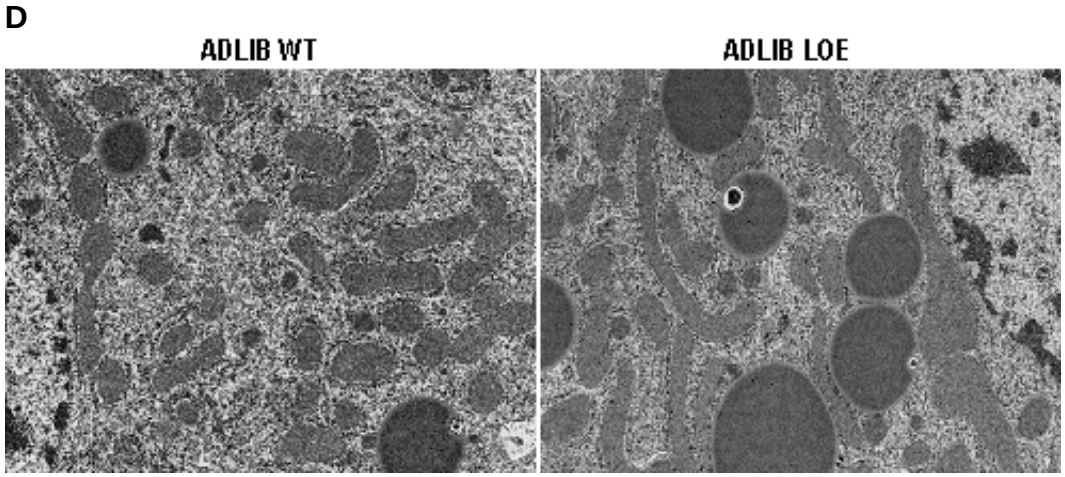

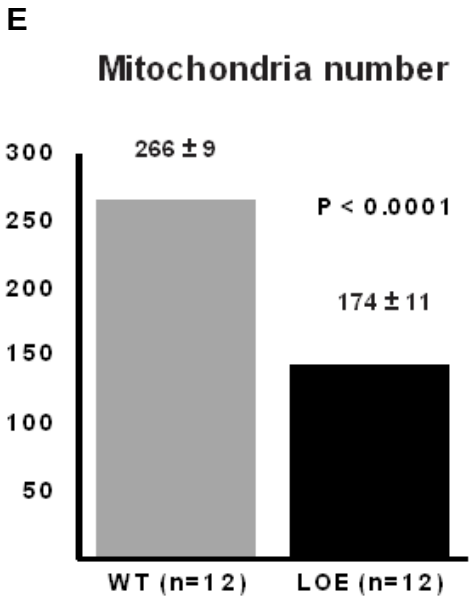

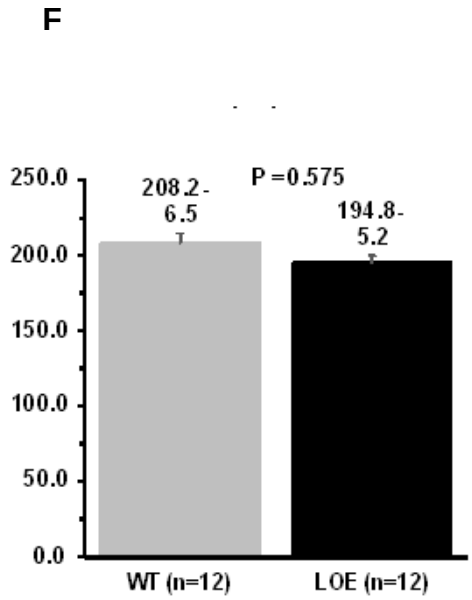

Figure 4.2 continued

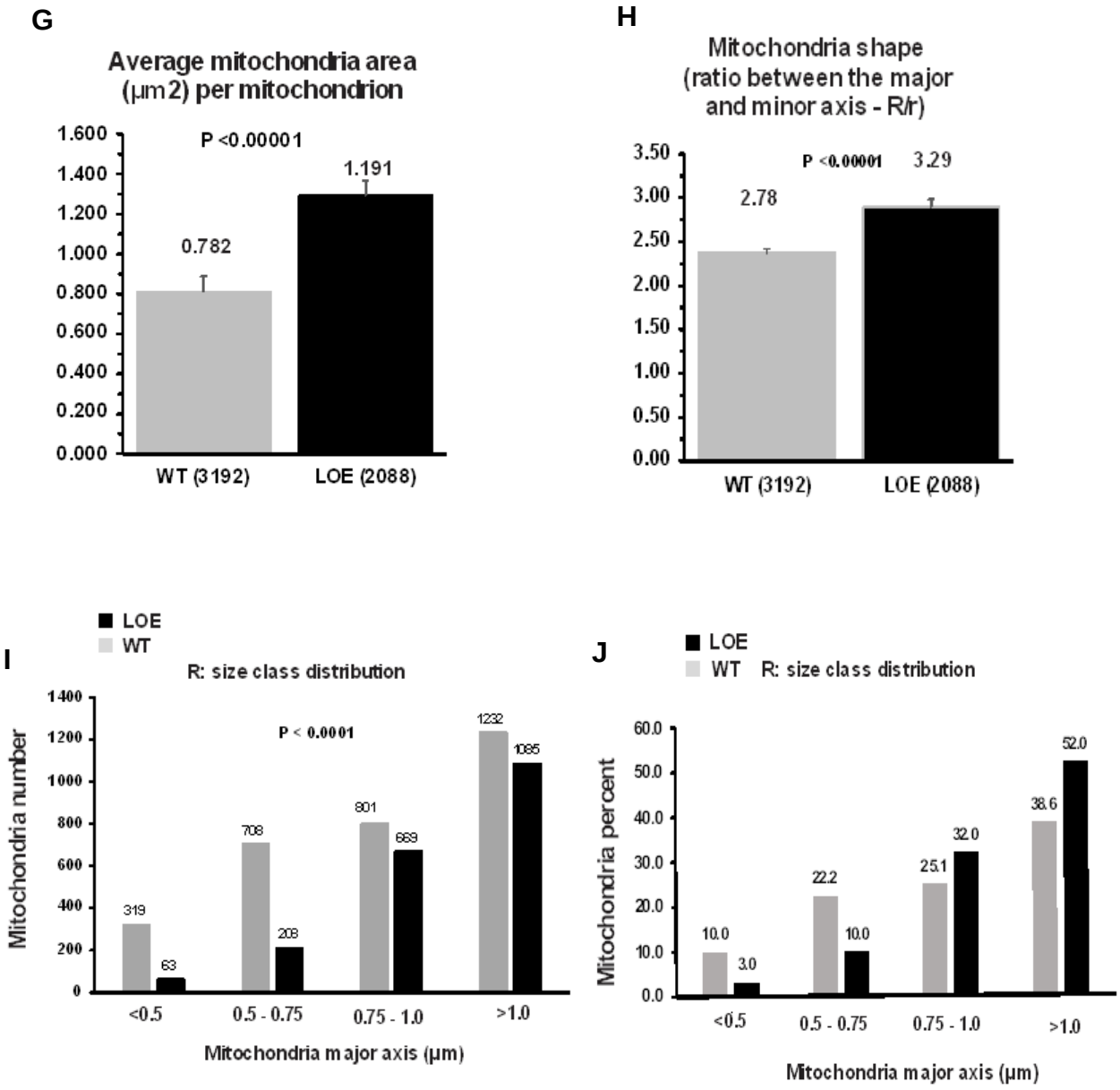

Figure 4.2 Overexpression of hepatic ABCB6 is linked to hyper-fusion of the mitochondrial network

(A) Representative western blot analysis of ABCB6 and Porin in *Abcb6LOE* and *Abcb6WT* mice. Porin is used as a loading control**.** (B) ImageJ analysis of protein bands normalized to porin. Average of three independent studies with 5 mice per group per study. Histograms are mean ±

SD (C) RTPCR analysis of *Abcb6* transcript levels in *Abcb6LOE* and *Abcb6WT* mice. Average of three independent studies with 5 mice per group per study. Histograms are mean ± SD. (D) Representative EM image of liver mitochondria used to study mitochondrial number, area and morphology. (E-J) Effect of ABCB6 overexpression on (E) average mitochondria number, (F) average mitochondria area per image, (G) average area per mitochondrion, (H) mitochondria shape, (I) mitochondria number major axis class distribution, (J) mitochondria percent major axis class distribution. Mitochondrial network dynamics were calculated in 12 images (2 images per mice per genotype) each of 980 μm^2 representing 6 *Abcb6LOE* and 6 *Abcb6WT* mice. Values represent mean ± SD.

Altered mitochondrial form in genetically engineered hepatic Abcb6 deficient and Abcb6 overexpressing mice results in altered mitochondrial function

Mitochondrial architecture, through the balance between fusion and fission events, represents a central mechanism for bioenergetic adaption (Cheng *et al.*, 2013; Liesa, et al., 2013; Nasrallah *et al.*, 2014). In general, elongated mitochondria (fusion) are considered to be in a state of increased bioenergetic efficiency, while in contrast shortened mitochondria (fission) are considered to be in a state of decreased bioenergetic efficiency (Liesa, et al., 2013). We hypothesized that increased mitochondrial elongation following ABCB6 overexpression would favor increased bioenergetic efficiency, while increased mitochondrial shortening in ABCB6 deficiency might favor decreased bioenergetic efficiency. To test this hypothesis, we measured the bioenergetic function of mitochondria isolated from wildtype, ABCB6 deficient and ABCB6 overexpressing livers by determining the oxygen consumption rate (OCR) using seahorse XF24 extracellular flux analyzer (Figure 4.3). Isolated mitochondria were loaded into different wells of the same seahorse plate and assayed with succinate as

fuel. Prior to the assay, we confirmed that equal amounts of functional mitochondria and mitochondrial content were present in all mitochondrial preparations by directly staining and imaging the wells of the XF24 flux analyzer plate with Mitotracker (Figure 4.3A), and by immunoblot analysis of mitochondrial preparations for equal protein content (Figure 4.3B). Extracellular flux analyzer studies revealed a significant decrease in basal respiration, ATP-synthesizing respiration (state III) and maximal respiratory capacity induced by uncoupling with FCCP (maximal) in *Abcb6LKO* mitochondria compared to *Abcb6WT* mitochondria (Figure 4.3C). In contrast these same parameters were significantly increased in *Abcb6LOE* mitochondria compared to *Abcb6WT* mitochondria (Figure 4.3D).

The oxidative phosphorylation system, consisting of the four multimeric enzyme complexes (CI–CIV) of the respiratory chain, and the ATP synthase complex (CV), drives the synthesis of ATP in most cells and defines the bioenergetic efficiency of the mitochondria. We wondered whether altered expression of oxidative phosphorylation complexes contributed to the differential bioenergetic capacity of the hepatic mitochondria in ABCB6 deficient and ABCB6 overexpressing mice. To test this, we performed a denaturing gel electrophoresis of mitochondrial proteins isolated from *Abcb6LKO*, *Abcb6LOE*, and *Abcb6WT* mice liver. We first confirmed that equal amounts of protein were loaded by staining western blot membranes with the non-specific protein dye Ponceau S (Figure 4.3E & Figure 4.3F). To control for mitochondrial protein loading, we normalized bands to the mitochondrial protein Porin, which did not vary significantly between samples. Surprisingly, western blot analysis revealed no significant difference in the protein levels of any of the complexes in either the

Abcb6LKO or *Abcb6LOE* mice compared to *Abcb6WT* controls (Figure 4.3G and 4.3H). Quantification of the protein bands in the immunoblots allowed confirmation of the lack of significant differences in the expression of respiratory complexes between the *Abcb6* genotypes (Figure 4.3I and Figure 4.3J).

With the advent of native electrophoretic gel systems that could separate large membrane complexes, respiratory super complexes were shown in a wide variety of eukaryotes, including yeast, plants, and animals (Genova, et al., 2014; Schagger *et al.*, 2000). These super complexes have been hypothesized to be important in stabilizing the levels of the individual respiratory complexes themselves, and increasing the efficiency of electron transport, thus enhancing the overall respiratory complex activity and mitochondrial function (Greggio *et al.*, 2017; Lapuente-Brun *et al.*, 2013). Given the lack of difference in respiratory complex protein levels in *Abcb6LKO* and *Abcb6LOE* mitochondria, we speculated if the differences in respiratory capacity could be due to changes in the assembly of respiratory super complexes. To test this, we analyzed super complex assembly in *Abcb6LKO*, *Abcb6LOE* and *Abcb6WT* mitochondria using native gel electrophoresis (blue native PAGE; BNPAGE). As with the denaturing gel electrophoresis, in BNPAGE we first confirmed that equal amounts of protein were loaded by normalizing bands to the mitochondrial protein VDAC, which did not vary significantly between samples. We first labeled in detail the specific SCs in *Abcb6WT* mice using the most recent description and characterization of SC structure in mammalian tissues (Greggio, et al., 2017). In line with previous reports, CI was mostly found in super-assembled species. CII existed predominantly, but not exclusively, as a single band. CIII and CIV existed both as free and super-assembled species (Figure

4.3K). Interestingly, blue native PAGE revealed an overall decrease in the assembly of SCs (specifically SCs I+III+IV) in *Abcb6LKO* mice, while an overall increase in SC assembly was observed in *Abcb6LOE* mice, compared to control *Abcb6WT* mice (Figure 4.3L). Quantification of BNPAGE confirmed significant differences in SCs in *Abcb6LOE* and *Abcb6LKO* mice (Figure 4.3M). To establish this observation further we analyzed the distribution of CI and CIII SCs, the two most prominent SCs in mammals. We observed that the fraction of CI and CIII allocated to SCs were lower in Abcb6LKO mice and higher in *Abcb6LOE* mice compared to the *Abcb6WT* controls (Figures 4.3N and 4.3O). Quantification of BNPAGE CI and CIII SCs allowed us to confirm a significant change in the assembly of SCs I and III between the genotypes (Figures 4.3P and 4.3Q).

Taken together our results suggest that ABCB6 expression dependent change in mitochondrial function is driven by reorganization of the OXPHOS super complexes without any significant change in the overall expression of the individual protein complexes.

Figure 4.3

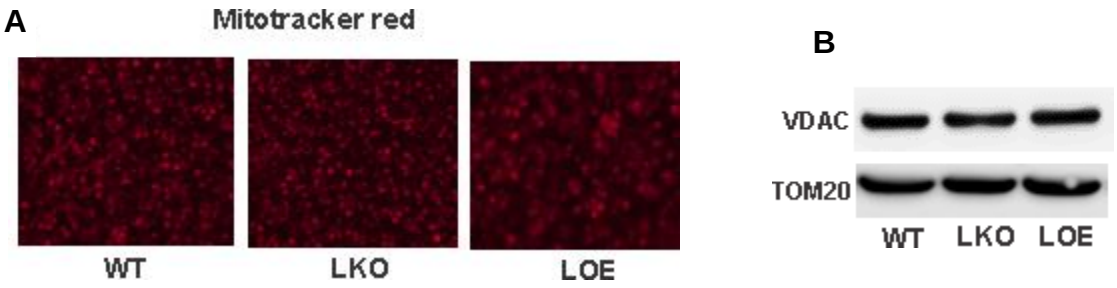

Figure 4.3 cont

C

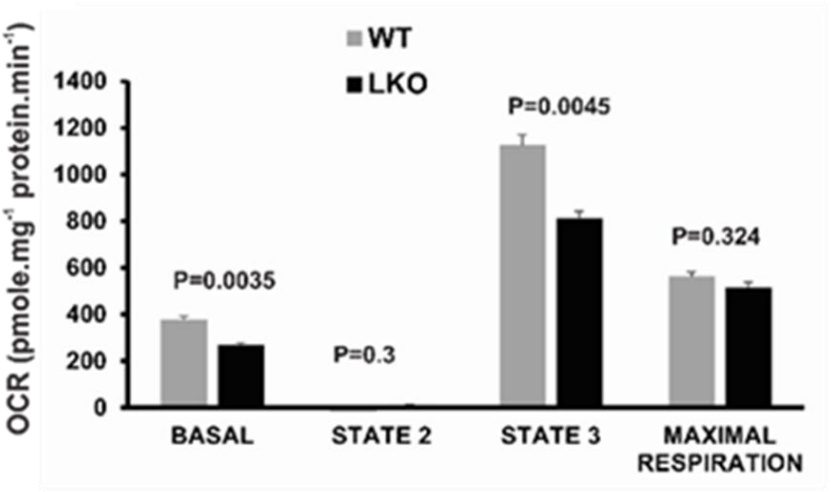

D

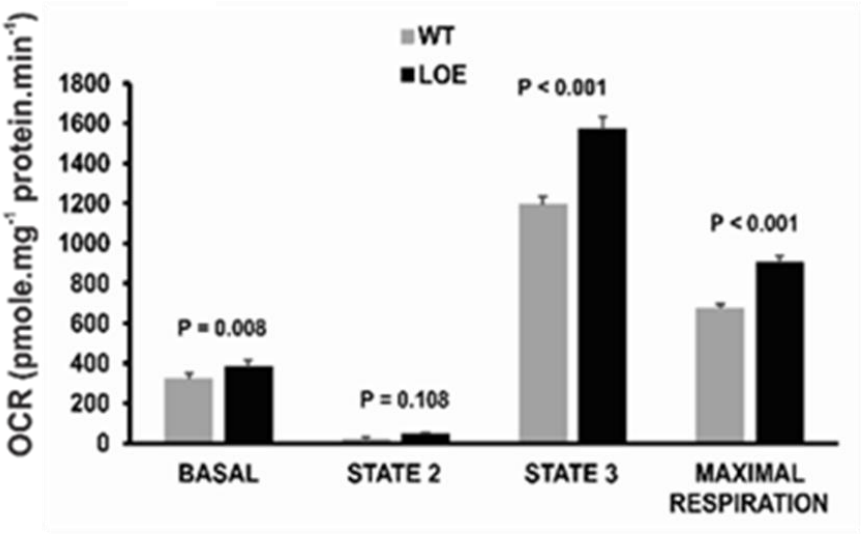

Figure 4.3 cont

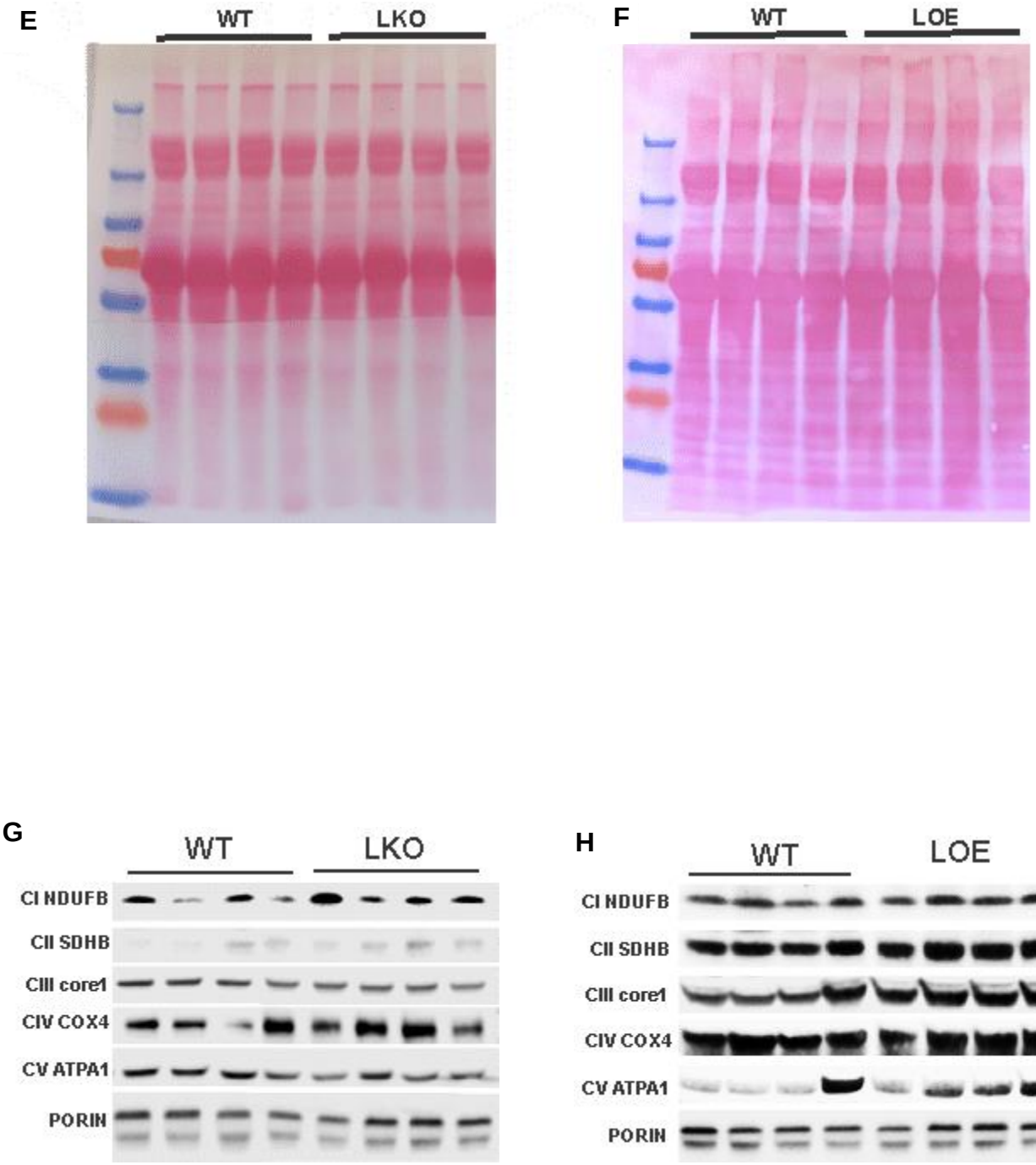

Figure 4.3 continued

I

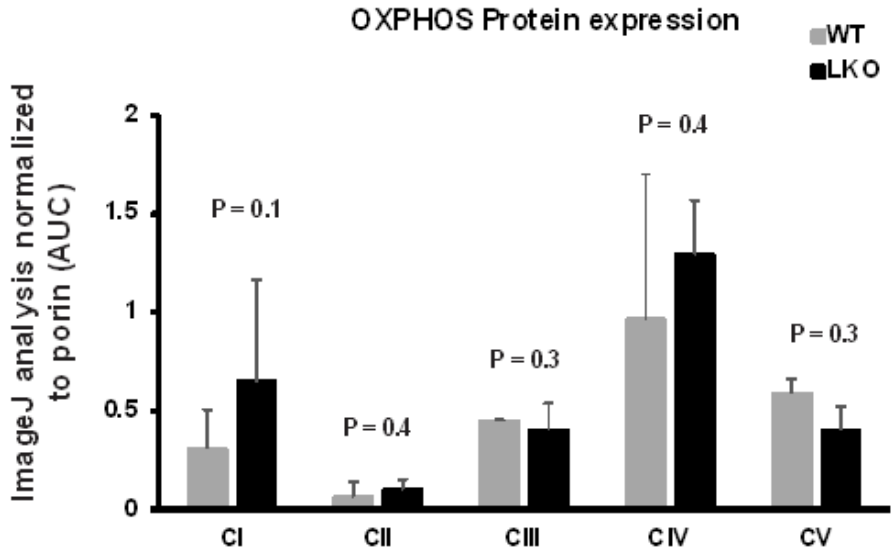

J

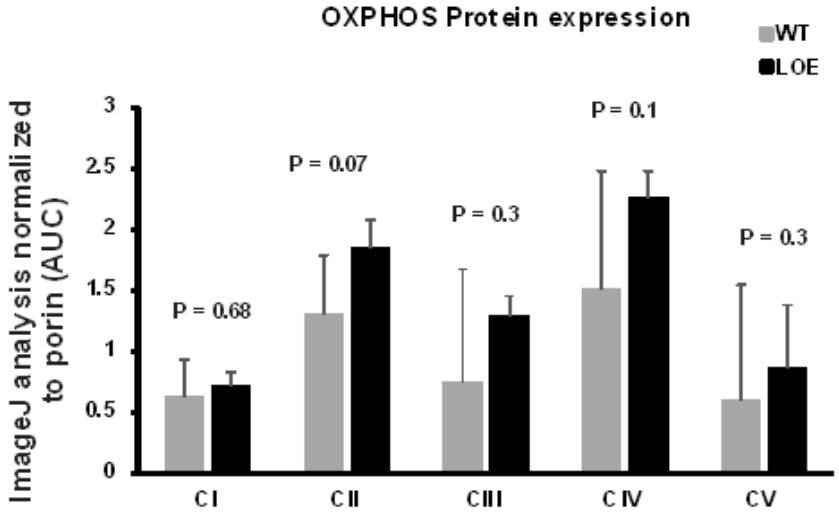

Figure 4.3 continued

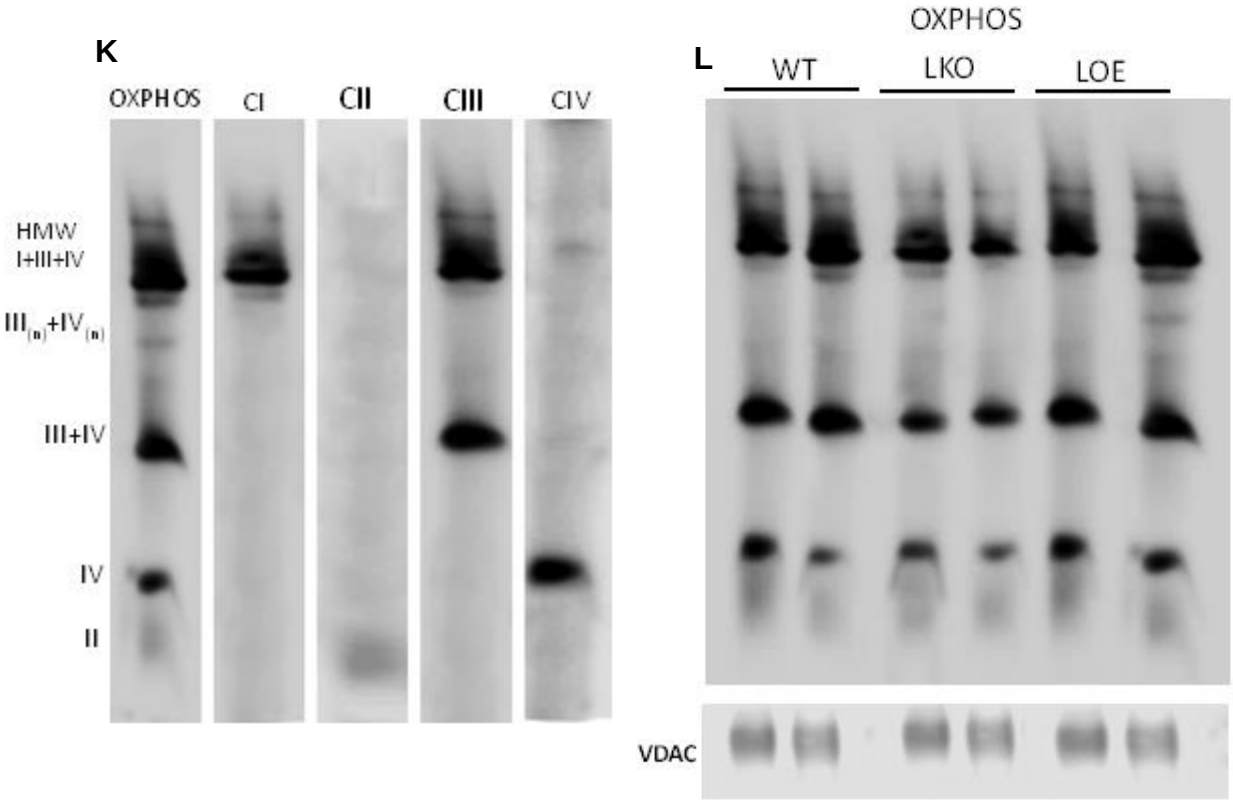

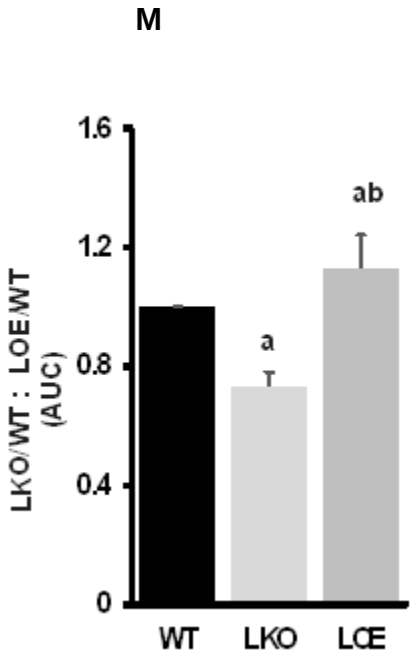

Figure 4.3 continued

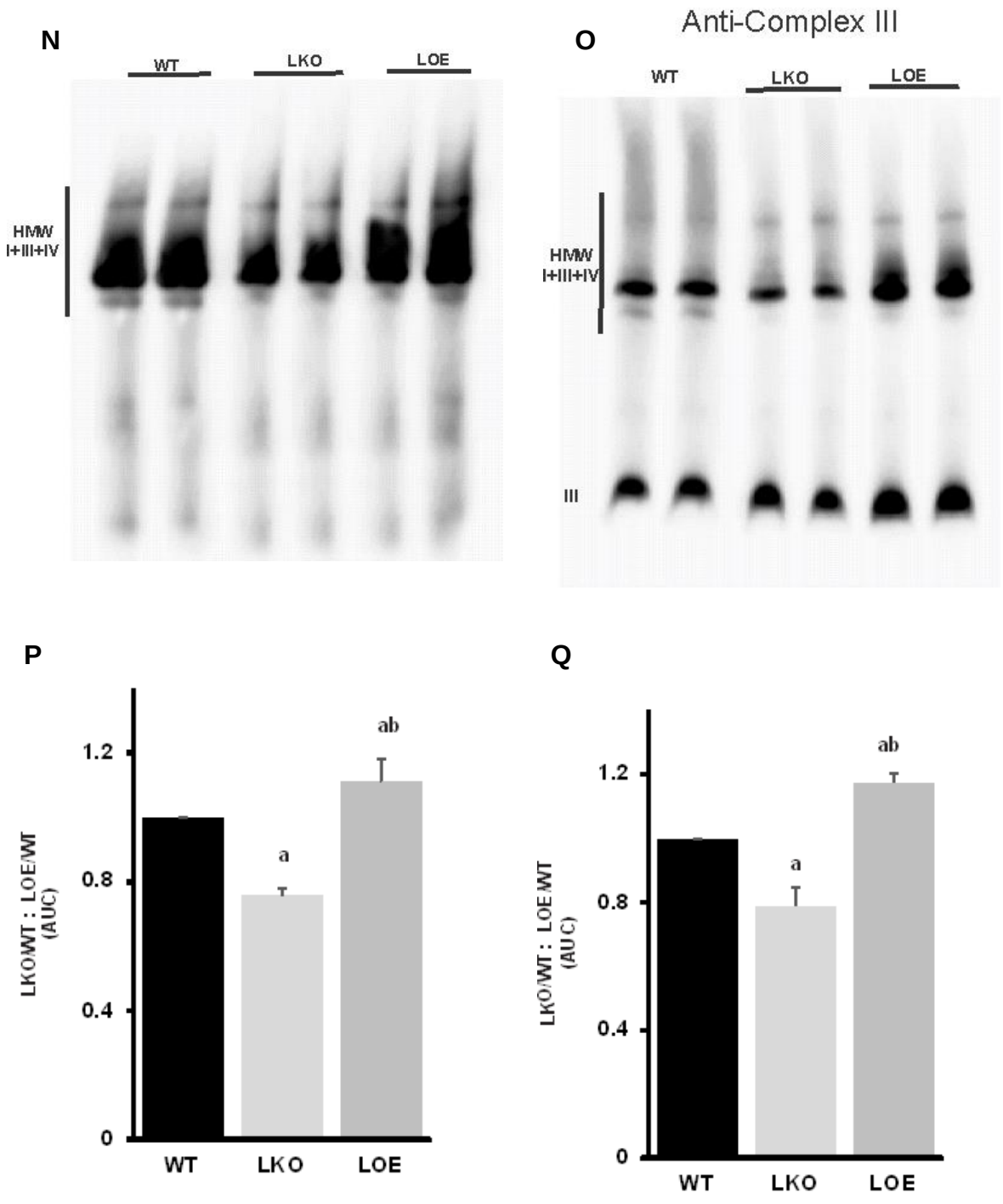

Figure 4.3 ABCB6 expression affects hepatic bioenergetic capacity

(A) Representative fluorescence microscopy image of Seahorse respirometry plate wells containing isolated mitochondria stained with MitoTracker Red. (B) Representative Immunoblot

analysis of VDAC and Tom20 in mitochondria that were in the Seahorse respirometry plates. (C - D) Quantification of OCR at different mitochondrial respiratory states in a representative experiment using mitochondria isolated from (C) *Abcb6WT* and *Abcb6LKO* mice and (D) *Abcb6WT* and *Abcb6LOE* mice, driven with succinate. ADP, oligomycin, FCCP, and antimycin were sequentially injected to assess mitochondrial respiratory states. 4-6 replicates per group. (E and F) Western blot analysis of (E) *Abcb6WT* and *Abcb6LKO* mitochondria and (F) *Abcb6WT* and *Abcb6LOE* mitochondria stained with the dye Ponceau S for total protein loading. (G-H) Representative western blot analysis of OXPHOS complex subunits I-V (CI-CV) in mitochondria isolated from (G) *Abcb6WT* and *Abcb6LKO* mice and (H) *Abcb6WT* and *Abcb6LOE* mice. Porin is used as a loading control. (I-J) Quantification of OXPHOS complex subunits (average of n=5 independent isolations) normalized to Porin loading control in mitochondria isolated from (I) *Abcb6WT* and *Abcb6LKO* mice and (J) *Abcb6WT* and *Abcb6LOE* mice. (K) Representative BN-PAGE analysis of mitochondrial extracts from *Abcb6WT* mice. Specific antibodies against individual ETC complexes were used separately. The high molecular weight bands (HMW), were mainly composed of SC I_n+III_n. The strong band below the HMW, primarily composed of I, III, and IV, were defined as SC I+III+IV. (L) Representative BN-PAGE of mitochondrial extracts from *Abcb6WT*, *Abcb6LKO* and *Abcb6LOE* mice probed with OXPHOS antibody cocktail. (M) Quantification of the total amount of SCs (average of n=5 independent isolations) in *Abcb6WT*, *Abcb6LKO* and *Abcb6LOE* mice. *Abcb6WT* SC content was used to normalize *Abcb6LKO* and *Abcb6LOE* SC expression. Values represent mean ± SD. ‘a’ significantly different from Abcb6WT; $p<0.001$. ‘b’ significantly different from Abcb6LKO; $p< 0.01$

(N and O) BNPAGE analysis of (N) complex I and (O) complex III super-assemblies in mitochondria isolated from *Abcb6WT*, *Abcb6LKO* and *Abcb6LOE* mice. (P and Q) Quantification of the total amount of SCs I and III in *Abcb6WT*, *Abcb6LKO* and *Abcb6LOE* mice; Average of n=5 independent isolations. *Abcb6WT* SC content was used to normalize *Abcb6LKO* and

Abcb6LOE SC expression. ‘a’ significantly different between *Abcb6WT* vs *Abcb6LKO*; p<0.001. ‘b’ significantly different between *Abcb6WT* vs *Abcb6LOE*; p< 0.01. Histograms represent mean ± SD

Hepatic ABCB6 expression oscillates in sync with fasting and feeding signals.

Multiple lines of evidence demonstrate that in the liver, mitochondrial dynamics of fusion and fission is closely linked to support the changing bioenergetic demand (Jacobi *et al.*, 2015; Lionetti *et al.*, 2014; Smith, et al., 2018b). Based on the strong association between hepatic mitochondrial form and function, and the *Abcb6* genotype, we wondered whether under physiological conditions ABCB6 expression was regulated to link bioenergetic demand to mitochondrial dynamics. To test this, we measured ABCB6 expression in two physiological relevant mouse models, postprandial (Figure 4.4A) and circadian rhythm (Figure 4.4B), where mitochondria undergo cyclical changes in their shape, size and distribution to adapt their bioenergetic and biosynthetic output to the ever-changing anabolic/catabolic state of the liver (Jacobi, et al., 2015; Sood *et al.*, 2014). We used the activation of nutrient-sensing mechanistic/mammalian target of rapamycin complex 1 (mTORC1) to confirm that mice were responsive to the fasting and feeding protocol used in our studies (Albert *et al.*, 2015; Laplante *et al.*, 2009, 2012) (Figure 4.4E). Similarly, we used circadian oscillation of Period Circadian Regulator 2 (Per2) to confirm circadian rhythm in our mouse models (Schmutz *et al.*, 2012) (Figure 4.4G and 4.4H). ABCB6 expression was evaluated in these models at both the transcription and translational levels. We found that in the postprandial mouse model (Figure 4.4A) ABCB6 expression was induced in response to fasting, while feeding decreased ABCB6 expression (Figure4.4E). More interestingly we found that fasting dependent increase in

ABCB6 expression was regulated at the transcriptional level (Figure 4.4D) with the highest expression seen after an overnight fast ~12 h. In contrast to fasting, feeding mediated decrease in ABCB6 expression appeared to be regulated at the post-transcriptional level, as we did not observe any change in the ABCB6 transcript following feeding (Figure 4.4D). Quantification of ABCB6 protein bands in immunoblots confirmed significant decrease in ABCB6 expression (Figure 4.4F).

To confirm the feeding dependent decrease in ABCB6 expression and to explore the dynamics of this process we developed an *ex vivo* model of postprandial using primary hepatocytes isolated from *Abcb6WT* mice. In this *ex vivo* model *Abcb6WT* mouse primary hepatocytes were cultured in either low nutrient (5 mM glucose) or high nutrient (25 mM glucose) media to replicate the *in vivo* fasting and feeding conditions. Further, to define the dynamics of feeding on ABCB6 expression we analyzed the time dependent decrease in ABCB6 protein by western blot. Consistent with the *in vivo* results, *ex vivo* ABCB6 expression was eliminated following 5 h of culturing in high nutrient media (Figure 4.4I). More importantly we observed a significant decrease (> 75%) in ABCB6 protein as early as 1 h of culturing in high nutrient media (Figure 4I). Quantification of the protein bands in immunoblots confirmed significant decrease in ABCB6 expression in response to nutrient load in primary hepatocytes (Figure 4.4J).

In the circadian rhythm model, we found a rather sluggish synchronization of the *Abcb6* transcript with the circadian clock (Figure 4.4C). However, in contrast to the *Abcb6* transcript, ABCB6 protein showed robust synchronization with the diurnal rhythm (Figure 4.4G). Quantification of the immunoblot protein bands allowed us to plot the circadian

profile of the ABCB6 protein which was phase reversed to the circadian oscillation of Per2 protein (Figure 4.4H).

Taken together these results suggest that hepatic ABCB6 expression is in sync with physiological and environmental stimuli where hepatic bioenergetic and biosynthetic output requires reprogramming to meet the ever-changing metabolic state.

Figure 4.4

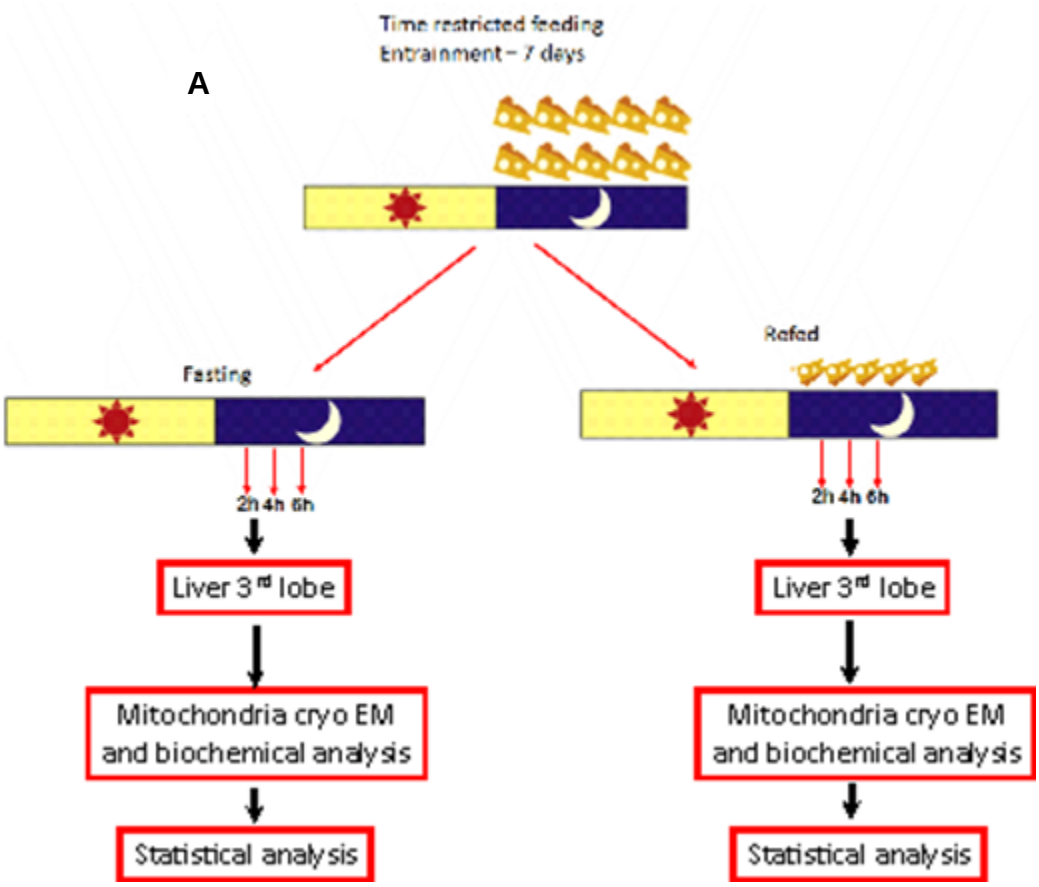

Figure 4.4 cont

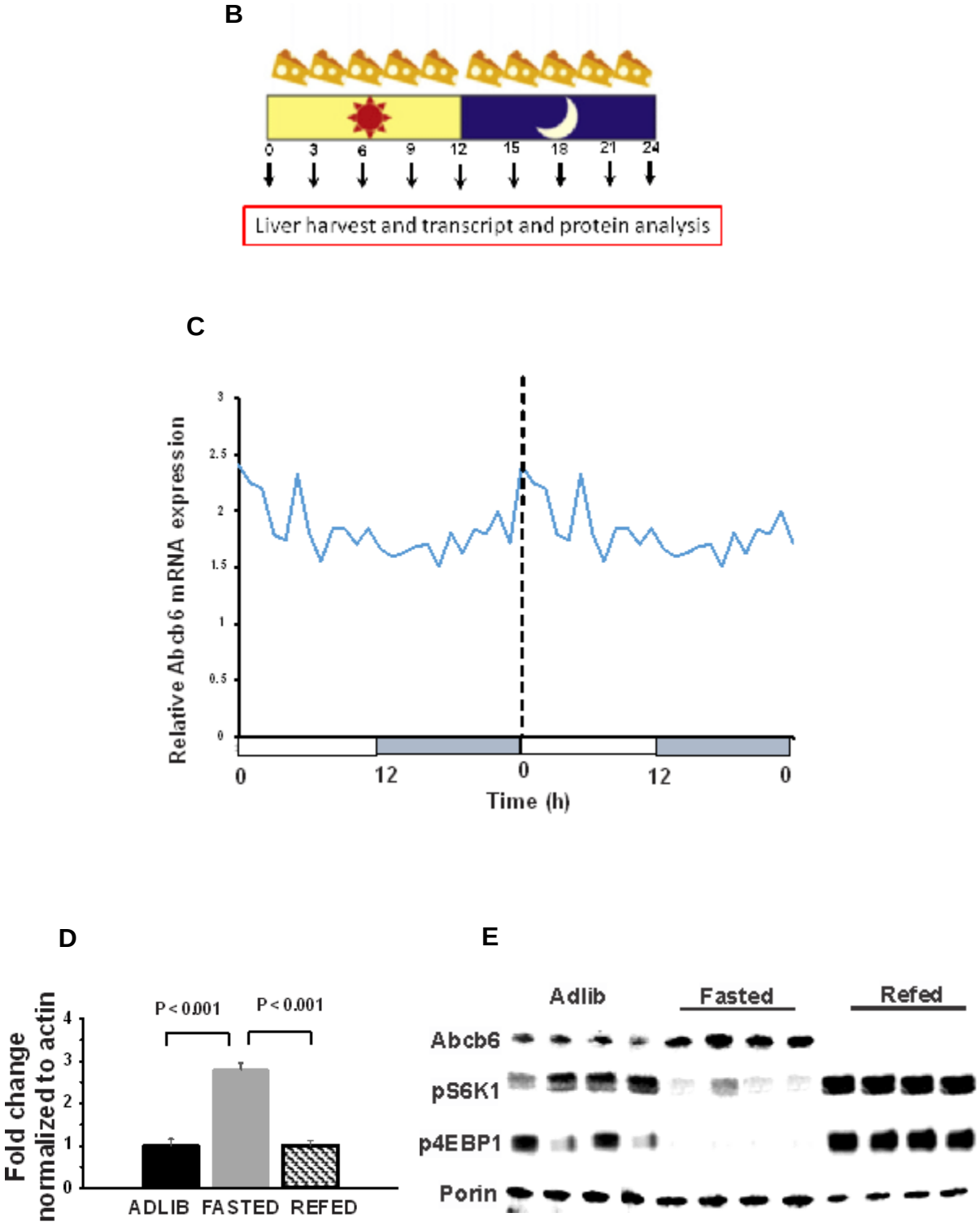

Figure 4.4 continued

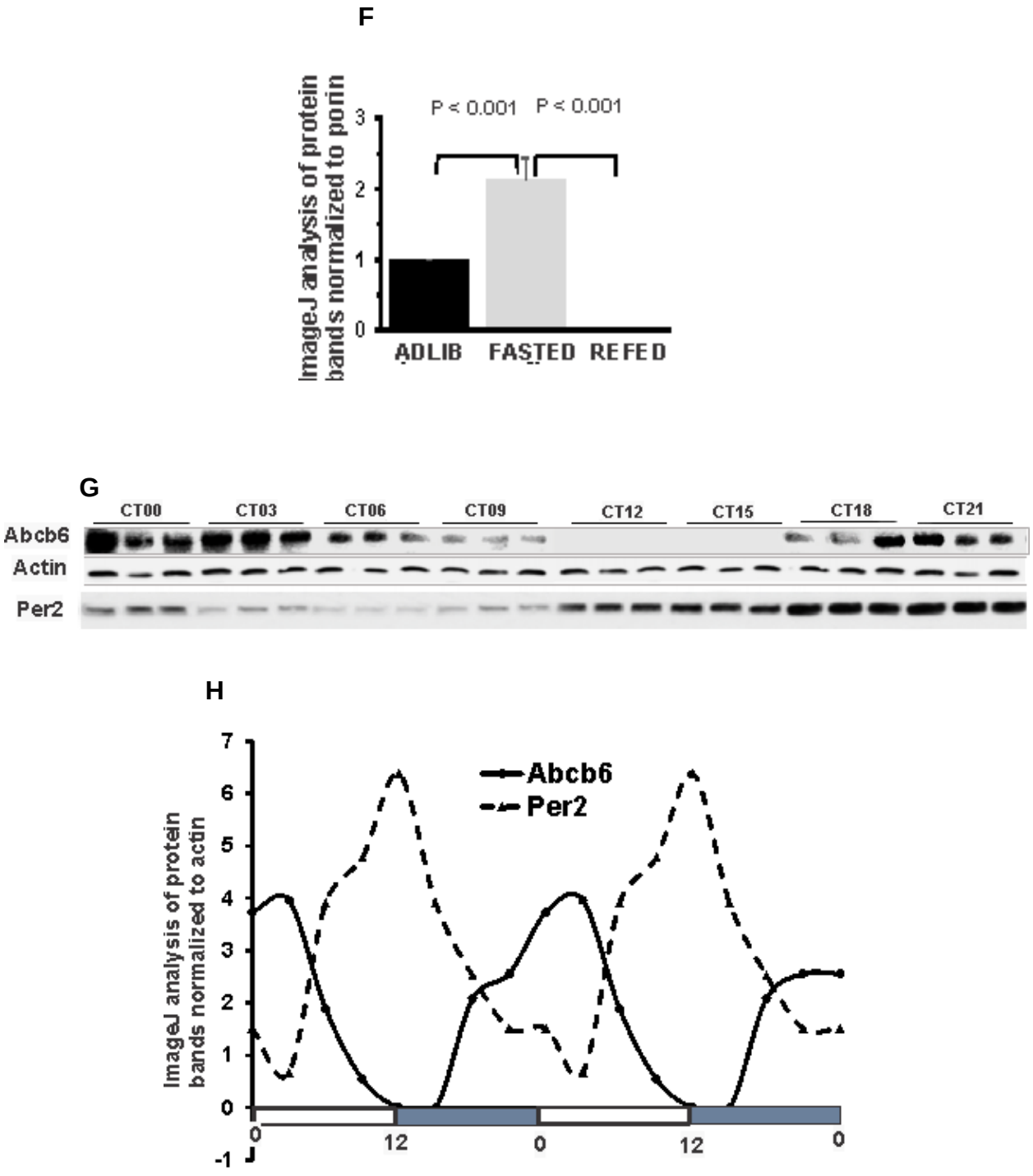

Figure 4.4 continued

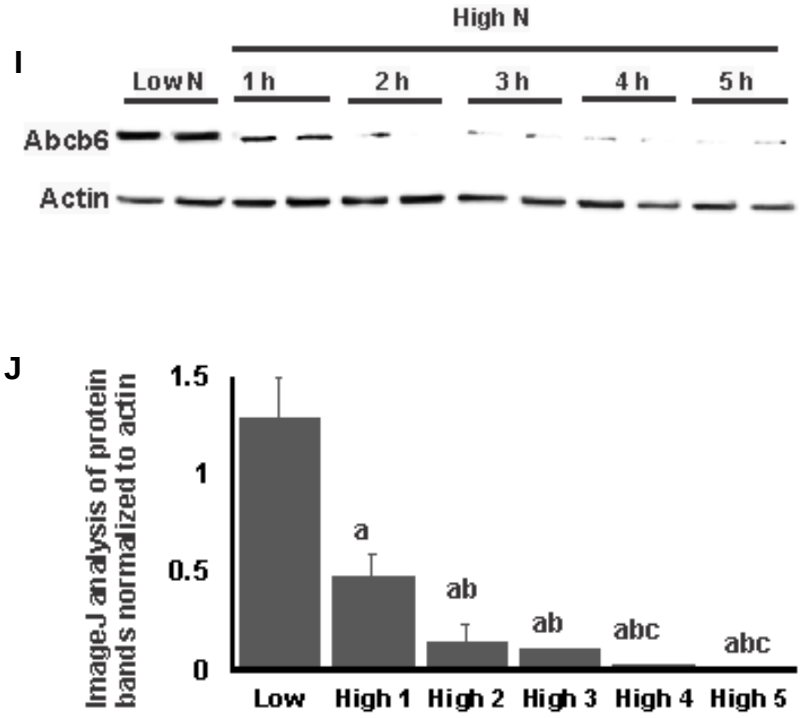

Figure 4.4 Hepatic ABCB6 expression in response to diurnal bioenergetic demand (A) Schematic representation of the postprandial model used in this study. (B) Schematic representation of the circadian model used in this study. (C) Double-plotted average (±SEM, n=4) mRNA levels of *Abcb6* in liver at different times of the day. Transcript levels were measured by qRT-PCR and normalized to *Gapdh* mRNA levels. Broken line separates double plotted data.

(D) *Abcb6* mRNA transcript in *Abcb6WT* mouse liver in response to postprandial. (E) ABCB6 protein expression in *Abcb6WT* mouse liver in response to postprandial. pS6K1 and p4EBP1 were used to confirm feeding and fasting responses and Porin was used as loading control. (F) Quantification of ABCB6 protein in Immunoblots normalized to Porin loading control (average of n= 3 independent experiments with 4-5 mice per group per experiment). (G) Circadian expression of ABCB6 protein in *Abcb6WT* mouse livers. Liver samples were collected every 3

hours for 24 hours (n=3-4 mice/time point). Per2 expression was used to confirm circadian rhythm and Porin was used as loading control. (H) Quantification of ABCB6 and Per2 Immunoblots normalized to Porin loading control (average of n=3 independent experiments with 3-4 mice per group per experiment). The white and black bar represents light cycle and dark cycle, respectively. Zeitgeber time 0; lights on; 12; lights off. The dotted line separates one 24 h (day and night) cycle. (I) Representative Immunoblot analysis of ABCB6 protein expression in primary hepatocytes isolated from *Abcb6WT* mice livers cultured in the presence of either low-nutrient (5 mM glucose) or high nutrient (25 mM glucose) for the indicated periods. Actin is used as a loading control. (J) Quantification of immunoblots normalized to actin (average of n=3 independent primary hepatocyte isolations). Values represent mean ± SD. 'a' significantly different from low nutrient; $p < 0.001$. 'b' significantly different from high nutrient at 1 h; $p < 0.001$. 'c' significantly different from high nutrient at 3 h; $p<0.001$. High 1, High 2, High 3, High 4, and High 5 represent hepatocytes treated with high nutrient media for 1 h, 2 h, 3 h, 4 h and 5 h respectively.

Dynamic changes in hepatic ABCB6 expression is required to accommodate mitochondrial form and function in response to hepatic bioenergetic demand.

Based on the synchronization of hepatic ABCB6 expression with bioenergetic demand and mitochondrial form and function, we hypothesized that dynamic changes in ABCB6 expression may be essential to accommodate hepatic bioenergetic demand to the mitochondrial life cycle of fusion and fission. To test this hypothesis, we first determined the dynamic changes in mitochondrial form and function in *Abcb6WT* mice in response to fasting and feeding using the postprandial mouse model described in Figure 4.4A. In *Abcb6WT* mice, a shift from ad libitum feeding to fasting reprogramed hepatic

mitochondria into a more fused or elongated morphology (Figure 4.5A) with a significant decrease in mitochondrial number (Figure 4.5B) without any significant change in total mitochondrial area (data not shown). Consistent with the more fused morphology, *Abcb6 WT* mitochondria displayed increased basal respiration, ATP-synthesizing respiration (state III) and maximal respiratory capacity (FCCP uncoupled) (Figure 4.5C). In contrast, a shift from fasting to refeeding resulted in shortened or fragmented mitochondria with a significant decrease in basal respiration, ATP-synthesizing respiration (state III) and maximal respiratory capacity (Figure 4.5A – 5C).

Using the mitochondrial form and functional changes observed in the *Abcb6WT* mice liver as the benchmark we next tested how these parameters were altered in *Abcb6LKO* and *Abcb6LOE* mice livers. We found that in *Abcb6LKO* mice, hepatic mitochondria were unable to undergo fusion (Figure 4.5D), decrease mitochondrial number (Figure 4.5E) or increase mitochondrial bioenergetic profile in response to energy demand (fasting) (Figure4.5F). However, in the fed conditions *Abcb6LKO* mice responses were similar to the *Abcb6WT* mice (Figure 4.5D-5F). In contrast to *Abcb6LKO* mice, *Abcb6LOE* mice were unable to undergo fission (Figure 4.5G), increase mitochondrial number (Figure 4.5H) or decrease bioenergetic efficiency in response to nutrient availability (feeding) (Figure 4.5I). However, in the fasted condition *Abcb6LOE* mice responses were similar to the *Abcb6WT* mice (Figure 4.5G – 5I). Together these results confirm our hypothesis and suggest that disturbances in hepatic ABCB6 expression results in an inability of these respective mitochondria to adapt their mitochondrial form and function to the changing energetic demands. By extension these results imply that

ABCB6 expression is an essential component in linking bioenergetic demand to mitochondrial form and function.

Figure 4.5

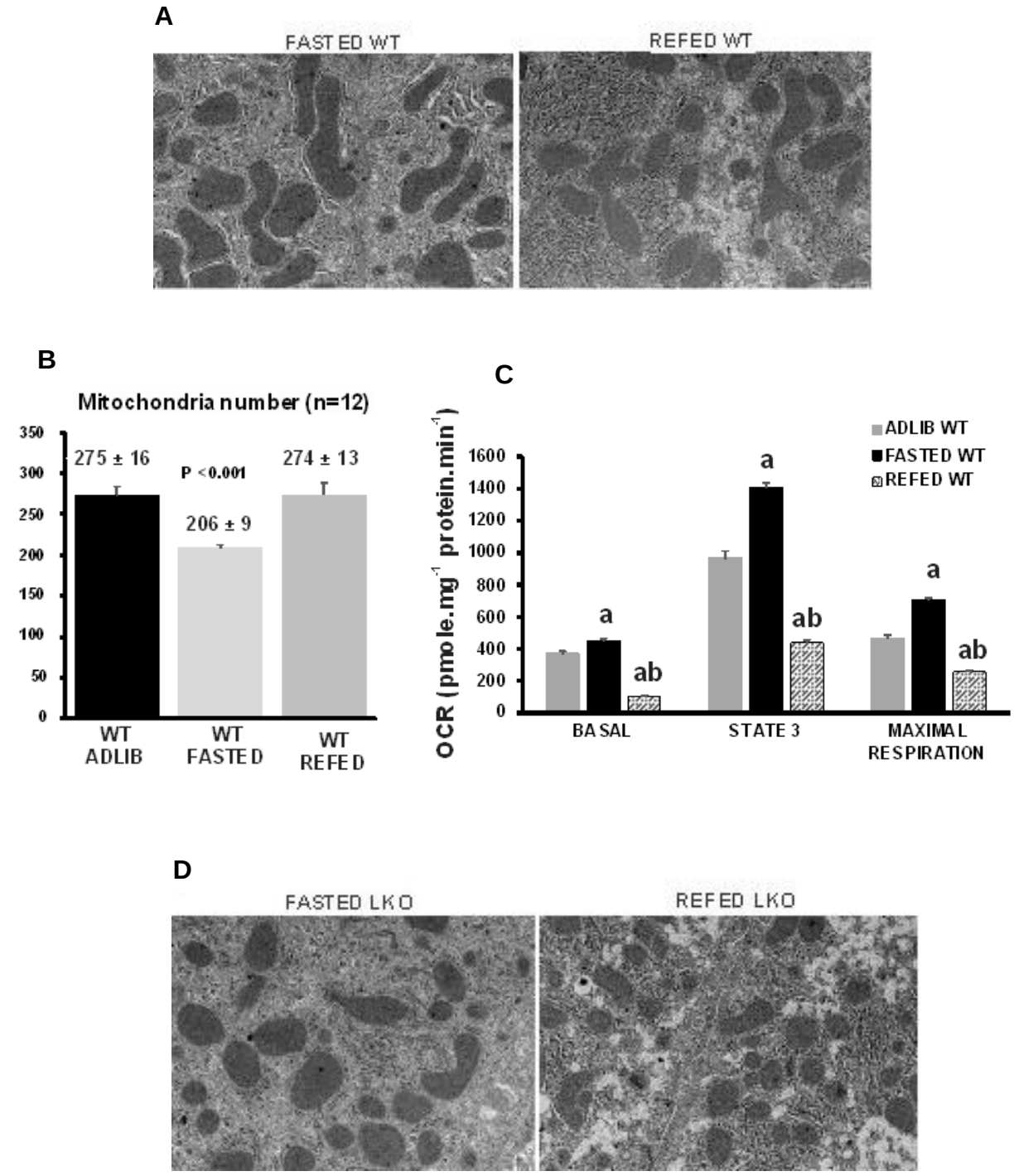

Figure 4.5 (A-I) continued

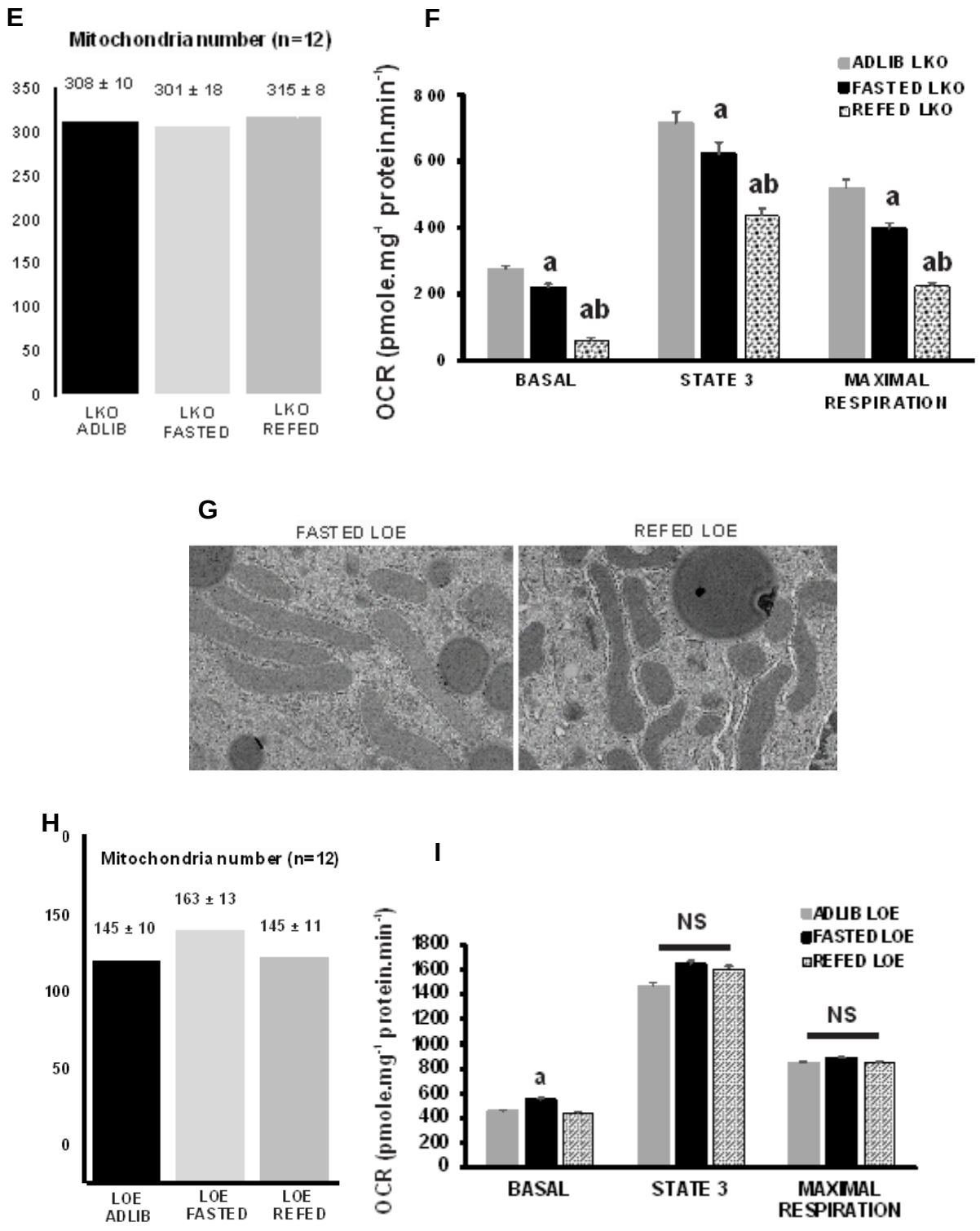

Figure 4.5 (A-I) ABCB6 expression affects postprandial remodeling of mitochondrial form and function and metabolic homeostasis (A, D, G) Representative EM images showing mitochondrial ultrastructural morphology in response to fasting and refeeding in (A) *Abcb6WT*, (D) *Abcb6LKO* and (G) *Abcb6LOE* mitochondria. (B, E, H) Mitochondrial number changes in response to fasting and feeding in (B) *Abcb6WT,* (E) *Abcb6LKO* and (H) *Abcb6LOE* mice. Mitochondrial number was calculated in 12 images (2 images per mice per genotype per condition) each of 980 μm^2 representing 6 mice per genotype per condition. Values represent mean ± SD. (C, F, I) Quantification of OCR at different mitochondrial respiratory states in a representative experiment using mitochondria isolated from (C) *Abcb6WT*, (F) *Abcb6LKO* and (I) *Abcb6LOE* in response to fasting and feeding.

Dynamic changes in hepatic ABCB6 expression is required to accommodate hepatic metabolic flexibility in response to hepatic bioenergetic demand.

A key aspect of synchronizing mitochondrial form and function in response to bioenergetic demand is to drive cellular adaptations that facilitate efficient use of available nutrients (glucose, lipids, and amino acids) (Gao, et al., 2014; Pintus, et al., 2012; Singer, 2013). Such adaptations promote hepatic metabolic homeostasis (metabolic flexibility) (Cheng, et al., 2013; Smith, et al., 2018b). Conversely, loss of this synchronization impairs metabolic homeostasis (Chowdhury *et al.*, 2013; Corpeleijn, et al., 2009; Lopez-Lluch, 2017). We speculated whether an inability to accommodate mitochondrial form and function to nutrient status in *Abcb6LKO* and *Abcb6LOE* mice results in impaired metabolic flexibility. To test this hypothesis, we first defined the parameters of energy usage, including fed and fasted hepatic ketone body production, glycogen depletion and triacylglycerol accumulation in *Abcb6WT* mice. Consistent with previous observations

(Arias *et al.*, 1997; Geisler *et al.*, 2016; Seitz *et al.*, 1977), fasting *Abcb6WT* animals showed increased hepatic ketone body production, glycogen depletion and triacylglycerol accumulation (Figures 4.5J – 5L and Figures 4.5P-5Q), while feeding *Abcb6WT* animals showed repletion of glycogen stores, and decreased beta-oxidation (Figures 4.5M – 5O).

Using the metabolic adaptations observed in *Abcb6WT* mice as benchmark we then tested how these parameters were altered in *Abcb6LKO* and *Abcb6LOE* mice. We found that *Abcb6LKO* mice were blunted in their ability to mobilize hepatic ketone body production (Figure 4.5J) and glycogen depletion (Figure 4.5K and Figure 4.5P) in response to fasting. In addition, fasting hepatic triglyceride content was significantly increased in the *Abcb6LKO* mice compared to *Abcb6WT* mice (Figures 4.5L and 4.5Q). However, in the fed state *Abcb6LKO* mice display features that are consistent with the *Abcb6WT* mice with repletion of hepatic glycogen stores and inhibition of beta-oxidation, although these parameters were much more significantly affected in *Abcb6LKO* mice compared to *Abcb6WT* mice (Figures.4.5M – 5O).

In contrast to *Abcb6LKO* mice, in *Abcb6LOE* mice fasting induced hepatic ketone body production and liver glycogen content were higher than that observed in the *Abcb6WT* mice (Figures 4.5J and4.5K respectively). However, these values did not reach statistical significance. In contrast to serum ketones and liver glycogen content, the liver triglyceride content of fasting *Abcb6LOE* mice was significantly lower compared to *Abcb6WT* mice (Figure 4.5L). Interestingly in the fed state no significant differences were observed between *Abcb6LOE* and *Abcb6WT* mice with respect to liver glycogen content or liver triglyceride levels (Figures 4.5M – 5O). Together these observations suggest that *Abcb6LKO* mice appear to be in a fed state with an inability to adapt to the metabolic

demands of the fasted state, while *Abcb6LOE* mice appear to show metabolic features, some of which, are consistent with the fasted state.

Figure 4.5 (J-Q)

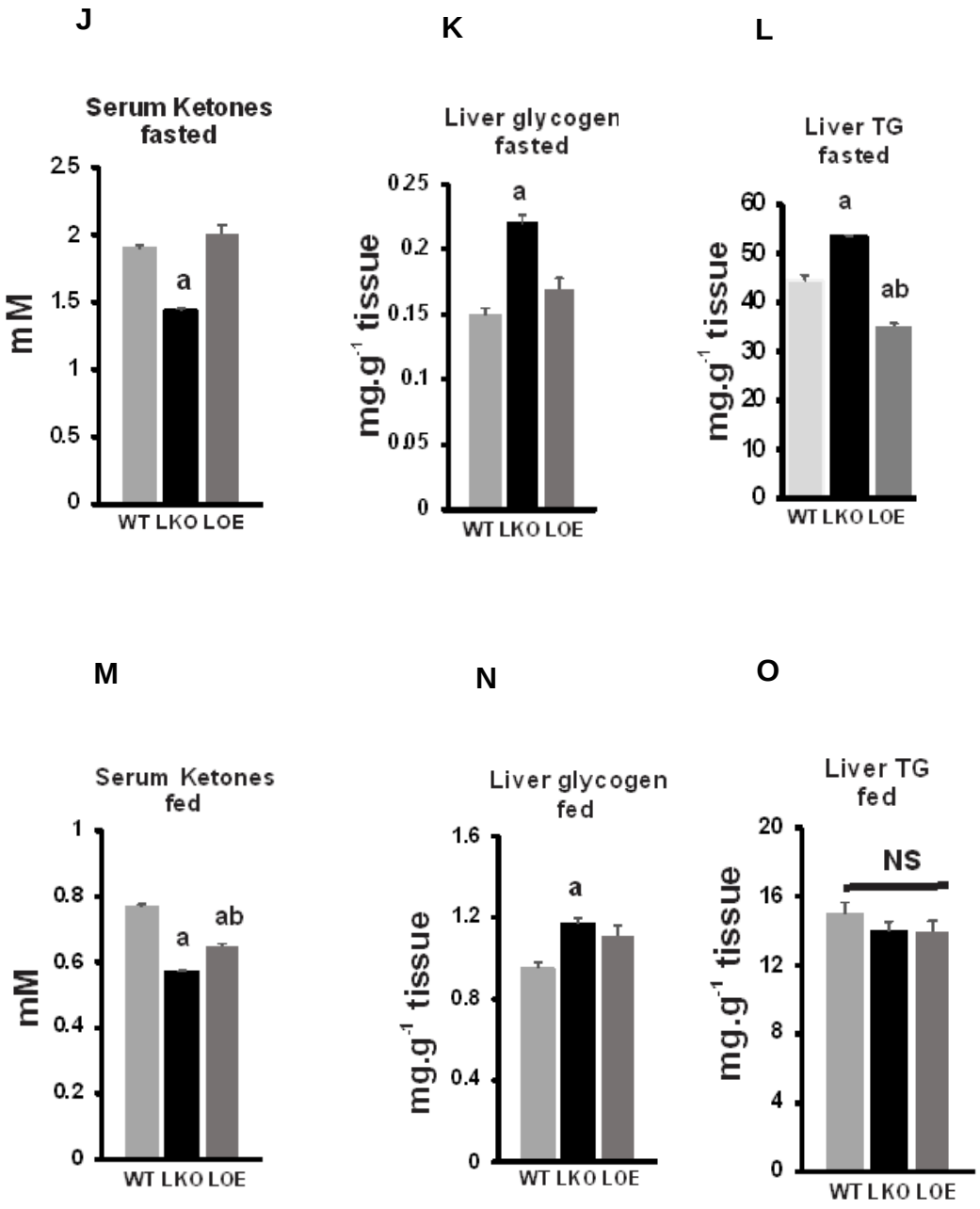

Figure 4.5 (J-Q) continued

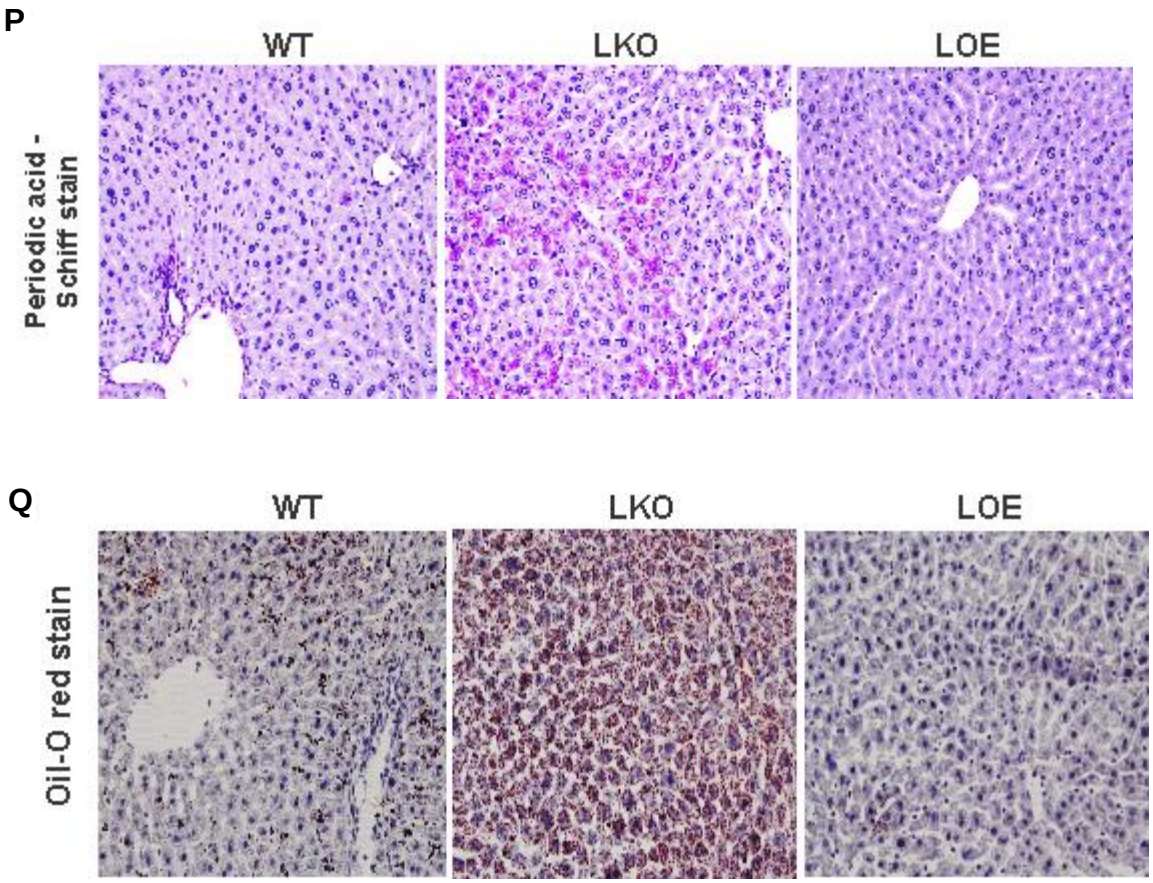

Figure 4.5 (J-Q) ABCB6 expression affects postprandial remodeling of mitochondrial form and function and metabolic homeostasis (J and M) Serum ketones, (K and N) Liver glycogen, and (L and O) Liver TG in fasted (J-L) and fed (M-O) *Abcb6WT*, *Abcb6LKO* and *Abcb6LOE* mice. Values represent mean ± SD. N= 3 independent experiments with 5 mice per group per experiment per condition. (P) Representative tissue sections showing fasting liver glycogen content assessed using periodic acid-Schiff stain. (Q) Representative tissue sections showing fasting liver lipid content assessed using Oil-O Red stain. 'a' significantly different from Adlib values in panels 'C, F, and I' and significantly different from WT in panels 'J – O'; $p<0.001$. 'b' significantly different from

fasted values in panels ‘C, F, and I’ and significantly different from LKO in panels ‘J – O’; p<0.001. NS; values are statistically not significant.

Metabolic inflexibility in mice with altered ABCB6 expression leads to early signs of metabolic disease.

A lack of metabolic flexibility is a significant contributing factor in the development of metabolic disease which includes obesity, insulin resistance and other comorbidities of metabolic syndrome (Corpeleijn, et al., 2009; Galgani, et al., 2008; Sieber *et al.*, 2017; Smith, et al., 2018b). Given the strong association between ABCB6 expression and metabolic inflexibility, we wondered whether chronic hepatic ABCB6 deficiency or hepatic ABCB6 sufficiency contributes to metabolic comorbidities associated with metabolic inflexibility. To test this, we initiated a study to define how ABCB6 expression affected food consumption, body composition and body weight change as well as parameters of metabolic disease. We placed 4-week-old (post weaning) *Abcb6LKO*, *Abcb6LOE,* and *Abcb6WT* mice on chow diet with ad libitum feeding, and followed the changes in weight gain, and food consumption (Figures 4.6A-6C). We observed that during the first 5 weeks of this study (week 6 to week 10) both *Abcb6LKO* and *Abcb6LOE* mice consumed significantly less food than the *Abcb6WT* mice (Figure 4.6B). However, this pattern in food consumption changed dramatically in the next three weeks (week 11 to week 13) with *Abcb6LOE* mice consuming significantly more food than *Abcb6WT* mice, and *Abcb6LKO* mice consuming significantly less food than the *Abcb6WT* mice (Figure 4.6B). Interestingly, we found that the *Abcb6LKO* mice consistently gained weight compared to *Abcb6WT* mice when normalized to food consumption (Figure 4.6C). In contrast the *Abcb6LOE* mice showed no significant difference in normalized body weight (normalized

to food consumption) during the first 5 weeks (Figure 4.6C) of the study. However, this changed dramatically during the next three weeks (week 11 to week 13) with *Abcb6LOE* mice showing a significant decrease in normalized body weight (normalized to food consumption) compared to *Abcb6WT* mice (Figure 4.6C).

To identify parameters of metabolic disease mice in each group were subjected to glucose and insulin tolerant tests at the end of 13 weeks. We observed that the *Abcb6LKO* mice were glucose intolerant in the glucose tolerance test (Figure 4.6H) with the calculated area under the curve (AUC) being statistically significant (Figure 4.6I). We also observed that the *Abcb6LKO* mice were insulin resistant at later time points (90 and 120 min) in the insulin tolerance test (Figure 4.6J), however the calculated area under the curve (AUC) for insulin tolerance was not statistically significant (Figure 4.6K) compared to *Abcb6WT* mice. In contrast to *Abcb6LKO* mice, *Abcb6LOE* mice showed improved glucose tolerance and insulin sensitivity compared to *Abcb6WT* mice, although these differences were not statistically significant for the most part (Figures 4.6L – 6O).

To identify additional parameters of metabolic disease the chow diet study was terminated at the end of 13 weeks and mice in each group were sacrificed. Serum and tissues were collected from the sacrificed mice and parameters of metabolic disease including fed and fasted serum triglycerides (TG) and serum free fatty acids (FFA) were assessed. We found that in both the fed and fasted states, serum TG (Figures 4.6D and 4.6F), and serum FFA (Figures 4.6E and Figure 4.6G) were significantly higher in *Abcb*6LKO mice compared to *Abcb6WT* mice. In contrast in *Abcb6LOE* mice we

observed decreased serum FFA under fed conditions (Figure 4.6G) while fasting serum FFA and fasting serum TG were high compared to *Abcb6WT* mice (Figures 4.6D and 6E).

The unique pattern of serum parameters combined with the distinctive body weight changes seen in *Abcb6LKO* and *Abcb6LOE* mice prompted us to evaluate the size and weight parameters of liver and adipose tissue, two key organs that are thought to contribute to body weight changes and the observed serum metabolite changes. We found that in *Abcb6LKO* mice both the liver and the white adipose tissue were heavier (normalized to body weight) compared to the liver and white adipose tissue of *Abcb6WT* mice (Figures 4.6P and 4.6Q). In contrast in *Abcb6LOE* mice the liver and the white adipose tissue (normalized to body weight) were lighter compared to the liver and white adipose tissue of *Abcb6WT* mice (Figures 4.6P and 4.6Q). More importantly the organ to body weight ratio observed in *Abcb6LKO* mice were significantly higher than the organ to body weight ratio seen in *Abcb6LOE* mice (Figures 46P and 46Q).

Taken together these results suggest that in mice chronic hepatic ABCB6 deficiency contributes to the development of metabolic disease while ABCB6 overexpression might be protective.

Figure 4.6

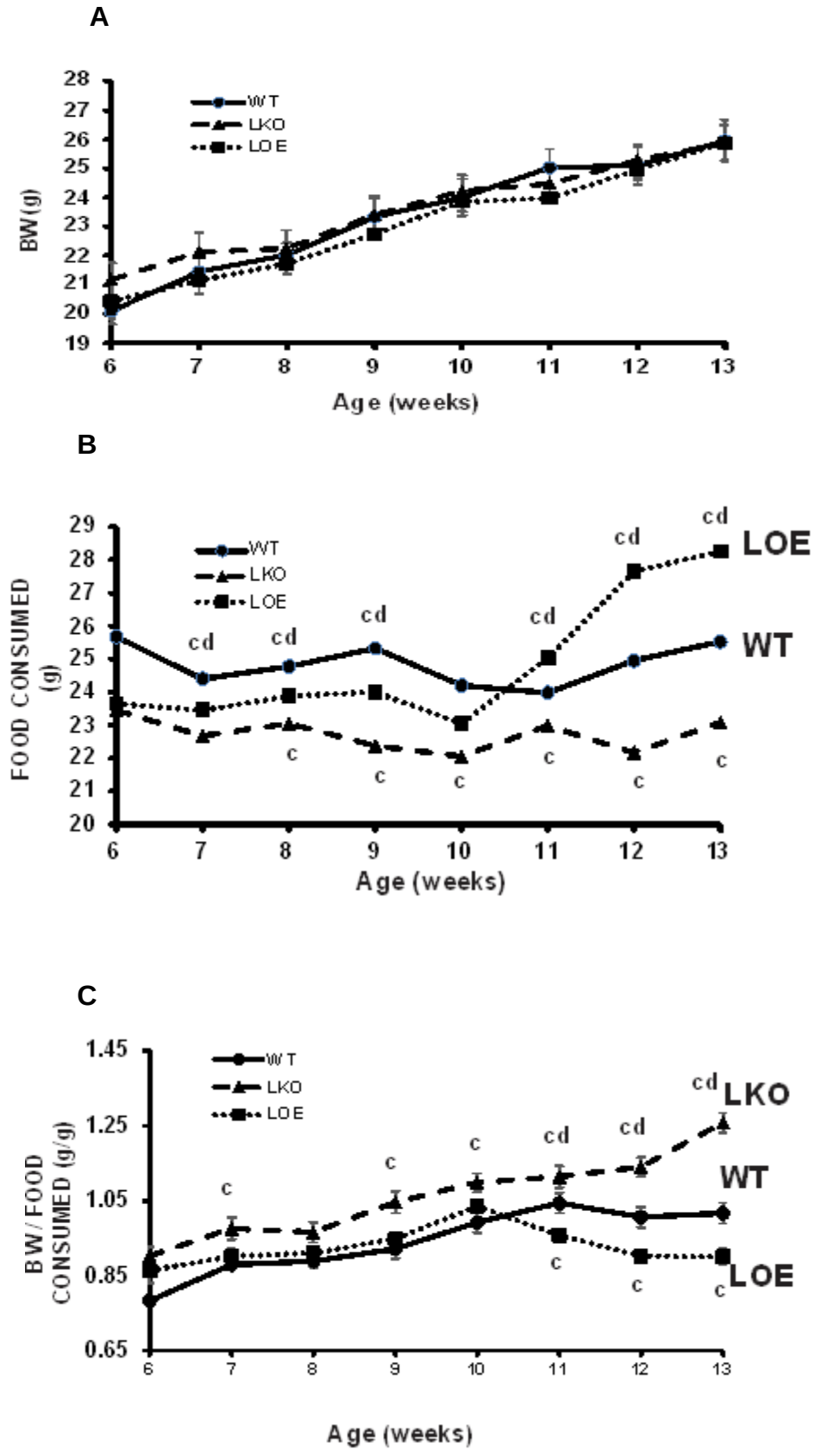
A
WT
LKO
LOE
BW(g)
Age (weeks)
B
WT
LKO
LOE
FOOD CONSUMED (g)
cd
c
LOE
WT
Age (weeks)
C
WT
LKO
LOE
BW / FOOD CONSUMED (g/g)
cd
c
LKO
WT
LOE
Age (weeks)

Figure 4.6 continued

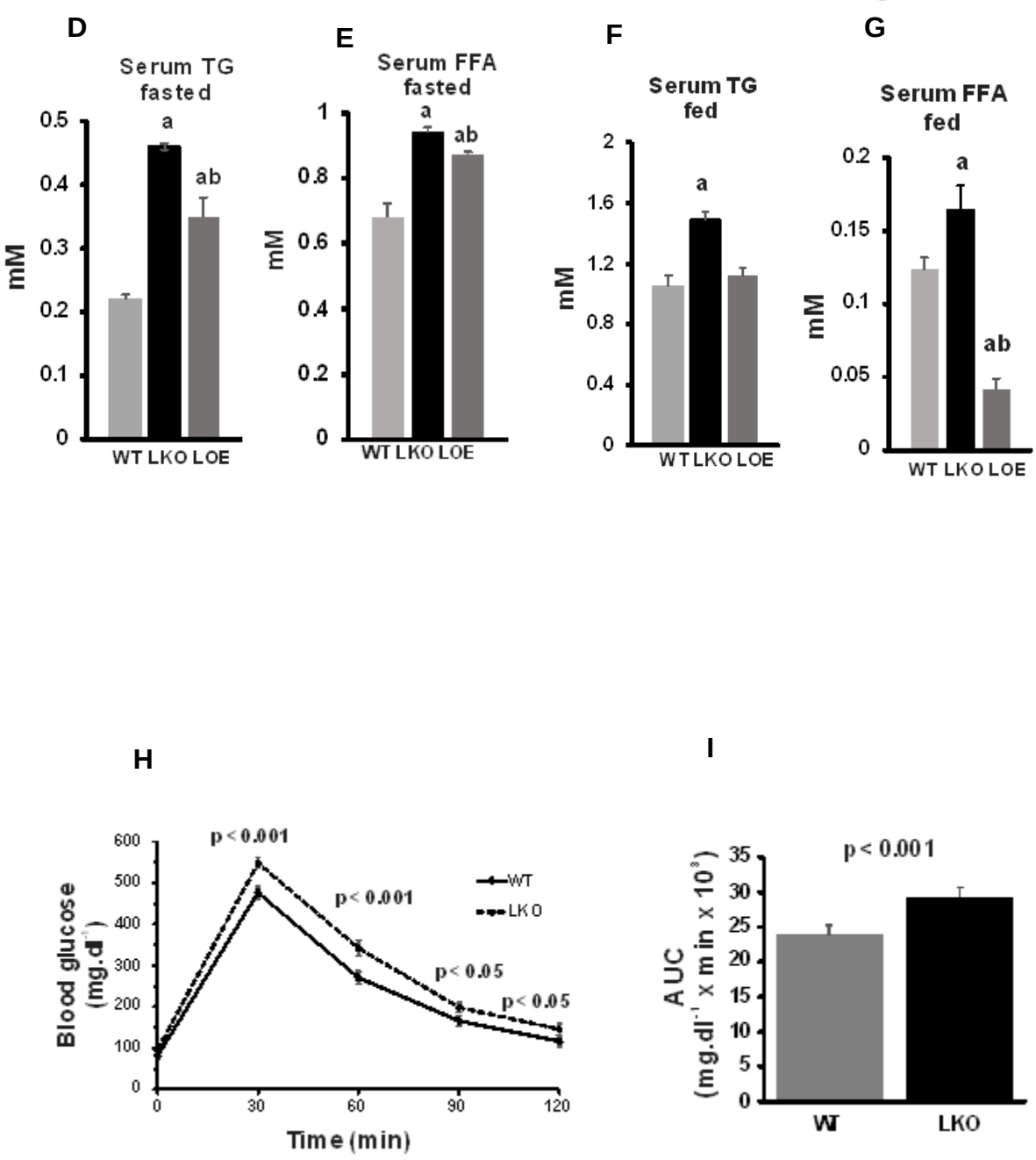

Figure 4.6 continued

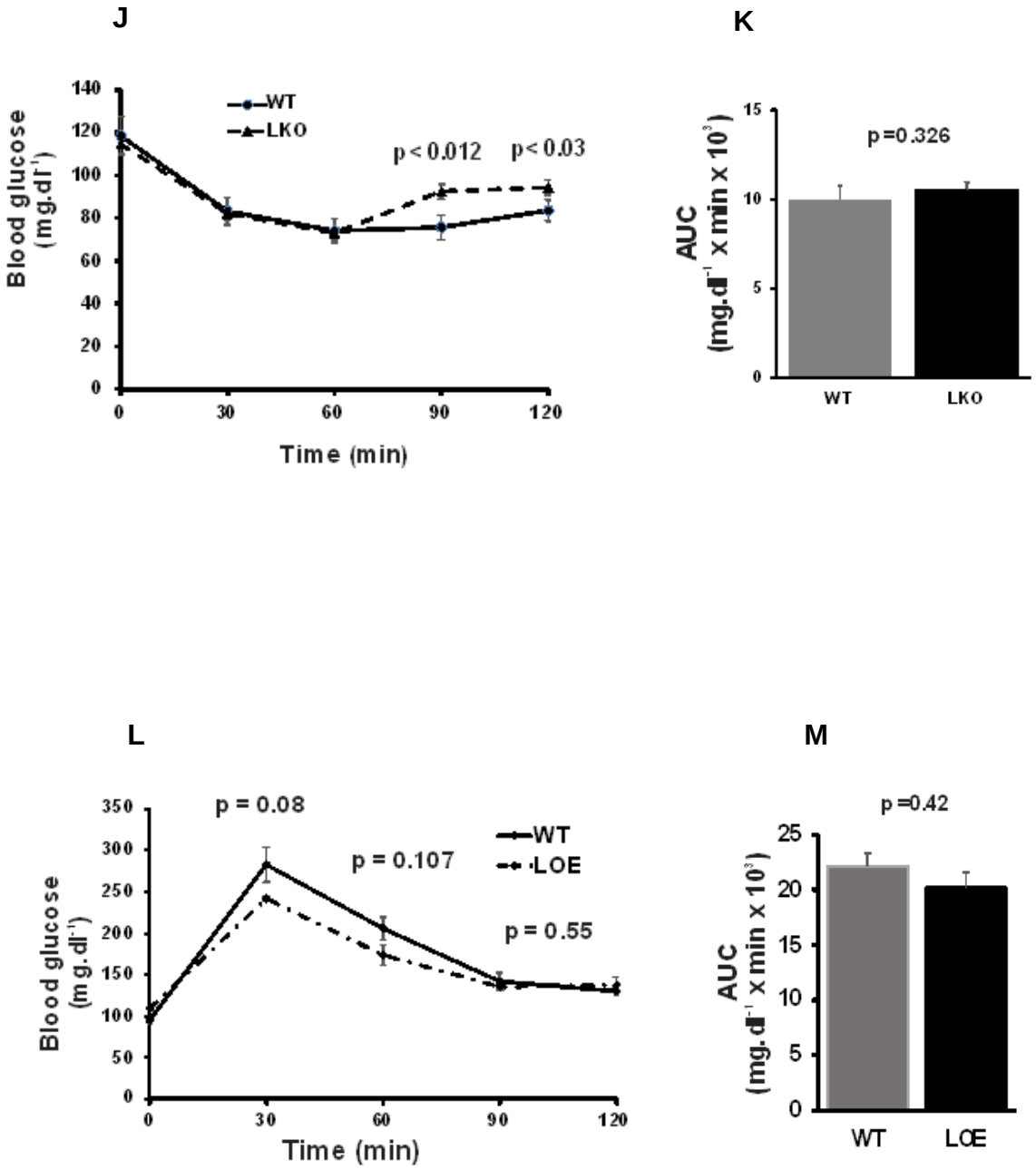

Figure 4.6 continued

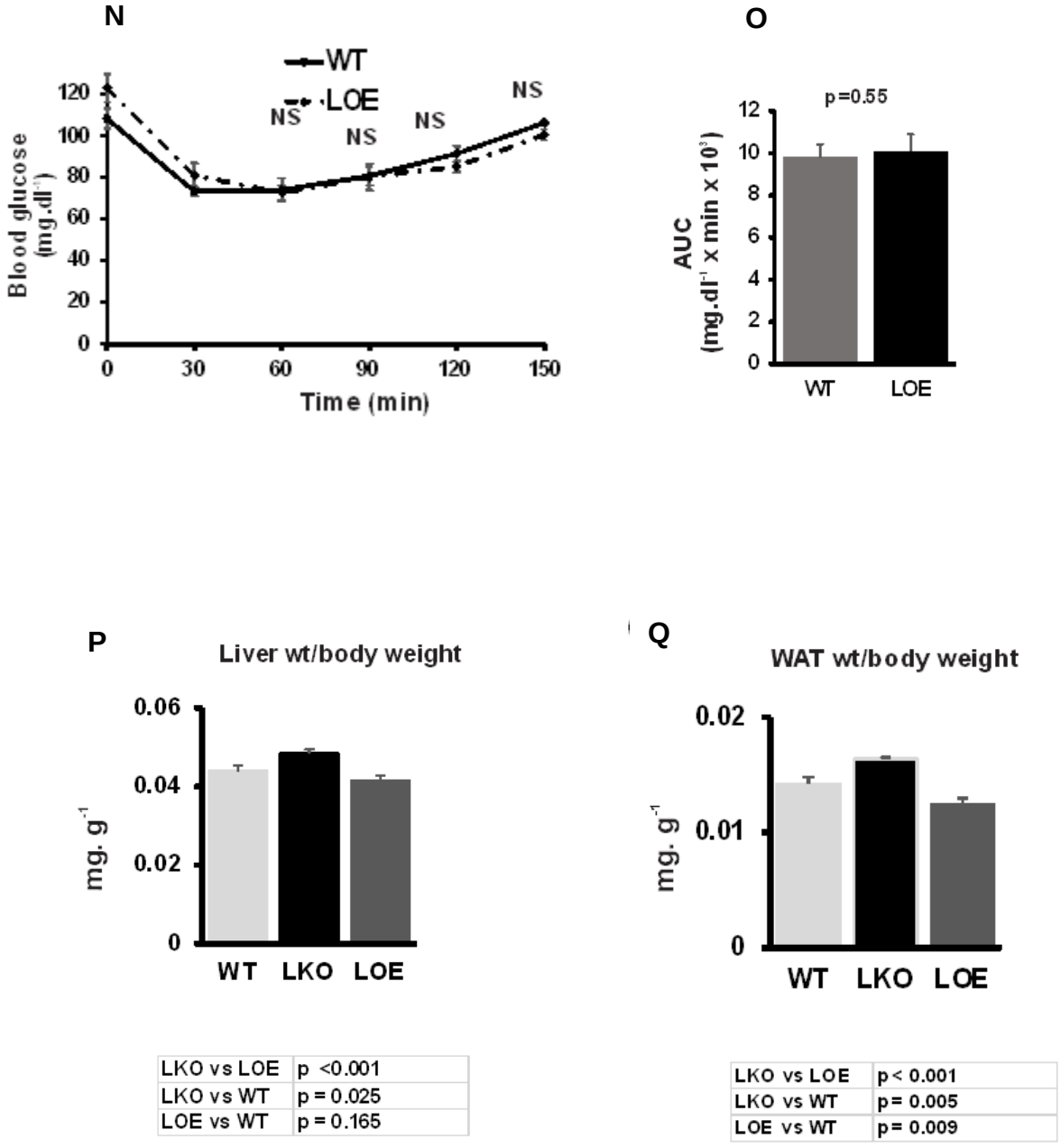

LKO vs LOE	p <0.001
LKO vs WT	p = 0.025
LOE vs WT	p = 0.165

LKO vs LOE	p< 0.001
LKO vs WT	p= 0.005
LOE vs WT	p= 0.009

Figure 4.6 Early signs of metabolic disease in male mice on chow diet as a result of chronic changes in hepatic ABCB6 expression

(A) Body weight, (B) food consumption and (C) body weight change normalized to food consumed in *Abcb6WT*, *Abcb6LKO* and *Abcb6LOE* mice. (D-G) serum biochemical parameters of *Abcb6WT*, *Abcb6LKO* and *Abcb6LOE* mice in (D, E) fasted and (F, G) fed conditions. (H, I) glucose and (J, K) insulin response in *Abcb6WT* and *Abcb6LKO* mice. (L, M) glucose and (N, O) insulin response in *Abcb6WT* and *Abcb6LOE* mice. 'a' significantly different from WT; $p<0.001$. 'b' significantly different from LKO; $p<0.001$ in serum biochemical parameters. 'c' significantly different from WT; $p<0.001$. 'd' significantly different from LOE; $p<0.001$ in body weight and food consumption. (P, Q) Organ to body weight ratios for *Abcb6LKO* and *Abcb6LOE* mice (p values listed). Results representative of 4 independent experiments with 5 – 6 mice per group per experiment. Values represent mean ± SD.

ABCB6 expression alters localization of mitochondrial fission and fusion proteins

To elucidate the mechanism by which ABCB6 expression affects mitochondrial morphology, we carried out cell fractionation experiments to determine the effect of ABCB6 on the expression and localization of the core proteins that regulate mitochondrial dynamics. In principal mitochondrial dynamics is controlled by the amount, localization and activity of the dynamin related proteins Mfn1, Mfn2, Opa1 and Drp1 (Bereiter-Hahn *et al.*, 1994; Ferree *et al.*, 2012; Hermann *et al.*, 1998; Lee *et al.*, 2016). In the following studies we first measured the expression of Mfn1, Mfn2, Opa1, and Drp1 in livers of *Abcb6LKO* and *Abcb6LOE* mice. We found no significant differences in the expression of any of the core mitochondrial fusion or fission proteins in either *Abcb6LKO* or *Abcb6LOE* mice (Figures 4.7A and 4.7E). We next tested whether mitochondrial localization of the fusion and fission proteins were different between the three mouse genotypes. We observed decreased mitochondrial localization of MFN2 and OPA1 and increased

mitochondrial localization of DRP1 in *Abcb6LKO* mice (Figures 4.7C and 4.7G). In contrast, in *Abcb6LOE* mice we found increased mitochondrial localization of Mfn2 and Opa1 and decreased mitochondrial localization of DRP1 compared to wildtype mice (Figures 4.7C and 4.7G). Quantification of the protein bands normalized to loading controls confirmed the immunoblot results (Figures 4. 7B, 4.7D, 4.7F & 4.7H). Collectively these results suggest that altered ABCB6 expression affects mitochondrial localization of MFN2, OPA1 and DRP1 some of which might contribute to ABCB6 mediated effects on mitochondrial dynamics.

Figure 4.7

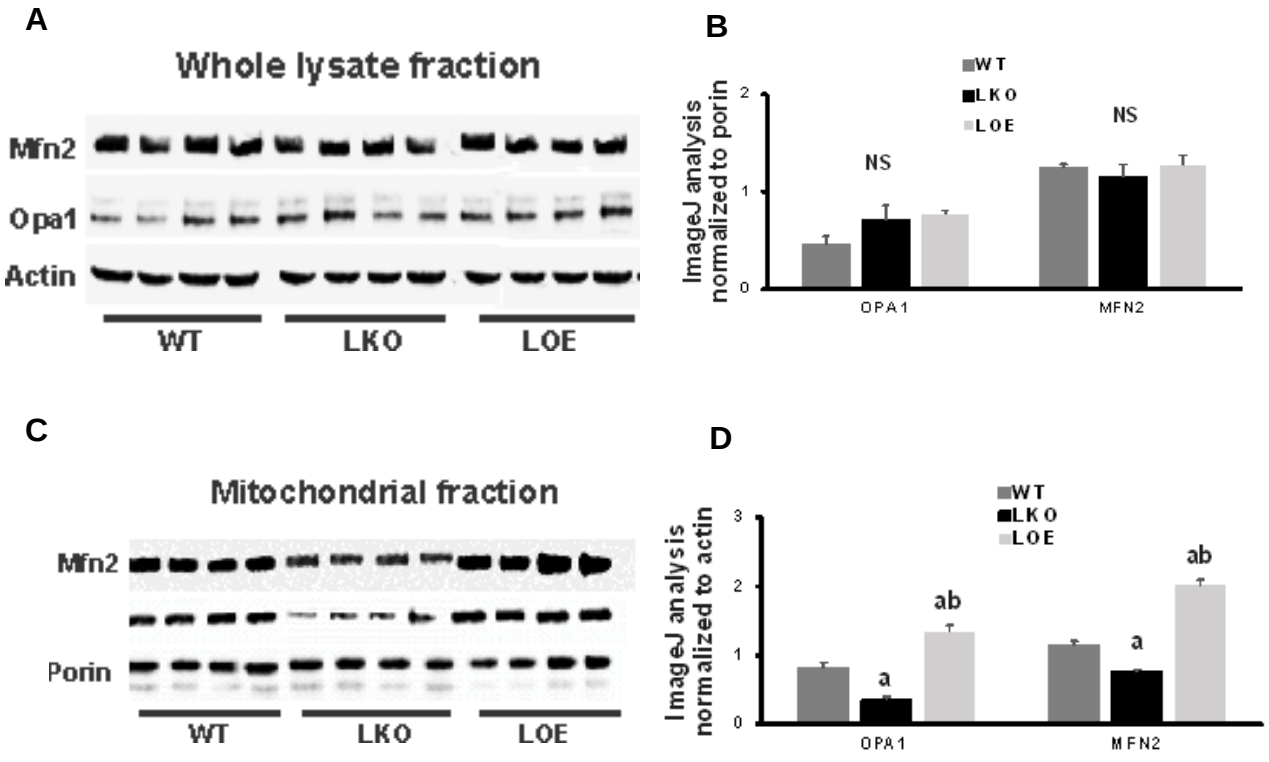

Figure 4.7 continued

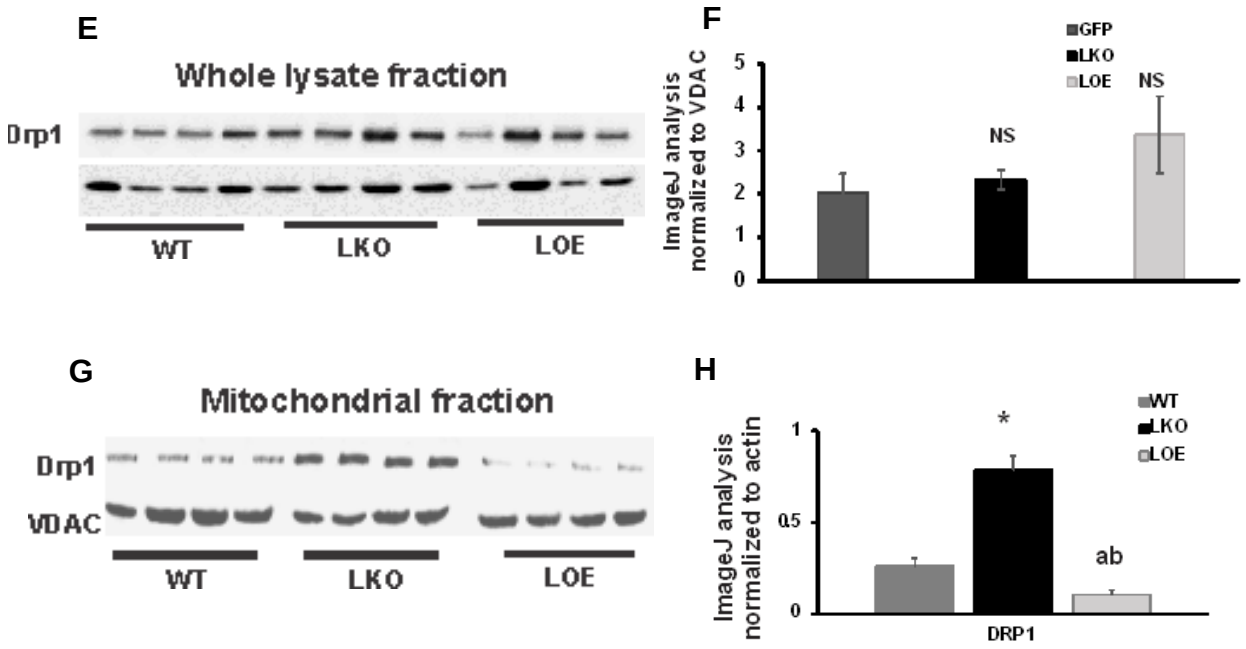

Figure 4.7 Effect of ABCB6 on the expression and mitochondrial localization of Mfn2, Opa1 and Drp1

(A-H) Representative western blot analysis of (A & C) fusion protein and (E & G) fission protein distribution between (A & E) whole liver lysate and (C & G) mitochondrial fractions. Porin and VDAC were used as loading controls for the mitochondrial fractions and actin was used as loading control for the total lysate fractions. (B, D, F, H) Quantification of immunoblots (n=5 independent experiments with 4-5 mice per group per experiment) normalized to Porin, VDAC and actin. Values represent mean ± SD. 'a' significantly different from WT; $p<0.001$. 'b' significantly different from LKO; $p<0.001$. NS; statistically non-significant.

4.5 Discussion

Mitochondria have a unique ability to change their morphology through fusion and fission events (Bereiter-Hahn, et al., 1994). This flexibility in mitochondrial morphology is

an important aspect of mitochondrial respiratory status which entails changes in energy and redox alterations, thereby integrating sensing and signaling processes that promote hepatic metabolic homeostasis. A major challenge has been to understand the molecular mechanisms that couple intracellular and environmental stimuli to mitochondrial dynamics. In this study we identify ABCB6, a mitochondrial outer membrane ABC transporter protein, as a physiologically controlled regulator of mitochondrial dynamics and hepatic energy homeostasis. To our knowledge, this is the first report of a mitochondrial ATP binding cassette transporter protein capable of modulating metabolic flexibility by simultaneous regulation of mitochondrial dynamics and mitochondrial function in the liver. Our studies suggest that hepatic ABCB6 expression is essential to promote whole-body metabolic homeostasis and dysregulation in its expression contributes to the development of metabolic disease.

ABCB6 mediated reprograming of mitochondrial function results from altered supra complex assembly of respiratory complexes

We found that ABCB6 mediated change in mitochondrial form reprograms mitochondrial bioenergetic efficiency. Bioenergetic efficiency during oxidative phosphorylation is carried out by the electron transport chain (ETC), a composite multi-protein system organized in four respiratory chain complexes (CI-CIV). The structural and functional organization of the ETC defines the efficiency of energy harvest by the mitochondria(Lenaz *et al.*, 2009). Recent studies suggest that the structural and functional organization of the ETC plastically changes from freely moving to super-assembled structures, called super complexes (Cogliati *et al.*, 2013). Indeed, change in mitochondrial morphology is thought to reorganize cristae architecture that promotes

higher order organization of the respiratory complexes into super assemblies, often without any significant change in the expression of the individual complexes (Cogliati, et al., 2013; Lenaz, et al., 2009; Schagger, et al., 2000). Such SCs are believed to reduce the diffusion distance required for the transfer of electrons from one complex to the other, thereby increasing the transport efficiency and overall mitochondrial function while limiting the production of reactive oxygen species (ROS) (Lapuente-Brun, et al., 2013; Maranzana *et al.*, 2013). In mice with differences in ABCB6 expression SCs appear to dynamically adapt to changes in mitochondrial morphology and be stabilized by cristae shape. This ABCB6 mediated adaptation of mitochondrial morphology and the ensuing super-assembly of respiratory complexes likely allows hepatocyte mitochondria to reprogram mitochondrial function. Consistent with the observation that such SC mediated changes in mitochondrial function do not translate into damaging amounts of ROS (Maranzana, et al., 2013), mitochondrial functional changes precipitated by differential ABCB6 expression does not lead to any significant change in ROS production (data not shown). However, whether a shift from dynamic change in ABCB6 expression to chronic gain or loss of ABCB6 expression leads to pathologically significant ROS levels requires further investigation.

ABCB6 deficiency or overexpression leads to compromised nutrient sensitivity

Normal energy metabolism is characterized by periodic shifts in glucose and fat oxidation as the mitochondrial machinery responsible for carbon combustion switches freely between alternative fuels according to physiological and nutritional circumstances (Gao, et al., 2014; Liesa, et al., 2013). This capacity of the mitochondria to switch between fuels is coupled to cellular and/or tissue changes, that promotes fasting and feeding

dependent glucose disposal, and lipid storage. An inability to accommodate such switch between fuel sources results in aberrant energy metabolism in the liver promoting the development of metabolic disease including obesity and insulin resistance (Bournat *et al.*, 2010; Galgani, et al., 2008; Gomes *et al.*, 2011b; Smith, et al., 2018b).

In mice with hepatic ABCB6 deficiency or hepatic ABCB6 overexpression mitochondrial capacity to switch between fuels is compromised. *Abcb6* deficient mice, because of their blunted ability to switch between carbon sources (blunted fat oxidation and glycogen depletion in the fasted state), appear to be in a state of over-nutrition and unabated substrate competition leading to a phenotype associated with metabolic comorbidities of glucose intolerance, and insulin resistance. In contrast ABCB6 overexpressing mice appear to be glucose tolerant and insulin sensitive. Interestingly, ABCB6 deficient mice respond to this state of unabated substrate competition by decreasing their food intake. Although the cause of anorexia in these animals should be further investigated, the observed feeding adaptation may be a compensatory mechanism to slow down excessive weight gain because of low energy efficiency. This is consistent with the observation that metabolic signals relating to energy surplus usually trigger compensatory changes, including decreased food intake and increased physical activity to maintain energy balance (Lenard and Berthoud, 2008). In this context it will be informative to assess if *Abcb6LKO* mice are physically more active either in the form of spontaneous physical activity or voluntary physical activity (commonly thought of as “exercise”).

In contrast to *Abcb6LKO* mice, *Abcb6LOE* mice respond to a state of under-nutrition with increased food consumption. Although, the underlying molecular mechanisms that

allow *Abcb6LOE* mice to increase food consumption needs to be elucidated, the observed response is consistent with activation of mechanisms that facilitate coping with an energy deficit. Under normal circumstances a decrease in fuel availability will be signaled to the brain by elevated ghrelin levels and low levels of all other gut hormones and a dip in leptin levels (Lenard and Berthoud, 2008). In this context it would be informative to evaluate if signaling mechanisms, regulated by hormones such as leptin and ghrelin, are altered in these mice to promote fasting responses in brain activity.

Most interestingly, in both *Abcb6LKO* and *Abcb6LOE* mice, despite the adaption in the feeding habits, chronic metabolic pressures appear to compromise nutrient sensitivity leading to increased body weight gain in ABCB6 deficient mice and low body weight in ABCB6 overexpressing mice. We hypothesize that the increased liver and white adipose tissue weight in *Abcb6LKO* mice results from increased lipogenesis and ensuing lipid accumulation in the liver and increased mobilization of fat for storage in adipocytes along with decreased lipolysis. Such a hypothesis would be consistent with the observation that the *Abcb6LKO* mice appear to be in a constant fed state and would also help explain the increased serum FFA and TG in *Abcb6LKO* mice irrespective of the nutrient status (fed or fasted).

In contrast to Abcb6LKO mice, we hypothesize that in *Abcb6LOE* mice the decreased liver and white adipose tissue weight results from decreased lipogenesis in liver and increased lipolysis in white adipose tissue resulting in increased mobilization of fat from the adipocytes as a potential source of fuel. Consistent with such a hypothesis the *Abcb6LOE* mice show increased serum FFA which would be expected with enhanced lipolysis under fasting conditions.

However, it is evident from the discussion presented in the above paragraphs, that a detailed analysis of the signaling pathways altered in *Abcb6LKO* and *Abcb6LOE* mice, not only in the liver but also in white and brown adipose tissue and the muscle, is required for a detailed understanding of the complex metabolic phenotype observed in these genetically modified mice.

ABCB6 expression is linked to nutrient status

Our studies demonstrate that ABCB6 expression is in sync with hepatic bioenergetic demands, and that ABCB6 is a required component of the metabolic and cell signaling events that enable crosstalk and cooperation between nutritional status and energy homeostasis. Fasting results in increased ABCB6 expression which appears to be regulated at the level of transcription, while feeding leads to loss of ABCB6 expression mediated by post-transcriptional mechanisms. However, at this stage, it is not clear what mechanisms link nutritional changes to ABCB6 expression. Three major nutritional sensors, mammalian target of rapamycin (mTOR), AMP-activated kinase (AMPK) and Sirtuins are involved in the control of mitochondrial physiology (Albert, et al., 2015; Bullon *et al.*, 2016; He *et al.*, 2017; Laplante, et al., 2012; Li, 2013; Ross *et al.*, 2016; Sengupta *et al.*, 2010). These nutritional sensors control mitochondrial biogenesis, mitochondrial dynamics and mitochondrial turnover through mitophagy/autophagy. Future studies will explore if ABCB6 is regulated by these pathways, and if so how these pathways are integrated to promote metabolic homeostasis.

ABCB6 expression is casually linked to regulation of core protein machinery that governs mitochondrial shape.

It has been established that the Dynamin-like GTPases form the core machinery that govern mitochondrial shape. The mammalian orthologues of mitofusin 1 and mitofusin 2 (*Mfn1* and *Mfn2*) and Optic Atrophy 1 (OPA1) are required to maintain a reticular mitochondrial network in cells, while the Dynamin-related protein 1 (DRP1) is required to promote mitochondrial fragmentation. Indeed, genetic ablation of mitofusin-1 and mitofusin-2 as well as the inner mitochondrial membrane (IMM) GTPase optic atrophy 1 is embryonic lethal (Chen, et al., 2003; Davies, et al., 2007). Similarly, the loss of the core fission GTPase Drp1 is also lethal (Ishihara, et al., 2009). However, unlike the phenotypes observed with the complete loss of these Dynamin-like GTPases, adaptive mitochondrial response to physiological and environmental stimuli appears to require a tighter regulation in their expression and activity. Indeed, the recent characterization of several regulatory proteins that control the activity and localization of the core dynamin related GTPases indicate that the molecular mechanisms regulating and controlling the morphology and function of mitochondria are more elaborate and complex in vertebrates (Ali *et al.*, 2018; Chandhok *et al.*, 2018; MacVicar *et al.*, 2016; Santel *et al.*, 2008). Our findings demonstrate that ABCB6 might function as a regulatory protein that controls the activity of the core dynamin related GTPases by modifying their mitochondrial localization. However, the precise mechanism, by which ABCB6 expression regulates differential localization of the core fusion/fission machinery requires further investigation.

Chapter 5. Alterations of the Hepatic Metabolome of Fasted and Refed Wild-type and *Abcb6* genetically altered mice

5.1 Abstract

Inbred mouse strains are frequently used as a model to study metabolic flexibility. Central to these studies are responses during pre-absorptive and post-absorptive states. Previous studies demonstrated that liver-specific *Abcb6* deficient (*Abcb6LKO*) and liver-specific *Abcb6* over expressing (*Abcb6LOE*) mice, alterations in metabolic flexibility responses were manifested in altered food consumption, respiratory exchange ratio, and disrupted glucose homeostasis. Further, in these mice, metabolic inflexibility was associated with disrupted mitochondrial dynamics. However, the mechanistic details of how altered ABCB6 expression leads to disruptions in mitochondrial dynamics are unclear. Given that ABCB6 is a membrane transport protein, we hypothesized that the phenotype observed in ABCB6 deficiency or over expression might arise from or loss of metabolite homeostasis. As a first step in testing this hypothesis, we performed an untargeted analysis of hepatic metabolites. To our surprise, preliminary analysis of the results demonstrates a role for hepatic ABCB6 in the reorganization of three prominent mitochondrial metabolic networks including bile acid, amino acid, and phospholipid homeostasis.

5.2 Introduction

Metabolic flexibility is the set of physiological adaptations to energy supply and demand. The primary facet of flexibility is the ability to preferentially utilize either carbohydrates or lipids as an energy source in response to environmental cues. Societal trends of decreased physical activity and increased caloric intake have led to increased average body weight and impaired metabolic flexibility that are accompanied by comorbidities such Type II diabetes, and metabolic syndrome (Goodpaster *et al.*, 2017).

Metabolic flexibility is needed under drastic circumstances such as physical exertion and starvation as well as circadian-driven eating patterns. Ensuing the diurnal sleep period, the is the fasted state. During this period, stored lipids are utilized to ensure adequate blood glucose primarily for the brain and resting metabolic processes. In the waking state, food consumption is utilized to maintain blood glucose and excess energy is stored as lipids in fat deposits for future use.

Maintenance of energy homeostasis through flexibility is accomplished via the coordination of interlinked metabolic pathways in multiple tissues. The liver, skeletal muscle, adipose tissue, heart, brain, and pancreas orchestrate the utilization, trafficking, and storage of energy substrates in response to endocrine signaling. Energy supply and demand drives enzymatic activity unique to individual organs that ensures rapid switching between carbohydrate and lipid metabolism. These responses are fine-tuned by energy sensing transcriptional programs (Smith *et al.*, 2018a).

Quantitative analysis of energy pathway metabolites has the potential to pinpoint derangements in the function or regulation of metabolic flexibility pathways. Analysis of metabolites in individual metabolic tissues under various energy supply conditions

would uncover how organ systems contribute to metabolic flexibility. Comparisons of the responses from individual metabolic tissues could also elucidate the how organ-organ crosstalk regulates overall metabolism. As a first step in understanding how individual organs contribute to maintaining energy homeostasis, and how physiological responses are integrated during nutrient state transitions, we initiated the analysis (completed by Metabolon Inc, Research Triangle Park, NC) of global metabolites in fasted (18 hours) and refed (6 hours) mouse liver in wild-type (WT), *Abcb6* liver-specific knock out (*Abcb6LKO*), and Abcb6 liver-specific over expressing (*Abcb6LOE*) 8-week male mice.

To our knowledge, this is the first study of its kind and as such, will assist in further defining the liver's role in metabolic flexibility. Also, this knowledge base of hepatic responses to nutrient state in wild-type mice can serve as a basis of comparison for other pharmacological or genetic treatments. In the case of our ABCB6 model of metabolic inflexibility, this study is especially appropriate and will potentially assist in describing the physiological role of ABCB6 in mammals.

5.4 Results

Summary of Super Pathway Changes in Fasted and Refed Mouse Liver

Data analysis was organized in a hierarchical manner with "Super pathways" being a large group of physiologically related sub pathways and with individual biochemicals (metabolites) being grouped within the sub pathways. The nomenclature "pathway"

does not necessarily indicate biochemical pathways per se, but rather, a convenient way to organize related biochemicals. For instance, the “Energy” super pathway contains metabolites generated from Krebs cycle and oxidative phosphorylation activities. Figures 5.1 A-H show the magnitude of change of the 8 “super pathways” Amino Acids, Carbohydrates, Energy, Lipids, Nucleotides, Peptides, Vitamins, and Xenobiotics from the fasted to refed state in WT, *Abcb6LKO*, and *Abcb6LOE* mice.

Values represented are the average sums of all metabolite peak values within the super pathway. In WT mice, food intake resulted in an increase in 6 of the 8 super pathways (Amino Acids, Carbohydrates, Energy, Peptides, Vitamins, and Xenobiotics). The Carbohydrate, Vitamin, and Xenobiotic super pathways reached statistical significance (Figures 5.1A-1C and 5.1F-1H). In contrast, the Lipid and Nucleotide super pathways in WT mice were decreased in the refed state with the Lipid super pathway reaching statistical significance (Figures 5.1D and 5.1E).

In *Abcb6LKO* mice, the same 6 super pathways were increased in the refed state with the Amino Acid, Carbohydrate, Vitamin, and Xenobiotic categories reaching statistical significance (Figures 5.1A- 1C, and 5.1F-1H). Lipid and Nucleotide super pathways were reduced in LKO mice as in the WT group. Again, with only the Lipid super pathway decrease reaching significance statistically (Figures 5.1D and 5.1E). In *Abcb6LOE* mice, the Amino Acid, Peptide, and Vitamin super pathways were not increased in response to feeding (Figure 5.1A, 5.1F, and Figure 5.1G). Both the Lipid and Nucleotide super pathway fasting mediated increase reached significance in *Abcb6LOE* mice (Figures 5.1D and 5.1E). Refed *Abcb6LOE* mice had significantly lower Vitamin super pathway values than both WT and *Abcb6LKO* mice (Figure 5.1G).

Although the super pathway analysis showed significant differences between the experimental condition (fasted or refed), this type of analysis did not demonstrate significant changes in the super pathway values between the genotypes (WT, LKO, and LOE).

Figure 5.1

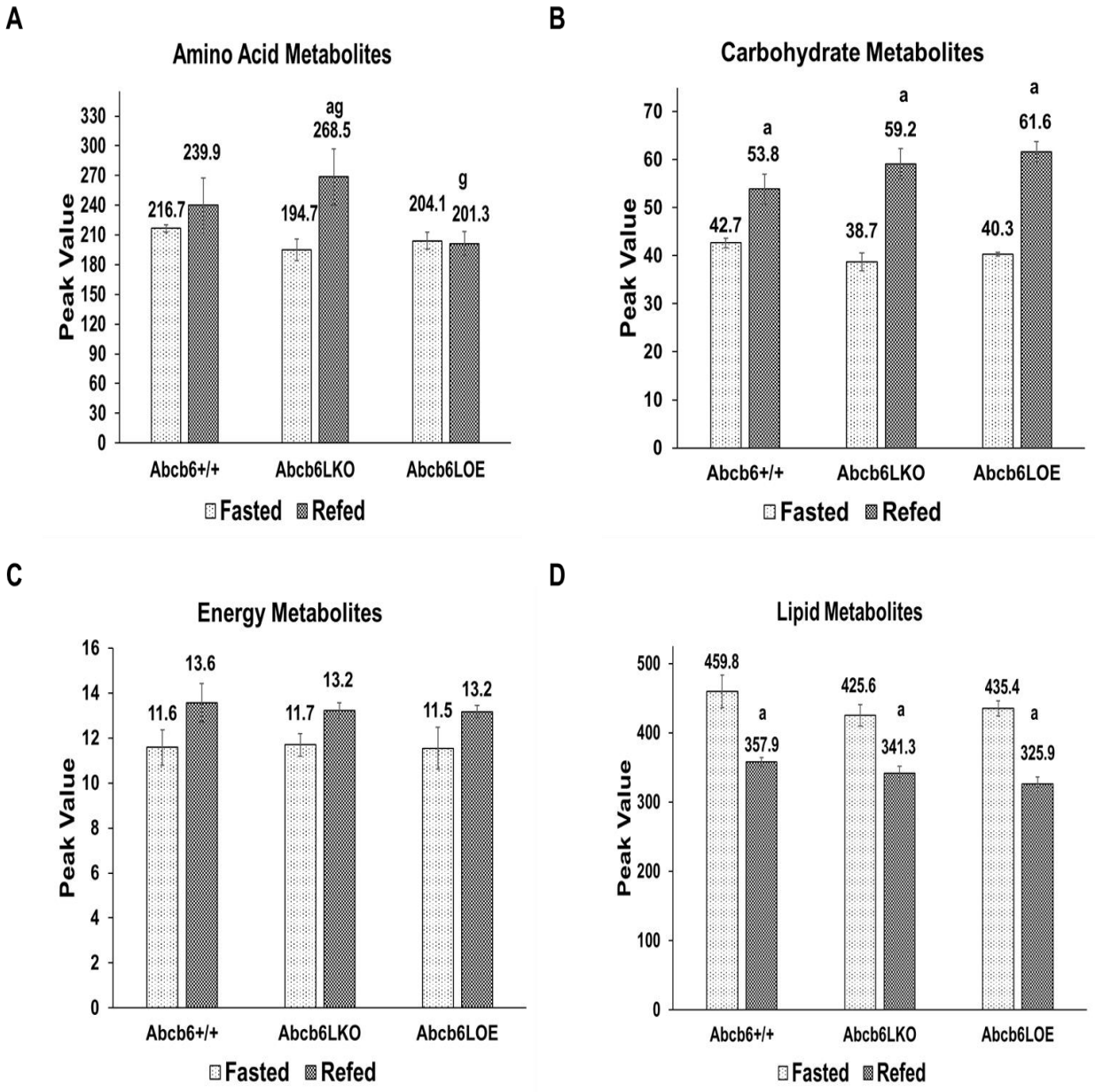

Figure 5.1 continued

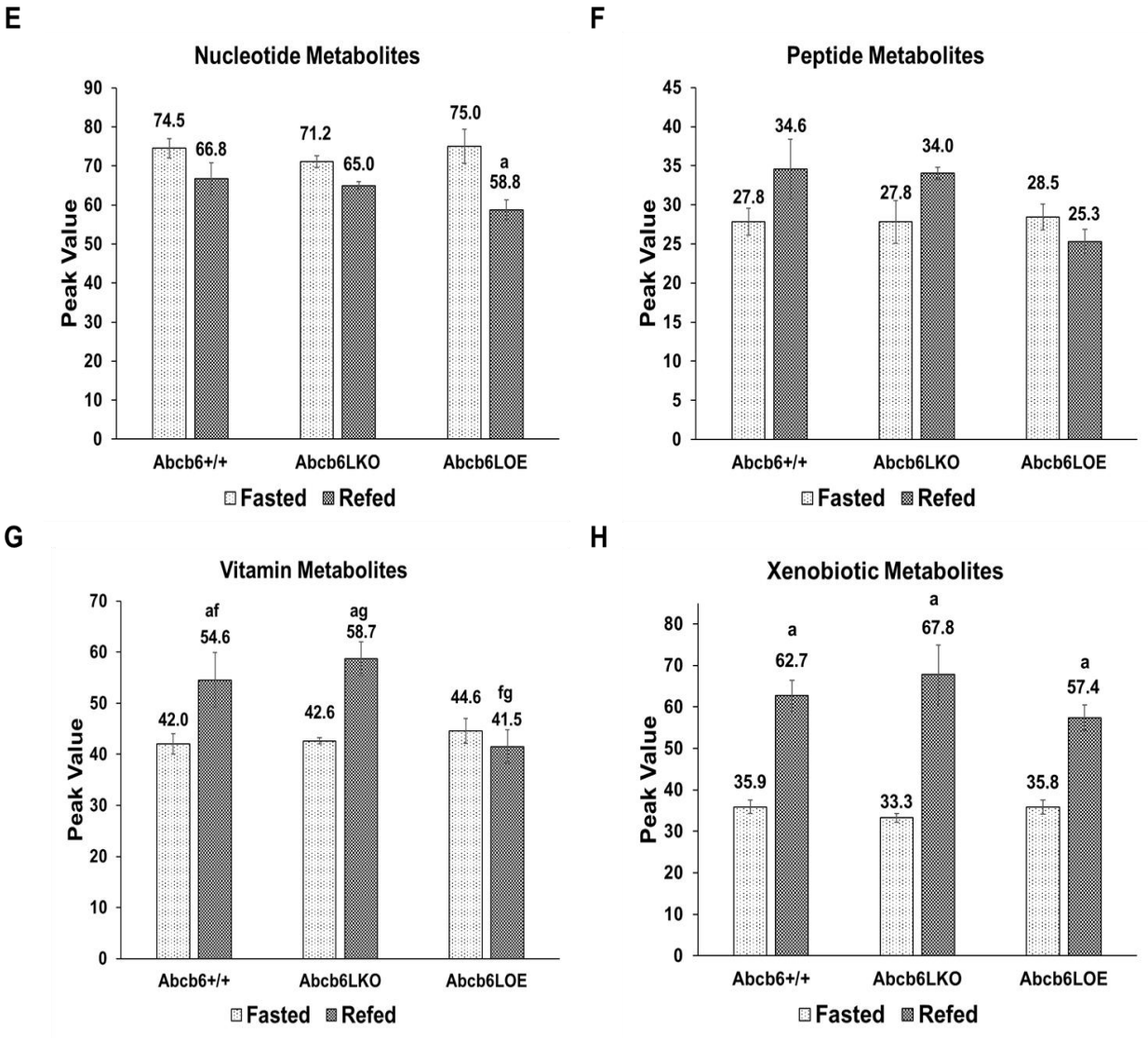

Fasted vs Refed	a
Fasted WT vs LKO	b
Fasted WT vs LOE	c
Fasted LKO vs LOE	d
Refed WT vs LKO	e
Refed WT vs LOE	f
Refed LKO vs LOE	g

Figure 5.1. Metabolic super pathway changes in response to fasting and refeeding in WT, *Abcb6LKO*, and *Abcb6LOE* mouse liver (A)-(H) Total peak values in the Amino Acid, Carbohydrate, Energy, Lipid, Nucleotide, Peptide, Vitamin, and Xenobiotic super pathways. N=4.

Amino Acid Metabolites in Fasted and Refed Mouse Liver

The liver utilizes amino acids for protein synthesis as well as for a glucogenic or ketogenic energy source. They are obtained exogenously from meals via portal circulation, de novo synthesis, or from protein and peptide degradation. In WT mice, total amino acids were slightly but non-significantly increased in response to feeding (Figure 5.1A). The main contributing factor to the overall increase in amino acids was the significant increase in the glutathione sub pathway (Figure 5.2A). The Methionine/Cysteine/SAM/Taurine sub pathway metabolites are necessary for glutathione production and intuitively, were also increased in the refed state (Figure 5.2B). Conversely, the glucogenic amino acid sub pathways Alanine/Aspartate and Histidine were increased in the fasted state with the Alanine/Aspartate sub pathway reaching statistical significance (Figures 5.2C and 5.2D). The ketogenic amino acid sub pathway Lysine was also significantly increased in the fasted state with the other major ketogenic sub pathway, Leucine/Isoleucine/Valine also being increased but not reaching statistical significance (Figures 5.2E and 5.2F). Within the Glutathione sub pathway, the reduced form of glutathione (GSH) metabolite was the main contributor to the increase in response to feeding (data not shown). The observed feeding induced increase in GSH in this study agrees with published data in rat liver (Yamada *et al.*, 2018). Higher glucogenic and ketogenic amino acid levels seen in WT mouse liver in the fasted state

may indicate increased import from extrahepatic tissues in the fasted state to support increased gluconeogenesis and ketosis.

As previously noted, *Abcb6LKO* refed mice had a significantly higher Amino Acid super pathway levels compared to fasted LKO mice (Figure 5.1A). Like the WT group, the major contribution to the increase was the Glutathione sub pathway (also due to GSH) with the Methionine/SAM/Taurine sub pathway following the same expected trend. Strikingly, the increases in the Amino Acid super pathway, Glutathione and Methionine/SAM/Taurine sub pathways were not seen in *Abcb6LOE* mouse liver (Figures 5.1A,5.2A, and 5.2B). Rather, these pathways were not significantly changed in response to feeding. In fact, *Abcb6LOE* Amino acid levels were significantly lower than *Abcb6LKO* in the fed state (Figures 1A, 5.2A, and 5.2B). Glucogenic amino acids in the Histidine and Alanine/Arginine sub pathways in the *Abcb6LKO* and *Abcb6LOE* followed the same fasting-induced increase trend as WT mice with feeding response reaching statistical significance. However, the fasted *Abcb6LKO* Alanine/Aspartate sub pathway level was significantly lower than both the WT and *Abcb6LOE* groups (Figure 5.2C and 5.2D). The ketogenic Leucine/Isoleucine/Valine sub pathway was, as in the WT group, increased in response to fasting in *Abcb6LKO* and *Abcb6LOE* mice with only the *Abcb6LOE* group reaching significance (Figure 5.2F). The other ketogenic sub pathway, Lysine, was also increased in response to fasting in *Abcb6LKO* and *Abcb6LOE* groups but only in the *Abcb6LKO* group did the increase reach significance. However, in both *Abcb6LKO* and *Abcb6LOE* mice, the fasted level of the Lysine sub pathway was significantly lower compared to WT mice (Figure 5.2E).

The two main concepts derived from analysis of amino acid sub pathways are, glutathione metabolism is increased in response to feeding and glucogenic/ketogenic amino acids are increased in the fasted state in mouse liver. In *Abcb6LOE* mice, the feeding-induced glutathione increase is extremely blunted. Also, both *Abcb6LKO* and *Abcb6LOE* mice had generally less drastic increases in glucogenic/ketogenic amino acids in response to fasting. (Figure 5.2A and Figures 5.2C-2F).

Figure 5.2

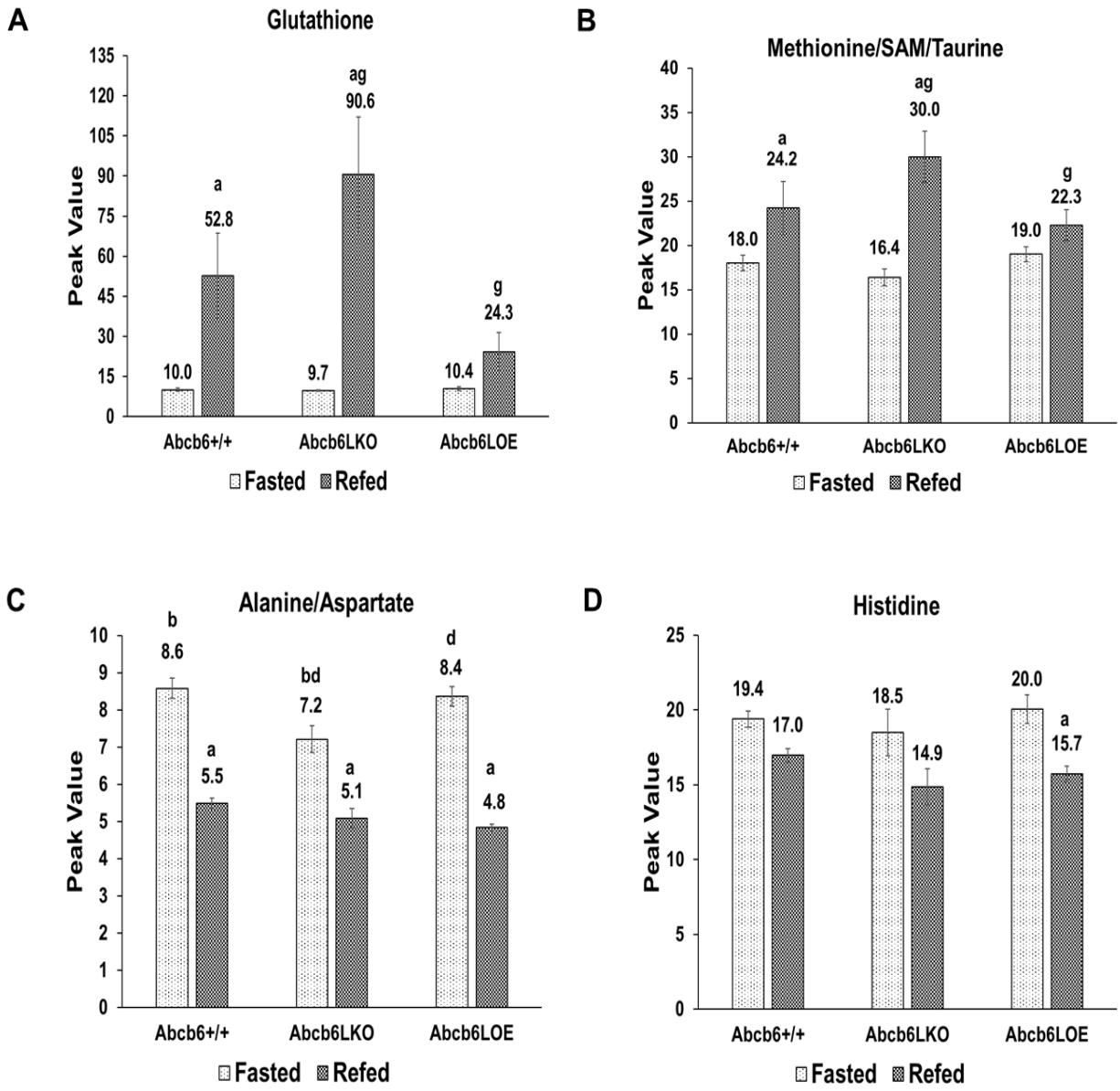

Figure 5.2 continued

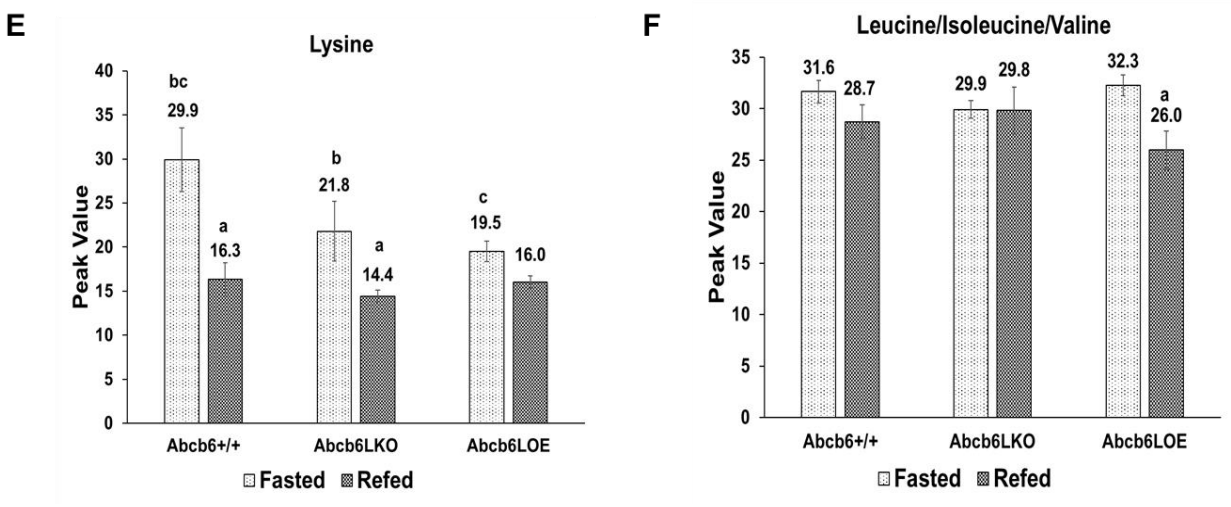

Fasted vs Refed	a
Fasted WT vs LKO	b
Fasted WT vs LOE	c
Fasted LKO vs LOE	d
Refed WT vs LKO	e
Refed WT vs LOE	f
Refed LKO vs LOE	g

Figure 5.2. Metabolic Amino Acid sub pathway changes in response to fasting and refeeding in WT, *Abcb6LKO*, and *Abcb6LOE* mouse liver (A)-(F) Total peak values in the Glutathione, Methionine/SAM/Taurine, Alanine/Aspartate, Histidine, Lysine, and the Leucine/Isoleucine/Valine sub pathways. N=4.

Carbohydrate Metabolites in Fasted and Refed Mouse Liver

A major function of the liver is to maintain blood glucose within a narrow range in both fasted and fed conditions. In the fed state, excess carbohydrates are stored as glycogen or are converted to fatty acids via de novo lipogenesis. During a fast, hepatic glycogen stores are converted to glucose which is subsequently exported to circulation. Concomitantly, hepatic gluconeogenesis activity increases to maintain blood sugar as glycogen stores are depleted. During the fasted period, the liver foregoes maintenance of its own glucose supply to provide for extrahepatic tissues. This phenomenon is demonstrated in our study with a greater than 2-fold reduction of hepatic glucose in the fasted state in WT mouse liver (Figure 5.3A). In the WT group, the carbohydrate super pathway was significantly increased in response to feeding (Figure 5.1B). The Glycogen sub pathway was expectedly significantly increased in the refed state (Figure 5.3B). The Fructose/ Mannose/Galactose sub pathway also contributed to the overall increase in hepatic carbohydrates presumably due to metabolism of diet-derived sugars (Figure 5.3C). Conversely, the Nucleotide Sugar sub pathway in WT mouse liver was significantly decreased in the refed state possibly due to the fact certain nucleotide sugars are precursors for glycogen synthesis (Ball *et al.*, 2011) (Figure 5.3D). In WT mice, hepatic lactate, a product of glycolysis, was significantly higher in the refed state (Figure 5.3E). However, the upstream glycolysis intermediate, pyruvate was not significantly altered in response to feeding (Figure 5.3F).

Abcb6LKO and *Abcb6LOE* mice had no significant variations from WT mice in hepatic glucose, the Carbohydrate super pathway, Glycogen, Fructose/Mannose, Lactose, or Pyruvate sub pathways in either nutritional state. (Figures 5.3A, 5.1B, 5.3B,

5.3C, 5.3E, and 5.3F). However, several changes were seen in the Nucleotide sugars sub pathway. Although both *Abcb6LKO* and *Abcb6LOE* groups had increases in nucleotide sugars in response to fasting, only the *Abcb6LOE* group was statistically significant. Also, *Abcb6LKO* mice had significantly lower nucleotide sugars in the fasted state compared to WT. Finally, in the refed state, *Abcb6LOE* mice had significantly lower refed nucleotide sugar levels.

The carbohydrate super pathway and most carbohydrate sub pathways were increased in the refed state with virtually no differences in sub pathway levels or responses between any genetic treatment groups. The exception to this trend was a relative increase in nucleotide sugars in the fasted state in all groups with *Abcb6LKO* and *Abcb6LOE* mice having lower fasted state nucleotide sugar levels compared to WT.

Figure 5.3

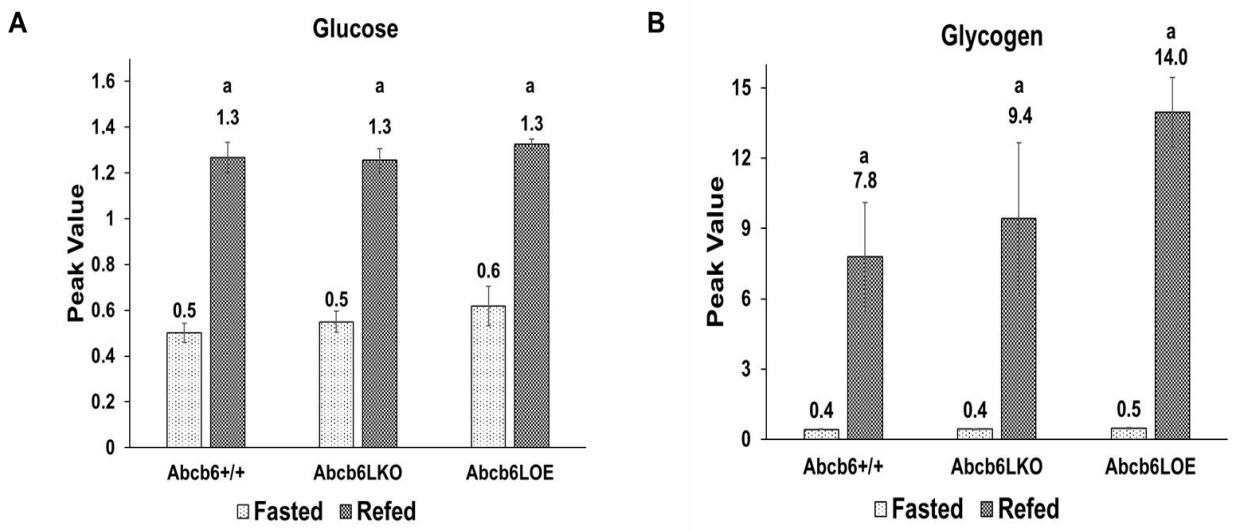

Figure 5.3 continued

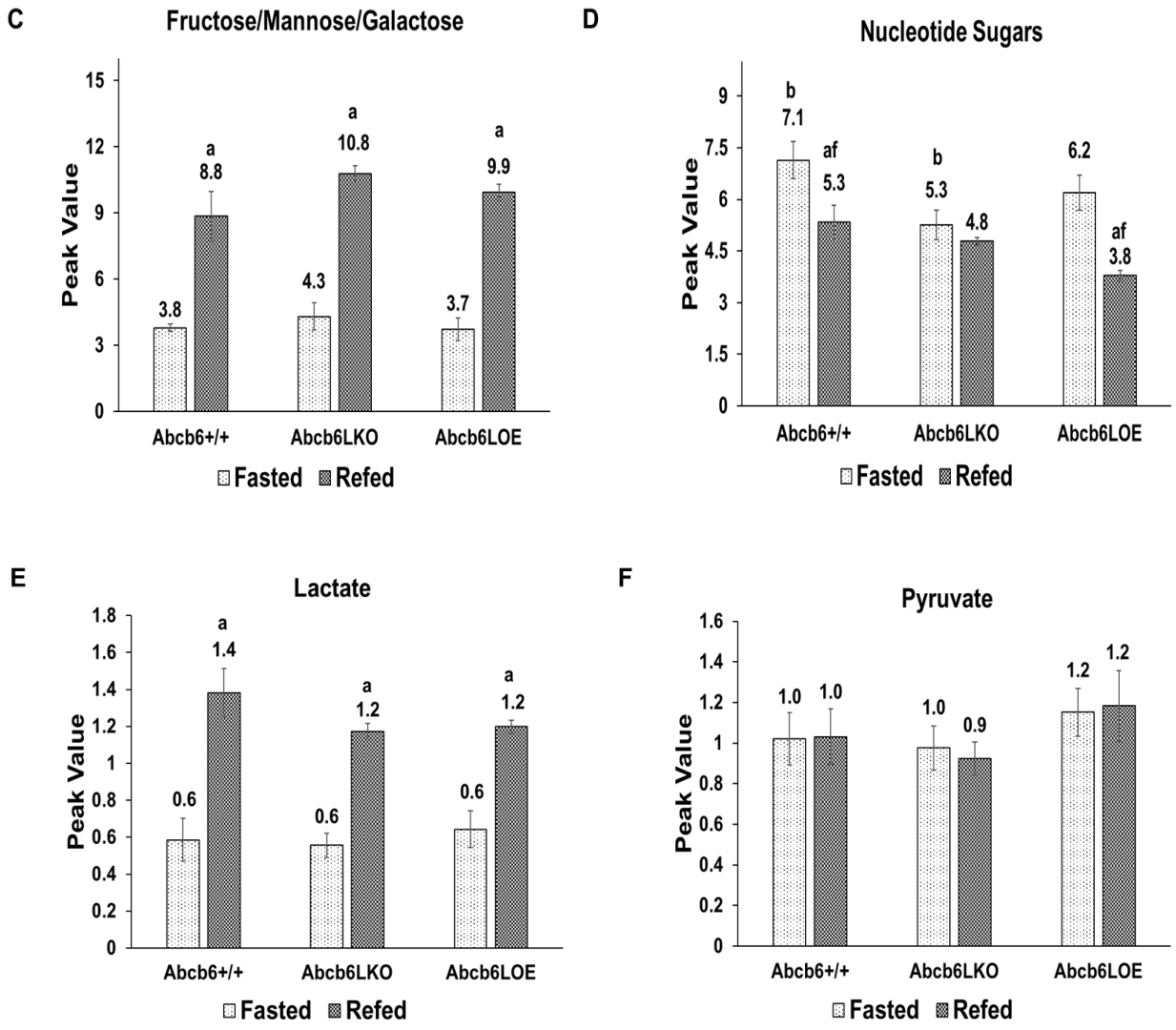

Fasted vs Refed	a
Fasted WT vs LKO	b
Fasted WT vs LOE	c
Fasted LKO vs LOE	d
Refed WT vs LKO	e
Refed WT vs LOE	f
Refed LKO vs LOE	g

Figure 5.3. Metabolic Carbohydrate sub pathway changes in response to fasting and refeeding in WT, *Abcb6LKO*, and *Abcb6LOE* mouse liver (A)-(F) Peak values of glucose,

Glycogen, Fructose/Mannose/Galactose, and Nucleotide sugars sub pathways, lactate, and pyruvate. N=4.

Energy Metabolites in Fasted and Refed Mouse Liver

In this analysis, the Energy super pathway is comprised of oxidative phosphorylation and tricarboxylic acid (TCA) cycle sub pathways. The Energy super pathway was not significantly altered in response to feeding in any of our treatment groups (Figure 5.1C) nor did the *Abcb6LKO* or *Abcb6LOE* group responses significantly differ from the WT group. However, several TCA derivative metabolites were significantly altered. In WT mice, the metabolite that had the highest magnitude of upregulation in response to feeding was succinyl carnitine (Figure 5.4A). Conversely, alpha-ketoglutarate was significantly decreased in the refed state (Figure 5.4B). These significantly altered intermediates may indicate cataplerotic/anaplerotic exit and entry points of the TCA cycle.

Abcb6LKO mice did not differ significantly from WT mice in the parameters listed above (Figures 5.1C, 5.4A, and 5.4B). Energy super pathway and succinyl carnitine levels were similar to WT and *Abcb6LKO* mice in *Abcb6LOE* mice. However, fasting did not illicit an increase in alpha-ketoglutarate (Figures 5.1C, 5.4A, and 5.4B).

The Energy super pathway was only very slightly decreased upon fasting in all treatment groups; supportive of the concept that the liver contributes to energy homeostasis through metabolic flexibility responses.

Figure 5.4

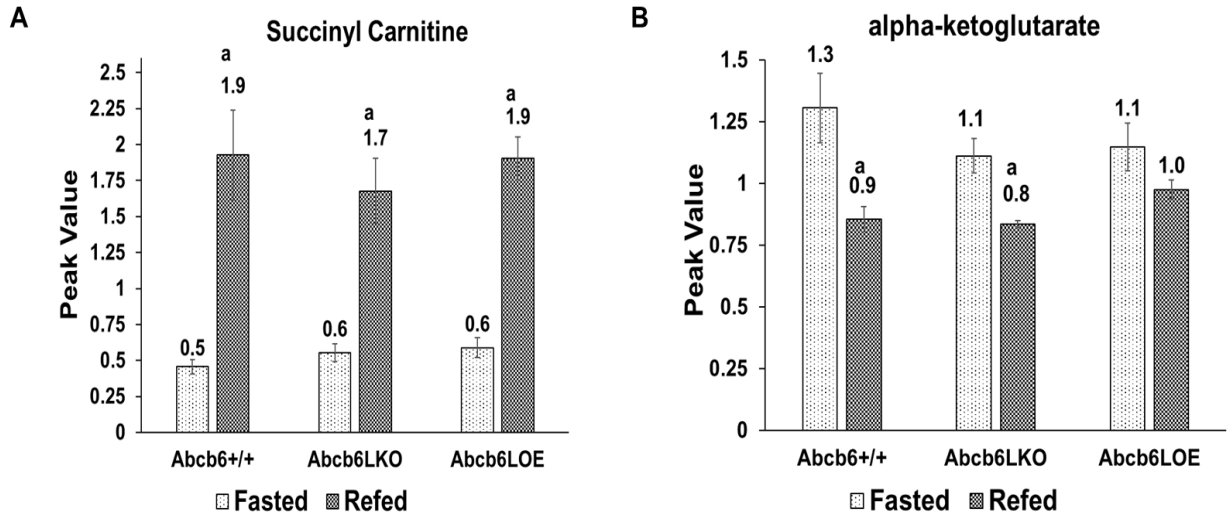

Fasted vs Refed	a
Fasted WT vs LKO	b
Fasted WT vs LOE	c
Fasted LKO vs LOE	d
Refed WT vs LKO	e
Refed WT vs LOE	f
Refed LKO vs LOE	g

Figure 5.4 Metabolic Energy metabolite changes in response to fasting and refeeding in WT, *Abcb6LKO*, and *Abcb6LOE* mouse liver (A) Succinyl carnitine total peak values. (B) Pyruvate total peak values. N=4.

Lipid Metabolites in Fasted and Refed Mouse Liver

At the start of the fasting period, blood lipid levels fall. Through beta-adrenergic signaling, free-fatty acids are liberated through lipolysis in adipose deposits and fatty acids are taken up by the liver. It is well established that as a result, total hepatic lipids are increased in the fasted state (Geisler, et al., 2016; Rui, 2014). Our analysis was in

accord, showing an increase in the Lipid super pathway in response to fasting in all treatment groups (Figure 5.1D). The free-fatty acids are either oxidized into ketones or packaged into VLDL particles for use by extrahepatic tissues. In WT mice, the Diacylglycerol sub pathway contributed to the greatest increase within the super pathway (Figure 5.5A). Long and medium chain fatty acid sub pathways were also significantly increased in the fasted state. (Figures 5.5B and 5.5C). Polyunsaturated fatty acids (n-3 and n-6) were also increased in the fasted state in keeping with previously published results (Figure 5.5D) (Marks *et al.*, 2015). The increased hepatic fatty acid and diacylglycerol content was likely due to the well-characterized influx of adipose fatty acids due to increased lipolysis and hepatic fatty acid uptake. The Ketone and Oxidized fatty acid sub pathways were also significantly increased in the fasted state (Figures 5.5E and 5.5F). The increase in ketone bodies is intuitive due to the expected switch to utilization of lipids for energy in the fasted state. Oxidized fatty acids such as 4-hydroxynonenal (the sole metabolite assessed in this study) have been associated with increased beta-oxidation (Li *et al.*, 2013). The Mevalonate sub pathway was also significantly increased in the fasted group (Figure 5.5G) in agreement with previously published data (Wiss *et al.*, 1977) that describes increased cholesterol synthesis in the fasted state. The increase seen in mevalonate may be a compensatory action to increase endogenous cholesterol production in absence of an exogenous supply.

Despite the fasting-mediated increase of most hepatic lipids, WT glycerophospholipids were significantly increased in the refed state with the significant increases seen in phosphatidylcholine (PC), phosphatidylethanolamine (PE),

phosphatidylinositol (PI) and phosphatidylglycerol (PG) (Figures 5.5H-5K). The relative decrease in hepatic phospholipid content due to fasting is consistent with published results (Ikeda *et al.*, 2014).

An essential function of the liver is the production of bile acids which are the main component of bile (also containing cholesterol and phospholipids), a substance that aids in the intestinal absorption of fats and fat-soluble nutrients through its surfactant action on lipids. Primary bile acids originate from the liver while secondary acids are produced through bacterial reactions in the intestine. Primary bile acids from the liver are routed to the ileum through the common hepatic bile duct and are also stored in the gall bladder (in mice). Primary and secondary bile acids are reabsorbed from the intestinal lumen and returned to the liver through portal circulation. The total amount of bile acids existing this enterohepatic circulation is referred to as the bile acid pool. In WT mice, Primary and Secondary bile acid sub pathways had a slight, non-significant increase in response to feeding suggesting increased hepatic bile acid synthesis and a larger bile acid pool. (Figures 5.1D, 5.5L, and 5.5M)This response is in agreement with published data (Chiang, 2013).

Hepatic diacylglycerol and fatty acid fasting-induced increases in *Abcb6LKO* and *Abcb6LOE* mice were similar to WT mice (Figures 5.5A-5D). Likewise, oxidized fatty acids and beta-hydroxybutyrate levels were increased in response to fasting in both *Abcb6LKO* and *Abcb6LOE* mouse liver. However, in *Abcb6LKO* and *Abcb6LOE* mice, fasting beta-hydroxybutyrate was lower compared to the WT group with the *Abcb6LOE* group reaching statistical significance. Also, both *Abcb6LKO* and *Abcb6LOE* mouse liver had lower oxidized fatty acids in the fasted state compared to the WT groups but

the decrease did not reach statistical significance (Figures 5.5E and 5.5F). The *Abcb6LKO* and *Abcb6LOE* Mevalonate sub pathway levels increased in response to fasting as was the case in the WT group. However, both *Abcb6LKO* and *Abcb6LOE* fasted levels were significantly lower as compared to WT (Figure 5.5G). Feeding induced glycerophospholipids in a similar manner in *Abcb6LKO* and *Abcb6LOE* mice with the exception being the *Abcb6LOE* Phosphatidylcholine sub pathway which was not significantly increased in response to feeding (Figures 5.5H-5K). In contrast to the slight feeding-induced increase in bile acids seen in WT mice, the *Abcb6LKO* group refed levels were virtually identical to fasted state levels. Remarkably, *Abcb6LOE* mice had an opposite response compared to the WT group with relatively lower bile acids in the refed state with the fasted levels being significantly higher than both WT and *Abcb6LKO* groups (Figures 5.5.L and 5.5.M).

In summary, hepatic lipids were generally increased in the fasted state except for glycerophospholipids which were decreased in response to fasting in WT mice. Products of fatty acid oxidation are also increased in WT mice in the fasted state. *Abcb6LKO* and *Abcb6LOE* mice had blunted fasting-induced beta-oxidation and cholesterol responses as compared to WT. Finally, genetic manipulation of ABCB6 expression clearly disrupted the feeding induced increase of hepatic bile acids.

Figure 5.5

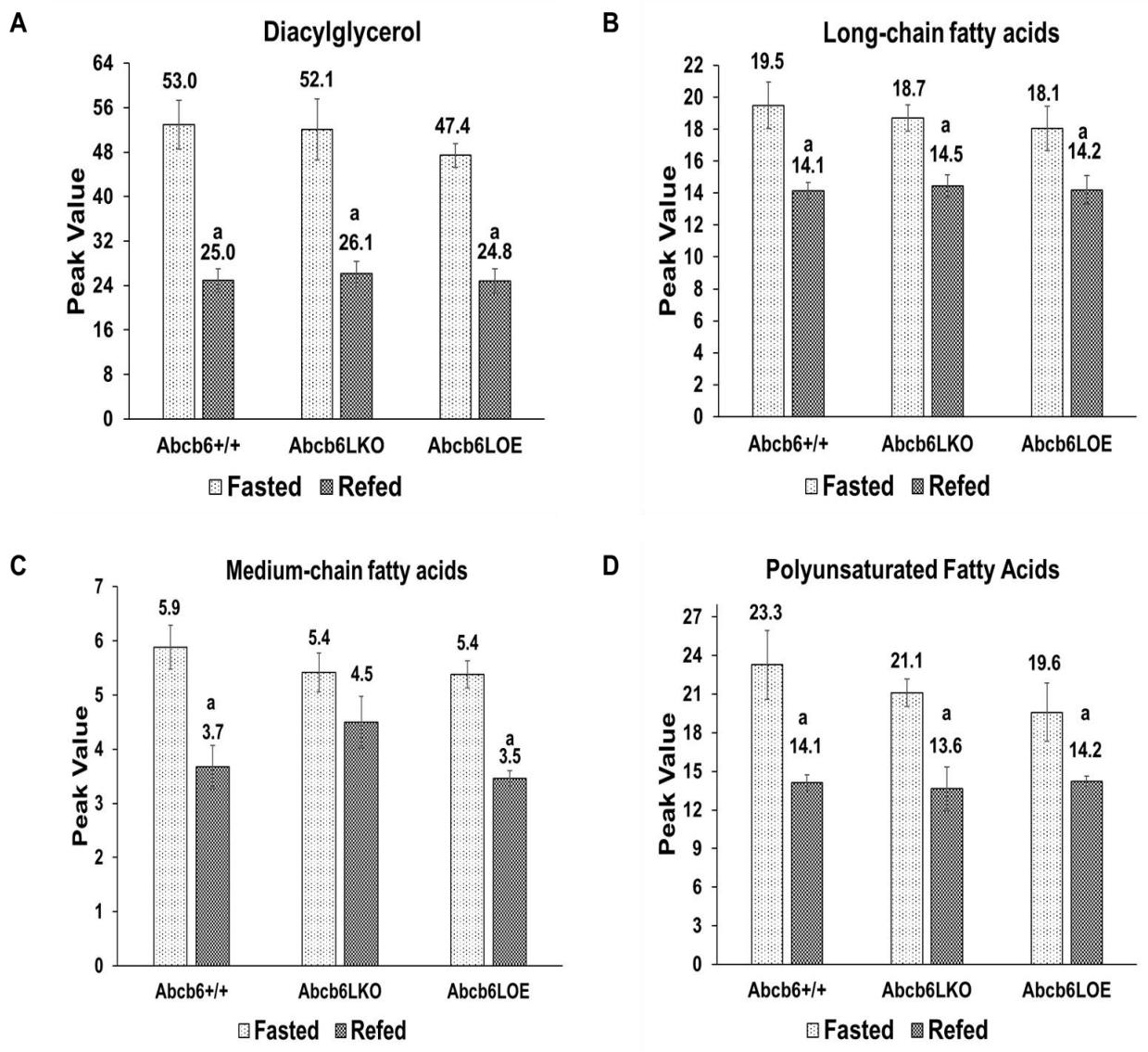
A
Diacylglycerol
Peak Value
64
56
48
40
32
24
16
8
0
53.0
a
25.0
52.1
a
26.1
47.4
a
24.8
Abcb6+/+
Abcb6LKO
Abcb6LOE
Fasted
Refed
B
Long-chain fatty acids
Peak Value
22
20
18
16
14
12
10
8
6
4
2
0
19.5
a
14.1
18.7
a
14.5
18.1
a
14.2
Abcb6+/+
Abcb6LKO
Abcb6LOE
Fasted
Refed
C
Medium-chain fatty acids
Peak Value
7
6
5
4
3
2
1
0
5.9
a
3.7
5.4
4.5
5.4
a
3.5
Abcb6+/+
Abcb6LKO
Abcb6LOE
Fasted
Refed
D
Polyunsaturated Fatty Acids
Peak Value
27
24
21
18
15
12
9
6
3
0
23.3
a
14.1
21.1
a
13.6
19.6
a
14.2
Abcb6+/+
Abcb6LKO
Abcb6LOE
Fasted
Refed

Figure 5.5 continued

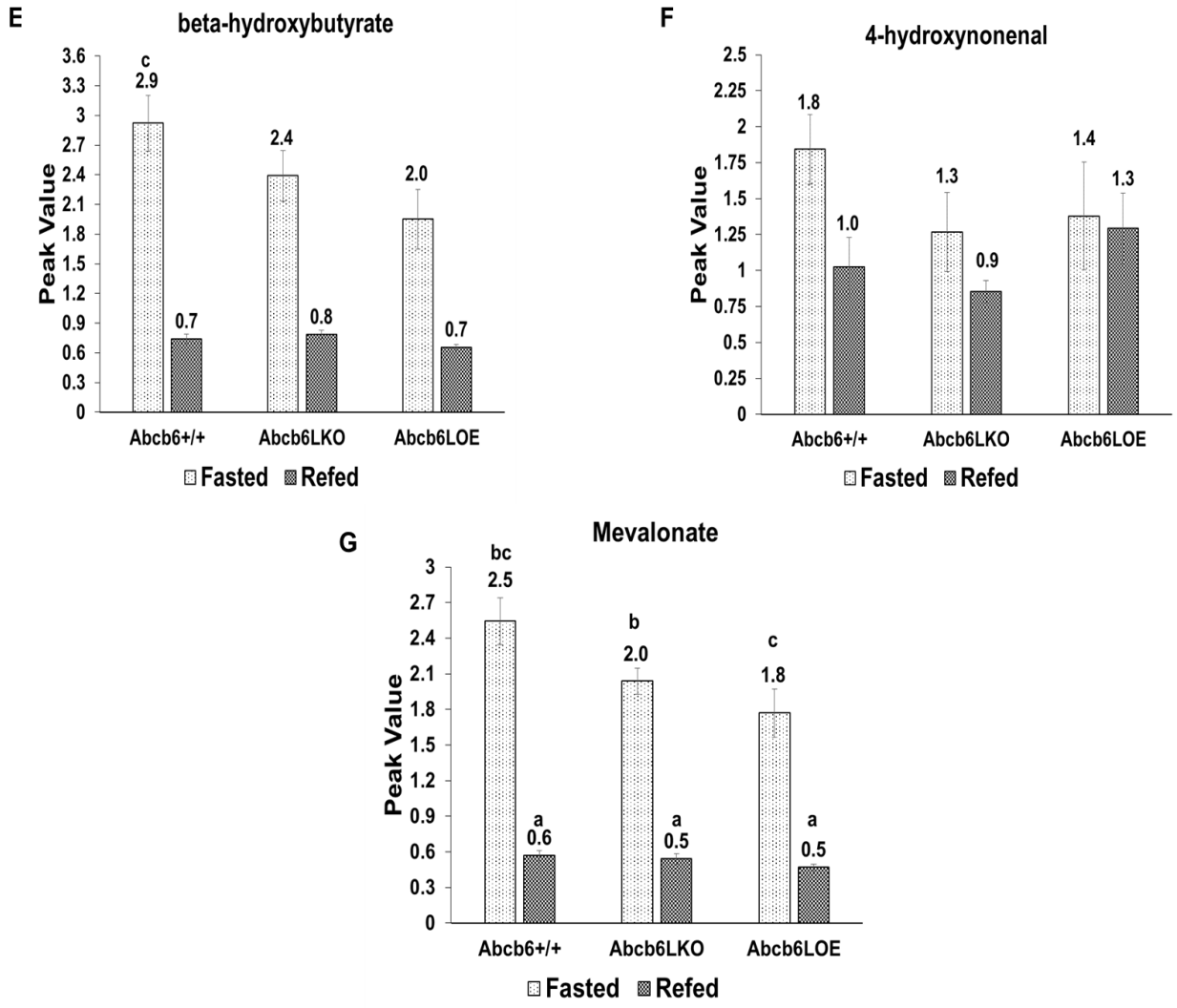

Figure 5.5 continued

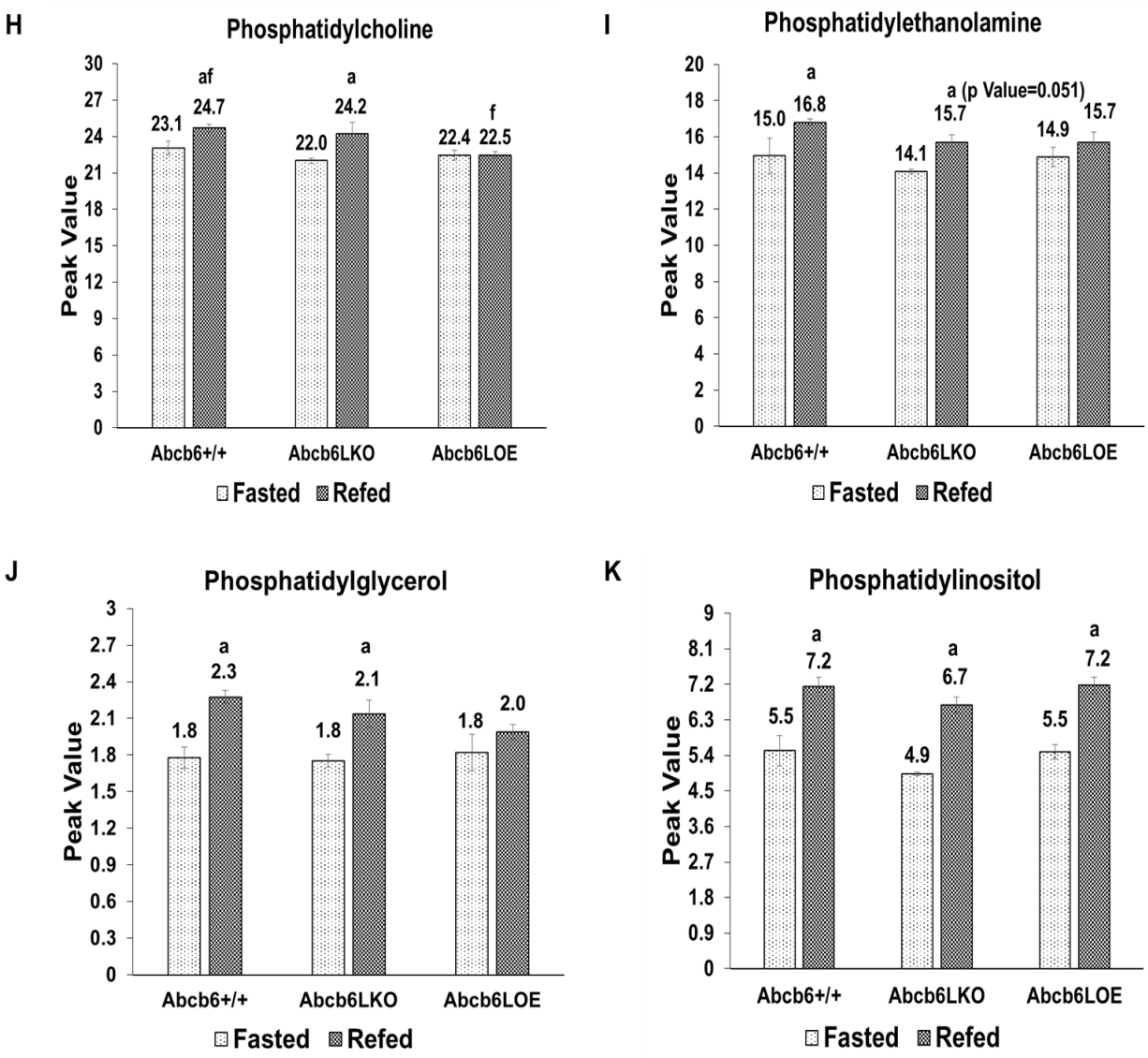

Figure 5.5 continued

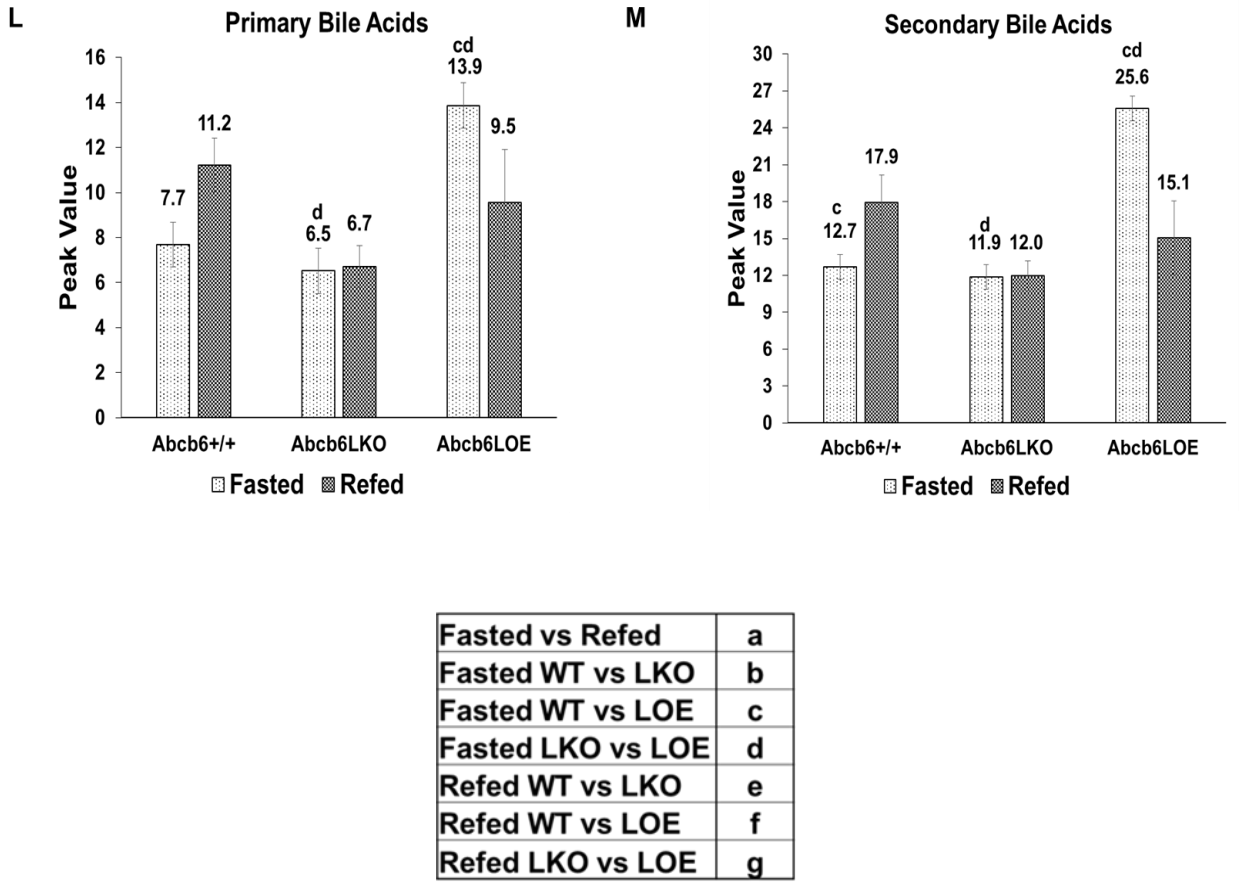

Fasted vs Refed	a
Fasted WT vs LKO	b
Fasted WT vs LOE	c
Fasted LKO vs LOE	d
Refed WT vs LKO	e
Refed WT vs LOE	f
Refed LKO vs LOE	g

Figure 5.5. Metabolic Lipid sub pathway changes in response to fasting and refeeding in WT, *Abcb6LKO*, and *Abcb6LOE* mouse liver (A)-(M) Total peak values in the diacylglycerol, long chain, medium chain, and polyunsaturated fatty acid, ketone, oxidized fatty acid, mevalonate, PC, PE, PI, PG, primary bile acid, and secondary bile acid sub pathways N=4.

Nucleotide Metabolites in Fasted and Refed Mouse Liver

The liver is the main site of nucleotide biosynthesis through the salvage and de novo synthesis pathways (Fustin *et al.*, 2012). Integral to all biological functions, they are found in energy molecules such as adenosine triphosphate (ATP), cofactors such as

flavin adenine dinucleotide (FAD), and nucleic acids in DNA and RNA. In WT mice, the Nucleotide super pathway was decreased in the refed state (Figure 5.1E) but the overall decrease did not reach statistical significance. Purine sub pathways in WT mice were decreased in response to feeding with the Adenosine and Inosine/Xanthine sub pathways reaching statistical significance (Figures 5.6A-6C). Pyrimidines in the Cytidine, Thymine, and Uracil sub pathways were also significantly decreased in the refed state in the WT group. The Orotate sub pathway was the exception to this downward trend in the fed state with this pyrimidine precursor being significantly increased in response to feeding (Figures 5.6D-6G). The overall trend of increased nucleotides in the WT fasted mice may be consistent with published data that indicate increased glucagon induces RNA degradation to yield an overall increase in nucleotides (Bleiberg-Daniel *et al.*, 1994).

Purine metabolites in *Abcb6LKO* group followed the same general trend as WT except that *Abc6LKO* mice had no significant increase in the Adenine sub pathway (Figures 5.1E and 5.6A-6C). In the *Abcb6LOE* group, the fasting mediated increase in the Nucleotide super pathway as well as Purine sub pathways reached statistical significance (Figures 5.1E and 5.6A-6C). Also, *Abcb6LOE* mice had significantly lower Guanine sub pathway levels compared to WT mice (Figure 5.6B). As in the WT group, *Abcb6LKO* and *Abcb6LOE* mice had lower levels of most pyrimidine sub pathway levels in the fed state with the *Abcb6LOE* group reaching significance. As in the WT group, the Orotate sub pathway was increased in the refed state for both *Abcb6LKO* and *Abcb6LOE* mice. However, *Abcb6LKO* and *Abcb6LOE* mice had lower refed orotate levels compared to WT with the *Abcb6LKO* group reaching statistical significance

(Figures 5.6D-6G). In the Uracil pyrimidine sub pathway, *Abcb6LOE* mice had significantly lower levels in the refed state compared to *Abcb6LKO* (Figure 5.6F).

Purines and pyrimidines (Nucleotide super pathway) increased in the fasted state with respect to the refed state except for the pyrimidine precursor, orotate which displayed an opposite trend. This trend was true for all treatment groups with orotate levels being lower in the *Abcb6LKO* and *Abcb6LOE* groups compared to WT in both nutritional states. Because orotate is a precursor to de novo pyrimidine synthesis, it is possible that it is not degraded in response to fasting.

Figure 5.6

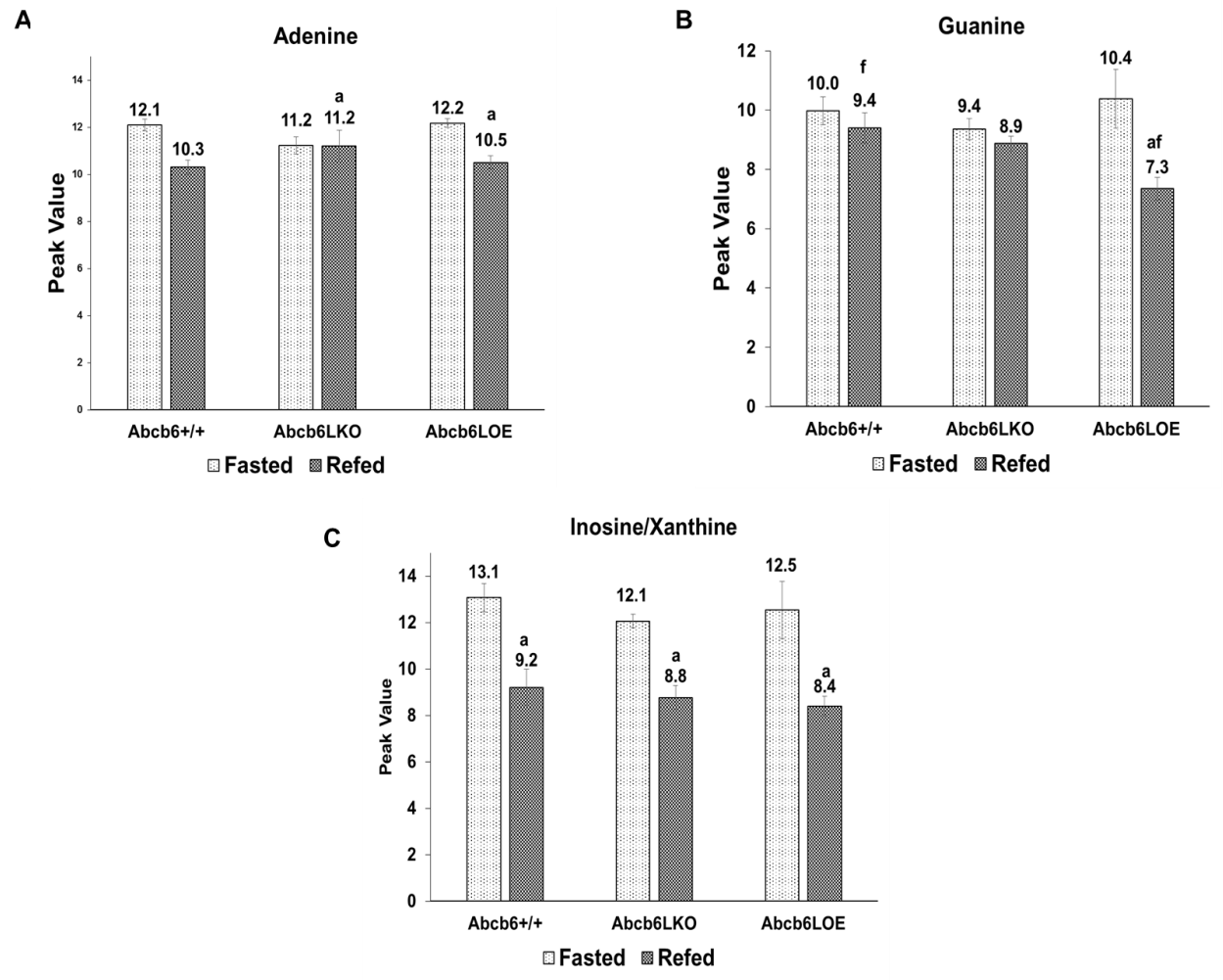

Figure 5.6 continued

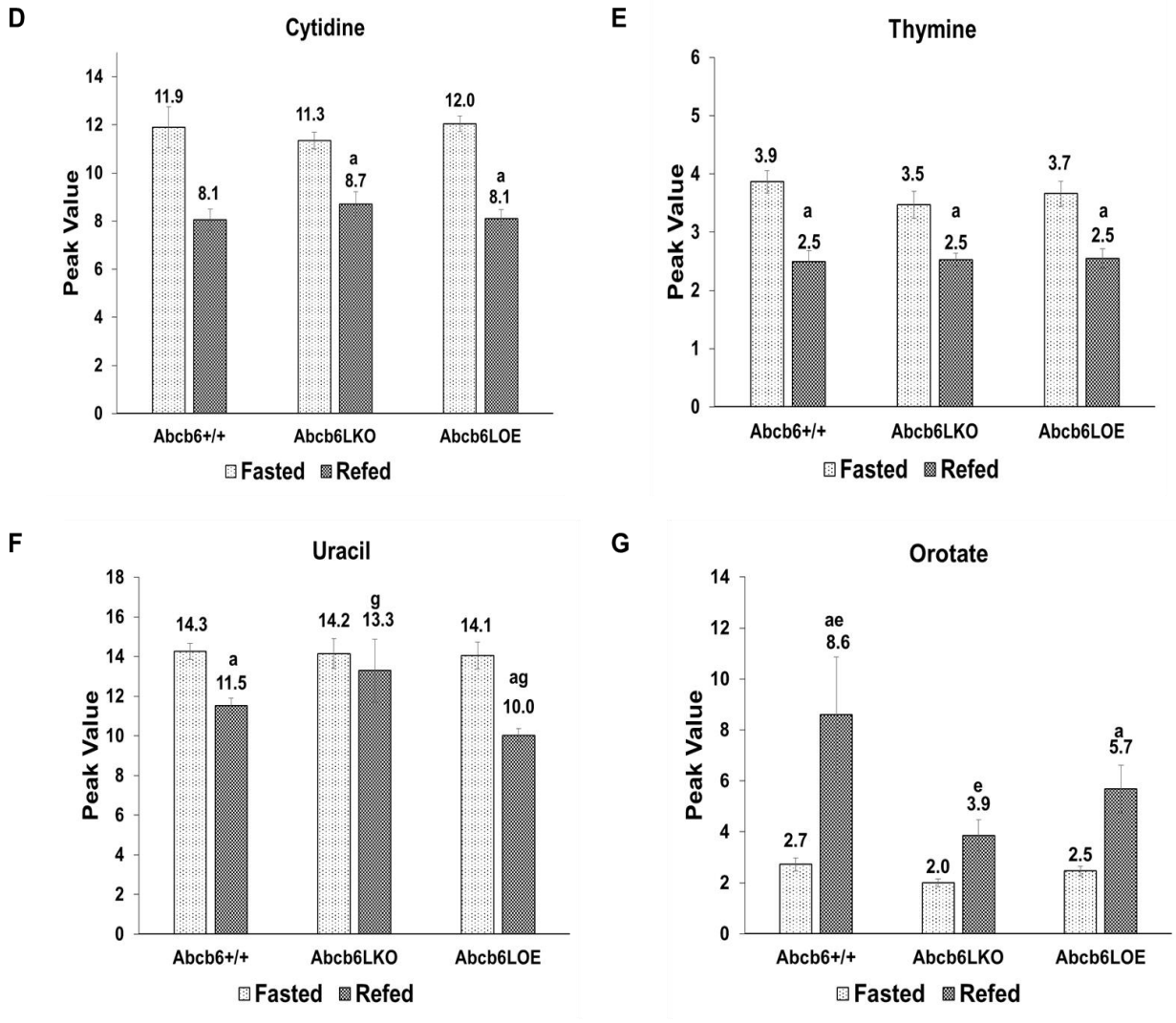

Fasted vs Refed	a
Fasted WT vs LKO	b
Fasted WT vs LOE	c
Fasted LKO vs LOE	d
Refed WT vs LKO	e
Refed WT vs LOE	f
Refed LKO vs LOE	g

Figure 5.6. Metabolic Nucleotide sub pathway changes in response to fasting and refeeding in WT, *Abcb6LKO*, and *Abcb6LOE* mouse liver (A)-(G) Total peak values in the

Adenine, Guanine, Inosine/Xanthine, Cytidine, Thymine, Uracil, and Orotate sub pathways. N=4.

Peptide Metabolites in Fasted and Refed Mouse Liver

Peptides are oligomers of linked amino acids formed from the degradation of proteins (Fruton *et al.*, 1950). The source for peptides may be the proteolysis of endogenous proteins or they may be derived from diet. Peptides from a meal may be delivered to the liver from enterocytes through portal circulation where they are broken down through extracellular hydrolysis (Lochs *et al.*, 1986) for the delivery of amino acids. Hepatic lysosomes are they main source of endogenous peptides through protein degradation (Thamotharan *et al.*, 1997). In WT mice, feeding produced a slight, albeit non-statistically significant increase in the peptide super pathway (Figure 5.1F). Both the Dipeptide and Gamma-glutamyl sub pathways were increased in response to feeding with the Dipeptide sub pathway reaching statistical significance (Figures 5.7A and 5.7B). The increase in gamma-glutamyl peptides indicates an increase in the gamma-glutamyl transferase activity which regulates the gamma-glutamyl cycle (Orlowski *et al.*, 1976) and the increase in that sub pathway is in accordance with the increase in glutathione seen in the amino acid super pathway in WT mouse liver (Figure 5.1A).

Abcb6LKO mice were not significantly different from WT in the Peptide super pathway nor either sub pathway (Figures 5.1F, 5.7A, and 5.7B). *Abcb6LOE* mice however, had an opposite trend in the Peptide super pathway with a fasted mediated increase though not reaching statistical significance (Figure 5.1F). The same trend was seen in both sub pathways in *Abcb6LOE* mice although not reaching statistical

significance (Figures 5.7A and 5.7B). However, refed *Abcb6LOE* levels of both sub pathways were lower than WT and *Abcb6LKO* mice with the dipeptide sub pathway reaching statistical significance (Figures 5.7A and 5.7B).

In summary, peptides were increased in response to feeding in WT and *Abcb6LKO* mice with both sub pathways also being increased in the refed state. However, *Abcb6LOE* mice showed the opposite trend with an increase in the fasted state. This result correlates well with the previously data showing a relatively blunted glutathione response to feeding seen in the *Abcb6LOE* group because gamma-glutamyl peptides may be positively associated with glutathione levels.

Figure 5.7

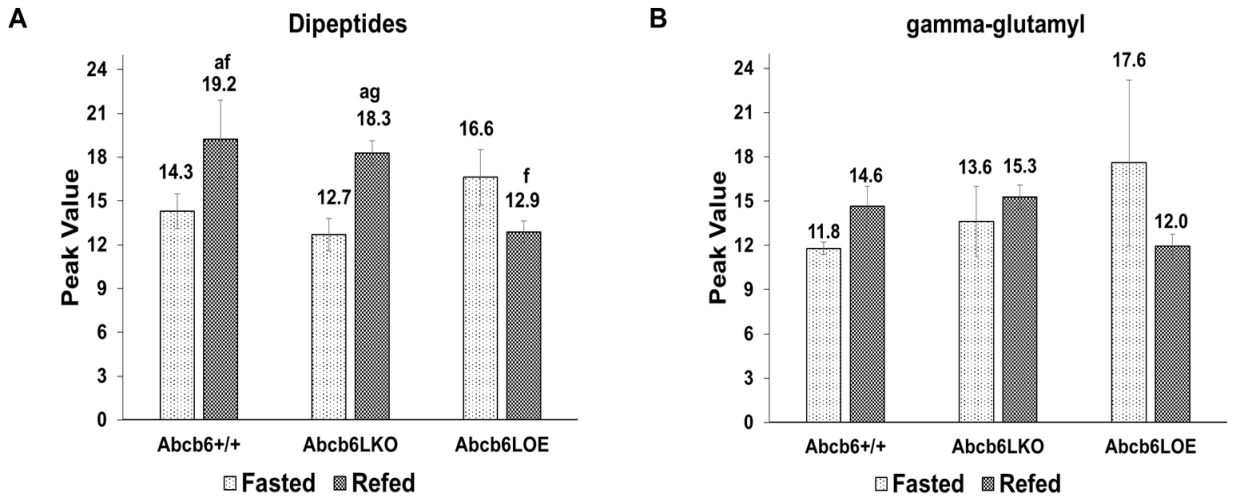

Fasted vs Refed	a
Fasted WT vs LKO	b
Fasted WT vs LOE	c
Fasted LKO vs LOE	d
Refed WT vs LKO	e
Refed WT vs LOE	f
Refed LKO vs LOE	g

Figure 5.7 Metabolic Peptide sub pathway changes in response to fasting and refeeding in WT, *Abcb6LKO*, and *Abcb6LOE* mouse liver (A) Total peak values in the Dipeptide sub pathway. (B) Total peak values in the gamma-glutamyl sub pathway. N=4.

Vitamin Metabolites in Fasted and Refed Mouse Liver

Vitamins and cofactors are essential for crucial enzymatic functions. While some vitamin levels can be maintained through endogenous biosynthesis, like humans, mice are reliant upon diet-derived biochemicals for survival (1995). In the WT group, the Vitamin super pathway was significantly increased in the fed state (Figure 5.1G). Interestingly, there were several vitamin sub pathways that were significantly reduced in the fed state including Folate, Riboflavin, Vitamin B6, and Thiamine sub pathways (Figures 5.8A-8D) even though the standard diet used for this study included the biochemicals from these sub pathways. The Vitamin A, Vitamin E (tocopherol), and Pantothenate/ CoA sub pathways were significantly increased in response to feeding (Figures 5.8E-8G). The decreases seen in some sub pathways could be due to hepatic transport and metabolism at the time-point chosen for this study.

In *Abcb6LKO* mouse liver, the Vitamin super pathway was also significantly increased in response to feeding. However, *Abcb6LOE* mice had a slight (non-significant) decrease of the Vitamin super pathway in the fed state (Figure 5.1G). In the vitamin sub pathways that were decreased in response to feeding in the WT group (Folate, Riboflavin, Vitamin B6, and Thiamine), *Abcb6LKO* and *Abcb6LOE* mice also had lower levels in the refed state (Figures 5.8A-8D). With the only notable alteration being that *Abcb6LOE* mice had a slight but significant increase in the Thiamin sub pathway in the fasted state compared to *Abcb6LKO* mice (Figure 5.8D). In the vitamin

sub pathways that were increased in response to feeding in the WT group (Vitamin A, and Vitamin E (tocopherol), Pantothenate/ CoA), *Abcb6LKO* and *Abcb6LOE* mice also showed the same increased trend in response to feeding (Figures 5.8E-8G). However, *Abcb6LOE* mice had drastically lower refed values in the refed state compared to WT and *Abcb6LKO* mice (Figures 5.8E-8G). The lower values in these sub pathways contributed to the significantly lower refed *Abcb6LOE* values in the Vitamin super pathway.

The Vitamin super pathway included the Heme sub pathway in which, heme was the sole metabolite. ABCB6 has been shown to be involved in heme biosynthesis *in vitro (Krishnamurthy, et al., 2006)* but *in vivo* studies suggest that ABCB6 expression is dispensable for heme production (Chavan, et al., 2015; Helias, et al., 2012). In this study, there was no significant difference in hepatic heme levels in *Abcb6LKO* or *Abcb6LOE* mice in either nutritional state. However, in WT mice heme was slightly elevated in response to feeding while in *Abcb6LKO* and *Abcb6LOE* mice, the was a slight decrease in the refed state (Figure 5.8H). Interestingly, Vitamin A and Vitamin E sub pathway level changes in the refed state seemed to follow the heme levels seen in the refed state. Published data suggests that hepatic levels of vitamins A and E are positively influenced by dietary iron (a component of the standard diet used for this study) (Domitrovic *et al.*, 2008).

In summary, vitamins were differentially affected by feeding with increases seen in some sub pathways and decrease seen in others. The major difference between the treatment groups in this pathway was *Abcb6LOE* mice tended to have lower increases in vitamins upon feeding.

Figure 5.8

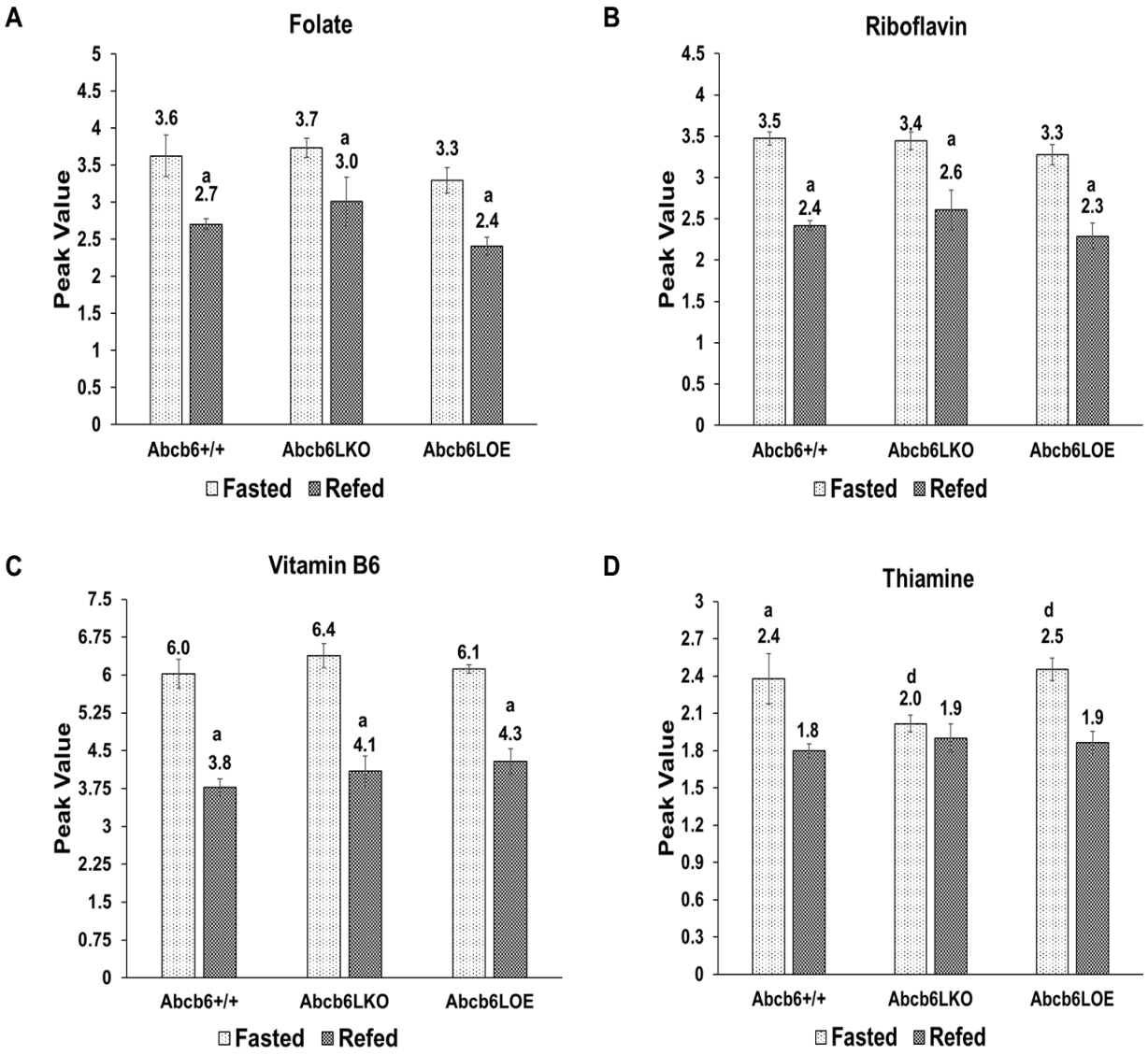
A
Folate
Peak Value
3.6
a
2.7
3.7
a
3.0
3.3
a
2.4
Abcb6+/+
Abcb6LKO
Abcb6LOE
Fasted
Refed
B
Riboflavin
Peak Value
3.5
a
2.4
3.4
a
2.6
3.3
a
2.3
Abcb6+/+
Abcb6LKO
Abcb6LOE
Fasted
Refed
C
Vitamin B6
Peak Value
6.0
a
3.8
6.4
a
4.1
6.1
a
4.3
Abcb6+/+
Abcb6LKO
Abcb6LOE
Fasted
Refed
D
Thiamine
Peak Value
a
2.4
1.8
d
2.0
1.9
d
2.5
1.9
Abcb6+/+
Abcb6LKO
Abcb6LOE
Fasted
Refed

Figure 5.8 continued

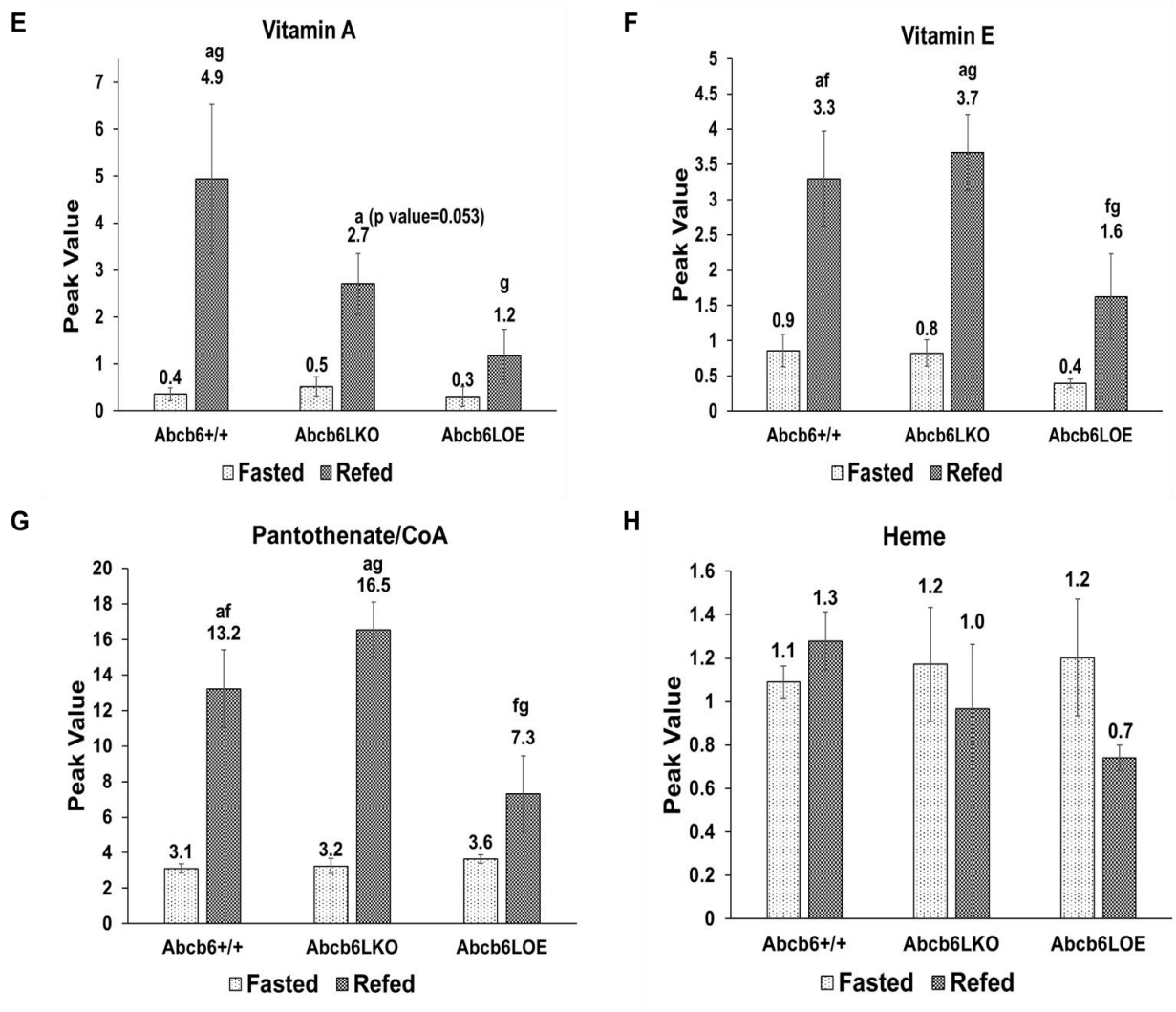

Fasted vs Refed	a
Fasted WT vs LKO	b
Fasted WT vs LOE	c
Fasted LKO vs LOE	d
Refed WT vs LKO	e
Refed WT vs LOE	f
Refed LKO vs LOE	g

Figure 5.8 Metabolic Vitamin sub pathway changes in response to fasting and refeeding in WT, *Abcb6LKO*, and *Abcb6LOE* mouse liver (A)-(H) Total peak values in the Folate,

Riboflavin, Vitamin B6, Thiamine, Vitamin A, Vitamin E, Pantothenate/CoA, and Heme sub pathways. N=4.

Xenobiotic Metabolites in Fasted and Refed Mouse Liver

Xenobiotics are by definition, exogenous compounds received from environmental sources such as food, water, and air. The liver is the major organ involved in metabolizing xenobiotics as it receives ingested materials from the alimentary tract via portal circulation. As expected, feeding significantly increased the Xenobiotic super pathway in WT mouse liver (Figure 5.1H). Food and Benzoate sub pathways were also both significantly increased in response to feeding (Figure 5.9A and 5.9B). Compounds in the Benzoate sub pathway included 3-phenyl propionate and hippurate that are known metabolites from gut microbiota (Gautam *et al.*, 2015). Feeding-induced stimulation of intestinal microbe metabolism likely explains the drastic increase in these biochemicals in the (Figures 5.9C and Figures 5.9D).

Xenobiotics were increased in response to feeding for all groups with the *Abcb6LOE* again having a less drastic increase in response to feeding as compared to WT with the *Abcb6LKO* group showing the opposite trend (greater magnitude of increase in the refed state) as compared to WT.

Figure 5.9

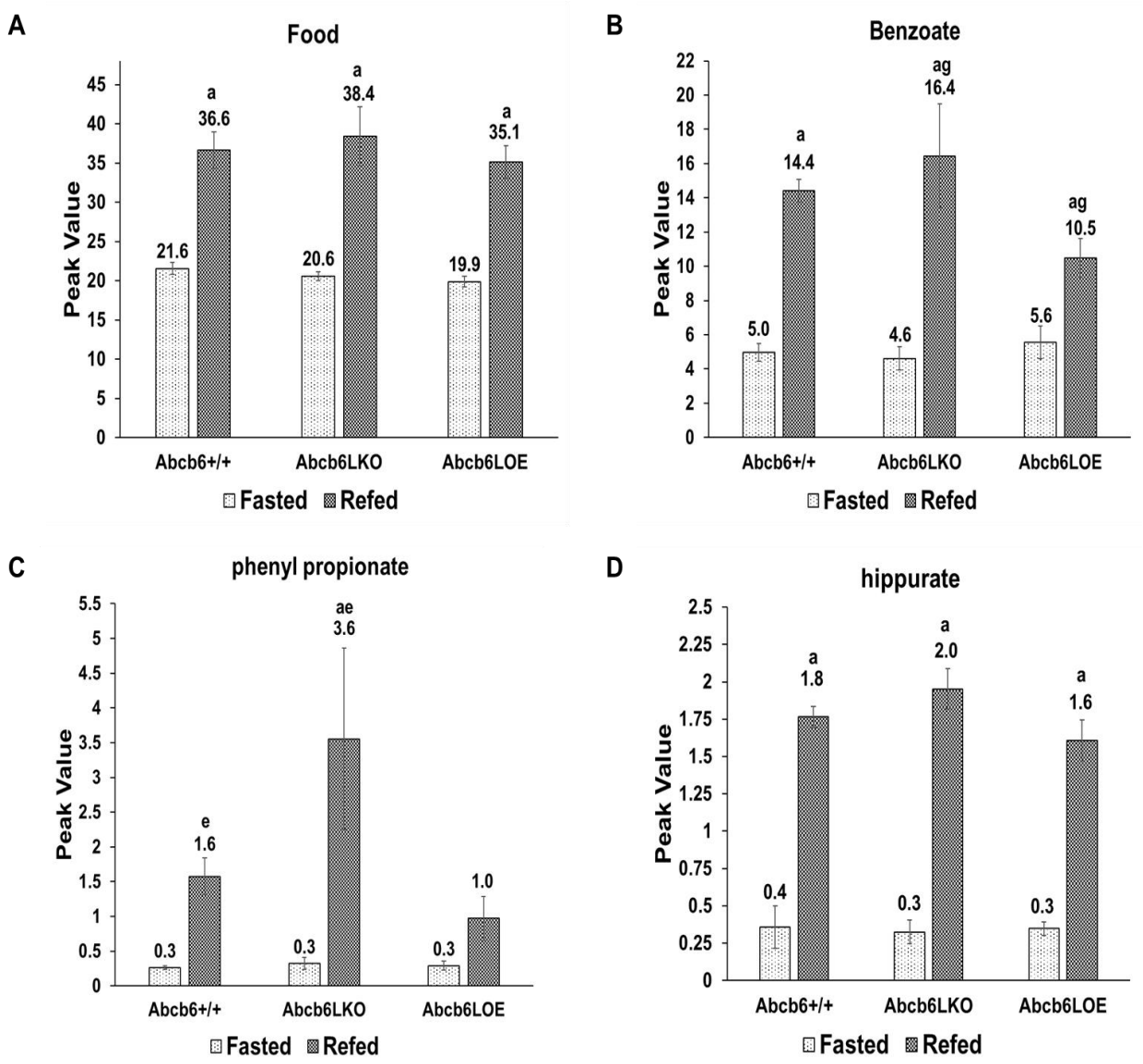

Fasted vs Refed	a
Fasted WT vs LKO	b
Fasted WT vs LOE	c
Fasted LKO vs LOE	d
Refed WT vs LKO	e
Refed WT vs LOE	f
Refed LKO vs LOE	g

Figure 5.9 Metabolic Xenobiotic sub pathway changes in response to fasting and refeeding in WT, *Abcb6LKO*, and *Abcb6LOE* mouse liver (A) Total peak values in the Food

sub pathway. (B) Total peak values in the Benzoate sub pathway. (C) Peak values of phenyl propionate. (D) Peak values of hippurate. N=4.

5.5 Discussion

Metabolic inflexibility plays an important role in the development of metabolic disease. Hepatic physiological responses to fasting and feeding are crucial to maintaining appropriate adaptation to nutritional status. Here, we present analysis of liver metabolites in fasted and refed states in WT, *Abcb6LKO*, and *Abcb6LOE* mice.

Because the liver receives macromolecules from portal circulation in the post-absorptive state, an increase in most hepatic metabolic super pathways would be expected. Indeed, we saw increases in 6 out of 8 super pathways in WT and *Abcb6LKO* mice in response to feeding. Interestingly, in *Abcb6LOE* mice, only 4 out of 8 super pathways were increased in response to feeding.

This study's analysis of hepatic metabolites reinforced previously established general maxims regarding physiological responses to fasting and feeding such as glycogen depletion, increased hepatic lipid uptake, and increased ketone production during a fast and increased hepatic carbohydrates and xenobiotics in response to feeding.

This set of data provides the first, to our knowledge, benchmark levels for hepatic metabolites in fasted and refed mice fed a standard chow diet. In the future, this study may be utilized to compare metabolite levels in other metabolic studies such as diet induced obesity or other dietetic alterations as well as genetic treatments effecting hepatic metabolism.

With respect to the genetic treatment groups (*Abcb6LKO* and *Abcb6LOE*) used in this study. The most striking departures from the WT group were seen in amino acid and lipid metabolism. As previously mentioned, dipeptides can be imported and degraded to generate hepatic amino acid supply. In our study, disruption of ABCB6 expression lowered select hepatic dipeptides and amino acids. Members of the ABC transport super family have been shown to be involved in the transport of dipeptides and amino acids. (Vasiliou, et al., 2009; Young *et al.*, 2001). Future studies could explore the possible transport dipeptide or amino acid transport function of ABCB6.

Cholesterol is the required substrate for bile acid synthesis. We found that genetic manipulation of ABCB6 resulted in lower hepatic cholesterol and bile acid levels and altered responses to feeding in these sub pathways. Again, published data indicates that ABC transporters play important roles in bile acid and cholesterol metabolism (Borst, et al., 2000) so it is conceivable that ABCB6 could have a transport function in either cholesterol or bile acid homeostasis.

There were relatively modest changes in phospholipid levels in *Abcb6LKO* and *Abcb6LOE* mouse liver compared to WT. Previous data demonstrates that *Abcb6LKO* and *Abcb6LOE* mice have altered mitochondrial morphology. It is likely that these changes are accompanied by altered mitochondrial membrane composition that may contribute to phospholipid changes seen in the whole lysate used for this study. Future analysis of isolated mitochondrial would be useful in pinpointing the source of altered phospholipids seen in this model.

Disruption of any one of the drastically altered pathways mentioned here could possibly explain our observation of metabolic inflexibility in *Abcb6LKO* and *Abcb6LOE*

mice. This study has provided a roadmap for future studies that will result in increased understanding of the contribution of ABCB6 to mammalian physiology. Supplemental assays such as RNA sequencing and mitochondrial metabolomics will direct future studies involving the potential role of ABCB6 in lipid and amino acid metabolism and will expand our understanding of tissue-specific metabolic flexibility adaptations in general.

Study Limitations

The present study is a “snap-shot” of both nutritional states (18 hour fasted, and 6 hours refed). Time course evaluation of both states would be informative regarding physiological responses. The liver plays an important role in whole-body metabolic flexibility, but additional studies of major metabolic organs would provide a more complete picture of the responses necessary to maintain energy homeostasis. Further, our report does not venture to discern between endogenous and exogenous levels of metabolites.

Chapter 6: Conclusions and Future Directions

This dissertation provides a detailed description of the metabolic consequences of altered ABCB6 expression in mice. The present studies show that ABCB6 deficiency or overexpression has a profound impact on energy homeostasis which is associated with changes in mitochondrial form and function. Despite previous *in vitro* and *ex vivo* data that suggested ABCB6 was associated with heme biosynthesis, multiple experiments determined that ABCB6 ablation or overexpression did not result in significant changes in heme levels *in vivo*. Therefore, the phenotypes described here are independent of changes in heme biosynthesis.

Chapter 2 Prior to this study, ATP-binding cassette transporter, ABCB6 was shown to be involved in the heme biosynthesis pathway in cell-based models (Krishnamurthy, et al., 2006). Additional studies confirmed that loss of ABCB6 is associated with several mammalian pathologies such as ocular coloboma, familial pseudo hyperkalemia, and atherosclerosis (Andolfo, et al., 2013; Murphy, et al., 2014; Wang, et al., 2012). Because these conditions have not been found to be directly linked to a disruption in heme synthesis, it is probable that ABCB6 has additional non-heme related physiological functions.

To better understand ABCB6 function *in vivo,* we utilized a whole-body *Abcb6* knockout mouse model. We observed metabolic disturbances in homozygous Abcb6 whole-body knock-out in male and female mice. Suggestive of a role in development, a portion of *Abcb6* KO offspring had stunted growth. Over time, these smaller mice surpassed wild-type liter mates in body weight despite no difference in food consumption. We discovered that the increased body mass was due to increased

adipose tissue. The obesogenic phenotype was accompanied by lower energy expenditure, metabolic syndrome-like characteristics such as disrupted glucose metabolism and disturbances in pathways that regulate energy homeostasis. Interestingly, through these studies, we discovered that hepatic ABCB6 expression is suppressed in obesity. Through EM imaging and bioenergetic flux assays, we found that ABCB6 deficiency resulted in increased fragmentation and decreased function in hepatic mitochondria. These results lead to the hypothesis that the metabolic disturbances in whole-body KO mice were due to ABCB6-mediated mitochondrial alterations.

Most of the analysis of mitochondrial form and function was done in liver. However, because the driving force of the obesogenic phenotype is likely due to reduced energy expenditure and physical activity, analysis of other tissues that regulate this aspect should be performed in the future. Endocrine system components such as the hypothalamus, thyroid, and pituitary contribute to overall energy balance and activity. Along with skeletal muscle and the brain, macro and micro anatomical analysis as well as mitochondrial form and function studies of these tissues in *Abcb6* KO mice would possibly result in a better understanding of origins of the observed phenotype.

Because the disruption of mitochondrial morphology and function was observed prior to the onset of obesity, it seems clear that mitochondrial dysfunction precedes metabolic syndrome in this model. However, it is presently unclear at what timepoint mitochondrial changes occur. Earlier observations of possible embryonic lethality seem to suggest that alteration of ABCB6 expression would have a developmental impact. At what point do mitochondrial abnormalities occur in *Abcb6* KO mice and if in early development,

how does this contribute to the metabolic syndrome seen in adulthood are still open questions. A full developmental study of *Abcb6* KO mice could partially address these questions. Additionally, because we currently have an *Abcb6* "floxed" mouse model, it is possible to alter ABCB6 expression using a universal promoter creating a whole-body KO or over expressing mouse after development is complete via intraperitoneal delivery of AAV8 Cre virus under a universal promoter. The combination of these two studies would give a clearer picture of how ABCB6 expression influences development and contributes to energy homeostasis in adulthood in absence of generational or developmental effects.

Chapter 3 The maintenance of whole-body energy homeostasis involves extensive inter-organ crosstalk. Also, we currently don't fully understand the developmental or generational consequences of ABCB6 deletion. Although ABCB6 is expressed in all metabolic tissues, it is unknown whether this transporter has tissue-specific functions. These facts represented barriers to unraveling the mechanistic details of ABCB6-mediated homeostatic disruptions in whole-body KO mice. To overcome these impediments, we developed a tissue-specific, inducible system to control ABCB6 expression. This chapter discusses the phenotypes seen due to liver-specific deletion or overexpression of ABCB6 in 8-week male mice.

Following up on the mitochondrial dysfunction seen in Abcb6 whole-body knockout mice, we confirmed that liver-specific alteration of ABCB6 also resulted in mitochondrial morphological changes with *Abcb6LKO* having increased fragmentation and *Abcb6LOE* having increased elongation in their respective mitochondrial populations. We also

discovered that function followed form in this model with fragmentation being associated with decreased mitochondrial function and elongation resulting in increased function in *Abcb6LKO* and *Abcb6LOE* mice respectively.

Based upon the previous observation that ABCB6 expression is downregulated in the obese state and the known association between mitochondrial dynamic changes in response to nutrient status, we investigated ABCB6 hepatic expression patterns in response to the diurnal feeding cycle. We found that ABCB6 expression was upregulated in low-nutrient (fasted) state and downregulated in high-nutrient (post-absorbent) state mirroring the mitochondrial morphology and function seen in the *Abcb6LOE* and *Abcb6LKO* models respectively.

In *Abcb6LKO* mouse liver, the expression of mitochondrial fusion proteins was decreased while fission protein expression was increased. In *Abc6LOE* mouse liver fusion protein expression was increased, and fission proteins were downregulated. This data supported the hypothesis that ABCB6 is responsive to nutrient signals and mediates a homeostatic response via interaction with mitochondrial fission and fusion machinery thus regulating metabolic flexibility. Indeed, *Abcb6LKO* and *Abcb6LOE* mice have altered food consumption and respiratory exchange ratio in response to dietary challenges as compared to wild-type mice as measured by indirect calorimetry assays. The loss of metabolic flexibility in *Abcb6LKO* and *Abcb6LOE* mice resulted in abnormal hepatic lipid and carbohydrate metabolism as well as disrupted glucose and insulin signaling. This study illustrates that ABCB6 plays a crucial role in maintaining energy homeostasis as suggested in the *Abcb6* whole-body KO studies. Remarkably, either

knockdown or overexpression of ABCB6 in a single organ, the liver, manifested systemic metabolic syndrome-like characteristics.

Future studies are needed to understand the mechanisms by which nutrient status influences ABCB6 expression and the downstream effects of this transporter's regulation. Our previous studies showed that ABCB6 expression was post-translationally downregulated by acute or chronic high nutrient status. Therefore, it is likely that ABCB6 degradation pathways are dynamically activated in response to increased nutrient supply. Inhibition of selected protein degradation pathways could uncover details of how nutrient sensing pathways are linked to the rapid regulation of ABCB6 expression.

Chapter 3 describes phenotypes seen after a set time point after genetically altering ABCB6 expression (10 days post IP delivery of AAV8 virus). It would be informative to discover the rapidity of mitochondrial morphological/functional changes in response to the loss or gain of ABCB6 expression. Such experiments could include analysis of ABCB6 expression and mitochondrial form and function as early as 24 hours post-injection and tracking those changes up to the 10 day point previously studied. Alternatively, it would be interesting to discover if the severity of the 10-day phenotypes would be more drastic after a longer period of ABCB6 knockdown/overexpression or conversely, would compensatory responses overcome the metabolic disturbances seen in this study. Any observable compensatory responses would no doubt, be informative.

Because the liver is crucial maintaining whole-body energy homeostasis and because ABCB6 is highly expressed in the liver, we chose this organ as the first tissue-specific study. However, crosstalk between the liver and other metabolic organs is well

documented and this study did not fully explore the effects of hepatic alteration of ABCB6 in other tissues. Changes in ectopic lipid accumulation, fuel selection in non-hepatic tissues, adipose hypertrophy or biogenesis, and hormonal responses are just a few examples of non-hepatic aspects that could be explored using this model. Information gained using this approach could shed further light upon the role of ABCB6 in maintaining energy homeostasis.

In addition, ABCB6 is also highly expressed in other tissues. Adipose, pancreas, muscle, testes, and brain-specific viruses are commercially available by which, further studies could explore the impact of changing ABCB6 expression in these tissues. Would gain or loss of ABCB6 have the same mitochondrial effects in these tissues? If so, what would be the impact on energy metabolism and other metabolic tissues in which ABCB6 expression was not targeted? Since the physiological role of ABCB6 in mammals is unclear, is it possible that ABCB6 expression could have differential functionality based upon specific organs or tissues. For example, ABCB6 is highly expressed in testes. Would genetic alteration of ABCB6 testicular expression affect fertility? Based upon the lower than expected homozygous progeny seen in our whole-body *Abcb6* knockout mice, this is a worthy question. We also observed behavioral abnormalities in the whole-body knock out model. Because the nervous system is highly reliant on mitochondrial function and appetite control is an essential function of the brain, behavioral and metabolic studies using an *Abcb6* brain-specific model are likely warranted.

The temporal and tissue-specific control of gene expression is a powerful tool. In our model, we also can accurately assess spatial and tissue-specific expression of ABCB6 through LacZ/ X Gal staining. Comprehensive analysis of the tissue-specific effects of

changes in ABCB6 expression, compensatory ABCB6 expressional changes by non-targeted tissues, and differential ABCB6 expression patterns will provide crucial information needed to understand ABCB6 function in higher eukaryotes.

Chapter 4 details global metabolomic data from the livers of wild-type, *Abcb6LKO*, and Acb6LOE mice in fasted and refed states. The purpose of this study was two-fold. Firstly, changes in liver metabolites in response to fasting or feeding are descriptive of hepatic adaptive responses to nutrient status that are not yet fully understood. Because this is the first murine study under these conditions, we needed to establish baseline levels of metabolites in wild-type mouse as well as the change in these levels in response to nutrient status. Secondly, *Abcb6LKO* and *Abcb6LOE* mice exhibit metabolic inflexibility. We proposed that metabolomic analysis of mice in this model would be informative as to possible transport substrates and functions of ABCB6 in mouse liver.

Our WT metabolomic study re-enforced previously well-characterized hepatic adaptations to fasting and feeding such as increased lipid import and glycogenesis. The study also reveals less understood adaptations. In our study, select vitamins were increased upon feeding while others were decreased in the refed state. Also, previous studies have shown that hepatic lactate is increased in liver in the fasted state, but our study shows higher lactate levels in the refed state.

Abcb6LKO and *Abcb6LOE* mice had significant changes in amino acid/peptide, nucleotide, and lipid metabolism. Additional studies and additional analysis of the

metabolite study will likely aid in pinpointing how ABCB6 expression relates to metabolic flexibility.

Although this study was informative, future studies will greatly enhance the value and usefulness of this data. Since many metabolites analyzed in this study could originate from either exogenous sources (food) or endogenous metabolic pathways, it is impossible to discern whether some metabolite level changes are attributable to the intake of a particular metabolite (or parent compound further metabolized to the final metabolite), or from regulatory actions of endogenous pathways. Another complication involved in these studies is that some pathways share a common metabolite. It is conceivable that opposing physiological adaptations could increase a common metabolite thus confounding the ability to conclude which metabolic action is causative of the metabolite level change. A parallel RNA sequencing analysis would assist in resolving both issues. RNA sequencing would provide a detailed transcriptional picture in both nutritional states thus potentially allowing us to conclude through pathway analysis if level changes were of endogenous origins and from which metabolic response/s they arose.

Our metabolomic study was performed on liver tissue whole lysate. Additional analysis of isolated mitochondria from the same treatment groups would be beneficial in several aspects. Previous publications have suggested multiple sub cellular localizations for ABCB6. Analysis of the mitochondrial fraction would highlight metabolic disturbances associated with the mitochondrial form of ABCB6. Both this metabolomic and our previous studies suggest dramatic lipid metabolism alterations in this model. Cellular membrane content contributes substantially to the overall lipid profile of the

liver. Our previous data show drastic morphological changes in *Abcb6LKO* and *Abcb6LOE* mitochondria which are very likely accompanied by alterations in membrane composition. Performance of metabolomic analysis on the mitochondrial fraction would improve the resolution of mitochondrial lipid changes and possibly identify lipid-related mechanistic details of how mitochondrial dynamics are affected in our model.

Chapter 7: Methods and Materials

***Animal Studies*—** All animal experiments were approved by the University of Kansas Medical Center Institutional Animal Care and Use Committee. Mice were housed in polycarbonate cages (four per cage) and maintained on a 14-h/10-h light-dark cycle at 22 5 °C and 20% relative humidity. For *Abcb6* whole-body knock out studies, mice were provided standard chow diet and water ad libitum. Mice were fasted for 12 hours prior to tissue collection.

For liver-specific studies, mice were entrained to time-restricted feeding (food provided from 7:30 pm to 7:30 am only) for one week prior to tissue collection. Fasted groups were fasting for 18 hours. Refed groups were fed for six hours prior to collection. Water provided ad libitum.

Abcb6 Whole-Body Null Mice*—Abcb6* knock-out mice were generated on C57BL6/N background using ES cells developed by the trans-NIH Knock-Out Mouse Project. The ablation cassette (velocigene cassette [bacterial *J3*-galactosidase-polyadenylation signal-loxP (locus of X over P1) site-human ubiquitin C gene promoter-neomycin phosphotransferase-polyadenylation sig- nal-loxP site]) used to generate *Abcb6* knock-out mice replaces the *Abcb6* ORF containing exons 3–5 with the *J3*-galactosidase-hUBC/em7-neomycin-poly(A) cassette, where the neomycin expression cassette is flanked by loxP sites (24). Microinjection of ES cells and generation of *Abcb6* heterozygous mice were done according to standard procedures. Mice were genotyped using appropriate primers. The first primer pair anchors to exon 1 and exon 3 and amplifies 470 bp of the WT allele. The sequences of the primers are as follows: WT-F, 5'- GCCCCCAGTCTTATACTCTA- CACG-3', and WT-R, 5'-

CCCATGCCTCTCTCTGCTTTCC- 3'. The second primer pair anchors to exon 1 and the neomycin cassette and amplifies 620 bp of the mutant allele. The primer sequences are as follows: KO-F, 5'-CACACCTCCCCCTGAACCTGAAA-3', and KO-R, 5'-CGT-GACCCCTCTCAGAGTTAGGAAAG-3').

Weight recordings- For body weight analysis, animals on a regular chow diet (Harlan Teklad 2018; 18% calories from fat) or, when indicated, an HFD (Research Diets D12451; 45% of total calories from fat) were weighed at the indicated time points from week 5 till week 20. Food intake was measured daily for the entire duration of the study and was determined to the nearest 0.1g by weighing the remaining chow or HFD. Trained personnel performed weekly observations of all mice.

ECHOMRI- Quantitative Magnetic Resonance (ECHOMRI 1100) measurements were made were done on mice that were fed ad lib during the light phase (0900 hr.). Scans were performed by placing animals into a thin-walled plastic cylinder (1.5 mm thick, 4.7 cm inner diameter), with a cylindrical plastic insert added to limit movement. While in the tube, animals were briefly subjected to a low-density (0.05 Tesla) electromagnetic field to measure fat, lean mass, free water, and total body water. The general theoretical background and specific technical details describing the basic functionality of this system is well-described by Tinsley et al (Evaluation of a quantitative magnetic resonance method for mouse whole body composition analysis. *Tinsley FC, Taicher GZ, Heiman ML*. *Obes Res. 2004 Jan; 12(1):150-60.)*

Generation of genetically modified Abcb6 Liver-Specific mice- *Abcb6LKO* and *Abcb6LOE* mice were generated on a C57BL6/N background. The strategy for the generation of genetically modified Abcb6 mice is shown in Figure 3.1A. Mice were maintained on a 12 h dark/light cycle and housed in groups of two to four with unlimited access to water and chow diet (5053 PicoLab Rodent diet 20, Fort Worth, TX) as indicated for individual experiments. All animal procedures were performed in accordance with the Guide for Care and Use of Laboratory Animals of the NIH and were approved by the Institutional Animal Care and Use Committee of the University of Kansas Medical Center, Kansas. In this report all animal studies were done using male mice.

Production of Adeno Associated Viral (AAV) Particles- Purified AAV-TBG-PI-Cre and AAV-TBG-PI.eGFP viral particles were obtained from Penn Vector Core (University of Pennsylvania, Philadelphia, PA). Purified AAV-TBG-PI-*Abcb*6 and AAV-TBG-PI.eGFP (*Abcb6* control) viral particles were obtained from Vector Biolabs (Malvern, PA).

Postprandial mouse model. The strategy for the postprandial mouse is shown in Supplementary Figure 4A. Briefly, For ABCB6 expression studies, male mice (C57BL6/N) were trained to handling, and night time feeding and day time fasting for a period of 9 days to minimize variability linked to stress and food consumption. On the 10^{th} day mice were moved to fresh cages and grouped into mice that were scheduled to be fasted or mice that were scheduled to be fed. On the 10^{th} night mice scheduled to be fed were

given food for 6 h, while mice scheduled to be fasted were not given any food. At the end of 6 h feeding mice in all groups were sacrificed and liver biopsy and/or harvest followed.

For fed and fasted responses of genetically modified *Abcb6* mice studies *Abcb6*$^{flox/flox}$ male mice 5 weeks of age were given a single peritoneal injection of either AAV8-TBG-PI. Cre or AAV8-TBG-PI-eGFP or AAV8-TBG-PI-*Abcb6*. Injected mice were then trained to handling and night time feeding and day time fasting for a period of 9 days to minimize variability linked to stress and food consumption. On the 10th day mice were moved to fresh cages and grouped into mice that were scheduled to be fasted or mice that were scheduled to be fed. On the 10th night mice scheduled to be fed were given food for 6 h, while mice scheduled to be fasted were not given any food. At the end of 6 h feeding mice in all groups were sacrificed and liver biopsy and/or harvest followed.

Circadian mouse model. The strategy for the circadian rhythm is shown in Figure 3.4B. Briefly, mice were housed in barrier facilities with 12 h light and dark cycles. ZT0: lights on at 6 am; ZT12: lights off at 6 pm. Mice were fed ad libitum with chow diet (5053 PicoLab Rodent diet 20, Fort Worth, TX). For circadian studies male mice C57BL6/N 5 - 6 week of age were sacrificed every 3 hours for 24 hr. Liver tissue was harvested and was used to isolate RNA. RNA samples were used to analyze circadian oscillation of *Abcb6* transcript while total liver lysates were processed and used to analyze circadian oscillation of ABCB6 protein.

Hepatic H & E staining- Mouse liver sections were rinsed in phosphate buffered saline and immediately fixed in buffered 10% formaldehyde for 48 hours followed by a 24-hour incubation in 70% ethanol. Tissues were then processed for 6 hours in a Leica ASP300S tissue processor. Paraffin-embedded tissues were sectioned to 6uM and stained with hematoxylin and eosin and imaged with an Olympus DP71 microscope.

Oil O Red Staining- Liver sections were collected and embedded in embedding medium. (Tissue-Tek® O.C.T. Compound, SAKURA, USA) and frozen on dry ice. Frozen sections (6 mm thick) were cut in a cryostat and stained with oil red O and hematoxylin for studying lipid accumulation with an Olympus DP71 microscope.

Periodic Schiff stain- Glycogen was visualized in paraffin-embedded tissue sections using a periodic acid – Schiff (PAS) staining kit (Sigma Aldrich, St Louis, MO). Tissue sections were also stained with standard hematoxylin and eosin for general cell morphology.

Lipid and metabolite Analysis- Hepatic and serum ketones, triglyceride, free fatty acid, and total cholesterol were determined using BioVision Incorporated (155 South Milpitas Blvd. Milpitas, California) kits as per manufacturer's instructions.

Preparation of tissue lysates - Mouse liver lysates were prepared as follows. Approximately, 0.05 grams (wet weight) of frozen tissue was homogenized in 500uL 1X Ripa buffer (Thermo Scientific, Waltham, MA) with protease inhibitors (Roche Applied Science) using a glass dounce homogenizer on ice. The resulting solution was spun at 10,000 g for 10 minutes at 4 degrees Celsius in a tabletop centrifuge. The supernatant was then collected and following BCA protein estimation, mixed with 4X Laemmli buffer (Bio-Rad 161-0747) and 1:100 beta mercaptoethanol.

Immunoblotting- Approximately 50 μg of total protein was analyzed by polyacrylamide gel electrophoresis (PAGE). Commercial primary antibodies were used for relative protein detection. Immunoreactive proteins were detected by using polyclonal goat anti-rabbit or anti-mouse horseradish peroxidase IgG secondary antibodies (Thermo Scientific, Waltham, MA) and visualized using Supersignal chemiluminescent horseradish peroxidase substrate (Thermo Scientific, MA) or IRDye goat anti-rabbit/goat-anti-mouse secondary antibodies (Li-Cor Lincoln, NE, USA) and visualized by Li-Cor Imager model 2800. Densitometry analysis was performed using ImageJ analysis software (National Institutes of Health).

Mito Stress Test- Isolated mitochondrial function was assessed using Seahorse XF24[3] Mito Stress test as previously described (Rogers *et al.*, 2011). Primary mouse hepatocyte Mito Stress analysis was performed as previously described (Chavan *et al.*, 2017).

RNA isolation, reverse transcription, and Real-time PCR analysis- RNA isolation from tissue was accomplished using TRIZOL® reagent (Invitrogen, CA) following manufacturer's protocol. iScript (BioRad, CA) was used for cDNA synthesis using 1 µg of RNA according to manufacturer's protocol. Real-time PCR was performed using CFX384TM Real Time PCR System using gene specific primers and iTaq™ Universal SYBR® Green Supermix (Bio-Rad, Hercules, California) for amplification measurement.

Intraperitoneal glucose and insulin tolerance tests- Control diet fed male wild-type and knockout mice were fasted overnight (16 hours). Tail snipping was used to collect blood. Glucose levels were detected using One Touch Ultra Mini blood glucose meter at 0 hour and at 30, 60, 90 and 120 minutes after intraperitoneal injection of 2.0 g/kg glucose or 0.05 units/kg insulin.

Transmission electron microscopic imaging- Fixed tissue was rinsed with 0.1N Cacodylate buffer twice, 10 min each. Tissue was post-fixed in 1% osmium tetroxide buffered in 0.1M Cacodylate buffer for 1 hour in a fume hood. Samples were rinsed with distilled water 3 times, 10 min each. Samples were dehydrated in a series of graded ethanol as follows; 50%, 70%, 80%, 95%, 100%, 100% for 15 min each. Samples were placed into propylene oxide for 20 min, then into 1:1 solution of propylene oxide and Embed 812 resin formulation medium (Electron Microscopy sciences, Fort Washington, PA) overnight. The samples were then placed in fresh Embed 812 medium formula for 1 hour. Samples were then placed into 00 size micromolds with fresh resin and placed in a 65-degree oven overnight. Samples were sectioned at 70nm using a Diatome

diamond knife on a Leica UC-7 ultra-microtome. Sections were viewed at 100kv on a J.E.O.L. JEM 1400 transmission electron microscope.

Mitochondrial isolation- Mitochondrial isolation was performed using an established protocol (Chavan, et al., 2013; Krishnamurthy, et al., 2006). In brief, liver was homogenized in 4 ml cold isolation buffer (70 mM sucrose, 210 mM mannitol, 5 mM HEPES buffer, 1mM EGTA, and 0.5% fatty-acid free bovine serum albumin). Homogenization was achieved using a Dounce glass homogenizer at 12 strokes. Following two rounds of centrifugation at 800 x g for 10 min, the mitochondrial fraction was washed and pelleted at 8,000 x g for 10 min. The pellet was suspended in approximated 150 µL cold isolation buffer and either stored at -80^{0}C in 50 µg aliquots or used immediately for extracellular flux assays.

Primary hepatocyte isolation- Primary hepatocyte isolation and culturing were performed as previously described (Chavan et al., 2017).

Mitochondria number, area and size calculations- Low magnification EM images of the liver samples each measured 980 µm^2. A total of 12-16 images (of 980 µm^2) for each genotype was used to calculate the average mitochondrial number. On each of these images, every mitochondrion was identified manually, and the perimeter was outlined with an optical pen using the adobe Photoshop software. The shape of each mitochondrion was defined by the axis ratio of the oval that best fits the area of the organelle (Adobe Photoshop software). Data are expressed as means ± SD. The statistical significance of differences was assessed with a one-or two –sample Student t test. One-Way Analysis

of Variance (ANOVA) was used to compare between treatment groups in the fed and fasted conditions. Statistically significant results from ANOVA were computed further using all pairwise multiple comparison procedures (Holm-Sidak method). All calculations were performed with SPSS statistical software package Version 22 (IBM)

Mitochondria Respirometry- All procedures were performed with pre-chilled buffers, equipment, and consumables. Isolated mitochondria were re-suspended in respiration buffer (100 mM KCl, 10 mM KH_2PO_4, 5 mM $MgCl_2$, 5 mM HEPES, 1 mM EGTA, 0.24%BSA, pH 7.2) and kept on ice as described previously (Chao *et al.*, 2018; Chavan, et al., 2017). 10 micrograms per well were loaded into Seahorse XF24 microplate in 50 µL volume containing substrates. The loaded plate was centrifuged at 2,000 x g for 5 min at 4ºC and an additional 450 µL of buffer+substrate (14 mM succinic acid and 2 mM rotenone) was added to each well.

Fluorophore excitation/emission- Mitotracker red, was excited with 488 nm 25 mW Argon-ion laser and their emission captured through 500-550 nm band-pass filter.

Supercomplex detection, identification, and quantification- Were performed using an established protocol (Jha *et al.*, 2016).

SC detection- 10-50 µg mitochondrial extracts were solubilized in 20 µL solubilization buffer (50 mM Imidazole, 500 mM 6-aminohexanoic acid, EDTA 1 mM pH7.0). 8 mg digitonin/mg of protein was added, and samples were incubated on ice for 30 min. Solubilized samples were centrifuged at maximal speed in a microcentrifuge for 30 min at 4ºC. The clear supernatant was combined with 1 µL of 2.5% Coomassie G-250.

Samples were loaded into NativePage 3%-12% Bis – Tris gel (Invitrogen) and electrophoresed at 4ºC in a Sure-Lock Xcell Tank (Invitrogen) at constant voltage of 20V for 60 min and 200V for 120 min or until dye front exited the gel. Simultaneous detection of CI-CV was achieved with the anti-OXPHOS complex kit (Mitosciences, catalog number, dil. 1: 2,000).

SC identification- in total, 50 µg mitochondrial extracts (with digitonin 8 g/g protein and G-250 Coomassie blue) were individually loaded for the detection of each complex. After the transfer, the membrane was cut and incubated in the same primary antibodies used for western blotting.

Blood and tissue biochemistry- Blood was drawn at the time of sacrifice via retro-orbital puncture, and plasma was prepared. Tissues were processed according to the kit specific manufacturer's instructions. The following kits were used to determine metabolic parameters: triglyceride determination kit (BioVision, catalog # K622), total cholesterol kit (BioVision, catalog # K603), free fatty acids determination kit (BioVision, catalog # K652), glycogen determination kit (BioVision, catalog # K646), ketone determination kit (BioVision, catalog # K632).

Heme measurements- Hepatic heme measurements were done using UPLC-QTOFMS system as described (Chavan et al., 2015).

Statistical Analysis- Unless specified otherwise, all values presented in the text are mean ± standard deviation (SD). The statistical significance of differences was assessed

with a one-or two –sample Student t test. Where applicable, Two-Way Analysis of Variance (ANOVA) was used to compare between the genotypes and between the treatment groups. Statistically significant results from ANOVA were computed further using all pairwise multiple comparison procedures (Holm-Sidak method). All calculations were performed with SPSS (software package Version 22 IBM) and/or Sigma Plot (version 12.0). A difference was considered significant at the $p < 0.05$ level.

References

Ajioka, R. S., Phillips, J. D., and Kushner, J. P. (2006). Biosynthesis of heme in mammals. *Biochim Biophys Acta* **1763**(7), 723-36.

Al-Mehdi, A. B., Pastukh, V. M., Swiger, B. M., Reed, D. J., Patel, M. R., Bardwell, G. C., Pastukh, V. V., Alexeyev, M. F., and Gillespie, M. N. (2012). Perinuclear mitochondrial clustering creates an oxidant-rich nuclear domain required for hypoxia-induced transcription. *Sci Signal* **5**(231), ra47.

Albert, V., and Hall, M. N. (2015). mTOR signaling in cellular and organismal energetics. *Current opinion in cell biology* **33**, 55-66.

Ali, S., and McStay, G. P. (2018). Regulation of Mitochondrial Dynamics by Proteolytic Processing and Protein Turnover. *Antioxidants* **7**(1).

Andolfo, I., Alper, S. L., Delaunay, J., Auriemma, C., Russo, R., Asci, R., Esposito, M. R., Sharma, A. K., Shmukler, B. E., Brugnara, C., *et al.* (2013). Missense mutations in the ABCB6 transporter cause dominant familial pseudohyperkalemia. *Am J Hematol* **88**(1), 66-72.

Antoun, G., McMurray, F., Thrush, A. B., Patten, D. A., Peixoto, A. C., Slack, R. S., McPherson, R., Dent, R., and Harper, M. E. (2015). Impaired mitochondrial oxidative phosphorylation and supercomplex assembly in rectus abdominis muscle of diabetic obese individuals. *Diabetologia* **58**(12), 2861-6.

Arias, G., Asins, G., Hegardt, F. G., and Serra, D. (1997). The effect of fasting/refeeding and insulin treatment on the expression of the regulatory genes of ketogenesis in intestine and liver of suckling rats. *Archives of biochemistry and biophysics* **340**(2), 287-98.

Arruda, A. P., Pers, B. M., Parlakgul, G., Guney, E., Inouye, K., and Hotamisligil, G. S. (2014). Chronic enrichment of hepatic endoplasmic reticulum-mitochondria contact leads to mitochondrial dysfunction in obesity. *Nature medicine* **20**(12), 1427-35.

Bach, D., Naon, D., Pich, S., Soriano, F. X., Vega, N., Rieusset, J., Laville, M., Guillet, C., Boirie, Y., Wallberg-Henriksson, H., *et al.* (2005). Expression of Mfn2, the Charcot-Marie-Tooth neuropathy type 2A gene, in human skeletal muscle: effects of type 2 diabetes, obesity, weight loss, and the regulatory role of tumor necrosis factor alpha and interleukin-6. *Diabetes* **54**(9), 2685-93.

Ball, S., Colleoni, C., Cenci, U., Raj, J. N., and Tirtiaux, C. (2011). The evolution of glycogen and starch metabolism in eukaryotes gives molecular clues to understand the establishment of plastid endosymbiosis. *J Exp Bot* **62**(6), 1775-801.

Barth, P. G., Valianpour, F., Bowen, V. M., Lam, J., Duran, M., Vaz, F. M., and Wanders, R. J. (2004). X-linked cardioskeletal myopathy and neutropenia (Barth syndrome): an update. *American journal of medical genetics. Part A* **126A**(4), 349-54.

Benador, I. Y., Veliova, M., Mahdaviani, K., Petcherski, A., Wikstrom, J. D., Assali, E. A., Acin-Perez, R., Shum, M., Oliveira, M. F., Cinti, S., *et al.* (2018). Mitochondria Bound to Lipid Droplets Have Unique Bioenergetics, Composition, and Dynamics that Support Lipid Droplet Expansion. *Cell Metab* **27**(4), 869-885 e6.

Benard, G., Bellance, N., Jose, C., Melser, S., Nouette-Gaulain, K., and Rossignol, R. (2010). Multi-site control and regulation of mitochondrial energy production. *Biochim Biophys Acta* **1797**(6-7), 698-709.

Bereiter-Hahn, J., and Voth, M. (1994). Dynamics of mitochondria in living cells: shape changes, dislocations, fusion, and fission of mitochondria. *Microscopy research and technique* **27**(3), 198-219.

Bleiberg-Daniel, F., Lamri, Y., Feldmann, G., and Lardeux, B. (1994). Glucagon administration in vivo stimulates hepatic RNA and protein breakdown in fed and fasted rats. *Biochem J* **299 (Pt 3)**, 645-9.

Boengler, K., Heusch, G., and Schulz, R. (2011). Nuclear-encoded mitochondrial proteins and their role in cardioprotection. *Biochim Biophys Acta* **1813**(7), 1286-94.

Borst, P., Zelcer, N., and van Helvoort, A. (2000). ABC transporters in lipid transport. *Biochim Biophys Acta* **1486**(1), 128-44.

Bournat, J. C., and Brown, C. W. (2010). Mitochondrial dysfunction in obesity. *Current opinion in endocrinology, diabetes, and obesity* **17**(5), 446-52.

Boushel, R., Gnaiger, E., Schjerling, P., Skovbro, M., Kraunsoe, R., and Dela, F. (2007). Patients with type 2 diabetes have normal mitochondrial function in skeletal muscle. *Diabetologia* **50**(4), 790-6.

Bray, G. A. (2004). Medical consequences of obesity. *J Clin Endocrinol Metab* **89**(6), 2583-9.

Bruce, J. I., Giovannucci, D. R., Blinder, G., Shuttleworth, T. J., and Yule, D. I. (2004). Modulation of [Ca2+]i signaling dynamics and metabolism by perinuclear mitochondria in mouse parotid acinar cells. *J Biol Chem* **279**(13), 12909-17.

Bullon, P., Marin-Aguilar, F., and Roman-Malo, L. (2016). AMPK/Mitochondria in Metabolic Diseases. *Exs* **107**, 129-152.

Castro, A. V., Kolka, C. M., Kim, S. P., and Bergman, R. N. (2014). Obesity, insulin resistance and comorbidities? Mechanisms of association. *Arquivos brasileiros de endocrinologia e metabologia* **58**(6), 600-9.

Chan, D. C. (2006). Mitochondrial fusion and fission in mammals. *Annu Rev Cell Dev Biol* **22**, 79-99.

Chandhok, G., Lazarou, M., and Neumann, B. (2018). Structure, function, and regulation of mitofusin-2 in health and disease. *Biological reviews of the Cambridge Philosophical Society* **93**(2), 933-949.

Chao, X., Wang, S., Zhao, K., Li, Y., Williams, J. A., Li, T., Chavan, H., Krishnamurthy, P., He, X. C., Li, L., *et al.* (2018). Impaired TFEB-mediated Lysosome Biogenesis and Autophagy Promote Chronic Ethanol-induced Liver Injury and Steatosis in Mice. *Gastroenterology* doi: 10.1053/j.gastro.2018.05.027.

Chavan, H., Christudoss, P., Mickey, K., Tessman, R., Ni, H. M., Swerdlow, R., and Krishnamurthy, P. (2017). Arsenite Effects on Mitochondrial Bioenergetics in Human and Mouse Primary Hepatocytes Follow a Nonlinear Dose Response. *Oxid Med Cell Longev* **2017**, 9251303.

Chavan, H., Khan, M. M., Tegos, G., and Krishnamurthy, P. (2013). Efficient purification and reconstitution of ATP binding cassette transporter B6 (ABCB6) for functional and structural studies. *The Journal of biological chemistry* **288**(31), 22658-69.

Chavan, H., Li, F., Tessman, R., Mickey, K., Dorko, K., Schmitt, T., Kumer, S., Gunewardena, S., Gaikwad, N., and Krishnamurthy, P. (2015). Functional coupling of ATP-binding cassette transporter Abcb6 to cytochrome P450 expression and activity in liver. *J Biol Chem* **290**(12), 7871-86.

Chen, H., Detmer, S. A., Ewald, A. J., Griffin, E. E., Fraser, S. E., and Chan, D. C. (2003). Mitofusins Mfn1 and Mfn2 coordinately regulate mitochondrial fusion and are essential for embryonic development. *The Journal of cell biology* **160**(2), 189-200.

Cheng, Z., and Ristow, M. (2013). Mitochondria and metabolic homeostasis. *Antioxidants & redox signaling* **19**(3), 240-2.

Chiang, J. Y. (2013). Bile acid metabolism and signaling. *Compr Physiol* **3**(3), 1191-212.
Chowdhury, S. K., Smith, D. R., and Fernyhough, P. (2013). The role of aberrant mitochondrial bioenergetics in diabetic neuropathy. *Neurobiology of disease* **51**, 56-65.

Cogliati, S., Frezza, C., Soriano, M. E., Varanita, T., Quintana-Cabrera, R., Corrado, M., Cipolat, S., Costa, V., Casarin, A., Gomes, L. C., *et al.* (2013). Mitochondrial cristae shape determines respiratory chain supercomplexes assembly and respiratory efficiency. *Cell* **155**(1), 160-71.

Contreras, L., Drago, I., Zampese, E., and Pozzan, T. (2010). Mitochondria: the calcium connection. *Biochim Biophys Acta* **1797**(6-7), 607-18.

Corpeleijn, E., Saris, W. H., and Blaak, E. E. (2009). Metabolic flexibility in the development of insulin resistance and type 2 diabetes: effects of lifestyle. *Obesity reviews : an official journal of the International Association for the Study of Obesity* **10**(2), 178-93.

Course, M. M., and Wang, X. (2016). Transporting mitochondria in neurons. *F1000Res* **5**.

Cui, Y. X., Xia, X. Y., Zhou, Y., Gao, L., Shang, X. J., Ni, T., Wang, W. P., Fan, X. B., Yin, H. L., Jiang, S. J., *et al.* (2013). Novel mutations of ABCB6 associated with autosomal dominant dyschromatosis universalis hereditaria. *PLoS One* **8**(11), e79808.

Davidson, A. L., Dassa, E., Orelle, C., and Chen, J. (2008). Structure, function, and evolution of bacterial ATP-binding cassette systems. *Microbiol Mol Biol Rev* **72**(2), 317-64, table of contents.

Davies, V. J., Hollins, A. J., Piechota, M. J., Yip, W., Davies, J. R., White, K. E., Nicols, P. P., Boulton, M. E., and Votruba, M. (2007). Opa1 deficiency in a mouse model of autosomal dominant optic atrophy impairs mitochondrial morphology, optic nerve structure and visual function. *Human molecular genetics* **16**(11), 1307-18.

Dean, M. (2009). ABC transporters, drug resistance, and cancer stem cells. *Journal of mammary gland biology and neoplasia* **14**(1), 3-9.

Dean, M., and Allikmets, R. (2001a). Complete characterization of the human ABC gene family. *Journal of bioenergetics and biomembranes* **33**(6), 475-9.

Dean, M., Rzhetsky, A., and Allikmets, R. (2001b). The human ATP-binding cassette (ABC) transporter superfamily. *Genome research* **11**(7), 1156-66.

Di Meo, S., Reed, T. T., Venditti, P., and Victor, V. M. (2016). Role of ROS and RNS Sources in Physiological and Pathological Conditions. *Oxid Med Cell Longev* **2016**, 1245049.

Domitrovic, R., Tota, M., and Milin, C. (2008). Differential effect of high dietary iron on alpha-tocopherol and retinol levels in the liver and serum of mice fed olive oil- and corn oil-enriched diets. *Nutr Res* **28**(4), 263-9.

Elmore, S. (2007). Apoptosis: a review of programmed cell death. *Toxicol Pathol* **35**(4), 495-516.

Ernster, L., and Schatz, G. (1981). Mitochondria: a historical review. *J Cell Biol* **91**(3 Pt 2), 227s-255s.

Eura, Y., Ishihara, N., Yokota, S., and Mihara, K. (2003). Two mitofusin proteins, mammalian homologues of FZO, with distinct functions are both required for mitochondrial fusion. *J Biochem* **134**(3), 333-44.

Ferree, A., and Shirihai, O. (2012). Mitochondrial dynamics: the intersection of form and function. *Advances in experimental medicine and biology* **748**, 13-40.

Frenzel, M., Rommelspacher, H., Sugawa, M. D., and Dencher, N. A. (2010). Ageing alters the supramolecular architecture of OxPhos complexes in rat brain cortex. *Experimental gerontology* **45**(7-8), 563-72.

Frisdal, E., and Le Goff, W. (2015). Adipose ABCG1: A potential therapeutic target in obesity? *Adipocyte* **4**(4), 315-8.

Frohman, M. A. (2015). Role of mitochondrial lipids in guiding fission and fusion. *J Mol Med (Berl)* **93**(3), 263-9.

Fruton, J. S., and Simmonds, S. (1950). The metabolism of peptides. *Cold Spring Harb Symp Quant Biol* **14**, 55-64.

Fustin, J. M., Doi, M., Yamada, H., Komatsu, R., Shimba, S., and Okamura, H. (2012). Rhythmic nucleotide synthesis in the liver: temporal segregation of metabolites. *Cell Rep* **1**(4), 341-9.

Galgani, J. E., Moro, C., and Ravussin, E. (2008). Metabolic flexibility and insulin resistance. *American journal of physiology. Endocrinology and metabolism* **295**(5), E1009-17.

Gao, A. W., Canto, C., and Houtkooper, R. H. (2014). Mitochondrial response to nutrient availability and its role in metabolic disease. *EMBO molecular medicine* **6**(5), 580-9.

Gautam, A., D'Arpa, P., Donohue, D. E., Muhie, S., Chakraborty, N., Luke, B. T., Grapov, D., Carroll, E. E., Meyerhoff, J. L., Hammamieh, R., *et al.* (2015). Acute and chronic plasma metabolomic and liver transcriptomic stress effects in a mouse model with features of post-traumatic stress disorder. *PLoS One* **10**(1), e0117092.

Geisler, C. E., Hepler, C., Higgins, M. R., and Renquist, B. J. (2016). Hepatic adaptations to maintain metabolic homeostasis in response to fasting and refeeding in mice. *Nutr Metab (Lond)* **13**, 62.

Genova, M. L., and Lenaz, G. (2014). Functional role of mitochondrial respiratory supercomplexes. *Biochim Biophys Acta* **1837**(4), 427-43.

Gohil, V. M., and Greenberg, M. L. (2009). Mitochondrial membrane biogenesis: phospholipids and proteins go hand in hand. *J Cell Biol* **184**(4), 469-72.

Gomes, L. C., Di Benedetto, G., and Scorrano, L. (2011a). During autophagy mitochondria elongate, are spared from degradation and sustain cell viability. *Nature cell biology* **13**(5), 589-98.

Gomes, L. C., Di Benedetto, G., and Scorrano, L. (2011b). Essential amino acids and glutamine regulate induction of mitochondrial elongation during autophagy. *Cell cycle* **10**(16), 2635-9.

Goodpaster, B. H., and Sparks, L. M. (2017). Metabolic Flexibility in Health and Disease. *Cell Metab* **25**(5), 1027-1036.

Gray, M. W. (2017). Lynn Margulis and the endosymbiont hypothesis: 50 years later. *Mol Biol Cell* **28**(10), 1285-1287.

Greggio, C., Jha, P., Kulkarni, S. S., Lagarrigue, S., Broskey, N. T., Boutant, M., Wang, X., Conde Alonso, S., Ofori, E., Auwerx, J., *et al.* (2017). Enhanced Respiratory Chain Supercomplex Formation in Response to Exercise in Human Skeletal Muscle. *Cell metabolism* **25**(2), 301-311.

He, L., Zhou, X., Huang, N., Li, H., Tian, J., Li, T., Yao, K., Nyachoti, C. M., Kim, S. W., and Yin, Y. (2017). AMPK Regulation of Glucose, Lipid and Protein Metabolism: Mechanisms and Nutritional Significance. *Current protein & peptide science* **18**(6), 562-570.

Heilbronn, L. K., Gan, S. K., Turner, N., Campbell, L. V., and Chisholm, D. J. (2007). Markers of mitochondrial biogenesis and metabolism are lower in overweight and obese insulin-resistant subjects. *The Journal of clinical endocrinology and metabolism* **92**(4), 1467-73.

Helias, V., Saison, C., Ballif, B. A., Peyrard, T., Takahashi, J., Takahashi, H., Tanaka, M., Deybach, J. C., Puy, H., Le Gall, M., *et al.* (2012). ABCB6 is dispensable for erythropoiesis and specifies the new blood group system Langereis. *Nature genetics* **44**(2), 170-3.

Herlan, M., Bornhovd, C., Hell, K., Neupert, W., and Reichert, A. S. (2004). Alternative topogenesis of Mgm1 and mitochondrial morphology depend on ATP and a functional import motor. *J Cell Biol* **165**(2), 167-73.

Hermann, G. J., and Shaw, J. M. (1998). Mitochondrial dynamics in yeast. *Annual review of cell and developmental biology* **14**, 265-303.

Hirsch-Ernst, K. I., Gaini-Rahimi, S., Ernst, B. P., Schmitz-Salue, C., Blume, S., and Kahl, G. F. (1998). Molecular cDNA cloning and tissue distribution of mRNA encoding a novel ATP-binding cassette (ABC) half-transporter. *Biochem Biophys Res Commun* **249**(1), 151-5.

Hu, C., Huang, Y., and Li, L. (2017). Drp1-Dependent Mitochondrial Fission Plays Critical Roles in Physiological and Pathological Progresses in Mammals. *Int J Mol Sci* **18**(1).

Hutson, S. M., Sweatt, A. J., and Lanoue, K. F. (2005). Branched-chain [corrected] amino acid metabolism: implications for establishing safe intakes. *J Nutr* **135**(6 Suppl), 1557S-64S.

Ikeda, I., Metoki, K., Yamahira, T., Kato, M., Inoue, N., Nagao, K., Yanagita, T., Shirakawa, H., and Komai, M. (2014). Impact of fasting time on hepatic lipid metabolism in nutritional animal studies. *Biosci Biotechnol Biochem* **78**(9), 1584-91.

Ishihara, N., Nomura, M., Jofuku, A., Kato, H., Suzuki, S. O., Masuda, K., Otera, H., Nakanishi, Y., Nonaka, I., Goto, Y., *et al.* (2009). Mitochondrial fission factor Drp1 is essential for embryonic development and synapse formation in mice. *Nature cell biology* **11**(8), 958-66.

Jacobi, D., Liu, S., Burkewitz, K., Kory, N., Knudsen, N. H., Alexander, R. K., Unluturk, U., Li, X., Kong, X., Hyde, A. L., *et al.* (2015). Hepatic Bmal1 Regulates Rhythmic Mitochondrial Dynamics and Promotes Metabolic Fitness. *Cell Metab* **22**(4), 709-20.

Jha, P., Wang, X., and Auwerx, J. (2016). Analysis of Mitochondrial Respiratory Chain Supercomplexes Using Blue Native Polyacrylamide Gel Electrophoresis (BN-PAGE). *Current protocols in mouse biology* **6**(1), 1-14.

Jheng, H. F., Tsai, P. J., Guo, S. M., Kuo, L. H., Chang, C. S., Su, I. J., Chang, C. R., and Tsai, Y. S. (2012). Mitochondrial fission contributes to mitochondrial dysfunction and insulin resistance in skeletal muscle. *Mol Cell Biol* **32**(2), 309-19.

Johnson, M. A., Vidoni, S., Durigon, R., Pearce, S. F., Rorbach, J., He, J., Brea-Calvo, G., Minczuk, M., Reyes, A., Holt, I. J., *et al.* (2014). Amino acid starvation has opposite effects on mitochondrial and cytosolic protein synthesis. *PLoS One* **9**(4), e93597.

Kaminski, W. E., Piehler, A., and Wenzel, J. J. (2006). ABC A-subfamily transporters: structure, function and disease. *Biochim Biophys Acta* **1762**(5), 510-24.

Kay, C., Woodward, K. D., Lawler, K., Self, T. J., Dyall, S. D., and Kerr, I. D. (2012). The ATP-binding cassette proteins of the deep-branching protozoan parasite Trichomonas vaginalis. *PLoS Negl Trop Dis* **6**(6), e1693.

Khraiwesh, H., Lopez-Dominguez, J. A., Lopez-Lluch, G., Navas, P., de Cabo, R., Ramsey, J. J., Villalba, J. M., and Gonzalez-Reyes, J. A. (2013). Alterations of ultrastructural and fission/fusion markers in hepatocyte mitochondria from mice following calorie restriction with different dietary fats. *J Gerontol A Biol Sci Med Sci* **68**(9), 1023-34.

Kim, J. A., Wei, Y., and Sowers, J. R. (2008). Role of mitochondrial dysfunction in insulin resistance. *Circulation research* **102**(4), 401-14.

Kohler, P. (1985). The strategies of energy conservation in helminths. *Molecular and biochemical parasitology* **17**(1), 1-18.

Koshiba, T., Detmer, S. A., Kaiser, J. T., Chen, H., McCaffery, J. M., and Chan, D. C. (2004). Structural basis of mitochondrial tethering by mitofusin complexes. *Science* **305**(5685), 858-62.

Krishnamurthy, P., and Schuetz, J. D. (2011). The role of ABCG2 and ABCB6 in porphyrin metabolism and cell survival. *Curr Pharm Biotechnol* **12**(4), 647-55.

Krishnamurthy, P., Xie, T., and Schuetz, J. D. (2007). The role of transporters in cellular heme and porphyrin homeostasis. *Pharmacol Ther* **114**(3), 345-58.

Krishnamurthy, P. C., Du, G., Fukuda, Y., Sun, D., Sampath, J., Mercer, K. E., Wang, J., Sosa-Pineda, B., Murti, K. G., and Schuetz, J. D. (2006). Identification of a mammalian mitochondrial porphyrin transporter. *Nature* **443**(7111), 586-9.

Kulkarni, S. S., Joffraud, M., Boutant, M., Ratajczak, J., Gao, A. W., Maclachlan, C., Hernandez-Alvarez, M. I., Raymond, F., Metairon, S., Descombes, P., *et al.* (2016). Mfn1 Deficiency in the Liver Protects Against Diet-Induced Insulin Resistance and Enhances the Hypoglycemic Effect of Metformin. *Diabetes* **65**(12), 3552-3560.

Kurashima-Ito, K., Ikeya, T., Senbongi, H., Tochio, H., Mikawa, T., Shibata, T., and Ito, Y. (2006). Heteronuclear multidimensional NMR and homology modelling studies of the C-terminal nucleotide-binding domain of the human mitochondrial ABC transporter ABCB6. *J Biomol NMR* **35**(1), 53-71.

Laplante, M., and Sabatini, D. M. (2009). mTOR signaling at a glance. *Journal of cell science* **122**(Pt 20), 3589-94.

Laplante, M., and Sabatini, D. M. (2012). mTOR signaling in growth control and disease. *Cell* **149**(2), 274-93.

Lapuente-Brun, E., Moreno-Loshuertos, R., Acin-Perez, R., Latorre-Pellicer, A., Colas, C., Balsa, E., Perales-Clemente, E., Quiros, P. M., Calvo, E., Rodriguez-Hernandez, M. A., *et al.* (2013). Supercomplex assembly determines electron flux in the mitochondrial electron transport chain. *Science* **340**(6140), 1567-70.

Lee, H., and Yoon, Y. (2016). Mitochondrial fission and fusion. *Biochemical Society transactions* **44**(6), 1725-1735.

Lenaz, G., and Genova, M. L. (2009). Structural and functional organization of the mitochondrial respiratory chain: a dynamic super-assembly. *Int J Biochem Cell Biol* **41**(10), 1750-1772.

Li, Q., Sadhukhan, S., Berthiaume, J. M., Ibarra, R. A., Tang, H., Deng, S., Hamilton, E., Nagy, L. E., Tochtrop, G. P., and Zhang, G. F. (2013). 4-Hydroxy-2(E)-nonenal (HNE) catabolism and formation of HNE adducts are modulated by beta oxidation of fatty acids in the isolated rat heart. *Free Radic Biol Med* **58**, 35-44.

Li, X. (2013). SIRT1 and energy metabolism. *Acta biochimica et biophysica Sinica* **45**(1), 51-60.
Liesa, M., and Shirihai, O. S. (2013). Mitochondrial dynamics in the regulation of nutrient utilization and energy expenditure. *Cell Metab* **17**(4), 491-506.

Lionetti, L., Mollica, M. P., Donizzetti, I., Gifuni, G., Sica, R., Pignalosa, A., Cavaliere, G., Gaita, M., De Filippo, C., Zorzano, A., *et al.* (2014). High-lard and high-fish-oil diets differ in their effects on function and dynamic behaviour of rat hepatic mitochondria. *PloS one* **9**(3), e92753.

Locher, K. P. (2009). Review. Structure and mechanism of ATP-binding cassette transporters. *Philos Trans R Soc Lond B Biol Sci* **364**(1514), 239-45.

Lochs, H., Morse, E. L., and Adibi, S. A. (1986). Mechanism of hepatic assimilation of dipeptides. Transport versus hydrolysis. *J Biol Chem* **261**(32), 14976-81.

Lombardi, A., Silvestri, E., Cioffi, F., Senese, R., Lanni, A., Goglia, F., de Lange, P., and Moreno, M. (2009). Defining the transcriptomic and proteomic profiles of rat ageing skeletal muscle by the use of a cDNA array, 2D- and Blue native-PAGE approach. *Journal of proteomics* **72**(4), 708-21.

Lopez-Lluch, G. (2017). Mitochondrial activity and dynamics changes regarding metabolism in ageing and obesity. *Mechanisms of ageing and development* **162**, 108-121.

Lopez-Lluch, G., Santos-Ocana, C., Sanchez-Alcazar, J. A., Fernandez-Ayala, D. J., Asencio-Salcedo, C., Rodriguez-Aguilera, J. C., and Navas, P. (2015). Mitochondrial responsibility in ageing process: innocent, suspect or guilty. *Biogerontology* **16**(5), 599-620.

Ma, H., and Patti, M. E. (2014). Bile acids, obesity, and the metabolic syndrome. *Best Pract Res Clin Gastroenterol* **28**(4), 573-83.

MacVicar, T., and Langer, T. (2016). OPA1 processing in cell death and disease - the long and short of it. *Journal of cell science* **129**(12), 2297-306.

Maranzana, E., Barbero, G., Falasca, A. I., Lenaz, G., and Genova, M. L. (2013). Mitochondrial respiratory supercomplex association limits production of reactive oxygen species from complex I. *Antioxidants & redox signaling* **19**(13), 1469-80.

Marks, K. A., Marvyn, P. M., Henao, J. J., Bradley, R. M., Stark, K. D., and Duncan, R. E. (2015). Fasting enriches liver triacylglycerol with n-3 polyunsaturated fatty acids: implications for understanding the adipose-liver axis in serum docosahexaenoic acid regulation. *Genes Nutr* **10**(6), 39.

Mattenberger, Y., James, D. I., and Martinou, J. C. (2003). Fusion of mitochondria in mammalian cells is dependent on the mitochondrial inner membrane potential and independent of microtubules or actin. *FEBS Lett* **538**(1-3), 53-9.

McKenzie, M., Lazarou, M., Thorburn, D. R., and Ryan, M. T. (2006). Mitochondrial respiratory chain supercomplexes are destabilized in Barth Syndrome patients. *Journal of molecular biology* **361**(3), 462-9.

McQuibban, G. A., Saurya, S., and Freeman, M. (2003). Mitochondrial membrane remodelling regulated by a conserved rhomboid protease. *Nature* **423**(6939), 537-41.

Meeusen, S., McCaffery, J. M., and Nunnari, J. (2004). Mitochondrial fusion intermediates revealed in vitro. *Science* **305**(5691), 1747-52.

Miller, W. L. (2017). Steroidogenesis: Unanswered Questions. *Trends Endocrinol Metab* **28**(11), 771-793.

Mitchell, T., and Darley-Usmar, V. (2012). Metabolic syndrome and mitochondrial dysfunction: insights from preclinical studies with a mitochondrially targeted antioxidant. *Free Radic Biol Med* **52**(5), 838-40.

Mitra, K., Wunder, C., Roysam, B., Lin, G., and Lippincott-Schwartz, J. (2009). A hyperfused mitochondrial state achieved at G1-S regulates cyclin E buildup and entry into S phase. *Proc Natl Acad Sci U S A* **106**(29), 11960-5.

Mitsuhashi, N., Miki, T., Senbongi, H., Yokoi, N., Yano, H., Miyazaki, M., Nakajima, N., Iwanaga, T., Yokoyama, Y., Shibata, T., *et al.* (2000). MTABC3, a novel mitochondrial ATP-binding cassette protein involved in iron homeostasis. *J Biol Chem* **275**(23), 17536-40.

Molina, A. J., Wikstrom, J. D., Stiles, L., Las, G., Mohamed, H., Elorza, A., Walzer, G., Twig, G., Katz, S., Corkey, B. E., *et al.* (2009). Mitochondrial networking protects beta-cells from nutrient-induced apoptosis. *Diabetes* **58**(10), 2303-15.

Moller, D. E., and Kaufman, K. D. (2005). Metabolic syndrome: a clinical and molecular perspective. *Annual review of medicine* **56**, 45-62.

Mootha, V. K., Lindgren, C. M., Eriksson, K. F., Subramanian, A., Sihag, S., Lehar, J., Puigserver, P., Carlsson, E., Ridderstrale, M., Laurila, E., *et al.* (2003). PGC-1alpha-responsive genes involved in oxidative phosphorylation are coordinately downregulated in human diabetes. *Nature genetics* **34**(3), 267-73.

Morino, K., Petersen, K. F., Dufour, S., Befroy, D., Frattini, J., Shatzkes, N., Neschen, S., White, M. F., Bilz, S., Sono, S., *et al.* (2005). Reduced mitochondrial density and increased IRS-1 serine phosphorylation in muscle of insulin-resistant offspring of type 2 diabetic parents. *The Journal of clinical investigation* **115**(12), 3587-93.

Morris, S. M., Jr. (2002). Regulation of enzymes of the urea cycle and arginine metabolism. *Annu Rev Nutr* **22**, 87-105.

Murphy, A. J., Sarrazy, V., Wang, N., Bijl, N., Abramowicz, S., Westerterp, M., Welch, C. B., Schuetz, J. D., and Yvan-Charvet, L. (2014). Deficiency of ATP-binding cassette transporter B6 in megakaryocyte progenitors accelerates atherosclerosis in mice. *Arterioscler Thromb Vasc Biol* **34**(4), 751-8.

Nasrallah, C. M., and Horvath, T. L. (2014). Mitochondrial dynamics in the central regulation of metabolism. *Nature reviews. Endocrinology* **10**(11), 650-8.

Neumann, J., Rose-Sperling, D., and Hellmich, U. A. (2017). Diverse relations between ABC transporters and lipids: An overview. *Biochim Biophys Acta Biomembr* **1859**(4), 605-618.

Nunnari, J., and Suomalainen, A. (2012). Mitochondria: in sickness and in health. *Cell* **148**(6), 1145-59.

Nutrient Requirements of Laboratory Animals: Fourth Revised Edition, 1995 doi: 10.17226/4758, Washington (DC).

Ono, T., Isobe, K., Nakada, K., and Hayashi, J. I. (2001). Human cells are protected from mitochondrial dysfunction by complementation of DNA products in fused mitochondria. *Nat Genet* **28**(3), 272-5.

Orlowski, M., and Wilk, S. (1976). Metabolism of gamma-glutamyl amino acids and peptides in mouse liver and kidney in vivo. *Eur J Biochem* **71**(2), 549-55.

Patti, M. E., Butte, A. J., Crunkhorn, S., Cusi, K., Berria, R., Kashyap, S., Miyazaki, Y., Kohane, I., Costello, M., Saccone, R., *et al.* (2003). Coordinated reduction of genes of oxidative metabolism in humans with insulin resistance and diabetes: Potential role of PGC1 and NRF1. *Proceedings of the National Academy of Sciences of the United States of America* **100**(14), 8466-71.

Perfettini, J. L., Roumier, T., and Kroemer, G. (2005). Mitochondrial fusion and fission in the control of apoptosis. *Trends Cell Biol* **15**(4), 179-83.

Pintus, F., Floris, G., and Rufini, A. (2012). Nutrient availability links mitochondria, apoptosis, and obesity. *Aging* **4**(11), 734-41.

Polireddy, K., Chavan, H., Abdulkarim, B. A., and Krishnamurthy, P. (2011). Functional significance of the ATP-binding cassette transporter B6 in hepatocellular carcinoma. *Mol Oncol* **5**(5), 410-25.

Pondarre, C., Campagna, D. R., Antiochos, B., Sikorski, L., Mulhern, H., and Fleming, M. D. (2007). Abcb7, the gene responsible for X-linked sideroblastic anemia with ataxia, is essential for hematopoiesis. *Blood* **109**(8), 3567-9.

Procko, E., O'Mara, M. L., Bennett, W. F., Tieleman, D. P., and Gaudet, R. (2009). The mechanism of ABC transporters: general lessons from structural and functional studies of an antigenic peptide transporter. *FASEB J* **23**(5), 1287-302.

Putti, R., Sica, R., Migliaccio, V., and Lionetti, L. (2015). Diet impact on mitochondrial bioenergetics and dynamics. *Front Physiol* **6**, 109.

Quazi, F., Lenevich, S., and Molday, R. S. (2012). ABCA4 is an N-retinylidene-phosphatidylethanolamine and phosphatidylethanolamine importer. *Nat Commun* **3**, 925.

Reichert, A. S., and Neupert, W. (2002). Contact sites between the outer and inner membrane of mitochondria-role in protein transport. *Biochim Biophys Acta* **1592**(1), 41-9.

Ritov, V. B., Menshikova, E. V., He, J., Ferrell, R. E., Goodpaster, B. H., and Kelley, D. E. (2005). Deficiency of subsarcolemmal mitochondria in obesity and type 2 diabetes. *Diabetes* **54**(1), 8-14.

Rogers, G. W., Brand, M. D., Petrosyan, S., Ashok, D., Elorza, A. A., Ferrick, D. A., and Murphy, A. N. (2011). High throughput microplate respiratory measurements using minimal quantities of isolated mitochondria. *PLoS One* **6**(7), e21746.

Ross, F. A., MacKintosh, C., and Hardie, D. G. (2016). AMP-activated protein kinase: a cellular energy sensor that comes in 12 flavours. *The FEBS journal* **283**(16), 2987-3001.

Rui, L. (2014). Energy metabolism in the liver. *Compr Physiol* **4**(1), 177-97.

Santel, A., and Frank, S. (2008). Shaping mitochondria: The complex posttranslational regulation of the mitochondrial fission protein DRP1. *IUBMB life* **60**(7), 448-55.

Schagger, H., and Pfeiffer, K. (2000). Supercomplexes in the respiratory chains of yeast and mammalian mitochondria. *The EMBO journal* **19**(8), 1777-83.

Scharwey, M., Tatsuta, T., and Langer, T. (2013). Mitochondrial lipid transport at a glance. *J Cell Sci* **126**(Pt 23), 5317-23.

Schmitz, G., Kaminski, W. E., and Orso, E. (2000). ABC transporters in cellular lipid trafficking. *Current opinion in lipidology* **11**(5), 493-501.

Schmutz, I., Albrecht, U., and Ripperger, J. A. (2012). The role of clock genes and rhythmicity in the liver. *Molecular and cellular endocrinology* **349**(1), 38-44.

Schou, J., Tybjaerg-Hansen, A., Moller, H. J., Nordestgaard, B. G., and Frikke-Schmidt, R. (2012). ABC transporter genes and risk of type 2 diabetes: a study of 40,000 individuals from the general population. *Diabetes Care* **35**(12), 2600-6.

Sebastian, D., Hernandez-Alvarez, M. I., Segales, J., Sorianello, E., Munoz, J. P., Sala, D., Waget, A., Liesa, M., Paz, J. C., Gopalacharyulu, P., *et al.* (2012). Mitofusin 2 (Mfn2) links mitochondrial and endoplasmic reticulum function with insulin signaling and is essential for normal glucose homeostasis. *Proceedings of the National Academy of Sciences of the United States of America* **109**(14), 5523-8.

Seitz, H. J., Muller, M. J., Krone, W., and Tarnowski, W. (1977). Coordinate control of intermediary metabolism in rat liver by the insulin/glucagon ratio during starvation and after glucose refeeding. Regulatory significance of long-chain acyl-CoA and cyclic AMP. *Archives of biochemistry and biophysics* **183**(2), 647-63.

Sengupta, S., Peterson, T. R., Laplante, M., Oh, S., and Sabatini, D. M. (2010). mTORC1 controls fasting-induced ketogenesis and its modulation by ageing. *Nature* **468**(7327), 1100-4.

Shoffner, J. M. (2001). An introduction: oxidative phosphorylation diseases. *Semin Neurol* **21**(3), 237-50.

Sieber, M. H., and Spradling, A. C. (2017). The role of metabolic states in development and disease. *Current opinion in genetics & development* **45**, 58-68.

Singer, P. (2013). From mitochondrial disturbances to energy requirements. *World review of nutrition and dietetics* **105**, 1-11.

Skulachev, V. P. (1999). Mitochondrial physiology and pathology; concepts of programmed death of organelles, cells and organisms. *Mol Aspects Med* **20**(3), 139-84.

Smeitink, J., van den Heuvel, L., and DiMauro, S. (2001). The genetics and pathology of oxidative phosphorylation. *Nat Rev Genet* **2**(5), 342-52.

Smith, R. L., Soeters, M. R., Wust, R. C. I., and Houtkooper, R. H. (2018a). Metabolic Flexibility as an Adaptation to Energy Resources and Requirements in Health and Disease. *Endocr Rev* **39**(4), 489-517.

Smith, R. L., Soeters, M. R., Wust, R. C. I., and Houtkooper, R. H. (2018b). Metabolic flexibility as an adaptation to energy resources and requirements in health and disease. *Endocrine reviews* doi: 10.1210/er.2017-00211.

Song, Z., Chen, H., Fiket, M., Alexander, C., and Chan, D. C. (2007). OPA1 processing controls mitochondrial fusion and is regulated by mRNA splicing, membrane potential, and Yme1L. *J Cell Biol* **178**(5), 749-55.

Sood, A., Jeyaraju, D. V., Prudent, J., Caron, A., Lemieux, P., McBride, H. M., Laplante, M., Toth, K., and Pellegrini, L. (2014). A Mitofusin-2-dependent inactivating cleavage of Opa1 links changes in mitochondria cristae and ER contacts in the postprandial liver. *Proceedings of the National Academy of Sciences of the United States of America* **111**(45), 16017-22.

Stephenson, E. J., and Hawley, J. A. (2014). Mitochondrial function in metabolic health: a genetic and environmental tug of war. *Biochimica et biophysica acta* **1840**(4), 1285-94.

Suen, D. F., Norris, K. L., and Youle, R. J. (2008). Mitochondrial dynamics and apoptosis. *Genes Dev* **22**(12), 1577-90.

Sunny, N. E., Kalavalapalli, S., Bril, F., Garrett, T. J., Nautiyal, M., Mathew, J. T., Williams, C. M., and Cusi, K. (2015). Cross-talk between branched-chain amino acids and hepatic mitochondria is compromised in nonalcoholic fatty liver disease. *Am J Physiol Endocrinol Metab* **309**(4), E311-9.

Tait, S. W., and Green, D. R. (2012). Mitochondria and cell signalling. *J Cell Sci* **125**(Pt 4), 807-15.

Thamotharan, M., Lombardo, Y. B., Bawani, S. Z., and Adibi, S. A. (1997). An active mechanism for completion of the final stage of protein degradation in the liver, lysosomal transport of dipeptides. *J Biol Chem* **272**(18), 11786-90.

Tondera, D., Grandemange, S., Jourdain, A., Karbowski, M., Mattenberger, Y., Herzig, S., Da Cruz, S., Clerc, P., Raschke, I., Merkwirth, C., *et al.* (2009). SLP-2 is required for stress-induced mitochondrial hyperfusion. *EMBO J* **28**(11), 1589-600.

Tsuchida, M., Emi, Y., Kida, Y., and Sakaguchi, M. (2008). Human ABC transporter isoform B6 (ABCB6) localizes primarily in the Golgi apparatus. *Biochem Biophys Res Commun* **369**(2), 369-75.

Tupone, D., Madden, C. J., and Morrison, S. F. (2014). Autonomic regulation of brown adipose tissue thermogenesis in health and disease: potential clinical applications for altering BAT thermogenesis. *Front Neurosci* **8**, 14.

Uhlen, M., Fagerberg, L., Hallstrom, B. M., Lindskog, C., Oksvold, P., Mardinoglu, A., Sivertsson, A., Kampf, C., Sjostedt, E., Asplund, A., *et al.* (2015). Proteomics. Tissue-based map of the human proteome. *Science* **347**(6220), 1260419.

van der Bliek, A. M., Shen, Q., and Kawajiri, S. (2013). Mechanisms of mitochondrial fission and fusion. *Cold Spring Harb Perspect Biol* **5**(6).

Vasiliou, V., Vasiliou, K., and Nebert, D. W. (2009). Human ATP-binding cassette (ABC) transporter family. *Hum Genomics* **3**(3), 281-90.

Wang, L., He, F., Bu, J., Zhen, Y., Liu, X., Du, W., Dong, J., Cooney, J. D., Dubey, S. K., Shi, Y., *et al.* (2012). ABCB6 mutations cause ocular coloboma. *Am J Hum Genet* **90**(1), 40-8.

Wang, L., Ishihara, T., Ibayashi, Y., Tatsushima, K., Setoyama, D., Hanada, Y., Takeichi, Y., Sakamoto, S., Yokota, S., Mihara, K., *et al.* (2015). Disruption of mitochondrial fission in the liver protects mice from diet-induced obesity and metabolic deterioration. *Diabetologia* **58**(10), 2371-80.

Westermann, B. (2008). Molecular machinery of mitochondrial fusion and fission. *J Biol Chem* **283**(20), 13501-5.

Westermann, B. (2012). Bioenergetic role of mitochondrial fusion and fission. *Biochim Biophys Acta* **1817**(10), 1833-8.

Wiedemann, N., Stiller, S. B., and Pfanner, N. (2013). Activation and degradation of mitofusins: two pathways regulate mitochondrial fusion by reversible ubiquitylation. *Mol Cell* **49**(3), 423-5.

Willems, P. H., Rossignol, R., Dieteren, C. E., Murphy, M. P., and Koopman, W. J. (2015). Redox Homeostasis and Mitochondrial Dynamics. *Cell Metab* **22**(2), 207-18.

Wiss, O., and Wiss, V. (1977). The influence of fasting on the synthesis of cholesterol, squalene, fatty acids, and ubiquinones in liver, small intestine, and kidney of rats in vivo. *Helv Chim Acta* **60**(8), 2566-75.

Xu, W., Barrientos, T., and Andrews, N. C. (2013). Iron and copper in mitochondrial diseases. *Cell Metab* **17**(3), 319-28.

Yamada, H., Ono, S., Wada, S., Aoi, W., Park, E. Y., Nakamura, Y., and Sato, K. (2018). Statuses of food-derived glutathione in intestine, blood, and liver of rat. *npj Science of Food* **2**(1), 3.

Yamashita, N., Hoshida, S., Nishida, M., Igarashi, J., Taniguchi, N., Tada, M., Kuzuya, T., and Hori, M. (1997). Heat shock-induced manganese superoxide dismutase enhances the tolerance of cardiac myocytes to hypoxia-reoxygenation injury. *J Mol Cell Cardiol* **29**(7), 1805-13.

Youle, R. J., and van der Bliek, A. M. (2012). Mitochondrial fission, fusion, and stress. *Science* **337**(6098), 1062-5.

Young, L., Leonhard, K., Tatsuta, T., Trowsdale, J., and Langer, T. (2001). Role of the ABC transporter Mdl1 in peptide export from mitochondria. *Science* **291**(5511), 2135-8.

Zhan, M., Brooks, C., Liu, F., Sun, L., and Dong, Z. (2013). Mitochondrial dynamics: regulatory mechanisms and emerging role in renal pathophysiology. *Kidney Int* **83**(4), 568-81.

Zhang, C., Li, D., Zhang, J., Chen, X., Huang, M., Archacki, S., Tian, Y., Ren, W., Mei, A., Zhang, Q., *et al.* (2013). Mutations in ABCB6 cause dyschromatosis universalis hereditaria. *J Invest Dermatol* **133**(9), 2221-8.

Zhang, S., Zeng, X., Ren, M., Mao, X., and Qiao, S. (2017). Novel metabolic and physiological functions of branched chain amino acids: a review. *J Anim Sci Biotechnol* **8**, 10.

Zhang, Y., Jiang, L., Hu, W., Zheng, Q., and Xiang, W. (2011). Mitochondrial dysfunction during in vitro hepatocyte steatosis is reversed by omega-3 fatty acid-induced up-regulation of mitofusin 2. *Metabolism* **60**(6), 767-75.

Zuo, L., Zhou, T., Pannell, B. K., Ziegler, A. C., and Best, T. M. (2015). Biological and physiological role of reactive oxygen species--the good, the bad and the ugly. *Acta Physiol (Oxf)* **214**(3), 329-48.